



THE UNIVERSITY *of* EDINBURGH

This thesis has been submitted in fulfilment of the requirements for a postgraduate degree (e.g. PhD, MPhil, DClinPsychol) at the University of Edinburgh. Please note the following terms and conditions of use:

This work is protected by copyright and other intellectual property rights, which are retained by the thesis author, unless otherwise stated.

A copy can be downloaded for personal non-commercial research or study, without prior permission or charge.

This thesis cannot be reproduced or quoted extensively from without first obtaining permission in writing from the author.

The content must not be changed in any way or sold commercially in any format or medium without the formal permission of the author.

When referring to this work, full bibliographic details including the author, title, awarding institution and date of the thesis must be given.

The effect of on-going and persistent infection on acute respiratory infection with influenza A

Gareth Hardisty



Doctor of Philosophy

The University of Edinburgh

2015

Declaration

I declare that all work included in this thesis is my own, except where otherwise stated. No part of this work has been, or will be, submitted for any other degree or professional qualification.

Gareth Hardisty - 2015

The Roslin Institute & R(D)SVS,

The University of Edinburgh,

Easter Bush,

Midlothian,

EH25 9RG.

Acknowledgements

I would like to express my sincere gratitude to my supervisor Professor Bernadette Dutia, not only for the opportunity to undertake my PhD but also for her continuous encouragement at every stage. I have valued her guidance and I am ever thankful for everything I have learned under her supervision.

Many thanks also to my second supervisor, Professor John Hopkins for sharing his immunological knowledge and mentoring me with his 'belts, braces and self-supporting trousers' approach to research.

I would also like to thank Professor Tony Nash, for his invaluable advice and inspiration during lab meetings and Mr Ian Bennet for navigating me through the lab and sharing his technical skill during the early days of my research.

A huge debt of thanks is owed to the three post-docs of the Nash/Dutia group. Thank you to Dr Karen Bryson and Dr Yvonne Ligertwood for their endless wisdom and for allowing themselves to be roped into ever more complicated experiments that I would never have been able to achieve without them. My heartfelt appreciation also goes to Dr Marlynne Quigg-Nicol who has always been enthusiastic towards my project from start to finish and has kept me laughing throughout. I am extremely fortunate to have had the opportunity to work alongside such a friendly and committed group.

Thanks also to everyone in the Taylor lab, principally Dr Matt Taylor and Dr Johanna Knipper for allowing me to invade their lab space, exploit their parasitology knowledge and for enduring more than a few long days in a flow hood squashing lymph nodes. I am very grateful to you both. Similarly, many thanks to Dr Pip Beard for her kind and valuable direction with all of the histology work.

And last but not least, thank you to my family and loved ones for their love and support over my never-ending student years and many thanks to my friends, particularly those I have met along the way who have shaped the whole experience massively for the better.

Abstract

Humans are subject to infection with a wide range of commensal and pathogenic organisms. Each pathogen requires an appropriate immune response to eliminate or control the invading organism and minimise pathology. Many pathogens have evolved strategies to subvert or manipulate the immune response and establish on-going infections. Similarly acute respiratory infection with virulent strains of influenza A virus are often poorly controlled by the immune system and can cause severe immunopathology and even fatality as a result of an inappropriate and excessive inflammatory response called a 'cytokine storm'.

Morbidity due to influenza infection and exacerbation by the immune response can vary greatly between individuals. The effect of underlying infection on the immune system could contribute to the variation in response. The aim of this project was therefore to determine if co-infection with two pathogens that establish on-going infections could alter the immune response to influenza A and impact the outcome of infection.

Persistent infections with filarial helminths can cause debilitating disease and significantly impact the immune response toward a skewed T_H2 or regulatory phenotype in order to control pathology. In contrast, infection with gammaherpesviruses in an immunocompetent host causes an initial inflammatory 'anti-viral' response before becoming an asymptomatic, latent infection. In an immunocompromised host, gammaherpesviruses can reactivate and lead to clinical presentation of disease. This suggests that these viruses require an on-going immune response to control all stages of infection. Both filarial helminths and gammaherpesviruses are common infections in human populations and therefore mouse models of these infections provide relevant systems to study their potential role in influenza virus infections.

In a BALB/c murine co-infection model, latent infection with the rodent gammaherpesvirus MHV-68 led to significantly decreased weight loss and clinical signs following high dose infection with A/WSN/33, (a H1N1 influenza A virus). This was coupled with decreased immunopathology in the lung and fewer infiltrating lymphocytes in the alveolar spaces and around larger airways, although infectious virus titres were not significantly reduced. This response was coupled with a decreased production of inflammatory cytokines and chemokines in co-infected mice 6 days post infection which correlated with the amelioration of pathogenesis in these animals.

A repeat of the study in 129Sv/Ev IFN γ R knock out mice showed the same protective effect in the co-infected mice, suggesting IFN γ is not critical for the protective phenotype. Mice infected with latent MHV-68 alone showed a significant increase in expression of T cell chemokines in

the lung and alveolar macrophages had a significantly increased production of suppressor of cytokine signalling (SOCS-1) suggesting latent MHV-68 infection may impact the phenotype of macrophages in the lung, modulating the response to influenza co-infection.

A co-infection model with a persistent rodent filarial helminth, *Litomosoides sigmodontis* and A/WSN/33 was also established in BALB/c mice. The L4 developmental stage of *L. sigmodontis* infection had no impact on co-infection with A/WSN/33. Adult stage worms, however, appeared to have a protective effect against A/WSN/33 pathogenesis. Co-infected mice had significantly delayed weight loss and clinical signs 3-5 days post infection. CD4⁺ and CD8⁺ T cells in the lung draining lymph nodes had significantly reduced T_H1 and T_H2 phenotypes (measured by cytokine production) compared with singly infected controls. IFN γ secreting CD4⁺ T cells in the lungs of co-infected mice also secreted increased levels of IL-10, suggesting an increase in regulation of the inflammatory response to A/WSN/33.

At the full patent stage of *L. sigmodontis* infection, co-infection with A/WSN/33 led to increased clinical signs and significantly exacerbated weight loss. CD4⁺ and CD8⁺ T cells in the lung draining lymph nodes were inflammatory in *L. sigmodontis* infected mice alone as well as co-infected mice and there were no differences in the percentage of CD4⁺ T cells in the lung secreting IL-10 and IFN γ between co-infected and influenza infected mice. A loss in regulatory responses during the patent stage of *L. sigmodontis* infection may therefore contribute to the loss of protection against A/WSN/33 at this time point within the co-infection model.

Understanding the impact of an underlying infection on the immune system could provide immune mechanisms that could be exploited to increase vaccine efficacy against influenza and similarly help to provide better treatment for individuals infected with influenza A. These results may also help predict the outcome of influenza A infection in individuals already infected with highly immunogenic, on-going infections.

List of Abbreviations

° c	degrees Celsius
129 Sv/Ev	Mouse strain
A/WSN/33	Influenza A Wilson Smith 1933 H1N1
AAMΦ	Alternatively activated macrophage
Ab	Antibody
Af	Alexofluor
Ag	Antigen
AIDS	Acquired immunodeficiency syndrome
AJ	Mouse strain
AMΦ	Alveolar macrophage
ANOVA	Analysis of variance
APC	Antigen presenting cell
APC	Allophycocyanin
ARDS	Acute respiratory distress syndrome
B cell	B lymphocyte
B10D2	Mouse strain
B220	CD45R
B6 Sle123	Mouse strain
BAL/F	Broncho-alveolar lavage / fluid
BALB/c	Mouse strain
BCL	B cell lymphoma protein
BHK	Baby hamster kidney
BLC	B lymphocyte chemotactic
B-LCL	B lymphoblastoid cell line
BMDMΦ	Bone marrow derived macrophage
BSA	Bovine serum albumin
Bv	Brilliant violet
C57BL/6	Mouse strain
C5a	Complement anaphylatoxin 5a
CD#/L	Cluster of differentiation number/ligand
cDNA	Complimentary DNA
CFA	Circulating filarial antigen
CIITA	Class 2 transactivator

CO ₂	Carbon dioxide
CTLA-4	Cytotoxic T-lymphocyte-associated protein 4
D.P.I	Days post infection
DBA/2J	Mouse strain
DC	Dendritic cell
dH ₂ O	Deionised water
DMEM	Dulbecco's minimum essential medium
DNA	Deoxyribonuclease
EAE	Experimental autoimmune encephalomyelitis
EBV	Epstein barr virus
EDTA	Ethylenediaminetetraacetic acid
ELISA	Enzyme linked immunosorbant assay
EMEM	Eagles minimum essential medium
Eotaxin	Eosinophil chemotactic CCL11
ER	Endoplasmic reticulum
EtOH	Ethanol
FACS	Fluorescence activated cell sorting
FCS / FBS	Fetal calf serum / fetal bovine serum
FITC	Fluorescein isothiocyanate
Foxp3	Forkhead box protein 3
Gata-3	Trans-acting T-cell-specific transcription factor
G-CSF	Granulocyte colony stimulating factor
GLM	General linear model
GM-CSF	Granulocyte macrophage colony stimulating factor
GMEM	Glasgows minimum essential medium
H&E	Hemoxilin and eosin
H-2	Mouse histocompatibility complex
H ₂ SO ₄	Sulphuric acid
HA	Heamagglutinin
HBV	Hepatitis B virus
HCMV	Human cytomegalovirus
HHV-4	Human herpesvirus 4
HIV	Human immunodeficiency virus
HKx31	H3N2 influenza strain
HLA	Human leukocyte antigen

HSV-1	Herpes simplex virus 1
HVS	Herpesvirus simiae
I-309	CCL1
ICOS	Inducible T cell co-stimulator CD278
IFITM	Interferon-induced transmembrane protein
IFN	Interferon
Ig	Immunoglobulin
IL	Interleukin
iNOS	Inducible nitric oxide sythatase
IP-10	Interferon gamma induced protein 10 CXCL10
IRF	Interferon regulatory factor
ISG	Interferon stimulated gene
I-TAC	Interferon-inducible T-cell alpha chemoattractant CXCL11
JAK	Janus kinase
JE	CCL2
KC	CXCL1
KO	Knock out
KSHV	Kaposi sarcoma associated herpesviurs
L1/2/3/4	Larval stage 1/2/3/4
LCMV	Lymphocytic choriomeningitis
LD50	50% lethal dose
L-glut	L-glutamine
M1	Matrix protein 1
mAb	Monoclonal antibody
MARCO	Macrophage receptor with collagenous structure
MAV-1	Mouse adenovirus 1
MCMV	Mouse cytomegalovirus
MCP	
MCP-5	Monocyte chemotactic protein 5 CCL12
M-CSF	Macrophages colony stimulating factor
MDCK	Madin-Derby canine kidney cell
MHC	Major histocompatibility complex
MHV-68	Murine gammaherpesvirus 68
MHV-74	Murine gammaherpesvirus 74
MIG	Monokine induced by gamma interferon CXCL9

MIP-1 α /1 β /2	Macrophage inflammatory proteins CCL3/4/CXCL2
miR	microRNA
MNV	Murine norovirus
MuHV-4	Murine herpesvirus 4 (MHV-68)
Mx	Interferon-induced GTP-binding protein
M Φ	Macrophage
N	Number
NA	Neuraminidase
NaHCO ₃	Sodium bicarbonate
NBF	Neutral-buffered formalin
NEP	Nuclear export protein
NF κ B	nuclear factor kappa-light-chain-enhancer of activated B cells
NIAID	National institute of allergy and infectious diseases
NK	Natural killer cell
NKG2A	C-type lectin receptor CD94
NOD	Non-obese diabetic mouse strain
NOX2	NADPH oxidase 2
NP	Nucleoprotein
ORF	Open reading frame
OVA	Ovalbumin
P/S	Penicillin and streptomycin
PA	Polymerase acidic protein
PB1	Polybasic 1
PB2	Polybasic 2
PBS	Phosphate buffered saline
PCR	Polymerase chain reaction
PD-1	Programmed cell death 1
PE	Phycoerythrin
PFU	Plaque forming units
PI3K	Phosphatidylinositol-4,5-bisphosphate 3-kinase
PMA	Phorbol myristate acetate
PR8	Influenza A strain Puerto Rico 8 /1934 H1N1
PRR	Pathogen recognition receptor
Psi	Pounds per square inch
PTLD	Post-transplant lymphoproliferative disorder

qPCR	Quantitative polymerase chain reaction
qRT-PCR	Quantitative reverse transcription polymerase chain reaction
RAG	Recombination activating gene absent mouse strain
RANTES	Regulated on activation, normal T cell expressed and secreted CCL5
RBC	Red blood cell
RNA	Ribonuclease
RNP	Ribonucleoprotein
ROR- α	RAR-related orphan receptor alpha
ROS	Reactive oxygen species
RPMI	Roswell Park Memorial Institute medium
RSV	Respiratory syncytial virus
RT	Reverse transcription
SCID	Severe combined immunodeficient mouse strain
SDF-1	Stromal cell-derived factor 1 CXCL12
SEA	Soluble egg antigen
sICAM-1	Intercellular adhesion molecule 1 CD54
SOCS-1/3	Suppressor or cytokine signalling 1 /3
STAT	Signal Transducer and Activator of Transcription
T cell	T lymphocyte
TAP	Transporter associated with antigen presentation
TARC	Thymus and activation regulated chemokine CCL17
TB / mTB	Tuberculosis / mycobacterium tuberculosis
T-bet	T-box transcription factor TBX21
TCID50	50% tissue culture infective dose
TGF	Transforming growth factor
TH1/2/17/9	T helper cell
TIMP-1	Metallopeptidase inhibitor 1
TLR	Toll like receptor
TMB	3,3',5,5'-Tetramethylbenzidine
TNF	Tumour necrosis factor
TREM-1	Triggering receptor expressed on myeloid cells 1
WHO	World Health Organisation
WT	Wild type
x G	Gravitational constant
μ MT	B cell deficient mouse

Table of contents

Chapter 1 - Introduction.....	1
1.1 The human host	1
1.2 Modelling infection.....	1
1.3 Latent and persistent infections	2
1.4 Polarisation of the immune response by latent and persistent infection	2
1.5 Immune modulation by latent infection: herpesviruses.....	3
1.5.1 Introduction to herpesviruses	3
1.5.2 Lytic, latent and persistent infection of gammaherpesviruses	4
1.1.1 Innate immune responses to herpesviruses.....	5
1.1.2 Adaptive immune responses to herpesviruses.....	6
1.5.3 Herpesvirus and respiratory co-infections	9
1.5.4 Herpesvirus infection and autoimmunity.....	9
1.5.5 Herpesvirus infection and type 2 immunity	10
1.6 Immune modulation by persistent infection: filarial nematodes	10
1.6.1 Changes to host immunity by filarial helminth infections.....	10
1.6.2 Helminths and autoimmunity.....	12
1.6.3 Helminths and allergy	13
1.6.4 Effect of helminth infection on concurrent infection.....	13
1.6.5 Helminth-parasite co-infections	14
1.6.6 Helminth-bacterial co-infections.....	15
1.6.7 Helminth-fungi co-infections.....	15
1.6.8 Helminth-viral co-infections	16
– Helminth-influenza co-infection	18
1.7 Impact of co-infection on acute immunity - influenza A viruses	19
1.7.1 Structure and genome.....	19
1.7.2 Severity and disease in humans	20
1.7.3 Global pandemics of the last century.....	20
1.8 Immune responses to acute influenza A infection	21
1.8.1 Innate immunity	21

1.8.2 Adaptive immunity	23
1.9 Alteration to the lung by pre-existing infection	27
1.10 Imbalance in the immune response to influenza A	27
1.10.1 Hypercytokinemia	27
1.10.2 T _H 1 immunity during influenza infection – potential role of IFN γ	29
1.11 Co-infection with influenza A.....	31
1.11.1 Influenza A and bacterial superinfection.....	31
1.11.2 Pre-existing conditions and influenza A	32
Chapter 2 - Materials and Methods	35
2.1 Preparation of virus stocks	35
2.2 <i>Litomosoides sigmodontis</i> life cycle.....	36
2.3 <i>In vivo</i>	37
2.4 Dissection.....	38
2.5 Flow cytometry	39
2.6 ELISAs	42
2.7 RNA extraction	43
2.8 DNA extraction.....	43
2.9 cDNA production.....	44
2.10 ORF73 MHV-68 qPCR	44
2.11 Macrophage Q-PCRs	45
2.12 Mouse cytokine protein array.....	46
2.13 Histology	46
2.14 Statistics	47
Chapter 3 - Latent gammaherpesvirus and influenza A co-infection	49
3.1 Introduction	49
3.2 MHV-68 - Murid Herpesvirus 4 (MuHV 4).....	49
3.2.1 Pathogenesis	49
3.2.2 Co-localisation of infections	50
3.2.3 Genome	50

3.2.4 MHV-68 as a model for EBV / KSHV	51
3.3 Hypothesis	51
3.4 Results.....	52
3.4.1 Co-infection with latent MHV-68 and 'low dose' A/WSN/33	52
3.4.2 Co-infection with latent MHV-68 and 5×10^2 A/WSN/33	62
3.4.3 Co-infection with latent MHV-68 and 5×10^3 A/WSN/33.....	78
3.4.4 Co-infection with latent MHV-68 and 5×10^3 A/WSN/33 in WT 129 Sv/Ev mice.....	94
3.4.5 Co-infection with latent MHV-68 and 5×10^3 A/WSN/33 in IFN γ R ^{-/-} 129Sv/Ev mice	101
3.4.6 Latent MHV-68 infection	112
3.5 Discussion	117
3.5.1 Co-infection with latent MHV-68 and 'low dose' influenza A/WSN/33	117
3.5.2 Co-infection with latent MHV-68 and 5×10^2 influenza A/WSN/33.....	118
3.5.3 Co-infection with latent MHV-68 and 5×10^3 influenza A/WSN/33.....	120
3.5.4 Co-infection with latent MHV-68 and 5×10^3 influenza A/WSN/33 in wild type 129 Sv/Ev mice	123
3.5.5 Co-infection with latent MHV-68 and 5×10^3 influenza A/WSN/33 in IFN γ R ^{-/-} 129 Sv/Ev mice.....	125
3.5.6 Latent MHV-68 infection	126
 Chapter 4 - Persistent <i>Litomosoides sigmodontis</i> and influenza A co-infection	 129
4.1 Introduction	129
4.1.1 Strain and sex specificity	131
4.2 Co-infection model	131
A. L4 (immature) <i>Litomosoides sigmodontis</i> + A/WSN/33 co-infection.....	132
B. Adult (pre-patent) <i>Litomosoides sigmodontis</i> + A/WSN/33 co-infection.....	132
C. Adult (patent stage \pm microfilaria) <i>Litomosoides sigmodontis</i> + A/WSN/33 co-infection.....	132
4.3 Hypothesis	133
4.4 Results.....	133
4.4.1 Pathology associated with <i>Litomosoides sigmodontis</i> infection at each developmental stage	133
4.4.2 Co-infection with immature (L4) <i>Litomosoides sigmodontis</i> and 5×10^3 A/WSN/33.....	136

4.4.3 Co-infection with pre-patent (adult) <i>Litomosoides sigmodontis</i> and 5×10^3 A/WSN/33.....	147
4.4.4 Co-infection with patent (adult \pm mf) <i>Litomosoides sigmodontis</i> on co-infection with 5×10^3 A/WSN/33.....	165
4.5 Discussion	182
4.5.1 Co-infection with immature (L4) <i>Litomosoides sigmodontis</i> had no significant impact on A/WSN/33 pathogenesis	182
4.5.2 Co-infection with pre-patent (adult) <i>Litomosoides sigmodontis</i> delays the pathogenesis of A/WSN/33 infection	183
4.5.3 Co-infection with patent (adult \pm mf) <i>Litomosoides sigmodontis</i> exacerbates the pathogenesis of A/WSN/33 infection	187
 Chapter 5 - Discussion	 190
5.1 Hypotheses	190
5.2 Context.....	190
5.3 Interaction between divergent immune responses.....	191
5.3.1 Competing responses	191
5.3.2 Regulatory responses	193
5.3.3 Synergistic responses	193
5.4 Mouse strain	194
5.5 Antigen specificity.....	195
5.6 The role of IFN γ	195
5.7 Future directions.....	196
5.7.1 Lung homeostasis and early innate responses	196
5.7.2 Secondary infection and memory responses	198
5.7.3 Impact.....	199
 Chapter 6 - Appendix	 200
 Chapter 7 - References.....	 204

Table of figures and tables

Figures

Figure 1.1 Co-infection with helminths	14
Figure 3.1 Schematic representation of latent MHV-68 infection prior to co-infection	49
Figure 3.2 Murine model of gammaherpesvirus and influenza A co-infection	50
Figure 3.3 Co-infection has no effect on low dose A/WSN/33 pathogenesis	52
Figure 3.4 Low dose A/WSN/33 pathology is not affected by pre-existing MHV-68 infection	54
Figure 3.5 Low dose A/WSN/33 pathology score is not affected by pre-existing MHV-68 infection	56
Figure 3.6 A/WSN/33 infection significantly increases IL-1 β and MIP2 at 4 days post infection and IFN γ and IL-10 6 days post infection	58
Figure 3.7 Latent MHV-68 is not altered by low dose A/WSN/33 infection	60
Figure 3.8 Pre-existing latent MHV-68 infection reduces susceptibility to 5x10 ² A/WSN/33 infection	63
Figure 3.9 MHV-68 latent infection reduces the extent of 5x10 ² A/WSN/33 pathology in the lung	65
Figure 3.10 A/WSN/33 pathology score is reduced by latent MHV-68 infection	67
Figure 3.11 5x10 ² A/WSN/33 infection increases IL-10 and IFN γ in the lung 7 days post infection	69
Figure 3.12 MHV-68 viral load is unaltered by 5x10 ² A/WSN/33 infection in the spleen but significantly reduced in the lung	71
Figure 3.13 TH1 CD4+ T cell phenotype in lung draining lymph nodes is the same in A/WSN/33 and co-infected mice	73
Figure 3.14 CD8+ cells in the lungs of co-infected mice produce increased levels of inflammatory cytokines 7 days after 5x10 ² A/WSN/33 infection	75
Figure 3.15 MHV-68 latency significantly reduces susceptibility to high dose 5x10 ³ A/WSN/33	77
Figure 3.16 Co-infection with latent MHV-68 does not significantly reduce pathology of 5x10 ³ A/WSN/33 infection	80

Figure 3.17 The cytokine environment following 5x10 ³ A/WSN/33 is significantly ameliorated by pre-existing latent MHV-68 infection	82
Figure 3.18 Infection with 5x10 ³ A/WSN/33 reduces the MHV-68 viral load in the lung	88
Figure 3.19 TH1 CD4+ T cell phenotype in lung draining lymph nodes is the same in 5x10 ³ A/WSN/33 and co-infected mice	89
Figure 3.20 CD8+ cells in the lungs of co-infected mice produce significantly increased levels of inflammatory cytokines 7 days after 5x10 ³ A/WSN/33 infection	91
Figure 3.21 Effect of MHV-68 latency co-infection on pathogenesis of 5x10 ³ A/WSN/33 (129Sv/Ev)	93
Figure 3.22 Co-infection with latent MHV-68 does not alter pathology caused by A/WSN/33 infection in 129Sv/Ev mice	96
Figure 3.23 Co-infection has no significant impact on cytokine environment in WT 129Sv/Ev mice	98
Figure 3.24 A/WSN/33 infection does not alter MHV-68 viral load in 129Sv/Ev mice	100
Figure 3.25 Effect of latent MHV-68 co-infection on pathogenesis of A/WSN/33 in an IFN γ R ^{-/-} model	102
Figure 3.26 Latent MHV-68 infection causes severe pathology in the lung but is not exacerbated by co-infection with A/WSN/33	104
Figure 3.27 Inflammatory environment is not altered in IFN γ R ^{-/-} S129Sv/Ev mice	109
Figure 3.28 A/WSN/33 infection in IFN γ R ^{-/-} 129Sv/Ev mice reduces MHV-68 in the lung	109
Figure 3.29 Lung cytokine environment and CD4+ cells in the draining lymph node are not altered by latent MHV-68 infection	111
Figure 3.30 Latent MHV-68 infection increases SOCS-1 expression in lung macrophages	115
Figure 4.1 Lung pathology caused by <i>Litomosoides sigmodontis</i> infection	132
Figure 4.2 – Co-infection with immature (L4) <i>Litomosoides sigmodontis</i> has no effect on A/WSN/33 pathogenesis	135
Figure 4.3 Co-infection with immature (L4) <i>Litomosoides sigmodontis</i> does not alter pathology caused by A/WSN/33	138

Figure 4.4 IL-10 level is increased in mice co-infected with immature (L4) <i>Litomosoides sigmodontis</i> and A/WSN/33	140
Figure 4.5 Co-infection with immature (L4) <i>Litomosoides sigmodontis</i> has a subtle impact on T cell responses in the lung and thoracic draining lymph nodes	142
Figure 4.6 Co-infection with pre-patent (Adult) <i>Litomosoides sigmodontis</i> has a protective effect against A/WSN/33 pathogenesis	146
Figure 4.7 Co-infection with pre-patent (Adult) <i>Litomosoides sigmodontis</i> does not alter pathology caused by A/WSN/33.	148
Figure 4.8 Cytokine environment is not significantly altered in mice co-infected with pre-patent (Adult) <i>Litomosoides sigmodontis</i> and A/WSN/33	152
Figure 4.9 Pre-patent (Adult) <i>Litomosoides sigmodontis</i> co-infection alters the CD8+ T cell profile in the lung draining lymph nodes following A/WSN/33 infection.	153
Figure 4.10 Pre-patent (Adult) <i>Litomosoides sigmodontis</i> co-infection leads to an increased inflammatory CD8+ T cell population in the lung following A/WSN/33 infection.	155
Figure 4.11 Pre-patent (Adult) <i>Litomosoides sigmodontis</i> co-infection alters the CD4+ T cell profile in the lung draining lymph nodes following A/WSN/33 infection	156
Figure 4.12 Co-infection with A/WSN/33 reduces the number of CD4+ T cells in the lung during pre-patent (Adult) <i>Litomosoides sigmodontis</i> infection	159
Figure 4.13 Co-infection with patent (Adult \pm Mf) <i>Litomosoides sigmodontis</i> has a deleterious effect on A/WSN/33 pathogenesis	164
Figure 4.14 Effect of patent <i>Litomosoides sigmodontis</i> co-infection on pathology caused by A/WSN/33.	166
Figure 4.15 Cytokine environment is not significantly altered in mice co-infected with patent (adult \pm mf) <i>Litomosoides sigmodontis</i> and A/WSN/33	168
Figure 4.16 CD8+ T cells in the lymph node are producing IFN γ in all infected groups and therefore co-infection has no significant impact.	170
Figure 4.17 Patent (adult \pm mf) <i>Litomosoides sigmodontis</i> co-infection leads to an increased inflammatory CD8+ T cell population in the lung following A/WSN/33 infection	171
Figure 4.18 Patent (Adult \pm Mf) <i>Litomosoides sigmodontis</i> co-infection alters the CD4+ T cell profile in the	173

lung draining lymph nodes following A/WSN/33 infection.

Figure 4.19 Patent (Adult \pm Mf) infection with *Litomosoides sigmodontis* results in a mixed TH1/TH2 phenotype in the lung but does not alter cytokine production by CD4+ during A/WSN/33 co-infection 176

Tables

Table 1.1 Biological properties of herpesviruses	3
Table 1.2 Influenza pandemics of the last century	21
Table 1.3 Cytokines and chemokines involved in hypercytokinemia	28
Table 2.1 Intracellular flow cytometry staining	40
Table 2.2 Antibody isotypes and clones	40
Table 2.3 ELISA reagents and dilutions	42
Table 2.4 Q-PCR template	44
Table 2.5 Primer sequences for macrophage Q-PCRs	44
Table 2.6 Optimal primer concentrations and reaction conditions for macrophage Q-PCRs	45
Table 4.1 <i>Litomosoides sigmodontis</i> L4 worm burden	145
Table 4.2 <i>Litomosoides sigmodontis</i> adult worm burden	162

Chapter 1 - Introduction

1.1 The human host

Humans are subject to continual infection by commensal and pathogenic organisms. The site of these infections is often the epithelial barriers, including the lung and intestine (Murphy 2011). The human immune response is therefore persistently activated in response to multiple harmful and innocuous antigens and must mount targeted and appropriate responses in order to maintain homeostasis with commensals, eliminate harmful pathogens and dampen excessive responses to harmless allergens. While the immune response has evolved the capability to elicit highly specific, polarised responses to a range of infectious agents, many pathogens utilise evasive mechanisms in order to establish long-term and persistent infections with deleterious effects on the host. Evidence of this can be seen in cancer associated herpesvirus infections or persistent, debilitating nematode infections and their associated pathologies.

1.2 Modelling infection

Animal models of infection are often employed by researchers in order to better understand such host-pathogen relationships. This is of particular importance to identify dysfunction in the host immune system that could be targeted or improved with therapeutics to enhance resistance to acute and persistent pathogens. In recent years models of infection usually utilise in-bred, pathogen free, laboratory strain animals in order to encourage consistency within responses. Mathematical modelling is also commonplace and applies similar principles to depict direct interactions between individual proteins / cells or pathogens in a defined host.

In reality, genetics, environmental factors, pre-existing conditions, malignancies and lifestyle choices all contribute to the outcome of human infection. This explains the variation in response between individuals infected with the same pathogen. Therefore models of infection using outbred animals (Masuzawa, Beppu et al. 1992) and models that incorporate a second pathogene, confounding factor or pre-disposition are re-emerging and becoming more common (Zaccone, Raine et al. 2004; Pawlowski, Jansson et al. 2012; Castro Sanchez, Aerts et al. 2013) in order to delineate these interactions.

1.3 Latent and persistent infections

On-going immune responses required to control one infection have been shown to limit, counteract or in some cases heighten the immune response to a second, unrelated pathogen. Co-infecting pathogens can directly interact or indirectly alter clinical presentation or transmission and kinetics of other infections. This can complicate treatment and hinder vaccination strategies (Griffiths, Pedersen et al. 2011). In many communities chronic, latent and persistent infections occur at a very young age and are then maintained throughout the life of the host, obfuscating responses to new infections (Enders, Biber et al. 1990; Petney and Andrews 1998). Understanding the impact of on-going infection on the host is therefore important to understand the potential effect on the response to co-infection. Studies of this type, which observe the interaction between multiple pathogens and the immune response are rare.

1.4 Polarisation of the immune response by latent and persistent infection

The immune response has evolved the capability to produce polarised, pathogen type specific responses to infection. Lytic viruses, large parasitic multicellular organisms, opportunistic bacterial infections, fungi, pollutants and allergens all trigger distinct responses that aim to clear pathogens with minimal immunopathology and collateral damage to host tissues. The response for example, to clear a lytic viral infection is different to the response required to clear a helminth infection. A host already responding to a persistent helminth infection may respond differently to infection with a virus compared with an uninfected individual.

At the site of infection, recognition of pathogen associated molecular patterns (PAMPs) by antigen presenting cells, or mechanical damage to barrier tissues caused by infection releases damage associated molecular patterns (DAMPs) and induces the production of cytokines, chemokines and immunomodulatory molecules (Kourilsky and Truffa-Bachi 2001). This systematically activates appropriate adaptive immune responses, such as T_H0 differentiation (to T_H1 / T_H2 / T_H17 etc) or class switched antibody production by B cells and ultimately neutralises the infection (Zhu and Paul 2008; Walsh and Mills 2013). Innate immune cells resident at the site of infection continue to propagate responses, and recruit other immune cells as necessary resulting in changes to the homeostatic balance at the site of infection to a phenotype that is suitably anti-viral / anti-helminthic etc. depending on the causative agent (Walsh and Mills 2013).

During an acute infection this is rapidly followed by resolution and return to homeostasis. In chronic, latent or persistent infection, the pathogen is not cleared and an on-going immune response is required to control the pathogen. The host immune system is therefore skewed

towards a particular phenotype at the site of infection. This can impact responses to heterologous pathogen.

This project aims to identify how such changes caused by ongoing infection can impact the response to an unrelated acute, inflammatory viral infection with influenza A. As the immune response can be skewed towards significantly different phenotypes depending on the pathogen, two models of on-going infection will be considered; latent infection with an inflammatory gammaherpesvirus and persistent infection with an immunosuppressive lymphatic filarial nematode.

1.5 Immune modulation by latent infection: herpesviruses

1.5.1 Introduction to herpesviruses

Herpesviruses are a highly disseminated order of double stranded DNA viruses identified in most vertebrates and some bi-valve molluscs. The family may be subdivided into 3 sub-families alpha α , beta β , and gamma γ , containing 17 genera and 90 species (Davison 2010). Each species is usually found to naturally infect a single host species and is therefore thought to have co-evolved during speciation of the host (McGeoch, Rixon et al. 2006). Herpesviruses are defined by four biological properties, represented in table 1.1 below.

Table 1.1 Biological properties of herpesviruses

1. They specify a large array of enzymes involved in nucleic acid metabolism (e.g., thymidine kinase, thymidylate synthetase, dUTPase, ribonucleotide reductase), DNA synthesis (e.g., DNA polymerase, helicase, primase), and processing of proteins (e.g., protein kinases), although the exact array of enzymes may vary from one herpesvirus to another.
2. Virus gene transcription, synthesis of viral DNA, and nucleocapsid assembly occur in the nucleus. Most virions acquire at least part of their tegument and are enveloped in the cytoplasm.
3. Production of infectious progeny virus (lytic infection) is generally accompanied by the destruction of the infected cell.
4. The herpesviruses examined to date employ cellular latency as a mechanism for lifelong persistence in their hosts.

Taken from (Pellet 2001).

– Gammaherpesviruses

The gammaherpesviruses are found extensively within mammalian populations. These viruses have high affinity for a single host and are restricted to transmission within the host family or order (Pellet 2001). The gammaherpesvirus sub-family may be further subdivided into two main genera, the *Lymphocryptoviridae* including Epstein Barr virus (HHV-4) which are exclusive to primates and humans and *Rhadinoviridae*, containing Kaposi-sarcoma associated virus (KSHV or HHV-8). MHV-68 (MuHV-4) is a murine model of gammaherpesvirus infection.

1.5.2 Lytic, latent and persistent infection of gammaherpesviruses

Gammaherpesviruses initially cause a lytic acute infection in the upper respiratory tract. The virus then enters a latent state, predominantly in B and T lymphocytes and macrophages where viral replication is halted. Latency differs from chronic or persistent infection as progeny virus is not produced. Latency is distinguished from abortive infection by the ability of the virus to reactivate and produce infectious progeny virus.(Pellet 2001)

EBV is relatively ubiquitous throughout human populations, predominantly infecting B lymphocytes but may also be found in T lymphocytes and natural killer (NK) cells as well as epithelial cells (Borza and Hutt-Fletcher 2002; Isobe, Sugimoto et al. 2004; Martin 2007). KSHV also has the ability to establish latent infection in B lymphocytes; cells that are maintained for the life of the host. KSHV is less widespread and prevalence varies between populations. These viruses often lie dormant, to evade detection by the host however reactivation events are required intermittently in order to produce progeny virus, spread from cell to cell and transmit from host to host.

Gammaherpesviruses have also been shown to maintain persistent infections in the lung epithelium (Egan, Stewart et al. 1995; Stewart, Usherwood et al. 1998). As a result they can produce lytic, latent and persistent infections at any point during on-going infection. Sporadic reactivation applies an inflammatory selective pressure to the host immune system, which must continually mount appropriate responses to each stage of the gammaherpesvirus life cycle.

The requirement for continual control of these infections is evident in immunocompromised hosts. Gammaherpesviruses can cause lymphoproliferative disease and tumour formation if host immunity is impaired (Cesarman and Knowles 1999; Carbone, Gloghini et al. 2008). EBV is associated with a number of malignancies including Burkitt's lymphoma, Hodgkin's disease and Nasopharyngeal carcinoma (Fields, Knipe et al. 2007) and KSHV is commonly associated with Kaposi Sarcoma, a cancer commonly occurring in immunodeficient AIDS patients (Greene, Kuhne et al. 2007).

Latent herpesvirus infections therefore require continual immune responses to avoid disease. Murine gammaherpesvirus MHV-68 is present in the lung, at the site of influenza A infection. Understanding the immune response to latent herpesvirus infection could give insight into the potential interactions between concurrent infection with herpesvirus and influenza A.

1.1.1 Innate immune responses to herpesviruses

Viral infections are generally met with inflammatory ‘type 1’ immune responses during acute infection. Infections by herpesviruses in the lung continue to induce inflammation and interferon production in an attempt to limit replication after acute infection (Christensen, Cardin et al. 1999).

– Changes to cytokine environment in latent infection

IFN γ is a key surveillance cytokine during gammaherpesvirus latency. IFN γ is known to be disposable during the lytic stage of infection with murine MHV-68 (a model of human gammaherpesviruses), resulting in only marginally increased viral titres at day 12 and mildly delayed clearance from the lung around day 15 (Sarawar, Cardin et al. 1997). Early innate immune cells including NK cells and macrophages are key contributors to IFN γ production during acute infection. During latent infection, reactivation of gammaherpesviruses was more prevalent in those with reduced IFN γ levels. A single polymorphism in the IFN γ gene, resulting in reduced production of the cytokine has been identified as contributing to increased incidence of EBV associated post-transplant lymphoproliferative disorder (PTLD) in an immunocompromised mouse model (Dierksheide, Baiocchi et al. 2005) and in human renal transplant patients (VanBuskirk, Malik et al. 2001). Herpes simplex virus infection is also controlled by persistent IFN γ production in the trigeminal ganglia by virus specific CD8⁺ T cells (Shimeld, Whiteland et al. 1997; Decman, Kinchington et al. 2005). CD8⁺ T cells or IFN γ alone can block reactivation of HSV-1 *ex vivo* from latently infected neurons by decreasing expression of the viral ICP0 gene required for lytic replication (Liu, Khanna et al. 2000; Decman, Kinchington et al. 2005).

As the interferon system is a critical component of anti-viral immunity, disruption during gammaherpesvirus co-infection can interfere with subsequent viral infections. Nguyen *et al* 2008, showed that latent MHV-68 infection caused increased CCL2 and CCL5 chemokine levels in the lungs as a result of increased IFN γ expression. Expression of IFN β , IL-4 and CXCL1 was unaltered, as were chemokine levels in the spleen. When coinfection with mouse adenovirus type 1 (MAV-1), further increased CCL5 levels in the lung that lead to increased mononuclear infiltrates in the airways compared to MAV-1 infected mice. While lung MAV-1

titres remained unaltered by the co-infection, the levels of MAV-1 detectable in the spleen were reduced (Nguyen *et al* 2008).

Transcriptomic analysis of spleens from mice infected with MHV-68 also demonstrated increased inflammatory IFN γ and IL-18 receptor as well as type 1 interferon inducible gene expression and SOCS-3 (White, Suzanne Beard *et al.* 2012). These cytokines may therefore also have an important role in the lung during persistent infection.

The overall immune environment is fundamentally altered to an ‘anti-viral phenotype’ with increased production of IFN γ in response to latent herpesvirus infection, at both the site of persistent replication and during latency.

– Changes to antigen presenting cells in the lung

Latent gammaherpesvirus infection can modulate immune responses to secondary bacterial infections by modulating the function of antigen presenting cells. C57BL/6J mice latently infected with MHV-68 (for 4 and 12 weeks) were resistant to lethal doses of either gram positive *Listeria monocytogenes* or gram negative *Yersinia pestis* and showed decreased bacterial burdens in the spleen and lung respectively due to activation of bactericidal macrophages (Barton, White *et al.* 2007). Significant protection was also seen in mice infected with MCMV but not HSV, (perhaps due to restricted anatomical location) however protection by the latent herpesviruses was not universal. Mice challenged with West Nile virus succumb to infection with similarity to uninfected mice (Barton, White *et al.* 2007). Latent infection caused increased serum levels of pro-inflammatory cytokines TNF α and IFN γ . This was not observed following infection with an ORF73 stop mutant incapable of establishing latent infection and was therefore latency specific. CD8⁺ and CD4⁺ T cells were dispensable for protection when depleted before challenge with the bacterial pathogens suggesting a broadly acting innate cross-protection as a result of MHV-68 latency. However when present, CD4⁺ and CD8⁺ T cells along with bactericidal macrophages may all be elicited by bystander activation of inflammatory cytokines (Barton, White *et al.* 2007). Macrophages may therefore be a critical component during co-infection, as primary infection can significantly alter their phenotype prior to infection with a secondary pathogen.

1.1.2 Adaptive immune responses to herpesviruses

During asymptomatic HCMV infection (a betaherpesvirus with 60-100% prevalence within the human population) an average of 10% of all blood memory CD4⁺ and CD8⁺ T cells HCMV antigen specific (Sylwester, Mitchell *et al.* 2005). Similar proportions of CD8⁺ T cells of asymptomatic individuals, seropositive for EBV were EBV antigen specific (Tan, Gudgeon *et*

al. 1999). These cells rapidly reactivated to viral antigens and did not show functional exhaustion, as is the case with other long term infections such as HIV, HCV and LCMV (Kim and Ahmed 2010).

– Changes to CD8⁺ T cells

Despite efforts of the virus to avoid detection the continual presence of virus antigens leads to an increasing population of herpesvirus specific CD8⁺ cells. These cells can also have an unexpected impact on a second infection. In a cohort of 20 patients infected with hepatitis B virus (HBV), CD8⁺ T cells were analysed for activation (CD38 and HLA-DR) and proliferation markers (Ki-67/Bcl-2low). The hepatitis infected patients showed 25% of CD8⁺ T cells with elevated activation and proliferation markers. When tested for antigen specificity with MCMV, EBV and influenza MHC-pentamers, 12.5% of activated cells were HCMV specific and 30% EBV specific. There were no influenza specific CD8⁺ T cells identified. Cross reactivity may therefore be herpesvirus specific. The appearance and decrease of these herpesvirus specific cells mimicked the kinetics of the total activated CD8⁺ T cell population during the course of HBV infection (Sandalova, Laccabue et al. 2010). When repeated in patients with dengue fever, influenza or adenovirus infection, similar herpesvirus responsive cells were identified despite fewer overall CD8⁺ T cells as a result of these viral infections. The effect may be associated with IL-15 production which *in vitro* was capable of HCMV/EBV specific reactivation of CD8⁺ T cells. (Sandalova, Laccabue et al. 2010) Whilst it is plausible, due to the size of the herpesvirus genome and large number of antigens encoded by herpesviruses that these cells were activated by cross reactivity of antigens, it also remains possible that secondary infection is capable of reactivating herpesviruses by disruption of latent infection. Reactivation from latency would provide a source of antigen to stimulate EBV or HCMV specific T cells during heterologous infection that would not be available in the case of influenza infection. This would perhaps explain the source of herpes specific CD8⁺ T cells (White, Suzanne Beard et al. 2012) and contribute to the concept that incidence of antigen exposure increases proportions of herpesvirus specific lymphocytes with age (Torti and Oxenius 2012).

– Changes to CD4⁺ T cells

CD4⁺ T cells have multiple functions during herpesvirus latency. Fundamentally, CD4⁺ T cells are required during latent infection to maintain the function of CD8⁺ T cells. Presentation of CD40L to DCs encourages long term activation of CD8⁺ T cells (Ridge, Di Rosa et al. 1998). In I-A^{-/-} mice infected with MHV-68, inhibitory markers PD-1 and NKG2A are up regulated on CD8⁺ T cells, (Dias, Giannoni et al. 2010) however the cells retain cytolytic function and capacity to release IFN γ (Giannoni, Shea et al. 2008). This is unlike infection with the persistent

virus LCMV where CD4⁺ helper T cell depletion resulted in functional exhaustion of CD8⁺ T cells that also increased in expression of PD-1 (Freeman, Wherry et al. 2006), suggesting a difference in response due to the latent infection caused by MHV-68. In MHV-68 infection the CD4⁺ T cells maintain CD8⁺ T cell hierarchy, with depletion resulting in changes in responses to specific viral epitopes. The CD8⁺ T cell response to one epitope in particular, ORF8₆₀₄K^b became more dominant in CD4⁺ KO (MHC-II^{-/-}) infection (Freeman, Roberts et al. 2014).

CD4⁺ T cells have direct cytolytic function during both lytic and persistent gammaherpesvirus infection. Up to 80% killing coupled with IFN γ production was observed when CD4⁺ T cells specific for an EBV lytic antigen BHRF-1 were co-cultured with EBV-transformed B-lymphoblastoid cell lines (B-LCLs). This was also seen for EBNA-1 latency protein in blood samples from Burkitt's lymphoma sufferers where 0.5% of all peripheral blood CD4⁺ T cells were EBNA-1 specific. These cells were capable of recognising Burkitt's lymphoma cell lines, demonstrating a mechanism of adaptive immunity against the virus independent of MHC-I antigen presentation (Paludan, Bickham et al. 2002). Adoptive transfer of OVA specific CD4⁺ T cells prolonged survival of RAG mice (deficient in VDJ recombination gene / no mature T and B cells) infected with an OVA expressing MHV-68. This suggests a direct role for CD4⁺ T cells in viral regulation, independent of classical helper T cell and B cell class switching functions. Establishment of latency was impaired in these mice despite the absence of B and CD8⁺ T cell function (Sparks-Thissen, Braaten et al. 2004). Latently infected BALB/c mice had increased CD27, a marker for cytolytic function and CD107a/b, a marker for degranulation on virus specific CD4⁺ T cells in both the spleen and lung. These cells can kill viral antigen expressing cells *in vivo* (Stuller and Flano 2009).

These cells were IFN γ independent and represent a functionally different phenotype to the IFN γ secreting CD4⁺ population which did not require antigenic stimulation to release the pro-inflammatory cytokines. Total CD4⁺ T cells isolated from MHV-68 infected mice were capable of inhibiting reactivation from latency *in vitro* (Stuller, Cush et al. 2010) and had direct cytotoxicity against MHV-68 immortalised B cells preventing tumour formation (Liang, Crepeau et al. 2013). Removal of CD4⁺ T cells *in vivo* resulted in persistent replication of lytic virus, development of disease and increased numbers of latently infected splenocytes when coupled with depletion of IFN γ (Christensen and Doherty 1999) suggesting CD4⁺ derived IFN γ actively represses reactivation. CD4⁺ T cells have other non-cytolytic epigenetic functions through production of IFN γ , which is capable of directly repressing the ORF50 viral transcription factor required for lytic replication during MHV-68 infection (Goodwin, Canny et al. 2010).

CD4⁺ T cells have a role in modulation of adaptive immunity and polarisation of innate cells in the lung. Cytokine production during latent infection is a key component of the ability of gammaherpesviruses to modulate concurrent infection.

1.5.3 Herpesvirus and respiratory co-infections

Reports from human infections with herpesviruses that have led to hospitalisation show increased incidence of co-infection. Patients with suspected infectious mononucleosis showed a higher incidence (63.6%) of EBV and HCMV co-infection, along with respiratory infections (Wang, Yang et al. 2010). In a study of patients with non-typical bacteria induced pneumonia, the incidence of herpesvirus co-infection was higher than uninfected controls, particularly in the case of HCMV (Zhou, Lin et al. 2013). Interaction between two such infections can increase disease severity. These studies point to the lung as a potentially key site of co-infection with herpesviruses despite uncertainty about the presence of human gammaherpesviruses in the healthy lung.

1.5.4 Herpesvirus infection and autoimmunity

Changes in adaptive responses caused by herpesvirus infection can be protective against autoimmunity. Infection with acute MHV-68 increased the incidence of autoantibodies in lupus prone B6.sle123 mice whilst latent infection protected from development of autoimmunity by suppression of lymphocyte activation and vastly reduced production of autoantibodies. Infection with MHV-68 was also protective in mice that had already developed signs of disease, notably 4 weeks post infection when latency had established. Latent infection in 6-8 week old mice significantly decreased the activation (detected with CD69) of CD3⁺ CD4⁺/CD8⁺ T cells, follicular and marginal zone B220⁺ B cells, which was suggested to inhibit the lymphoid expansion caused by autoimmunity (Nguyen *et al* 2008). Herpesviruses are not universally protective against autoimmunity however. Latent infection of C57BL/6 with MHV-68 led to exacerbated EAE clinical signs due to CD4⁺ and virus-specific CD8⁺ infiltrations in the brain and spinal cord. Increased levels of pro-inflammatory IFN γ , TNF α cytokines and CXCL9 and CCL5 chemokines and decreased IL-17a were detected in the serum of infected mice along with a decreased anti-MOG (EAE inducing antigen) IgG1 vs IgG2a antibody ratio (Casiraghi, Shanina et al. 2012). Production of inflammatory mediators during latent infection with MHV-68 can therefore reduce IL-17a and IgG1 antibodies specific to EAE induction. In an IL-10^{-/-} model of inflammatory bowel disease, co-infection with MHV-68 exacerbated colonic disease scores, increased splenomegaly and showed reduced survival. MHV-68 titre was unaffected between IL-10^{-/-} and WT C57BL/6 control mice.

1.5.5 Herpesvirus infection and type 2 immunity

A number of studies discussed above have reported the effect of herpesvirus latency on inflammatory processes of subsequent infections, providing cross protection or exacerbating symptoms. Herpesvirus infections have also been shown to modulate type 2 immunity. EBV infection has been demonstrated to have an inverse correlation with asthma sensitisation during the early years of development, suggesting that herpesviruses play a role in suppressing allergic responses during development (Nilsson, Linde et al. 2005). Challenge of MHV-68 latently infected mice with *Heligmosomoides polygyrus* or *Schistosoma mansoni* eggs however leads to reactivation of the virus into lytic replication due to STAT6 activation and IL-4 production, (discussed in 1.6.8). In atopic patients and those prone to allergic responses, atypical presentation of herpesvirus infection and more frequent reactivation events have been observed. While herpesviruses may reduce inflammatory immune responses, latency is dependent on IFN γ and inflammatory cytokine signalling to control reactivation. A skew towards type 2 immunity can reactivate herpesvirus infection. Interaction between immune responses during co-infection may therefore be dependent on the type of pathogen involved and how systemically polarised the immune response is as a result.

1.6 Immune modulation by persistent infection: filarial nematodes

Helminths are large, multicellular organisms transmitted by direct contact, through contaminated water and food sources or through an insect vector. Helminth infection can result in debilitating disease and huge financial burdens for developing countries where such infections are endemic (Wynd 2007). Lymphatic filarial parasites are found within the lymph vessels and body cavities and can significantly alter or subdue the host immune response. As with latent herpesvirus infection they are highly prevalent in human populations, particularly in the tropics. Lymphatic filarial parasites *Wuchereria bancrofti*, *Brugia malayi* and *Brugia timori* cause repeat and persistent infections. Multi-parasitic infection is therefore common. The impact of these infections on unrelated pathogens requires better understanding.

1.6.1 Changes to host immunity by filarial helminth infections

Helminths are capable of producing long lived, persistent or repeat infections as a result of successful immune evasion strategies or manipulation of host immune mediated attack. Co-evolution of parasite and host immune response as well as the multicellular nature of these parasites means that helminths have driven diversification within the immune system and generated distinct immune mechanisms compared to that of microbial infections (Anthony,

Rutitzky et al. 2007). Immunity to many helminth infections is therefore governed by the type 2 cytokines IL-4, IL-5, IL-9, IL-10 and IL-13 and production of robust immunoglobulin E (IgE), eosinophil, basophil, alternatively activated macrophages (aaMΦ) and mast cell responses (MacDonald, Araujo et al. 2002). These responses combine to strengthen barrier defences, expel, inactivate and destroy large invading parasites, restrict growth and repair mechanical damage (Palm, Rosenstein et al. 2012). While herpesviruses influence host immunity by long term production of inflammatory cytokines, helminths polarise the immune system with suppressive and type 2 responses.

The centre point of type 2 responses during helminth infection is the IL-4 receptor and subsequent activation of CD4⁺ T_H2 cells. T cells are critical components in the immune response to filarial nematodes. Studies in nude mice lacking T cells (Suswillo, Owen et al. 1980) and SCID and RAG mice lacking both T and B cells (Nelson, Greiner et al. 1991; Babu, Shultz et al. 1999) have shown the requirement of T cell responses for elimination of *Brugia* helminths. The canonical helminth response is a T_H2 phenotype in T helper cells. Polarisation of the immune response in helminth infection to the T_H2 phenotype requires the production of IL-4. Therefore absence of IL-4, IL4R or STAT6 increases susceptibility to *Brugia* parasites. (Babu, Ganley et al. 2000; Spencer, Shultz et al. 2001) Filarial parasite infection can involve developmental stages during infection of the host. In *L. sigmodontis* infection, infection occurs with L3 stage larvae that progress to L4 and adult developmental stages in the host. Absence of IL-4 results in increased L4 parasite burden two weeks post infection with L3 larvae, with similarity to SCID mice. Additionally these mice were microfilaraemic by 10 weeks post infection. (Babu, Ganley et al. 2000)

The inflammatory cytokine IFNγ (usually considered the polar opposite of IL-4) has a role in susceptibility to filarial infection. IFNγ^{-/-} mice mount stronger IL-4 governed T_H2 responses and eliminate the infection at an earlier stage and so do not reach patent infection. (Babu, Ganley et al. 2000) IFNγ is produced by splenic lymphocytes in response to *L. sigmodontis* parasite antigens during the first 24 days post infection and from the point of patency at day 50 onwards in susceptible BALB/c mice (Taubert and Zahner 2001). In resistant C57BL/6 mice, high levels of IL-4, IL-5 and IFNγ are all increased between 10 and 30 days post infection compared to BALB/c mice. C57BL/6 had very low antibody titres whilst the high levels of IgG2a at day 10 in BALB/c suggests a T_H1 polarisation at early stage of infection (Babayán, Ungeheuer et al. 2003). A subdued T_H2 response at early stage of infection and in particular low levels of IL-5 (associated with larval growth (Babayán, Ungeheuer et al. 2003)) suggests susceptibility to filarial parasites is highly dependent on polarisation of the CD4⁺ T cell environment. The combination of T_H1 and T_H2 is central to protective immunity in filarial infection.

– Heterologous immunity with helminths

A number of studies have begun to demonstrate heterologous immunity afforded by helminth infection on concurrent infections (reviewed in 2014)). The pathology of a single helminth infection in humans is difficult to study, as it is more often the case that poly-parasitic infections are present (Raso, Luginbuhl et al. 2004). This is further complicated by interactions of the immune system with the natural microbiome and virome of the host as well as differences in susceptibility to each parasite between individuals as a result of genetic and environmental factors (Quinnell 2003; Walk, Blum et al. 2010). The encompassing factor between the majority of helminth infections is the polarisation towards T_H2 and T_{REG} immunity. Therefore information from different co-infection models allows insight into the extent of heterologous immunity afforded by parasitic infection.

– Helminths and the hygiene hypothesis

The ability of helminth infections to imprint selective pressure on the host immune response is seen in the hygiene hypothesis. There is strong evidence for an inverse relationship between helminthic infection and immunological diseases in the developed world. Common infectious agents that have co-evolved with the immune system for millennia have been eliminated as a result of better healthcare, medical treatment and hygiene practices. The hygiene hypothesis or microbial deprivation hypothesis suggests that removal of these selective pressures on a developing immune system can result in reduced immune tolerance and increased allergic and autoimmune disorders (Bloomfield, Stanwell-Smith et al. 2006; Okada, Kuhn et al. 2010).

1.6.2 Helminths and autoimmunity

Interaction of immune responses between helminth infections and autoimmune disorders has been observed. In the absence of T_H2 immunity ($IL-4^{-/-}$), the intestinal helminth, *Heligmosomoides polygyrus* induced regulatory $CD4^+$ $Foxp3^+$ T cell IL-10 production which was capable of limiting diabetes progression in non-obese diabetic (NOD) mice (Mishra, Patel et al. 2013). In the same NOD mice, *Schistosoma mansoni* soluble egg antigen (SEA) induced up-regulation of IL-2, IL-10 and C-type lectins on dendritic cells which then encouraged production of protective, disease limiting $Foxp3^+$ T_{REGS} and other $TGF\beta$ producing $CD4^+$ T cells (Zaccone, Burton et al. 2009). Similarly in a Piroxicam induced inflammatory bowel disease model in $IL-10^{-/-}$ mice, *Heligmosomoides polygyrus* infection altered IL-13 production at mucosal sites and limited pro-inflammatory IL-12 in the lamina propria thereby suppressing colitis pathology (Elliott, Setiawan et al. 2004). Helminth therapy has already been trialled in humans with Crohn's disease by infection with *Trichuris suis* ova. 79% of patients treated

displayed reduced Crohn's disease activity indexes after 24 weeks of treatment (Summers, Elliott et al. 2005). In a cohort of multiple sclerosis (MS) patients, infection with intestinal worms resulted in increased eosinophilia, increased production of regulatory cytokines IL-10 and TGF β by PBMC and decreased secretion of inflammatory cytokines IFN γ and IL-12. This was coupled with alleviated MS symptoms (Correale and Farez 2007). Inflammatory dysregulation may also be connected to the hygiene hypothesis. This suggests psychiatric diseases, (Rook, Lowry et al. 2013) depression (Raison, Lowry et al. 2010) and cancer (Rook and Dalglish 2011) incidences in the western world may be higher due to the elimination of certain infections although a direct role for helminths in such diseases has yet to be fully explored.

1.6.3 Helminths and allergy

Infection of ovalbumin (OVA) sensitised BALB/c mice with the intestinal nematode *Heligmosomoides polygyrus* suppressed T_H2 immunity and pathogenesis of asthma when these mice were challenged with OVA antigen compared with uninfected mice. Reduced eosinophilia and increased production of IL-10 was exhibited in parasite infected/OVA sensitised mice challenged with OVA antigen after adoptive transfer of CD4⁺ T cells from *Heligmosomoides polygyrus* infected mice suggesting a role for T_{REGS} in the protective effect (Kitagaki, Businga et al. 2006). Similarly in human *Schistosoma haematobium* infection a role for IL-10 production was identified in association with protection from atopy (van den Biggelaar, van Ree et al. 2000).

1.6.4 Effect of helminth infection on concurrent infection

The National Institute of Allergy and Infectious Diseases (NIAID, 2014) in the USA has formed the international collaborative network for the study of human helminth co-infections to better understand interactions between endemic parasitic infection and their outcome on disease, treatment and vaccine strategy in areas where co-infection is common (NIAID, 2014). Helminth co-infections are thought to occur in 800 million people worldwide (Hotez, Molyneux et al. 2007). Infection of humans by parasitic worms has been a longstanding relationship, as evidenced in whipworm (*Trichuris trichiura*) infection in Neolithic archaeological remains (Dickson, Oeggel et al. 2000). Helminths have therefore been an enduring selective pressure on the human immune system. The ubiquitous nature of helminthic infection around the tropics and sub tropics means that co-infection is frequently a confounding factor during the immune response to other infections. The nutritional and developmental impact of multiple parasitic infections is only recently being considered as a premeditator in outcome of subsequent infection (Pullan and Brooker 2008). The highly T_H2 and regulatory responses often induced by

chronic helminth infection has the potential to alter outcome or pathogenesis of heterologous infection (Cox 2001). This is a key area of research in pro-inflammatory type 1 infections, particularly those that share regions of transmission with helminths, such as HIV, TB and Malaria. See Figure 1.1 below.

Figure 1.1 Co-infection with helminths



Figure 1.1 World map showing the geographic distribution of co-infection with helminths together with tuberculosis, malaria and/or HIV infection of adults. (Salgame, Yap et al. 2013)

1.6.5 Helminth-parasite co-infections

Antagonism between helminths and the intestinal protozoan *Giardia lamblia* in a Bolivian cohort of patients has been demonstrated with *Giardia* less likely in helminth infected individuals, however it increases on anti-helminthic treatment (Blackwell, Martin et al. 2013). Persistent *Schistosoma haematobium* infection in Senegalese children has been shown to protect from the incidence of *Plasmodium falciparum* infection (Lemaitre, Watier et al. 2014).

In filarial helminth infection, the stage of development is critical to the influence on co-infection. Malaria co-infection is aggravated and results in severe weight loss in BALB/c mice co-infected with pre-patent *L. sigmodontis*. This weight loss was associated with a significant increase in IFN γ production by splenocytes in amicrofilaremic mice at this time point (Graham, Lamb et al. 2005). If co-infection with malaria occurs during patent *L. sigmodontis* infection however malarial infection is alleviated. In a computational model of infection, co-infection resulted in decreased prevalence of lymphatic filarial worm burden and simultaneously led to extended disease as a result of malaria infection (Slater, Gambhir et al. 2013). *In vivo* co-

infection of BALB/c mice with *Plasmodium chabaudi* and *L. sigmodontis* led to greatly decreased *L. sigmodontis* worm burden and unaltered plasmodium parasitaemia. Co-infection with *Plasmodium yoelii* and *L. sigmodontis* resulted in decreases in both parasite burdens across the first 30 days of both infections (Karadjian, Berrebi et al. 2014). Species specific differences therefore have a large impact on disease and can determine the outcome of co-infection.

1.6.6 Helminth-bacterial co-infections

Helminth infections increase susceptibility to and enhance pathogenicity of bacterial infections. *Schistosoma haematobium* infection of the urogenital tract in BALB/c mice induces production of IL-4 which can impair invariant NKT cell function, leaving previously resistant mice susceptible to urinary tract infection by *Escherichia coli* (UPEC) strain UTI89 (Hsieh, Fu et al. 2014). Equally, 100% of BALB/c mice infected with *Taenia crassiceps* or *Heligmosomoides polygyrus* for 6 weeks succumb to *Streptococcus pneumoniae* rapidly after infection, an effect that can be reversed by anti-helminthic treatment (Apiwattanakul, Thomas et al. 2014). An *In vivo* model of *Heligmosomoides polygyrus* co-infection with *Bordetella bronchiseptica* results in exacerbated disease for both pathogens, increased faecal egg counts and higher, potentially lethal bacterial loads (Lass, Hudson et al. 2013). *H. polygyrus* infection greatly exacerbates experimental colitis with *Citrobacter rodentium*. Interestingly, this is a result of AAMΦs becoming more susceptible to infection with *C. rodentium*, increasing bacterial burden and production of TNFα (Weng, Huntley et al. 2007). This study actively demonstrates how helminth infection can impair macrophage responses to subsequent, unrelated pathogens although filarial infection appears to have limited impact on bacterial infection. Patent infection with *L. sigmodontis* does not alter *Mycobacteria tuberculosis* (MTB) infection. Despite instigating T_H2 and hypo-proliferative responses, co-infection does not alter spleen cell proliferation to MTB antigen PPD or resulting IFNγ production, despite proximity of the two infections in the lung (Hubner, Killoran et al. 2012). Co-infection with *Strongyloides stercoralis* during TB infection however reduces mycobacterial specific T_H1 and T_H17 specific responses and circulating cytokines in an IL-10 dependent manner (George, Anuradha et al. 2014) demonstrating that co-infection can directly impact CD4⁺ T cell responses.

1.6.7 Helminth-fungi co-infections

A relatively recent observation is the correlation between some helminth and fungal infections. T_H1 humoral responses are generally required for clearance of fungal infection and therefore T_H2 responses are associated with susceptibility (Blanco and Garcia 2008). *Schistosoma mansoni* infection induces a lasting T_H2 polarised immune response with increased production

of immunosuppressive IL-10 (Pearce and MacDonald 2002) that in a Sudanese cohort, (where *S. mansoni* infection is endemic) enables establishment of fungal infection with *Madurella mycetomatis* (van Hellemond, Vonk et al. 2013). Molecular identification of *Pichia guilliermondii* from the blood of 197 / 222 microfilaraemic, *Wuchereria bancrofti* infected individuals in an Indian (West Bengal) study identify fungi as common co-infections with filarial pathogens (Saini, Gayen et al. 2014). Other individual infections have also been reported in immunocompetent patients (Prakash, Gupta et al. 2011). These studies isolate opportunistic fungi and yeast infections as potentially pathogenic following helminth infection but contribution of helminths to the outcome of fungi is yet to be explored thoroughly in animal models.

1.6.8 Helminth-viral co-infections

Many viruses elicit type 1 pro-inflammatory immune responses. Helminths produce type 2 and regulatory responses that are capable of facilitating or decreasing susceptibility to different viral infections (Kamal and El Sayed Khalifa 2006). Suppression of immune responses can result in exacerbated co-infection.

Following a 12 day infection with *Trichinella spiralis*, C57BL/6 mice were challenged with norovirus MNV-CW3. Co-infected animals showed reduced numbers and functional capacity of MNV specific CD8⁺ T cells as well as decreased MNV specific CD4⁺ T cells and reduced production of IFN γ and TNF α , compared with singly infected controls (Osborne, Monticelli et al. 2014). This was the same for oral and systemic infections suggesting the effect of such a suppressive helminth immune response can impact beyond the site of infection.

Infection with *Heligmosomoides polygyrus*, an intestinal nematode prior to MNV infection led to reduced MNV specific CD8⁺ T cell responses, decreased production of IFN γ and TNF α with significantly increased MNV titres in the ileum. These observations were found to be independent of microbiota when repeated in germ free mice (Osborne, Monticelli et al. 2014). Impaired anti-viral immunity was associated with STAT-6 dependent activation of AAM Φ determined by arginase 1 and YM1/2 expression (Osborne, et al. 2014).

Initiation of such T_H2 type responses can also effect the long term suppression of latent viruses. Murine gammaherpesvirus-68 (MHV-68) is reactivated *in vivo* from latency during *Heligmosomoides polygyrus* co-infection or as a result of challenge with *Schistosoma mansoni* eggs (Reese, Wakeman et al. 2014). *In vitro* stimulation of the MHV-68 infected bone marrow derived macrophages (BMDM) with IL-4 (antagonistic of IFN γ) resulted in expression of STAT6, a transcription factor induced during alternative activation of macrophages. Further analysis revealed that STAT6 directly binds MHV-68 gene 50 promoter allowing reactivation

from latency (Reese, Wakeman et al. 2014) thus T_H2 polarisation directly altered the immune response to an inflammatory 'T_{H1} inducing' pathogen.

This ability for helminth infection to alter viral pathogenesis and viral burden can also be seen in Puumala Hantavirus infection. In a study of *Myodes glareolus* bank voles (the natural reservoir species of Puumala Hantavirus), co-infection with helminth species *Heligmosomum mixtum* was associated with greater viral load. However *Aonchotheca muris-sylvatici*, (a rodent whipworm) co-infection showed significantly decreased viral loads of Hantavirus and incidence of co-infection (Salvador, Guivier et al. 2011). Infection with different helminths does not therefore always have similar influences on concomitant viral infection.

Some co-infections may even be beneficial. In an Egyptian cohort of human patients with Hepatitis C infection, (HCV) detection of *Schistosoma mansoni* antibodies correlated with decreased incidence of mixed cryoglobulinaemia, suggesting a protective effect of co-infection (Abbas, Omar et al. 2009). Mixed cryoglobulinaemia secondary to HCV is associated with increased type 1 cytokines, IFN γ and TNF α and T cell recruiting chemokines MIP-1 α , MIP-1 β and CXCR-3, (Saadoun, Papadopoulos et al. 2005) while *Schistosoma mansoni* infection induces a largely T_H2 response (Kaplan, Whitfield et al. 1998).

Co-infection effects have also been demonstrated in HIV infection. Peripheral blood mononuclear cells (PBMC) taken from patients with filariasis (*Loa loa*, *Wuchereria bancrofti* or *Onchocerca volvulus*) depleted of CD8⁺ T cells demonstrated greater viral replication when infected with human immunodeficiency virus (HIV) *in vitro*. Cells from patients with filariasis produced increased IL-4 but decreased expression of RANTES (Gopinath, Ostrowski et al. 2000). In a human cohort of HIV infected individuals in Chennai India, 5 - 9.5% displayed co-infection with *Wuchereria bancrofti*. Co-infected individuals showed a trend for lower filarial antigenemia than HIV negative individuals however this was not statistically significant (p=0.07) (Talaat, Kumarasamy et al. 2008). Similarly in a Tanzanian cohort with a HIV incidence of 7.9% and *Wuchereria bancrofti*-specific circulating filarial antigen (CFA) incidence of 43.5%, positive association was found between CFA and HIV infections whereas hookworm and HIV incidences shared no correlation (Nielsen, Simonsen et al. 2006).

Increased HIV susceptibility following filarial infection may be a result of changes to surface proteins on CD4⁺ T cells. CTLA-4 counteracts anti-viral CD28 expression and therefore unrestricted CTLA-4 expression by depleted CD28 expression (mAb) results in susceptibility to HIV infection (Riley, Schlienger et al. 2000). CTLA-4 is up-regulated on CD4⁺ T cells in a human population on the Cook Islands with *Wuchereria bancrofti* filarial infection, particularly during the microfilaraemic the stage of infection. An increase in IL-5 and decrease in IFN γ production suggests that CTLA-4 can also bias the T_H1/T_H2 paradigm in filariasis (Steel and

Nutman 2003). In the case of filarial co-infection, the stage of larval development may therefore alter outcome to viral resistance.

– Helminth-influenza co-infection

The immunosuppressive influence of helminth immune responses can significantly alter the progression of inflammation and subsequent disease by inducing a skew toward type 2 immunity. Respiratory infection with influenza is predominantly inflammatory and results in vast infiltration of immune cells and occlusion of alveolar spaces. Co-infection is hypothesised to dampen excessive type 1 responses to influenza infection.

Early studies in pigs pre-patently and patently infected with *Metastrongylus* (lungworms) then co-infected with A/Swine/Iowa/15/30 (S-15) (H1N1) showed increased pathogenesis, increased lung size due to leukocyte infiltration as well as increased temperature and clinical signs at both stages of infection (Nayak, Kelley et al. 1964). Influenza / helminth co-infection was performed in laboratory mice in 1972 by Chowaniec *et al.* Female Ha/ICR strain mice were infected with the intestinal parasite *Nematospiroides dubius* (now renamed *Heligmosomoides polygyrus bakeri*) at increasing doses (50 – 1000 larvae). Mice were then co-infected with a sub-lethal dose of A/Japan/170/62 E₃M₂₂E₂. Co-infected animals had reduced viral titre when compared with uninfected controls. Results also indicated co-infected mice showed significantly lower antibody levels to influenza haemagglutinin 21 days post infection than singly infected mice (Chowaniec, Wescott et al. 1972). Reduced antibody titres may be a result of IL-21 deficiency during *Heligmosomoides polygyrus* infection, a crucial cytokine for B cell differentiation (Reynolds, Filbey et al. 2012).

Non-specific immune suppression is a characteristic of many helminth infections. Mice infected with the nematode *Trichanella spiralis* are also less susceptible to pathology during influenza A infection. Clinical signs and weight loss as a result of influenza infection were not altered in co-infected mice however recovery from infection occurred quicker as a result of greatly reduced numbers of infiltrating CD4⁺ and CD8⁺ cells, as well as reduced production of IFN γ and IL-10 (Furze, Hussell et al. 2006). Mechanisms of reduced inflammation and influenza modulation may vary between parasites. A reduction in T cells appears to be independent of IL-10 in this particular co-infection.

T. gondii, is an intracellular protozoan capable of promoting NK cell derived IFN γ that is attributed to statistically increased survival rates in mice co-infected with lethal dose A/Hong Kong/483/1997 H5N1 influenza. This is an innate response, critical during the early stages of influenza infection that may be replicated by injection with exogenous IFN γ every 24 hours for

four days post infection (O'Brien, Schultz-Cherry et al. 2011). The viral titre 5 days post infection was significantly decreased following IFN γ treatment, (O'Brien, Schultz-Cherry et al. 2011) however in this instance, susceptibility to influenza was reduced by pre-existing inflammation, demonstrating the complexity with which helminth infection can modulate influenza infection. *Taenia crassiceps* is an intestinal/lung tapeworm that induces T_H2 responses, and down regulates T_H1 CD4⁺ T cells in the vicinity of the parasite. 8 week infection with the tapeworm *T. crassiceps* however had no effect on survival of BALB/c mice infected with Influenza A/Puerto Rico/8/34 (H1N1) (Apiwattanakul, Thomas et al. 2014). The site of infection may therefore contribute to the modulatory effect of co-infections.

1.7 Impact of co-infection on acute immunity - influenza A viruses

Chronic, latent and persistent infection can impact how the host responds to a second, unrelated infection. Both latent herpesvirus infections and persistent helminth infections have been shown to mediate the efficacy of the host immune response to a second pathogen. Influenza A viruses pose a significant health risk to the global population and are governed by highly inflammatory type 1 immune responses characteristic of respiratory viral infection. As the two previously discussed pathogens have high prevalence in human populations, and are resident in close proximity to the site of influenza infection, this project aims to determine if the influence of such co-infections can change the outcome of influenza A by adjusting the inflammation initiated by viral infection in the lung.

1.7.1 Structure and genome

Influenza A viruses of the family *Orthomyxoviridae* are a family of single stranded, negative sense, segmented RNA genome viruses capable of causing severe and highly contagious respiratory disease in human and animal hosts. They are generally observed in a spherical virion of 80-120 nanometres in diameter, however filamentous forms have also been observed up to 300 nm in length. The influenza A and B genera contain 8 segments in their RNA genome. The viruses are identified according to their genus, the host in which they were discovered, isolation location, strain number, year of isolation and surface glycoproteins, (hemagglutinin (HA) and neuraminidase (NA)) e.g. Influenza A/*Cygnus cygnus*/Germany/R65/2006 H5N1 (Fields, Knipe et al. 2007). There are currently 11 neuraminidase and 18 hemagglutinin subtypes known. Wild aquatic birds are the natural host of most influenza A viruses.

New strains occur as a result of reassortment of segments from two different influenza A viruses that infect the same cell. Successful reassortment results in increased fitness and the potential to infect a new host potentially resulting in pandemic influenza A outbreaks when a previously

naïve population with little immunity becomes subject to infection (Hay, Gregory et al. 2001). Of current importance is the possibility that individual avian and human tropic viruses capable of infecting the same mammalian host cells will recombine and introduce a novel, highly virulent strain capable of infecting the human population (Treanor 2004).

1.7.2 Severity and disease in humans

Influenza A viruses are a significant cause of morbidity and mortality worldwide and therefore pose large financial and socio-economic strain on both developed and developing countries. Influenza A infection occurs as both severe pandemic incidences such as the H1N1 outbreak in 2009 estimated to have killed ~284,500 globally and more frequent seasonal strains that result in serious disease in the elderly and individuals predisposed to infection by other health issues.

Symptoms of influenza A infections usually occur 2 days after infection by aerosol transmission, direct contact with infected individuals or contaminated surfaces. The height of viral replication in the lung occurs a few days after this (WHO 2014). Influenza can cause a combination of symptoms including muscle aching, cough, high fever, headaches and malaise. In severe cases strong inflammatory responses associated with immunopathology in lung epithelium known as a 'cytokine storm' has been reported as a result of cytokine profile changes, desensitization of toll receptors and alterations to apoptotic mechanisms (Chan, Cheung et al. 2005; Morens, Taubenberger et al. 2008). This can be life threatening depending on virulence and host susceptibility.

1.7.3 Global pandemics of the last century

The most severe example of an influenza A pandemic recorded occurred during the 1918 H1N1 'Spanish Flu' outbreak, thought to have killed 50 million. Case-fatality rates were 2.5% compared to other pandemics around 0.1% (Johnson and Seifert 1998). The outbreak occurred in three 'waves' as a result of antigenic drift; mutations that increased the strain's virulence (Fields, Knipe et al. 2007). It has now been determined that many of those who succumbed to infection, actually died as a result of pneumonia caused by secondary bacterial infection (Morens, Taubenberger et al. 2008). Surprisingly influenza has a basic reproduction number of only 2-3, (Mills, Robins et al. 2004) much lower than many infectious diseases, suggesting that the incubation period before onset of symptoms and susceptibility to secondary infection are key factors in the rapid spread of the virus.

Table 1.2 Influenza pandemics of the last century

Year	Name	Subtype	Fatalities
1918	Spanish influenza	H1N1	~ 40 - 50 million
1957	Asian influenza	H2N2	~ 1 million
1968	Hong Kong	H3N2	~ 1 - 4 million
1977	Russian influenza	H1N1	
2009	Swine flu	H1N1	~ 284,500

1.8 Immune responses to acute influenza A infection

The majority of influenza infections occur due to seasonal strains that circulate in human populations each year. While this accounts for an average of 8,000 deaths in the UK per year, (England 6 October 2014) the majority of immunocompetent people mount sufficient, neutralising immune responses that confer protection from repeat infection. The immune response to influenza A is a type 1 response and therefore requires inflammatory cytokine signalling (Monteiro, Harvey et al. 1998). Pre-existing inflammation in the lung as a result of latent herpesvirus infection or increased production of type 2 cytokines and regulatory cytokines by persistent filarial nematode infection may therefore impact the response to influenza A.

1.8.1 Innate immunity

– Initiation of response

Initiation of the immune response to influenza occurs at the epithelial cell barrier in the lung. Pathogen recognition receptors, including NOD like receptors, Toll like receptors and dsRNA helicase enzymes, (RIG-I and MDA-5) identify pathogen associated molecular patterns (PAMPs) in virally infected cells. The signalling pathways activated by binding of these receptors leads to the production of type 1 (α/β) and 3 (λ) interferons and other pro-inflammatory cytokines. Activation of the interferon system via JAK/STAT signalling leads to the up regulation of a number of interferon stimulated genes (ISGs) which produce proteins with anti-viral capacity e.g. Mx proteins. These anti-viral proteins and receptors are crucial for appropriate inflammatory responses and reduce the capability of influenza to replicate. NLRP3

inflammasome is also activated by type 1 interferon and changes to ionic concentrations caused by influenza infection. Further production of inflammatory cytokines, IL-1 α/β and IL-18 and increased MHC-II expression in response to IFN γ production leads to antigen specific CD4⁺ T cell recruitment to the lung. Initiation of the response to influenza infection in the lung therefore requires systematic activation of inflammatory cytokine networks that could be impaired due to pre-existing infection with an infection that exacerbates or hinders type 1 anti-viral immunity.

- Antigen presenting cells

Innate immune cells including antigen presenting cells have a key role in activating adaptive immunity to influenza infection.

Lung immunity is largely dependent on alveolar and tissue resident, interstitial macrophages which express similar markers, (F4/80⁺, CD11c^{hi} and CD11b^{int}) but provide different mechanisms of protection (Wissinger, Goulding et al. 2009). Alveolar macrophages are less readily activated. They produce IL-10 and TGF- β regulatory cytokines and express MHC-II at low levels (Thepen, Kraal et al. 1994). These cells have a role in regulating proliferation of T cells, through production of prostaglandins, (Roth and Golub 1993) whilst allowing activation and effector function (Upham, Strickland et al. 1995). Interstitial macrophages are more capable of IL-1 β and IL-6 production, coupled with increased presentation of MHC-II, in line with maintenance of homeostatic environment in the lung (Steinmuller, Franke-Ullmann et al. 2000).

Macrophages are required at early time points during influenza infection to phagocytose infected cells and limit viral replication. Macrophage responses can be polarised to heighten or suppress other immune responses. They are also critical for maintaining homeostatic balance within the lung and epithelial-macrophage interactions that are required in the initial response to influenza infection. CD200 receptor, a negative regulator of macrophage activation is engaged by increased CD200 on influenza infected epithelial cells (Snelgrove, Goulding et al. 2008). An absence of CD200 leads to a lower threshold of activation for macrophages in influenza infected mice and therefore greater immunity to viral infection (Goulding, Godlee et al. 2011). The impact of pre-existing infection on such molecules could influence the susceptibility of individuals to influenza.

Polarisation of macrophages can result in the formation of distinct phenotypes. M1 macrophages are defined by production of inflammatory mediators, TNF- α , IL-1 β , IL-12 and iNOS in response to IFN γ , GM-CSF or LPS. M2 regulatory macrophages may be subdivided into a number of subsets but are ultimately identified by production of IL-10, IL-1Ra, arginase 1, FIZZ and YM1/2 in the presence of IL-4/IL-13 or IL-10. M1 macrophages are associated with inflammatory responses during influenza infection whilst M2 macrophages are required for

tissue repair in the lung (Nicol and Dutia 2014). Polarisation of macrophages as a result of cytokine production can alter MHC-II expression, phagocytic capacity and their ability to produce reactive oxygen species (that can contribute to lung pathology). Targeting polarisation of these cells has been identified as a novel strategy for mediating infection and inflammatory diseases (Labonte, Tosello-Tramont et al. 2014).

As macrophages present in the lung are a heterogeneous population, it is unclear which macrophages change or respond to infection and whether all macrophages return to their basal state once inflammation is resolved. Increasing evidence suggests that tissue resident macrophages active during infection in the lung may be long-lived (Davies, Jenkins et al. 2013). Therefore persistent infection and resulting inflammation in the lung may alter the phenotype of these cells and their responsiveness to secondary infection with influenza infection (discussed further in 1.11.1).

Dendritic cells (DCs) are professional antigen presenting cells that sample antigen in the lung. While antigens displayed by MHC-II are usually exogenous and MHC-I endogenous, DCs have the capacity to cross-present antigen from exogenous source onto MHC-I (Waithman and Mintern 2012). The type of dendritic cells present in influenza infection is unclear. One study suggests influenza infection in mice requires langerin DCs to clear infection and present antigen to CD4⁺ and CD8⁺ cells. Resident CD8⁺ DCs were also known to present antigen to CD8⁺ T cells. (GeurtsvanKessel, Willart et al. 2008) Other studies indicated that CD103⁺ DCs were required for CD8⁺ antigen presentation. (Kim and Braciale 2009; Ho, Prabhu et al. 2011) Depletion of alveolar CD11c⁺ DCs with diphtheria toxin impacted CD8⁺ T cell responses to influenza suggesting a role for this cell type. (Belz, Smith et al. 2004) It is therefore likely many dendritic cell subsets are responsible for influenza antigen presentation.

Polarisation of DCs (as seen in macrophages) is apparent during infection. IL-4R is integral in these cells in order to polarise T cell responses optimally through IFN γ production whilst RELM α is required for optimal IL-10 and IL-13 production (Cook, Jones et al. 2012). Polarisation of T cells is largely dependent on antigen. Influenza infection can produce a mixed phenotype of T_H1, T_H2 and T_H17 responses (Oh and Eichelberger 2000). The impact of pre-existing infection on polarisation of T cell responses to influenza is unknown.

1.8.2 Adaptive immunity

The adaptive immune response to influenza is complex and varies between sub-types and animal models tested. Production of cytotoxic lymphocytes and neutralising antibody is required to control viral replication and eliminate the infection as well as protect against re-infection.

– CD4⁺ T cells

Activation of CD4⁺ T cells during influenza infection is due to antigen presentation by professional APCs; dendritic cells via MHC-II. After activation, differentiated effector CD4⁺ T cells are then recruited to the lung where they peak at day 6 post infection. These CD44⁺/CD49d⁺ cells secrete high levels of IFN γ and IL-2 and decline with viral clearance (Roman, Miller et al. 2002). CD4⁺ T cells are polarised during infection. T helper cell profiles can be identified by cytokine production. Influenza A infection induces various levels of T_{H1}, T_{H2} and T_{H17} cells. These cells are maintained in a careful balance in most individuals and subsequently activate appropriate CD8⁺ cytotoxic responses and neutralising antibody production following class switching on B cells. In some instances excessive production of inappropriate cytokines results in immunopathology in the lung. Potential unbalance due to pre-existing infection may therefore alter outcome of infection and impact other cell populations in the process.

Depletion of CD4⁺ T cells in mice with antibodies does not alter the outcome of infection with influenza A H3N2 (HKx31). Viral replication was unaltered and cytolytic function of CD8⁺ T cells was unchanged. Cytokine production by precursor cytolytic cells were impaired in H-2IAb^{-/-} mice for months after infection suggesting an important role for CD4⁺ T cells in cytokine production and CD8⁺ T cell help (Tripp, Sarawar et al. 1995). Pro-inflammatory cytokine production (IFN α , TNF α , CXCL9, IL-6, and MCP-1) at early stages of infection is integral to the outcome of infection. At potentially lethal doses of influenza, (LD50, H1N1 PR8) cytokine disruption results in altered lung pathology at later time points (Vogel, Harris et al. 2014).

Antibody-mediated protection is vital in influenza immunity. Classically CD4⁺ T cells have a significant role in mediating antibody production. Through production of the cytokine IL-21 and T cell costimulatory ICOS CD4⁺ T cells facilitate affinity maturation and germinal centre formation (Bauquet et al. 2009). In μ MT^{-/-} (B cell deficient) mice, the absence of CD4⁺ T cells resulted in fatality from normally sub-lethal doses of influenza (Mozdzanowska, Furchner et al. 2005).

CD4⁺ T cells are now also known to have direct cytolytic function. Adoptively transferred cytolytic CD4⁺ T cells were capable of conferring protection in naïve mice challenged with influenza H1N1 A/PuertoRico8/34 (Brown, Lee et al. 2012). CD4⁺ T cells increased the levels of anti-influenza antibodies. CD4⁺ T cells were protective by direct cytotoxic function in B cell KO mice (Brown, Dilzer et al. 2006).

Cytolytic influenza-specific CD4⁺ T cells are perforin dependent. Perforin deficient CD4⁺ T cells are less capable of protecting naïve mice from influenza infection than WT CD4⁺ T cells

(Brown, Lee et al. 2012). During influenza infection perforin-mediated cytolytic CD4⁺ T cells express pro-inflammatory cytokines TNF- α and IL-2 in the draining lymph node and IFN γ and IL-10 in the lung at the site of infection, suggesting differing roles depending on location. Cytolytic CD4⁺ T cells are not however restricted to the T_H1 phenotype and remain functional during influenza responses in the absence of IFN γ (Graham, Dalton et al. 1993). Although adoptive transfer of primed T_H2 CD4⁺ T cell clones from BALB/c mice into naïve hosts offered no cytolytic activity against influenza challenge. (Graham, Braciale et al. 1994). Therefore correct polarisation of CD4⁺ toward inflammatory responses may be important for optimal resolution of infection. This is an important consideration during co-infection, as T cell responses may be altered by pre-existing infection and cytokine production.

– CD8⁺ T cells

CD8⁺ T cells are activated in the lymphoid tissues and in the lung during influenza infection. They are primed by CD8⁺ DCs in the lymph node and CD103⁺ migrating DC's in the lung (Belz, Smith et al. 2004). Activation of CD8⁺ T cells requires direct antigen presentation through MHC-I by professional antigen presenting cells. Absence of dendritic cells migrating to the lung significantly impairs CD8⁺ T cell responses (McGill, Van Rooijen et al. 2008). CD8⁺ T cells have targeted lytic function, against infected cells through production of granzyme A and B and perforin. Granzymes punch holes in the infected cell membranes and encourage production of inflammatory cytokines that improve antigen presentation by MHC molecules. Perforin enters the cell and induces apoptosis. CD8⁺ T cells have an intrinsic role in limiting the replication of the virus and it's progression into neighbouring cells (Metkar, Menea et al. 2008). Cytotoxic lymphocytes (CTLs) also directly induce apoptosis via Fas/FasL interactions and TRAIL activation by DR5 expression on infected epithelial cells (Brincks, Katewa et al. 2008). CD8⁺ T cells interact with dendritic cells following infection. These interactions are also required during clearance of infection. This is dependent on inflammatory cytokine signalling. Treatment of mice with sphingosine-1-phosphate receptor agonist abrogated the cytokine storm and reduced efficacy of CD8⁺ T cell responses following influenza infection (Matheu, Teijaro et al. 2013). Changes to cytokine production at early time points of infection can therefore alter effector function and kinetics of adaptive immunity to influenza. Polarisation of the lung environment by pre-existing infection may alter the kinetics of the influenza CD8⁺ T cell response.

– B cells and antibody production

Neutralising antibody is the ultimate goal to create lasting and antigen specific protection in viral infection. Antibodies are capable of binding influenza directly and thereby limits

replication of the virus (Cooper and Nemerow 1984). A single antibody was identified in 2012 that could bind to a conserved region of influenza haemagglutinin and therefore protected against H1,2,3,9 and 12 sub-types, (Ekiert, Kashyap et al. 2012) demonstrating the efficacy of appropriate antibody responses. A combination of IL-2 regulation by Foxp3⁺ T_{REGS} and T_{FH} germinal centre formation and production of polarising cytokines is critical to provide antibody responses during influenza infection (Leon, Bradley et al. 2014). At the site of influenza infection, the epithelial surface, initial antibody production is largely of the IgA isotype. Production of IgA increases rapidly upon influenza infection and can bind the virus intracellularly. These antibodies tend to be targeted at the surface glycoproteins HA and NA. Similarly IgM antibody production is a first line defence against influenza infection and encourages complement mediated inhibition of viral entry into the cell until high affinity antigen specific responses are initiated. IgG responses are the dominant antibody in the lung (Renegar, Small et al. 2004). IgG is required for opsonisation of viruses, increased phagocytosis by Fc receptor bearing cells and increased cytotoxicity by NK cells [158]. IgG sub-type is determined by the CD4⁺ T cell response. In regards to influenza infection, BALB/c mice produce IgG1 (T_{H2} stimulated) responses whilst resistant strains and mice that survive infection had increased levels of IgG2a (T_{H1} stimulated) antibodies (Huber, McKeon et al. 2006). Vaccination strategies against influenza aim to increase IgG2a production (human IgG subtypes are named differently). CD4⁺ T cell dependent activation of B cell class switching is therefore vital to form resistance to re-infection. Co-infection and changes to CD4⁺ T cells by ongoing inflammation would therefore impair production of appropriate neutralising antibodies to influenza infection.

– Memory responses

M1 and NP proteins are the immunodominant targets of CD4⁺ T cells (Chen, Zanker et al. 2014). Memory cells responding to these antigens, acquired during seasonal infections are broadly protective against other sub-types of highly pathogenic influenza (Lee, Ha do et al. 2008). Memory CD4⁺ T cells have an important role in secondary infection and are the source of inflammatory cytokines within 48 hours of secondary infection (McKinstry, Strutt et al. 2010). Memory CD4⁺ T cells can display great heterogeneity and vary in maintenance and quality of response to secondary infection (Richards, Chaves et al. 2011). Memory CD8⁺ cells are subsequently produced to provide more rapid responses upon secondary infection. Memory CD8⁺ T cells are often specific for highly conserved influenza proteins PA, NP and M1 and can offer cross protection between strains (Wang, Lamberth et al. 2007). It is known that treatment of influenza with the anti-viral drug Oseltamivir reduces the efficacy of the CD8⁺ effector population and subsequent protection to re-infection. Generation of appropriate CD4 and CD8

memory responses during primary infection is therefore critical to developing neutralising immunity against re-infection. If pre-existing infection alters the CD4⁺ T cell function and changes the cytokine environment, memory responses may be compromised.

1.9 Alteration to the lung by pre-existing infection

The lung, unlike the blood or spleen is not a sterile environment. The lung immune system must respond appropriately to pathogenic invasion whilst ignoring the constant influx of harmless antigens (Raz 2007). The lung requires the ability to continuously adjust and regulate its responsiveness to antigen and danger signals through interactions between antigen presenting cells and the epithelial barrier (Raz 2007). Inflammation due to infection in the lung decreases CD200, IL-10 and TGF- β production by epithelial cells, allowing alveolar macrophages to untether, become inflammatory (increased OX40L expression) and increase TLR sensitivity. Resolution of inflammation is associated with increased CD200 expression and stunted TLR expression, reducing responsiveness and promoting regulation in the lung environment (Wissinger, Goulding et al. 2009). The impact of latent herpesvirus infections and helminth infection on homeostasis in the lung could demonstrate their potential impact on co-infection with influenza A. There is a high incidence of chronic, latent and persistent infections in human populations meaning influenza will rarely infect an individual that is not already infected with an on-going infection and the effect of such infections in the lung will likely impact the immune response to influenza.

1.10 Imbalance in the immune response to influenza A

As described in the previous section, successful immunity to influenza requires the careful balance of cytokine environment and subsequent stimulation of the inflammatory and regulatory arms of the human immune system. In pandemic outbreaks of influenza infection, young individuals can succumb to infection as a result of self-propagating inflammation and cytokine production known as hypercytokinemia or ‘cytokine storm’.

1.10.1 Hypercytokinemia

At the early stages of influenza infection, the respiratory tract becomes highly inflamed, identified by the levels of pro-inflammatory cytokines. Levels of IL-1 β , TNF α , IL-6 and type 1 interferons are all increased in bronchoalveolar lavage fluid and in lung homogenates in murine models of influenza infection (Julkunen, Sareneva et al. 2001). These cytokines are released from non-immune cells due to activation of the inflammasome by PRRs and production of type

1 interferon due to infection. This begins the signalling cascade and initiates pro-inflammatory, anti-viral immunity. The extent of hypercytokinemia is predictive of the outcome of infection, particularly in human infection with highly pathogenic strains such as H5N1, where chemokine and cytokine levels (IP-10, MCP-1, IL-8, IL-6 and IL-10) in serum may directly correlate with viral load (de Jong, Simmons et al. 2006). An excessive and damaging pulmonary increase in pro-inflammatory cytokines and chemokines is directly correlated with severe pathology, intensified symptoms of infection and increased chance of fatality in pandemic strains of influenza infection. This is evident if NFκB (a transcription factor integral for synthesis of a number of pro-inflammatory cytokines) is deficient. Infection of mice with the p50 subunit of NFκB deleted leads to dramatically reduced pathology and lack of hypercytokinemia. Viral replication is unaltered. (Droebner, Reiling et al. 2008). Therefore co-infection may provide a selective pressure on the immune response to limit or exacerbate inflammatory signalling as a result of on-going infection.

Table 1.3 Cytokines and chemokines involved in hypercytokinemia

IL-1α/β	<ul style="list-style-type: none"> – Neutrophil accumulation / activation of CD4⁺ T cells – Production of anti-viral IgM – Activation of the inflammasome 	(Schmitz, Kurrer et al. 2005; Ichinohe, Lee et al. 2009)
TNFα	<ul style="list-style-type: none"> – Earliest cytokine produced in epithelial cells – Primes cells to produce greater levels of other pro-inflammatory cytokines – Limits viral replication <i>in vitro</i> 	(Van Campen 1994; Seo and Webster 2002; Veckman, Osterlund et al. 2006)
IL-6	<ul style="list-style-type: none"> – Correlated with patients in intensive care – Associated with fever in human infection – IL-6^{-/-} does not confer protection against A/Mexico/4108/2009 – Initiates neutrophil mediated clearance of virus 	(Kaiser, Fritz et al. 2001; Dienz, Rud et al. 2012; Paquette, Banner et al. 2012)
IL-8	<ul style="list-style-type: none"> – Chemotaxis of neutrophils – Rapid clearance of necrotic cells – Potent pyrogen in humans (absent in mice) 	(Hammond, Lapointe et al. 1995; Arndt, Wennemuth et al. 2002)
MCP-1	<ul style="list-style-type: none"> – Monocyte recruitment from the blood – TNFα and iNOS production by monocytes – MCP^{-/-} leads to decreased epithelial integrity and apoptosis 	(Deshmane, Kremlev et al. 2009; Pamer 2009)

Specific cytokines and chemokines, seen in table 1.3 are associated with the initiation of a cytokine storm. Collectively IL-1β and TNFα are initiators of immunopathology during

influenza infection. Mice lacking TNF-R1 TNF-R2 and IL-1R1 showed a significant delay in mortality when infected with H5N1 and further decreased cytokine production and cellular infiltration (Perrone, Szretter et al. 2010). IL-6 is associated in a natural human infection with onset of clinical symptoms, including fever. IL-6 expression in childhood infection with H1N1 is associated with a high IL-1 β response (Chiaretti, Pulitano et al. 2013). IL-8 (CXCL-8) and MCP-1 (Monocyte chemotactic protein 1, CCL2) are key to recruiting monocytes and lymphocytes to the site of infection and therefore require balanced production to stop excessive infiltration, (although IL-8 is absent in mice).

In high pathogenicity influenza virus infection, IRF3 has been identified as a key signalling pathway for cytokine and chemokine induction, ablation of which leads to significantly reduced levels of IFN β , IFN λ and MCP-1 while TNF α remains unaltered (Hui, Lee et al. 2009). Such responses require an intricate network of intracellular signalling and transcriptional regulation. Therefore disruption of these pathways by underlying infection or inflammation may directly impact the response to influenza infection.

1.10.2 T_H1 immunity during influenza infection – potential role of IFN γ

The contribution of IFN γ appears to be integral to a variety of stages during influenza immunity, although it may also be causative in the cytokine storm response observed in fatal influenza infection. The role of IFN γ in influenza A infection is complicated. In the absence of IFN γ , CD4⁺ T cells produce greater levels of IL-17a. While direct cytolytic capacity is unaltered, IFN γ ^{-/-} CD4⁺ T cells cannot promote recovery in the lung as efficiently as WT CD4⁺ T cells (Brown, Lee et al. 2012). Similarly targeted disruption of the IFN γ gene results in alterations to antibody production, increase in type 2 cytokines and production of IgG1 (Graham, Dalton et al. 1993). In rats, activation with IFN γ , led to increased MHC-II expression and TNF α production by alveolar macrophages which conferred protection from challenge with *Listeria monocytogenes* (Steinmuller, Franke-Ullmann et al. 2000). Following influenza infection, up regulation of IFN γ can result in decreased macrophage phagocytosis, which contributes to susceptibility from bacterial pathogens (Wang, Zhou et al. 2014). Similarly, infection impacts the ability of DC's to cross present all exogenous antigens and therefore attenuates presentation of all MHC-I antigens (Smed-Sorensen, Chalouni et al. 2012). Induction of type 1 IFN during influenza infection results in decreased production of CCL2, impaired recruitment of macrophages and subsequently promotes the establishment of streptococcus pneumoniae colonisation (Nakamura, Davis et al. 2011). IFN γ ^{-/-} mice infected with influenza are also less susceptible to pneumococcal infection 48 hours after infection than WT mice (Sun and Metzger 2008).

Latent gammaherpesvirus requires IFN γ production to maintain latent infection. Persistent filarial nematode infection induces an opposing type 2 immune response and requires IFN γ for regulation. IFN γ has been shown as a source of dysregulation during influenza infection and therefore IFN γ may be a key cytokine to determine the effect of co-infection.

– IFN γ induced cytokines and chemokines

IFN γ activates a prototypical inflammatory immune response. IFN γ is also important for a number of other immune responses. The impact on the immune response due to increased or decreased IFN γ will alter the levels of other cytokines and chemokines.

IP-10 (Interferon gamma inducible protein 10 / CXCL10) has a significant T cell chemotactic role during influenza infection. Acute respiratory distress syndrome (ARDS) as a result of pandemic 2009 H1N1 influenza infection is correlated with serum levels of IP-10. IP-10 is a hallmark of severe respiratory distress (Bermejo-Martin, Ortiz de Lejarazu et al. 2009). IP-10 deficient mice have weakened T cell responses when stimulated with antigen, poor trafficking to sites of infection and as a result, debilitated protection against virus infection (Dufour, Dziejman et al. 2002). CD8⁺ T cells have been shown to produce IP-10 in response to co-stimulation to promote generation of effector cell populations (Peperzak, Veraar et al. 2013). Monoclonal antibodies (mAb) to IP-10 are capable of decreasing severity of immunopathology in murine models of infection, (Wang, Yang et al. 2013) likely due to abrogated T cell responses and similarly decreased infiltration of neutrophils (Ichikawa, Kuba et al. 2013). IP-10 is induced by epithelial cells undergoing apoptosis, (Law, Lee et al. 2010) which in response to influenza infection may explain its expression in only the most severe human cases where hypercytokinemia is induced.

MIG-1 (Monokine induced by IFN γ / CXCL9) is often correlated with severity of hypercytokinemia and severity of clinical presentation (Lee 2009). It is a chemokine responsible for T cell recruitment in viral infections of the liver and central nervous system (Liu, Armstrong et al. 2001; Arai, Liu et al. 2002). During H1N1 PR/8 pandemic strain infection or H3N2 seasonal infection, alveolar macrophages produce high levels of CXCL9 (Wang, Nikrad et al. 2012). The particular contribution of MIG-1 in influenza infection is not fully elucidated; however serum levels in high pathogenicity infections (H5N1) are greatly increased, suggesting an influence on the cytokine storm (Peiris, Yu et al. 2004).

RANTES (regulated on activation, normal T cell expressed and secreted / CCL5) is expressed in nasal and bronchial epithelial cells within 24 hours of infection *in vitro*. Expression of RANTES is dependent on PI3K transcriptional activation of NF κ B and IRF-3 (Chiou, Chen et al. 2011). RANTES is required for T cell, dendritic cell and eosinophil recruitment to the lung and is

therefore up regulated between day 5 and 15 of influenza infection, however in a RANTES^{-/-} mouse leukocyte transport was not impaired, suggesting functional redundancy between chemokines (Wareing, Lyon et al. 2004).

1.11 Co-infection with influenza A

The aim of this project is to determine if pre-existing concomitant infection during the acute response to influenza can regulate or unbalance the immune response, in turn modulating the outcome of infection, providing new insight into therapeutic targets and considerations in regards to vaccination in the human population.

1.11.1 Influenza A and bacterial superinfection.

The majority of research into influenza co-infection has looked at secondary infection as a result of influenza. Fatalities of the 1918 H1N1 influenza pandemic were almost always as a result of bacterial superinfection. Evidence suggests many of the bacterial pathogens were opportunistic infections of common bacteria usually found in the respiratory tract (Morens, Taubenberger et al. 2008). Death in the 1918 pandemic usually occurred at around day 7-9 post infection. Similarly in 2009, up to 34% of cases were complicated by secondary bacterial pathogens (Chertow and Memoli 2013). In a cohort of 183 co-infected, hospitalised children, the most common bacterial pathogens were *Staphylococcus aureus* (39%), *Pseudomonas* species (16%), *S. pneumoniae* (8%), *Haemophilus influenzae* (7%), and *S pyogenes* (4%) (Randolph, Vaughn et al. 2011). Such infections tend to occur around day 2-3 post infection in humans when viral shedding is at a peak (Rice, Rubinson et al. 2012).

A number of animal models of viral / bacterial co-infection have helped establish the mechanisms behind co-infection. Influenza has a profound effect on epithelial integrity in the lung. Sialic acid cleavage as a result of viral entry and release, disrupted ciliary beat and epithelial cell death due to immune mediated cytotoxicity of infected cells contribute to hypoxic areas of necrosis and airway constriction; factors which promote increased bacterial growth (Horner and Gray 1973; McCullers 2006). Bacteria such as *S. pneumococcus* are more capable of adhesion in the already inflamed lung, with increased receptor availability as a result of damage to the epithelia (McCullers and Tuomanen 2001). Influenza A encodes a number of proteins capable of evading the immune system. Bacterial infection of the lungs following viral infection is therefore facilitated by an impaired immune response. Anti-viral interferon α signalling decreases the number of $\gamma\delta$ T cells in the lung, key producers of anti-bacterial IL-17a. Absence of IFN α therefore led to successful clearance of secondary infection with *S. pneumoniae* and increased recruitment of neutrophils following influenza infection in a murine model (Li,

Moltedo et al. 2012). Correspondingly, IFN γ production by alveolar macrophages during influenza infection results in changes to receptor expression. Down regulation of the scavenger receptor MARCO on macrophages decreases their phagocytic capacity for bacterial pathogens, suppressing innate protection to heterologous infection (Sun and Metzger 2008). NK cell responses are also impaired by viral infection and cytokine production is vastly reduced in response to secondary pathogens (Small, Shaler et al. 2010). Synergistic inflammatory responses occur as a result of both bacterial and viral infection in the lung, therefore co-infection mutually increases inflammatory mediators and induces an enlarged influx of immune cells which heavily contributes to the onset of fatal pneumonia (McCullers 2014). Impairment of wound healing responses due to viral or bacterial infection can also reciprocally facilitate the pathogenicity of the other infection. This is evident in a model of 2009 pandemic H1N1 influenza and streptococcus pneumonia where co-infection was assisted by loss of repair responses and increased pulmonary damage (Kash, Walters et al. 2011). Onset of *S. pneumonia* infection is associated with a second ‘rebounding’ increase in viral titre, suggesting that bacterial infection is actively distorting the clearance of influenza from the lung (Smith, Adler et al. 2013).

These infections are a result of influenza induced pathology however they provide insight into the specific regions of the immune system that are affected by influenza infection. Pre-existing infections that also alter these responses will likely alter the outcome of influenza infection and furthermore could pre-dispose individuals to further infection with the bacterial pathogens discussed above.

1.11.2 Pre-existing conditions and influenza A

The majority of co-infections address influenza A as the primary infection. This project aims to address the role pre-existing and on-going infections can play on influenza susceptibility. HIV and asthma along with co-infection by other respiratory viruses represent a group of co-morbidities that have been addressed in this context of influenza co-infection.

- Respiratory viral infection

Human respiratory infection is often complicated by the number of potentially unidentified infectious agents. Clinical identification of viral agents in nasopharyngeal swabs or sputum samples in human infection has been greatly advanced by the introduction of multiplex PCR for common respiratory viruses (Deng, Ma et al. 2013). The influence of concurrent infection is evident in data collected during the H1N1 2009 pandemic.

Rhinovirus	Patients identified with rhinovirus co-infection tended to have less severe symptoms whilst non-rhinovirus infections were associated with worsened influenza prognosis (Esper, Spahlinger et al. 2011).
Influenza B	Co-infection with seasonal influenza B is significantly correlated with increased fatality and admission into intensive care units in hospitalised patients with H1N1 2009pdm strains (Goka, Vallely et al. 2013).
Adenovirus	In a cohort of ‘high risk’ military trainees during the 2009 pandemic, adenovirus co-infection was rare and not associated with worsened severity (Yun, Fugate et al. 2014). Individual cases of adenovirus co-infection with either RSV or H1N1 influenza have been identified as contributing factors to severity of disease (Yun, Fugate et al. 2014).
Respiratory syncytial virus	RSV co-infection shows an increased trend in influenza severity, for both hospitalisation and requirement for intensive care treatment with mechanical ventilation (Torres, Iolster et al. 2012). RSV infection is generally associated with increased chance of hospitalisation in young children (Bourgeois, Valim et al. 2009).
Seasonal influenza A	Co-infections with other H1N1 strains is rare and was only detected during the initial wave of 2009 cases. Other influenza A strains are often not detected by multiplex PCRs for respiratory co-infection and therefore their effect is under reported. (Peacey, Hall et al. 2010) Significance of such infections is therefore prominent for research into potential reassortment.
Others	Coronaviruses, metapneumovirus and parainfluenza viruses have all been identified as co-infectors during the 2009 pandemic however their specific clinical impact has not been identified (Stefanska, Romanowska et al. 2013).

– Human immunodeficiency virus (HIV)

There is very limited research addressing the effect of pre-existing HIV infection (despite the high prevalence) on influenza infection. Some individual studies have identified increased prevalence of acute lower respiratory tract infection and increased incidence of pneumococcal

secondary infection in influenza patients with HIV (Cohen, Moyes et al. 2013). However, others have shown decreased incidence of virally induced severe acute lower respiratory tract infection in young HIV patients (Madhi, Schoub et al. 2000). Despite individual reports, overall studies excluding for factors of co-morbidity are extremely limited. Early reports from the 2009 H1N1 pandemic reveal HIV positive individuals were not overrepresented in the initial wave of susceptible individuals (Gilsdorf and Poggensee 2009) however prevalence of morbidity and mortality from influenza in those with AIDS was increased in a number of case reports during 2009 H1N1 (Lee, Wu et al. 2010). This likely reflects the negative impact of HIV on the adaptive (CD4⁺) immune response.

– Asthma

In a cohort of H1N1 2009 pandemic sufferers, morbidity of patients with and without an underlying asthmatic condition was characterised. Despite the increased likelihood of chronic obstructive pulmonary disease, the requirement for mechanical ventilation, development of pneumonia and likelihood of death were all significantly reduced in patients with asthma (McKenna, Bramley et al. 2013). Similarly in a mouse model of asthma, during peak allergic response influenza infection was cleared rapidly, resulted in no weight loss and reduced interferon response, while infection with influenza during remodelling after an allergic response had no significant impact compared to WT controls (Samarasinghe, Woolard et al. 2014). In another study of human infection, increased resistance to influenza was associated with early inhaled steroid use (Semple, Strathdee et al. 2011). Both studies however point to mediation of responses to influenza due to pre-existing type 2 inflammation in the lung, an observation that could be key to understanding the variation in responses by individuals infected with influenza A.

1.12 Aims

The effect of persistent and latent co-infection on acute influenza A infection is poorly understood.

This project therefore aims to identify changes to innate and adaptive immune responses during latent infection with a murine model of gammaherpesvirus infection (MHV-68) and a murine model of persistent filarial nematode infection (*Litomosoides sigmodontis*).

The effect of these changes will then be observed in a co-infection model during an acute respiratory infection with a murine strain of influenza A.

The role of macrophages, inflammatory cytokines produced in the lung and CD4⁺ T cell activation in the lung draining lymph nodes will be investigated to determine if alterations to the immune system during co-infection can alter the severity and ultimate outcome of influenza A infection.

Chapter 2 - Materials and Methods

2.1 Preparation of virus stocks

– Influenza A/WSN/33 H1N1

The original virus stock of mouse adapted H1N1 A/WSN/33 was provided by Dr D. Jackson, University of St Andrews, UK. A T175 flask (Thermo, MA USA) containing Madin-Darby Canine Kidney (MDCK) cells in Dulbecco's minimum essential medium (DMEM) (Sigma, UK) with 100 µg/ml penicillin and streptomycin (Invitrogen, UK), 100µg/ml L-glutamine (Invitrogen) and 5% v/v foetal calf serum (FCS) were grown to confluence at 37°C with 5% CO₂ and infected at a multiplicity of infection of 0.001 by addition of virus in 2 ml serum free DMEM for 1 hour on a rocking platform at 37°C. After incubation, media was removed and cells were incubated in DMEM + 2.5µg/ml N-acetyl trypsin. After 48 hours infected cells had lifted from the monolayer. The supernatant, from the flask containing the virus was centrifuged at 8000 x g, 4°C for 10 min to remove cell debris. Supernatant containing the virus was frozen at -80°C in 50µl and 1ml aliquots. Thawed viral titre is determined by plaque assay on MDCK cells.

– A/WSN/33 Plaque Assay

Homogenised samples or viral stock samples were diluted in 10 fold serial dilutions in serum free DMEM from 10⁻¹ to 10⁻⁹. 400µl of each dilution was added to confluent monolayers of MDCK cells grown in 6 well plates (Thermo, MA USA); each dilution in duplicate. Plates were incubated at 37°C for 1 h, rocking every 10 mins to ensure complete monolayer coverage with the sample. After incubation samples were aspirated from the cell monolayer. 2ml overlay media (see below) was added to each well and when set (approximately 15 mins), the plates were turned upside down and incubated at 37°C for three days.

After 3 days plates were removed from 37°C and turned upright. Each well was fixed by the addition of 4ml 10% NBF (Leica, UK) and left for 24 h in a fume hood. The fixative and agarose plug were then removed and cells were stained with 0.1% toluidine blue O (Sigma) in dH₂O for 1 h. Plates were washed in H₂O and plaques counted under a light microscope. Plaques visible at the lowest two dilutions are used to calculate viral titre.

Overlay medium: 2% w/v agarose (Biogene, NJ USA) dissolved in dH₂O and warmed to 56°C was added in equal parts to 2x overlay media, composed of 100ml 10x Eagle's minimum essential media (EMEM) (Invitrogen CA USA), 28ml 7.5% w/v BSA (Fraction V, Sigma, UK), 10ml L-glutamine (Invitrogen), 20ml 7.5 NaHCO₂ (Invitrogen), 10ml 1M HEPES, 5ml 1% w/v

dextran, 10ml penicillin and streptomycin (Invitrogen) and 517ml dH₂O stored at 4°C. Overlay media was placed in a 37°C water bath in 25ml aliquots on the day of titration.

– MHV-68 g2.4

T175 flasks of baby hamster kidney (BHK) cells were grown at 37°C to confluence in Glasgow's minimum essential medium (GMEM) containing 100 µg/ml penicillin and streptomycin (Invitrogen, UK), 100µg/ml L-glutamine (Invitrogen), 10% v/v tryptose phosphate broth and 5% v/v FCS. Cells were removed from each flask with trypsin EDTA (Sigma) and resuspended at 1×10^7 /ml in 5ml medium. MHV-68 virus was added at a multiplicity of infection 0.001 and cells were incubated at 24°C on a shaker for 1 hr. Infected cells were seeded at low concentration (3×10^6 cells) per T175 flask and incubated for 7 days at 37°C until the cell monolayer was lysed by infection. After incubation, the cell suspension was collected and centrifuged at 18000 x g for 20 min at 4°C. The supernatant was discarded and cells were resuspended in a minimal volume of PBS. The cell pellet was then homogenised with a sterile glass Dounce homogenizer and the resulting cell suspension transferred to a glass universal and sonicated in an ice water bath for 15 min. After centrifugation at 18000 x g for 20 min at 4°C the supernatant containing the virus was collected. The remaining cell pellet was homogenised in PBS as before and centrifuged again. The second supernatant was pooled with the first and aliquots of 50 or 200µl were frozen at -80°C. The viral titre was determined by plaque assay using BHK cells. A cell lysate for use in sham infections was also prepared as above.

– MHV-68 g2.4 Plaque Assay

Homogenised sample or virus stock was diluted in 10 fold serial dilutions in complete GMEM (see previous section) from 10^{-1} to 10^{-9} . 0.2ml of each dilution was added to a single cell suspension of 1×10^7 BHK cells, vortexed and shaken at 27°C for 1 h. After incubation, tubes were vortexed and each sample was added to two 60mm plates with 3 ml GMEM containing 100 µg/ml penicillin and streptomycin (Invitrogen, UK), 100µg/ml L-glutamine (Invitrogen) and 5% v/v FCS and incubated for 4 days at 37°C. After incubation, cells were fixed with 10% NBF overnight. Fixative was removed and the cells stained with 0.1% toluidine blue O for 1 h. Plates were washed in H₂O and plaques were counted under a light microscope. The lowest two dilutions of each sample are used to calculate titre.

2.2 *Litomosoides sigmodontis* life cycle

Litomosoides sigmodontis life cycle is maintained in gerbils. *Ornithinyssus bacoti*, a mite vector takes a blood meal from the infected, microfilaraemic gerbils. The larvae then develop through the L1-L3 stages of the life cycle inside the mite. The mites were harvested after 15 days and

suspended in RPMI media. L3 larvae were extracted and counted under a light microscope. See: Hubner *et al* (Hubner, Torrero et al. 2009).

2.3 *In vivo*

BALB/c mice used in MHV-68 experiments were purchased from Harlan UK Ltd. Those used for *L. sigmodontis* co-infection were bred in house at the University of Edinburgh. 129 Sv/Ev and 129 Sv/Ev IFN γ R^{-/-} were purchased from B+K universal and bred in house. See: Huang *et al* (Huang, Hendriks et al. 1993). All work was reviewed by The University of Edinburgh ethics committee and carried out under a UK Home Office licence according to the Animals (Scientific Procedures) Act 1986. Project license: 60/4479 (19b8).

- Intranasal inoculation of A/WSN/33 or MHV-68 g2.4

Mice were anaesthetised using 5% isoflurane (Abbot Animal Health, IL USA) Animals were sedated within 1-2 min, where they may be retained short term (min) before intranasal infection.

- Viral inoculum A/WSN/33 and MHV-68 g2.4

Mice infected with A/WSN/33 were inoculated intranasally with 5×10^2 or 5×10^3 PFU in 40 μ l sterile Dulbecco's minimal essential medium (DMEM). Mock infected mice were inoculated with 40 μ l DMEM alone. Mice infected with MHV-68 g2.4 were inoculated intranasally with 5×10^4 PFU in 40 μ l sterile phosphate buffered saline (PBS) pH 7.4 (Invitrogen). Sham infected mice were inoculated with 40 μ l sterile PBS containing baby hamster kidney (BHK) cell lysate. (See MHV-68 g2.4 viral isolation above).

- Subcutaneous injection of *L. sigmodontis* L3 larvae

Mice were injected S.C. in the lower back with 25 x L3 *L. sigmodontis* larvae in <100 μ l RPMI-1640 media.

- Tail bleed (*L. sigmodontis* infected mice only)

Microfilaria count was determined in 50 μ l blood collected from the lateral tail vein. Blood was gathered in FACS lysing solution 1:10 in dH₂O (BD, NJ USA).

2.4 Dissection

- Blood samples

Blood samples were drawn within a minute of death by severing the hepatic artery or by cardiac puncture. These samples were chilled immediately to 4°C on ice. On the same day blood samples were centrifuged at 500 x g for 15 mins at 4°C, serum aspirated and stored at -80°C.

- Spleen samples

The spleen was removed and cut into three sections. The upper half was fixed into 10% neutral buffered formalin (NBF) for histology. The central segment was frozen on dry ice for DNA extraction and the bottom piece was placed in RNA Later (Invitrogen) at 4°C for subsequent RNA extraction.

- Pleural lavage (*Litomosoides sigmodontis* infected mice only)

12 ml RPMI was flushed into and collected from the pleural cavity to recover adult worms.

- Lymph nodes

Parathymic, posterior mediastinal and paravertebral lymph nodes were collected as a source of lymph nodes draining the lung and pleural cavity. Lymph nodes were passed through a 40µm cell strainer and resuspended in RPMI-1640 with 0.5% mouse serum (Caltag-MedSystems, UK) 100U/ml penicillin, 100µg/ml streptomycin and 2mM L-glutamine.

- Lungs

The left superior bronchi was tied off with elastic thread and the left lobe cut away and divided into three pieces. The top half was frozen on dry ice for homogenisation for ELISA analysis and influenza A/WSN/33 titre. The central segment was frozen on dry ice for DNA extraction and the bottom piece was placed in RNA later for subsequent RNA extraction.

The lungs were flushed with 3 x 1ml Hanks balanced salt solution (HBSS) (Invitrogen) containing 3mM EDTA (Invitrogen) using a cannulised needle in the trachea. BAL was stored at 4°C on ice before centrifugation at 500 x g for 5 min at 4°C. The lungs were inflated and fixed with 5ml 10% w/v NBF, the trachea tied off with elastic thread and the lungs removed and placed in 10% w/v NBF for histology.

2.5 Flow cytometry

– Intracellular cytokine staining

Prior to staining, lymph nodes were strained through 40µm cell strainers and the cells were suspended in 1ml RPMI. After centrifugation of the BAL fluid (BALF) or lymph node samples, the cell pellet was resuspended in 1ml FACS buffer (PBS + 2% foetal calf serum and 0.01% sodium azide) containing red blood cell lysis buffer (Imgenex, CA USA) at room temperature for 5 mins. 1ml FACS buffer was added before cells were centrifuged at 500 x g for 5 mins. The supernatant was discarded and cells were washed twice by resuspension in FACS buffer and centrifugation. After the second wash step, lymph node cells were counted and plated into 96 round bottomed well plate (Co-star, NY USA) at 2×10^6 cells in 100µl RPMI per well. BAL cells were not counted due to the low cell numbers. 0.5 µg/ml phorbol myristate acetate (PMA) (Cambridge Bioscience, UK) and 1µg/ml Ionomycin (Sigma) were added to each well and cells incubated for 2 hours at 37°C to stimulate T lymphocyte activation and cytokine production. After 2 hours 10µg/ml Brefeldin A (Acros Organics) was added to each well to indirectly inhibit transport of intracellular proteins from the Endoplasmic Reticulum to the Golgi. The cells were incubated at 37°C for a further 2 hours. Cells were centrifuged at 500 x g for 5 mins and washed twice in 200µl PBS. PBS was removed and cells were live/dead stained with 1:500 Zombie Cyan live/dead stain (Biolegend) in PBS. Cells were incubated at 4°C for 30 min before being washed twice in 200µl PBS. After the final wash, PBS was removed and cells were fixed in 100µl cytofix/cytoperm (BD) for 20 mins at 4°C. Cells were centrifuged at 500 x g for 5 mins and washed twice in 200µl 1:10 perm/wash buffer in dH₂O (BD). Cells were stored in perm/wash buffer at 4°C overnight. The following day non-specific antibody staining was blocked with 200µg/ml rat IgG for 20 min at 4°C and then washed twice in 200µl perm/wash buffer. Cells were then stained for cell surface markers and intracellular cytokine production (Table 2.1). Samples were run on a LSR II Fortessa (BD) and analysed with Flow-Jo V10 software (Flow-Jo, OR USA).

– Analysis

Analysis of FACS data was performed as outlined in Appendix Figure 6.2. Initially dead cells were removed by identification with Zombie live/dead stain (biolegend). Zombie dyes are fixable live / dead stains that react with primary amine groups on proteins. Live cells therefore exclude the dyes and dead cells appear labelled and can be detected in the aqua channel (525/50nm) by excitation with a violet 405nm laser. Doublet cells that passed through the machine attached to another cell were then excluded by comparison of FSC-height vs. FSC-area. Lymphocytes were then identified by size on a SSC-area vs. FSC-area plot. Cells that

appeared between 100-200K on each axis were considered lymphocytes. Antibodies directed against CD4⁺ and CD8⁺ lymphocytes were used to gate out cell types and intracellular staining used to identify relevant cytokine production. Identification of non-specific antibody staining was performed with appropriate isotype stained controls for each respective antibody used. Non-specific binding was subtracted from each positive sample. Compensation was performed in multi-colour staining by pooling samples of lymphocytes and staining for individual cytokines / markers. Single positive samples were then used to create a compensation template on the BD Fortessa LSR FACS machine.

Table 2.1 Intracellular flow cytometry staining

The cells were stained for the following markers and intracellular cytokines for detection with the BD LSRFortessa Cell Analyser.

BAL	Lymph Nodes		Fluorochrome	Brightness	FL	Excitation			Detection
	Th1/Th2	Th17				Laser	nm	%	Filter
CD4	CD4	CD4	Alexafluor 700	2	11	Red	640	48.1	730/45
CD8	CD8	CD8	PerCP-Cy5.5	3	3	Blue	488	98.4	710/50
Live/Dead	Live/Dead	Live/Dead	Aqua	5	5	Violet	405	36.7	525/50
IFN γ	IFN γ	IL-6	FITC	3	2	Blue	488	88.0	530/30
IL-5	IL-5	IL-17a	APC	5	10	Red	640	71.2	670/14
IL-4	IL-4		PE	5	7	Y/Green	561	94.3	586/16
TNF α	TNF α		BV605	5	8	Violet	405	99.1	610/20
IL-10	IL-10		BV421	5	4	Violet	405	98.2	450/50
IL-17a			PE-Cy7	4	17	Y/Green	561	94.9	780/60

Cells were stained in a final volume of 20 μ l in wash/perm buffer for 30 min in the dark at 4°C. Cells were then washed twice with wash/perm buffer and resuspended in MACS buffer (Miltenyi Biotec, Germany) containing 1% NBF.

Table 2.2 Antibody isotypes and clones

Marker	Fluorochrome	Marker Type	Dilution	Clone	Isotype	Distributor
CD4	Alexafluor 700	T cell	1:200	GK1.5	IgG2b κ	Biolegend
CD8	PerCP-Cy5.5	T cell	1:200	53-6.7	IgG2a κ	Biolegend
Live/Dead	Aqua	Live/Dead	1:500	Zombie Cyan	N/A	Biolegend
IFN γ	FITC	Cytokine	1:100	XMG1.2	IgG1 κ	Biolegend
TNF α	BV605	Cytokine	1:100	MP6-XT22	IgG1 κ	Biolegend
IL-4	PE	Cytokine	1:100	11B11	IgG1, κ	Biolegend
IL-5	APC	Cytokine	1:100	TRFK5	IgG1 κ	Biolegend
IL-6	FITC	Cytokine	1:100	MP5-20F3	IgG1 κ	eBioscience
IL-10	BV421	Cytokine	1:100	JES5-16E3	IgG2b κ	Biolegend
IL-17a	PE-Cy7	Cytokine	1:100	TC11-18H10.1	IgG1 κ	Biolegend
IL-17a	APC	Cytokine	1:100	TC11-18H10.1	IgG1 κ	Biolegend

2.6 ELISAs

ELISAs for inflammatory or regulatory cytokines were performed on lung homogenates. Each ELISA was tested for efficacy using homogenate samples. All buffers were stored at 4°C and antibodies at -20°C. Reagents were brought to room temperature prior to use. Immulon 4HBX flat bottom 96 well plates (Thermo MA, USA) were coated in pre-titrated capture antibody in a coating buffer, (50µl per well) sealed and incubated at 4°C overnight. Plates were washed 5 times by adding and decanting 150µl wash buffer (PBS + 0.05% Tween-20 (Thermo) pH 7.5) per well and patting plate against paper towels. To block the plate, 100µl blocking buffer was added to each well; the plate was sealed and left at room temperature on a shaker at 90 rpm for 1 hour. During this time standards were made by diluting the top concentration standard (either 1000 or 2000pg/ml) in halving serial dilutions. The plate was washed as before and 50µl neat samples and standards added to relevant wells. The plate was sealed and placed on a shaker for 2 hours at RT. The plate was washed and 50µl detection antibody added per well. The plate was sealed and shaken for 1-2 hours. The plate was washed and 50µl streptavidin-HRP or avidin-HRP added per well. The plate was protected from light and shaken at room temperature for 30 min. The plate was washed and 50µl 3,3',5,5'-Tetramethylbenzidine (TMB) substrate added per well. The plate was protected from light and incubated at RT without shaking for 15-30 min until colour developed. When the lowest standard well showed a colour change the reaction was halted by addition of 50µl 2N sulphuric acid (H₂SO₄) (SLS, UK) per well. Plates were read at 450 nm and 570 nm on a BioTek (VT, USA) absorbance plate reader. 570 nm background level was subtracted from 450 nm reading and the average of each duplicate sample was taken and analysed using <http://elisaanalysis.com/app> (4 parameter logistic regression) using the known standard curve. Alternatively optical density for each sample was divided by the mean optical density of all uninfected samples to determine the fold change compared with baseline expression in uninfected mice.

Table 2.3 ELISA reagents and dilutions

ELISA	Coating Buffer	Blocking Buffer	Assay Diluent	HRP
IFN γ	8.4g NaHCO_3 + 3.56g Na_2CO_3 in IL dH $_2$ O pH9.5	Assay diluent	10% FCS in PBS	1:1000 Avidin-HRP
TNF α	PBS	Assay diluent	1% BSA in PBS pH 7.2	1:100 Streptavidin-HRP
IL-10	PBS	Assay diluent	10% FCS in PBS	1:1000 Avidin-HRP
TGF β	PBS	5% Tween-20 in PBS +0.05% NaN_3	R and D reagent diluent concentrate 1	1:200 Streptavidin-HRP
IFN β	PBS	Assay diluent	RD1W	Anti-rabbit HRP
IL-2	Pre-coated plate	Pre-coated plate	RD1-14	1:100 Streptavidin-HRP
CXCL2 (MIP 2)	Pre-coated plate	Pre-coated plate	RD1W	1:100 Streptavidin-HRP
IL-1 β	Pre-coated plate	Pre-coated plate	RD1N	1:100 Streptavidin-HRP
GM-CSF	Pre-coated plate	Pre-coated plate	RD1W	1:100 Streptavidin-HRP

2.7 RNA extraction

Total RNA extraction was performed following the ‘RNeasy Mini Kit’ (Qiagen) protocol: Tissues were stored in RNALater at 4°C. 30mg or less of each lung or spleen sample was disrupted by homogenisation in a tissuelyser II (Qiagen) and suspended in buffer RLT containing β -mercaptoethanol to inactivate RNases. RNA was precipitated by adding ethanol and then a series of washing steps were performed according to Qiagen protocol before elution of the RNA in 50 μ l RNase-free water. RNase-free DNase 1, (Qiagen) an endonuclease was used during the washing stages to remove DNA contamination.

2.8 DNA extraction

Total DNA extraction was performed following the ‘DNeasy Blood and Tissue Kit’ (Qiagen) protocol: Up to 25mg of spleen or lung samples stored at -80°C were lysed and disrupted in buffer ATL containing proteinase K (Qiagen) by vortexing periodically during incubation at 56°C for 24 hours. DNA was precipitated by the addition of buffer AL and 100% ethanol and

purified by spin column centrifugation and a number of wash steps with AW1 and AW2 buffers. The DNA was then eluted in Buffer AE (10 mM Tris-Cl, 0.5 mM EDTA; pH 9.0) and stored at -20°C.

2.9 cDNA production

cDNA was produced using RNA extracted from spleens (see above) according to Invitrogen Superscript III reverse transcriptase protocol: First strand synthesis was undertaken by addition of 1µl 0.5µg/µl random primers or 1µl 0.5µg/µl Oligo(dT)15 primers, 1µl dNTPs and up to 11µl of total RNA (500ng - 1µg total) to a final volume of 13µl in nuclease free dH₂O. This was heated to 65°C for 5 min, then incubated on ice (4°C) for at least 1 minute to stop the reaction. After brief centrifugation to collect the contents of the tube, 4µl 5x first-strand synthesis buffer, 1 µl 0.1M DTT, 1µl RNaseOUT and 1 µl Superscript III RT were added. Samples were mixed by pipetting and incubated at 25°C for 5 min followed by 45 min at 50 °C and finally inactivated for 15 min at 70 °C. The cDNA was then stored at -20°C. (All reagents Invitrogen)

2.10 ORF73 MHV-68 qPCR

MHV-68 genome copy number was determined by an established qPCR in the Dutia group for ORF 73. The standard curve was previously determined to have a single product at >95% efficiency. 100 ng of sample DNA was added to a master mix containing fast start universal SYBR green (Roche, Switzerland) and 400 nM forward ACCCTCGGGATCAAATAACC and reverse CCCATCACCACCAGTGCC primers. Samples were then run on a Rotorgene 3000 qPCR machine with Rotorgene Q series software used for analysis using the template in table 2.4.

Table 2.4 Q-PCR template

Cycle Step	Temperature (°C)	Time (seconds)	Cycles
Hold	95	600	1
Denaturation	95	15	40
Extension	62	50	
Hold	94	20	1
Melt	60 → 99	-	1

2.11 Macrophage Q-PCRs

BALF sample were added to a flat bottom 96 well plate (Costar) for 1 hour. Samples were then removed and adherent cells washed twice in sterile PBS. Adherent cells were lysed in 200 µl RLT lysis buffer and RNA was isolated from samples as outlined above. Alveolar macrophages comprise the predominant adherent cell population within the BALF. No further positive or negative isolation was performed. Macrophage specific QPCR was then performed to identify phenotypes.

Q-PCRs used to determine macrophage subtype were designed and optimised by Gillian Campbell (previously of Dutia group). Primer sequences for genes of interest are listed in Table 2.5. Optimal primer concentrations and annealing temperatures are listed in Table 2.6. Each Q-PCR was measured as relative concentration against SDHA.

Table 2.5 Primer sequences for macrophage Q-PCRs

Gene	Forward	Reverse
SDHA	gctcctactgatgaaacctg	aactcaatcccttacagcaa
Arginase 1	ggcctttgttgatgtcccta	atgcttccaactgccagact
CD206	tgaaccctaatgtccagaaa	ctcgtaatcagcctccaatc
IL-10	ctttgctatgggtgcctttca	atctccctggtttctcttcc
iNOS	tgctactgagacaggaag	gacagtctccattcccaa
TNFα	caccaccatcaaggactcaa	gacagaggcaacctgaccac
SOCS-1	acagtgcctcaacggaact	aaggcagtcgaaggcttc

Table 2.6 Optimal primer concentrations and reaction conditions for macrophage Q-PCRs

Gene	Forward	Reverse	MgCl	Anneal
SDHA	400 nm	400 nm	2.5 mM	62°C
Arginase 1	400 nm	400 nm	3.0 mM	62°C
CD206	400 nm	400 nm	3.0 mM	62°C
IL-10	400 nm	400 nm	2.5 mM	62°C
iNOS	400 nm	400 nm	3.0 mM	62°C
TNF α	400 nm	400 nm	3.0 mM	65°C
SOCS-1	400nm	400nm	2.5 mM	62°C

2.12 Mouse cytokine protein array

Lung homogenate samples were thawed at room temperature. The array was performed following the protocol provided by R and D systems (MN USA). Membrane identification numbers were removed and the protocol for use with the Li-Cor imager (Li-Cor, NB USA) was followed for secondary staining. Protein Array membranes are blocked from non-specific binding by incubation for 1 hr at RT on a rocking platform shaker in wells containing buffer 6. 1 ml of each sample was added to 0.5 ml of buffer 4 and 15 μ l of reconstituted Mouse Cytokine Array Panel A Detection Antibody Cocktail. These samples were incubated at RT for 1 hr. Buffer 6 was removed and each sample was added to a well containing an antibody coated membrane. They were then incubated overnight at 4°C on a rocking platform shaker. Membranes were washed in 1x wash buffer and dH₂O in individual containers and secondary staining was performed. See: Protein array protocol here <http://www.rndsystems.com/Products/ARY006>). Membranes were dyed with IRDye 800cw infrared dye streptavidin (Li-Cor) at 1:2000 dilution for 30 min on a rocking shaker at room temperature. Membranes were then washed and stored in PBS protected from light. The membranes were scanned wet on a Li-Cor Odyssey (Li-Cor) at a resolution of 84 μ m, medium quality, 0.0mm focus offset. Optimal intensity was 3 and all membranes were analysed using Image Studio Lite version 4.0 (Li-Cor). Results are reported as fold change in fluorescence intensity compared with expression levels in uninfected mice.

2.13 Histology

10 μ m sections of lungs fixed in 10% NBF were stained with hemoxylin and eosin at the veterinary pathology unit, R(D)SVS, University of Edinburgh. Slides from each mouse were

scored and imaged using a Nikon Eclipse Ni series microscope and camera (Nikon, Japan) and Zen X software (Zeiss, Germany).

Pathology scores were valued from 0-3 for a number of observations with the help of Dr Phillipa Beard, University of Edinburgh. Influenza infection was assessed by peribronchial and perivascular infiltration / presence of inflammatory cells which were identified and described. Interstitial inflammation and necrosis along with epithelial necrosis were also evaluated and scored as determinants of infection severity. The total area of the lung was observed and damage caused by infection described as 0, 25, 50, 75 or 100%. For *Litomosoides sigmodontis* infection lungs were scored for different pathology, again on a scale of 0-3. Hypertrophic mesothelium and broncho-alveolar lymphoid tissue hyperplasia were recorded along with infiltration of neutrophils, lymphocytes and multi-nucleated giant cells.

2.14 Statistics

All statistical analysis was performed using Minitab 16.

During design of *in vivo* experiments data from previous experiments, predicted outcomes and variation in assay techniques were used to determine power of the experiment. Numbers of mice used per experimental group were calculated using 'sample size for estimation' in Minitab 16 allowing for statistical judgements that are accurate and reliable and responsible hypothesis testing. This method is in accordance with Home Office guidance for the 3 R's (reduce, refine and replace) of using animals for experimental procedures.

Initially all data were tested for normality using an Anderson Darling probability test, individual distribution identification or visualising data with a distribution histogram. If data was normally distributed then parametric statistical methods were used. If the data was not normal then transformation using either log, log (x+1) for positively skewed data or square root for negatively skewed data was used preferentially to normalise. If the data could not be normalised then non-parametric methods were undertaken.

In cases where 2 groups were being compared, for example with influenza titre data then students 2 sample t test was used. If the data could not be normalised then analysis with Mann-Whitney test was used.

In the case of 4 groups being compared, if all groups had equal numbers of values then a 2-way ANOVA was used to determine significance. If groups were unbalanced, for example if the control group was of smaller size then a general linear model was constructed on the same principles. All pairwise comparisons were performed by Tukey analysis at 95%, 99% and

99.9% confidence levels in comparison to the co-infected group. Similarly if data from two independent experiments was analysed then 'experiment' was added to the model as an additional variable, controlling for technical variation between experimental repeats. If the data required for such comparisons could not be normalised then Kruskal-Wallis analysis was used. Data was treated as in the case of a 1 way ANOVA and variation between all individual experimental groups was measured. If this analysis presented any suggestion of significant differences between groups of interest then Mann-Whitney analysis was undertaken to determine significance between individual groups. This measure was undertaken to avoid false positives by repeat testing and cross comparison of all groups.

Results are always represented with standard deviation as error and averages as mean average unless otherwise stated.

Chapter 3 - Latent gammaherpesvirus and influenza A co-infection

3.1 Introduction

All humans are infected with a range of commensal and pathogenic organisms. Gammaherpesviruses are common latent viruses present in all human populations. Latent viruses require an on-going immune response to control viral replication and prevent disease. Acute influenza A infection will often occur in individuals that harbour latent gammaherpesvirus infections.

This chapter aims to identify modulation to the host immune response by a latent murine gammaherpesvirus, MHV-68 and determine if its effect on the innate and adaptive immune response can alter subsequent infection with mouse attenuated influenza A/WSN/33 (H1N1).

3.2 MHV-68 - Murid Herpesvirus 4 (MuHV 4)

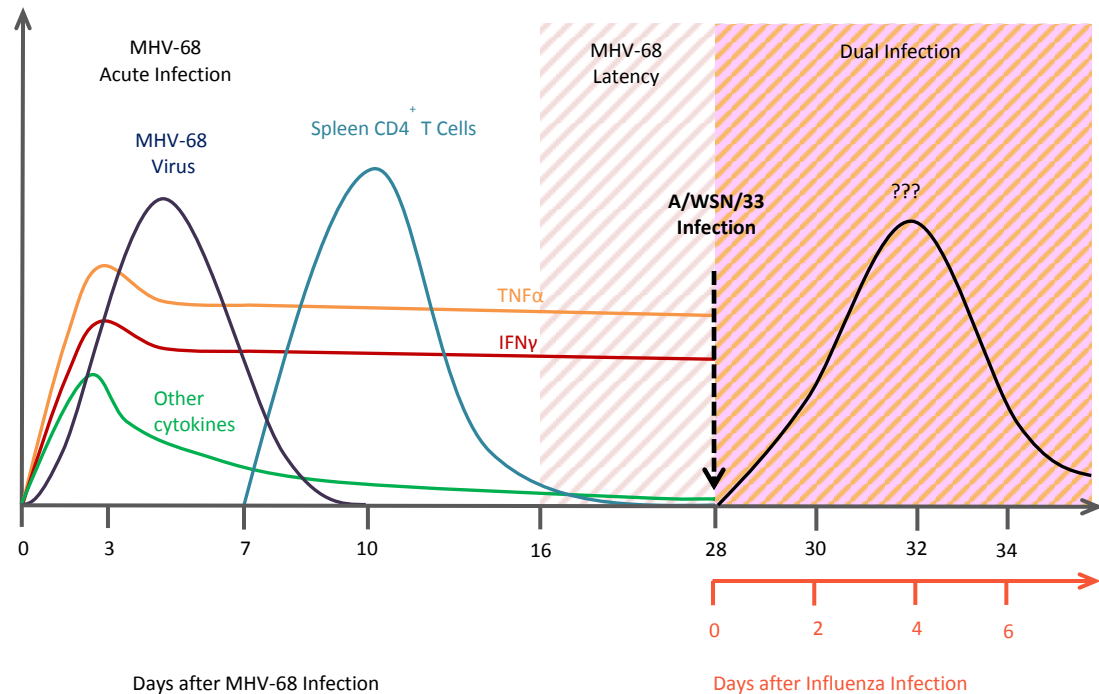
Murid herpesvirus 4 (MuHV 4) is a gammaherpesvirus in the genus *rhadinovirinae*. Five strains were originally isolated from bank voles (*Clethrionomys glareolus*) and wood mice (*Apodemus flavicollis*) in Slovakia, 1980 (Blaskovic, Stancekova et al. 1980). The archetypal strain MHV-68 readily infects laboratory strains of mice (*Mus musculus*).

3.2.1 Pathogenesis

Although the natural infection route is unknown, intranasal infection (a likely route) of BALB/c mice causes an acute infection of the lung alveolar epithelium and mononuclear cells for 10 d.p.i. Lymphoproliferation is also observed in the lungs, with homology to infectious mononucleosis caused in EBV sufferers (Sunil-Chandra, Efstathiou et al. 1992). The lytic infection is largely cleared in the lung within two weeks, with an observed decrease in inflammation. From here the virus enters the lymph node via macrophages and dendritic cells leading to establishment of latent infection in B lymphocytes (which spread the virus to distal organs e.g. spleen), macrophages and splenic dendritic cells for the life of the animal, Splenomegaly, a CD4⁺ T cell induced expansion of lymphocytes in the spleen occurs around day 10 (Simas and Efstathiou 1998; Nash, Dutia et al. 2001). In the long term latent virus is present in the lymph node and spleen as well as the lung where it is present at low levels in epithelial and lymphoid cells (Stewart, Usherwood et al. 1998). MHV-68 makes a useful animal model for the study of gammaherpesviruses such as EBV and KSHV *in vivo*, especially in regards to the lung and spleen immune responses. The kinetics of the acute MHV-68 murine

model of infection can be seen in Figure 3.1. A hypothetical dual infection is introduced at day 28, when latent infection is established in BALB/c mice.

Figure 3.1 Schematic representation of latent MHV-68 infection prior to co-infection



3.2.2 Co-localisation of infections

MHV-68 has been shown to persist in the epithelial cells in the lung, even after latency is established in the spleen (Stewart, Usherwood et al. 1998). Influenza viruses are usually restricted to a few cell types in the lung including epithelial cells and in some cases macrophages (Tate, Schilter et al. 2011). Cellular proteases play a role in the ability of influenza progeny virus to cleave from the surface of an infected cell (Choppin and Scheid 1979). A/WSN/33 virus encodes a neuraminidase capable of binding plasminogen. Active plasmin (a serine protease) then cleaves the virus hemagglutinin allowing the virion to infect new target cells. A/WSN/33 may therefore replicate in other tissues including the brain and spleen. In this model, MHV-68 and A/WSN/33 viral infections may therefore be present in both the lung and spleen.

3.2.3 Genome

MHV-68 has at least 73 identified genes, many of which are co-linear and homologous to both KSHV and EBV. The virus encodes homologues of cellular genes including Bcl-2 (M11), Cyclin D (ORF 72), complement regulatory protein (ORF 4) and an IL 8 receptor (ORF 74)

allowing suspension of apoptosis, manipulation of the host cell cycle, reductions in complement activation and chemokine attraction respectively (Simas and Efstathiou 1998).

3.2.4 MHV-68 as a model for EBV / KSHV

MHV-68 provides a model of KSHV and EBV human infections. All gammaherpesviruses have narrow host tropism. Whilst EBV will infect some primate species, the pathogenesis is very different to a natural infection (Tripp, Hamilton-Easton et al. 1997) and is therefore limited. MHV-68 is capable of causing a mononucleosis-like disease in laboratory mice with great similarity to that of EBV in a human host. It should however be noted that wood mice (*Apodemus sylvaticus*) are the natural host of MHV-68 (Blasdell, McCracken et al. 2003) and variations in response have been observed. The natural host displays lower viral replication during lytic infection, greater neutralizing antibody and more delineated secondary follicles in germinal centres in comparison to BALB/c mice (Hughes, Kipar et al. 2010).

A BALB/c model of infection was used in the following co-infection experiments. 5-6 week old female BALB/c mice were infected with 5×10^4 MHV-68 in PBS and 28 days later, once the MHV-68 infection has established latency, mice were infected with varying doses of A/WSN/33 influenza virus in DMEM. Figure 3.2 shows the time line of the experiments. An additional 3 experimental groups were used as controls.

Figure 3.2 Murine model of gammaherpesvirus and influenza A co-infection



3.3 Hypothesis

Increasing evidence from murine models is demonstrating the ability of herpesvirus latency to increase resistance to further infection by modulation of host immunity. These viruses have co-evolved with the human immune system and establish infection for the life of the host however very little is known of the positive influence of herpesvirus infection in humans. Discovery of potentially beneficial effects of such infections on acute concurrent infections may provide novel targets in the development of new therapies or vaccines for a range of other pathogens.

3.4 Results

The initial co-infection experiments with latent MHV-68 and A/WSN/33 were performed at a relatively low influenza dose. It was unknown how these two viruses would interact and therefore a low dose of 5×10^2 PFU A/WSN/33 was used to reduce the likelihood of a severe or negative outcome during co-infection. These co-infection experiments are referred to as 'low dose' from this point forward.

3.4.1 Co-infection with latent MHV-68 and 'low dose' A/WSN/33

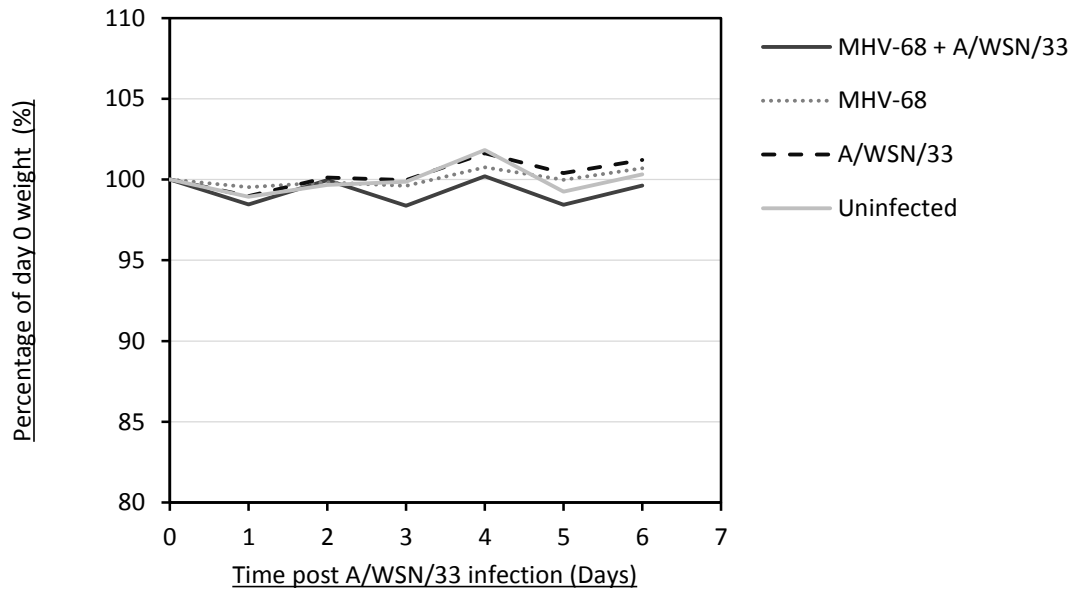
– Effect of latent MHV-68 on co-infection with A/WSN/33

Co-infection experiments with a low dose A/WSN/33 were performed intranasally at 28 days post MHV-68 infection. After the A/WSN/33 infection, the mice were monitored for signs of clinical signs and weight loss every 24 hours. Clinical signs of influenza infection including respiratory effort, decreased mobility, hunched stature, staring coat, trembling and pointed face were all scored 0 on a ranked scale of 0-3 for all experimental groups throughout the 6 day time course. This is a sub-threshold level on the severity rating system. There was no associated weight loss at low dose (5×10^2) A/WSN/33 infection and all experimental groups reached day 6 at a similar percentage of weight measured prior to infection. Mean percentages were 99.34%, 100.71%, 101.22% and 100.31 % for co-infected, MHV-68 infected, A/WSN/33 infected and uninfected groups respectively, with less than 2.5% variation within experimental groups (Figure 3.3A). Therefore there were no differences in clinical outcome of co-infection compared to singly and mock infected controls. Results are gathered from 4 independent experiments with cull dates at day 2 (single experiment), day 4 (2 experiments) and 6 days (2 experiments) post A/WSN/33 infection.

At these three time points following A/WSN/33 infection, animals were culled and lungs were harvested and frozen at -80°C . The left lobe of the lungs was homogenised and the homogenate was titrated in a dilution series as described in section 4.1 to determine the infectious viral load of A/WSN/33. In these experiments lung A/WSN/33 titre was normally distributed in all of the experimental groups. A two sample t test was performed to determine significant difference. Infectious titre of A/WSN/33 in singly infected (mean of 2.5×10^4 PFU ml^{-1} lung homogenate) and co-infected mice (mean of 1.81×10^4 PFU) did not significantly differ at day 2 ($p=0.526$). There was also no difference at the peak of viral replication at day 4 ($p=0.825$) where co-infected and singly infected mice again showed similar infectious titre, 1.64×10^4 and 1.89×10^4 PFU ml^{-1} . At day 6 post infection the difference in lung titre was significantly lower ($p=0.045$)

Figure 3.3 Co-infection has no effect on low dose A/WSN/33 pathogenesis

A. Weight loss



B. Influenza lung titre

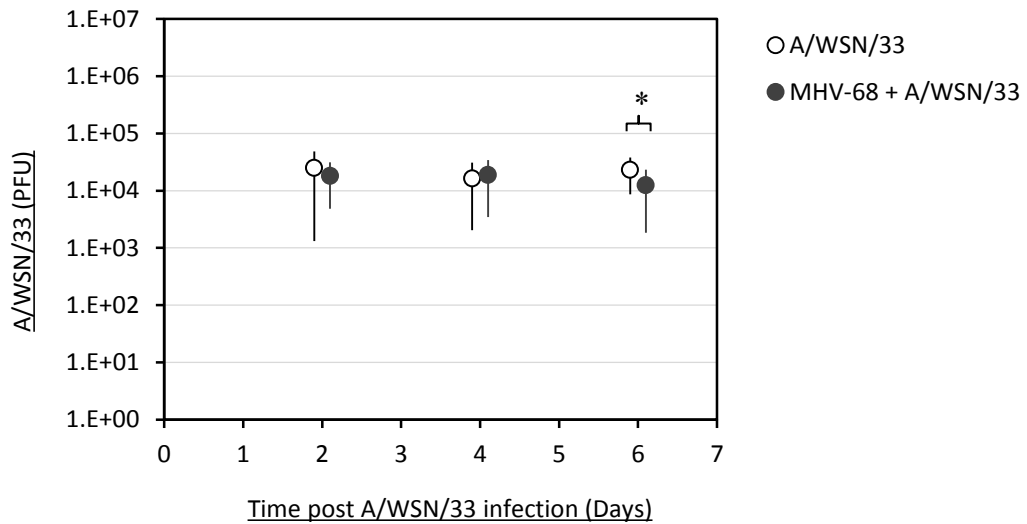


Figure 3.3 - 6 week old female BALB/c mice were inoculated I.N. with either 5×10^4 MHV-68 or $40 \mu\text{l}$ baby hamster kidney cell lysate. After 28 days, groups were infected I.N. with either low dose A/WSN/33 H1N1 or $40 \mu\text{l}$ Dulbecco's minimum essential medium. **A.** Influenza induced weight loss **B.** Mean A/WSN/33 titre in the lung. N=6 at day 2 from a single experiment. N=12 at day 4 and 7 from 3 repeat experiments. Error bars represent ± 1 standard deviation of the mean. Significance determined by students two sample T test (* = $p < 0.05$).

in co-infected mice. Co-infected mice had a lower mean titre (1.25×10^4 PFU ml⁻¹) than mice infected with A/WSN/33 alone (2.33×10^4 PFU ml⁻¹) and greater standard deviation from the mean, 14,500 PFU compared to 10,600 PFU in the co-infected mice (Figure 3.3B). The reduction in titre is subtle, however for this time point there were an increased number of mice per group (n=12).

– Pathology in the lung

Low dose A/WSN/33 infection is sufficient to cause significant changes to the lung environment. Viral replication results in epithelial cell death in the respiratory tract. Six days post infection with A/WSN/33, an increase in macrophages, lymphocytes and polymorphonuclear cells can be found in the lung, cuffing the airways and blood vessels. Extent of inflammation and cell infiltration was scored visually on a scale of 0-3 (Figure 3.5). There is some mild inflammation in the lung due to haemorrhage following cull by rising CO₂ and also lavage of the lungs to gather immune cells for FACS analysis (3.4A and 3.4B). Pre-existing infection with latent MHV-68 does not significantly alter the integrity of the lung (Figure 3.4C) however small lymphocyte foci accumulations are apparent in the interstitial spaces around the lung, (Figure 3.4D and 3.4E). There may be 1-4 of these foci within a cross section of the latently MHV-68 infected lung.

A/WSN/33 infection at low dose causes mild pathology. Infiltrations of cells (predominantly lymphocytes) are seen 6 days post infection around the blood vessels and airways within the lung (Figure 3.4F-H). These infiltrations are seen the same extent in mice co-infected with a pre-existing latent MHV-68 infection (Figure 3.4I-K). Co-infected mice therefore do not display a significant change in pathology in the lung compared with A/WSN/33 infected mice.

– Cytokine environment in the lung

Pathology caused by low dose A/WSN/33 was not altered by on-going co-infection with latent MHV-68. The reduction in infectious A/WSN/33 titre suggests an attenuated phenotype due to co-infection so to determine if the inflammatory environment in the lung is moderated, cytokine levels in the lung were measured at days 4 and 6 post infection by ELISA.

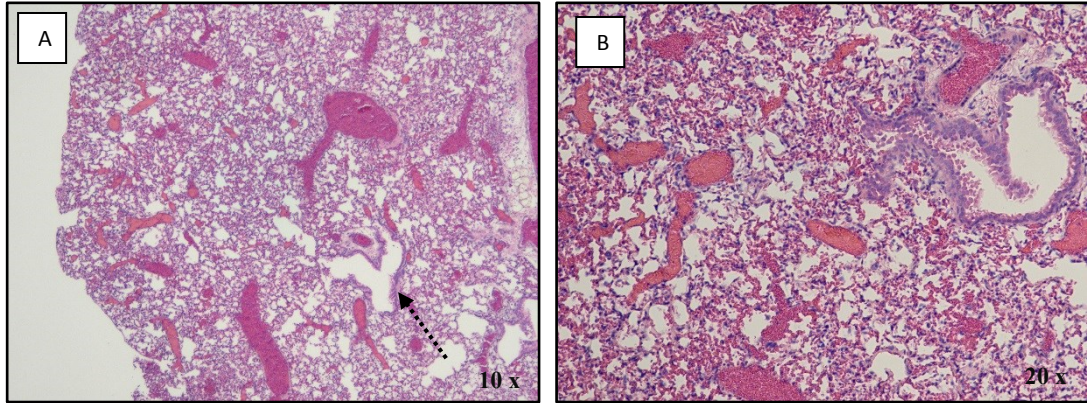
At day 4, IFN γ was detected in all experimental groups at an average of 75-100 pg ml⁻¹. Standard deviation within these groups was also similar, with variation around the mean of around 25-60 pg ml⁻¹. IFN γ levels were therefore not significantly different between groups.

TNF α levels at this time point were also not altered by infection. TNF α was expressed at lower levels than IFN γ and on average was detected at between 10 and 25 pg ml⁻¹ in all samples. The standard deviation was much greater, (up to 30 pg ml⁻¹ in the co-infected mice) as these results are often below the limit of detection in this ELISA and give results of 0 pg ml⁻¹ (Figure 3.6A).

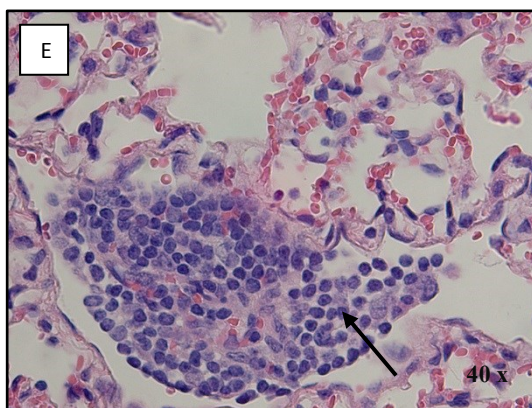
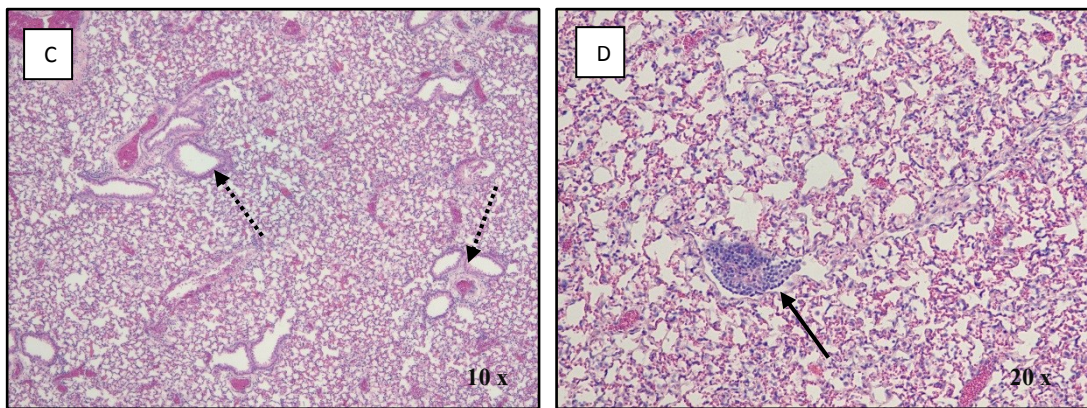
Figure 3.4 Low dose A/WSN/33 pathology is not affected by pre-existing MHV-68 infection

Histology sections



Uninfected



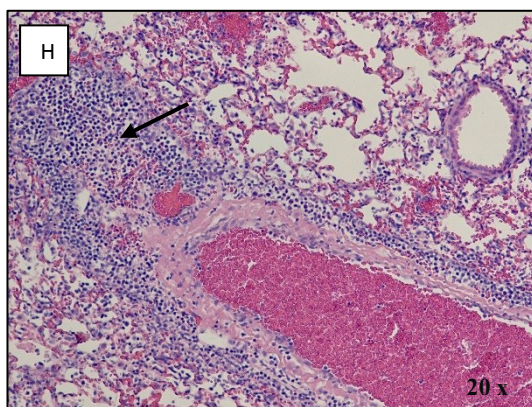
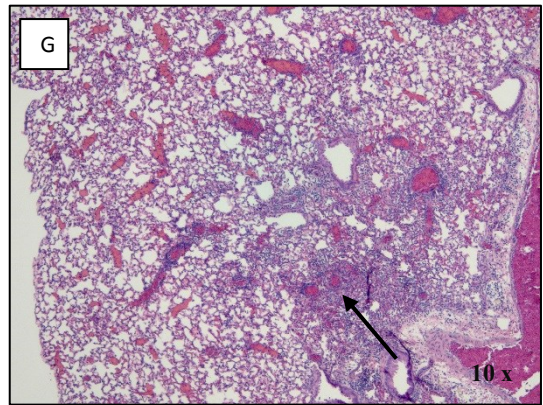
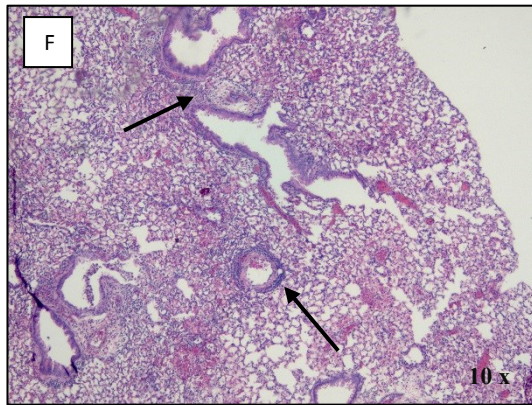
MHV-68 infected



Key:

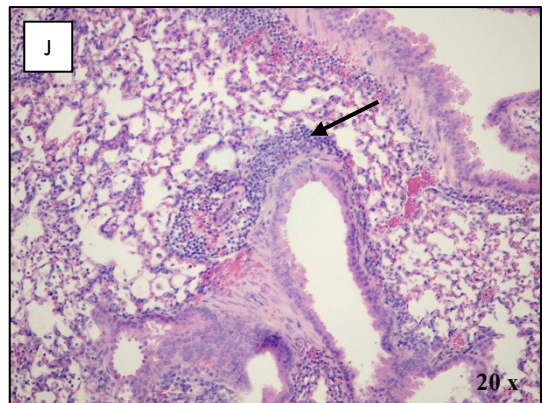
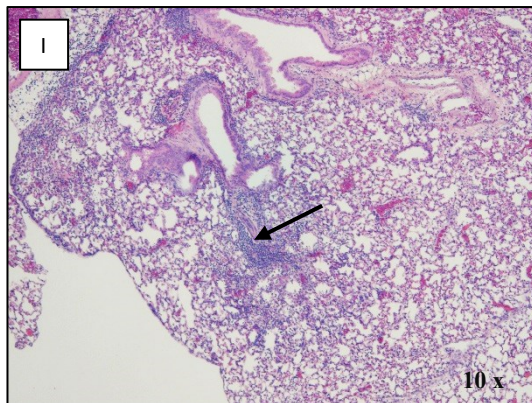
-  Normal lung structure
-  Lymphocyte infiltration / inflammation

Low dose A/WSN/33 infected



Key:
● Normal lung structure
▲ Lymphocyte infiltration / inflammation

MHV-68 + low dose A/WSN/33



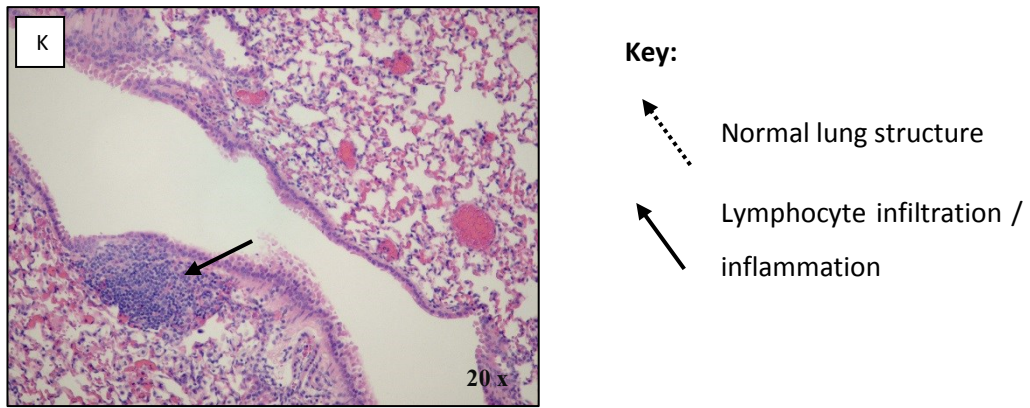


Figure 3.4 The right lung was inflated and fixed with 10% neutral buffered formalin. Lung sections were stained for hematoxylin and eosin. Representative sections are shown. Dashed arrows show areas of unaffected airways and blood vessels. Solid arrows demonstrate regions of lymphocytes infiltration and inflammation. **A-B** Lungs from uninfected mice. **C-E** Lungs from MHV-68 latently infected mice. **F-H** Lungs from A/WSN/33 infected mice. **I-K**. Images are representative from each infection group. Magnification is identified in the bottom right corner of each image.

Figure 3.5 Low dose A/WSN/33 pathology score is not affected by pre-existing MHV-68 infection

A. Pathology score

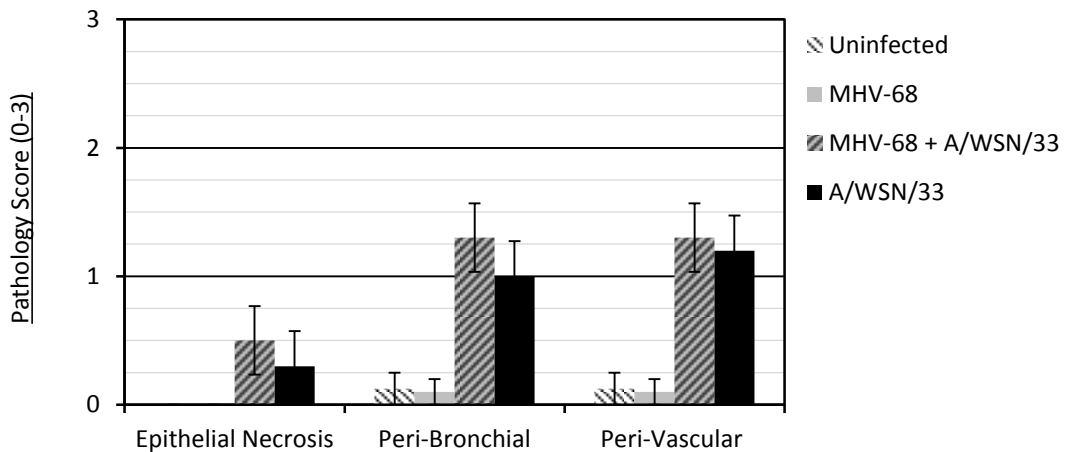


Figure 3.5 A. Complete lung cross-sections were scored for signs of inflammation and cell damage, N=6. Representative of 3 experiments. Results are displayed as mean average per group \pm 1 standard deviation.

Such results were not discounted as they still hold value statistically, and these results represent 2 independent experiments. Non-parametric testing was applied to account for zero values which cannot be normalised. There was no significant difference between the groups.

The regulatory cytokines IL-10 and TGF β were also not significantly changed by infection at day 4. Expression was detected between 25 and 80 pg ml⁻¹ in all groups for these two regulatory cytokines; however, there was a general trend for decreased expression in the influenza A/WSN/33 infected groups. Co-infected mice expressed 43.69 pg ml⁻¹ TGF β (\pm 22.76) and A/WSN/33 infected mice 32.64 \pm 15.64 pg ml⁻¹. On average this was lower than uninfected (73.89 \pm 31.13) and MHV-68 infected mice (75.17 \pm 52.10) however the variation in expression within these groups was high and therefore the decrease was not significant (Figure 3.6A).

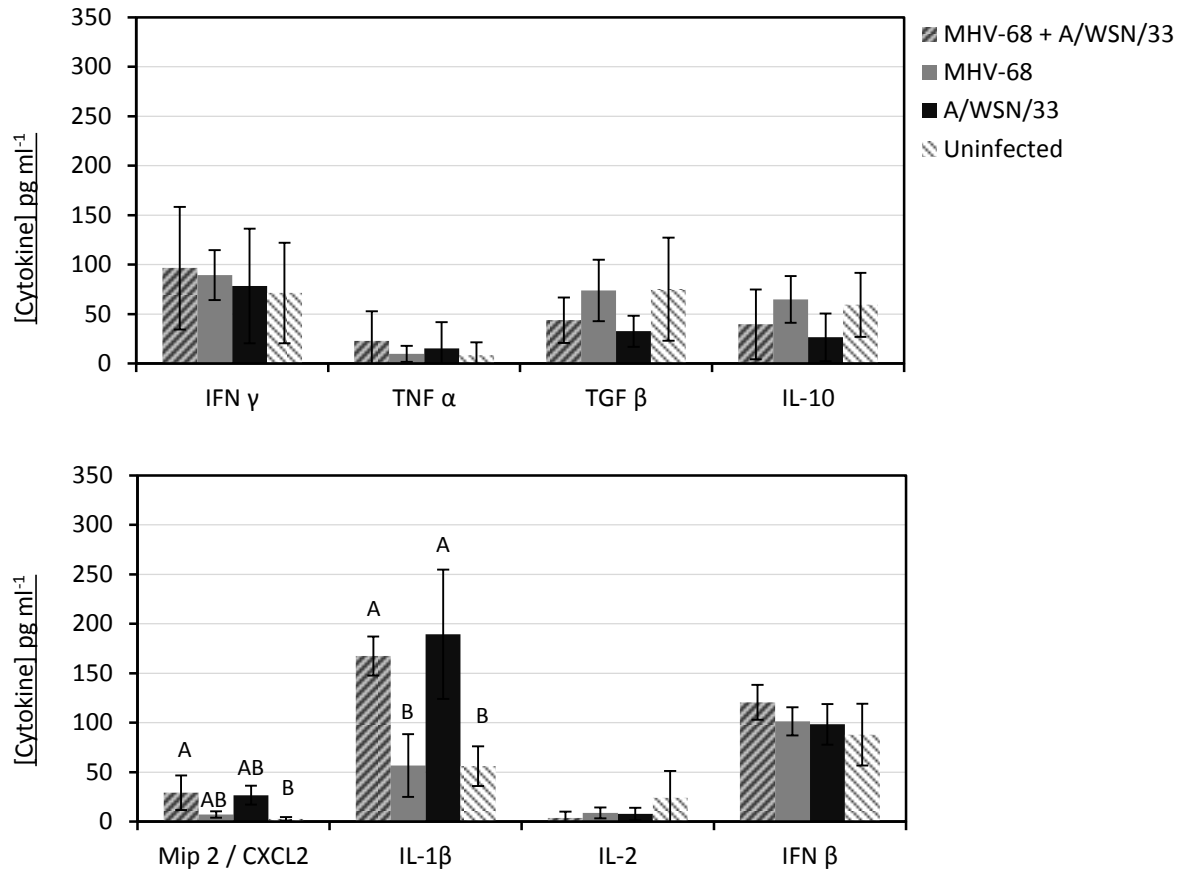
A similar pattern was observed for IL-10 expression where uninfected and MHV-68 infected mice express 64.58 and 59.29 pg ml⁻¹ of IL-10 whilst co-infected and A/WSN/33 infected mice had lower levels of 39.50 and 26.43 pg ml⁻¹ respectively. The standard deviation was similar across all groups (\sim 25-30 pg ml⁻¹) and therefore the decrease was not sufficient to gain any statistical significance.

A significant increase ($p < 0.05$ by GLM) in MIP2 (CXCL2) was observed in the co-infected mice 4 days post infection when compared with the uninfected group (29.19 \pm 17.38 pg ml⁻¹ compared with 2.71 \pm 1.82 correspondingly). A small increase in MIP2 in the MHV-68 infected group to 7.14 \pm 3.49 and a larger increase to 26.69 \pm 9.63 in the A/WSN/33 infected group was also observed however due to the low numbers of replicates in the case of this cytokine (data gathered from a single experiment) these differences are not statistically significant compared with the uninfected group. A significant increase in IL-1 β is also observed in both A/WSN/33 infected groups. Expression at 167.39 \pm 19.77 in the co-infected mice and 189.42 \pm 65.51 pg ml⁻¹ in the A/WSN/33 infected animals compared with mean expression of 56.01 and 56.78 pg ml⁻¹ in uninfected and MHV-68 infected control groups.

IL-2 and IFN β did not change in expression between experimental groups. IL-2 was only detectable in some samples as expression was at the point of detection in all groups. Mean averages of 3.67, 8.77, 7.65 and 23.89 pg ml⁻¹ were recorded in co-infected, MHV-68 infected, A/WSN/33 infected and uninfected groups respectively (Figure 3.6A). The uninfected group contained a single sample with 66.89 pg ml⁻¹ IL-2 which caused an increase in the average for this group and greater standard variation of \pm 27.21 pg ml⁻¹. This did not significantly increase the amount of IL-2 in the uninfected group compared with other experimental groups and standard deviations within the remaining groups were similar.

Figure 3.6 A/WSN/33 infection significantly increases IL-1 β and MIP2 at 4 days post infection and IFN γ and IL-10 6 days post infection

A. Day 4



B. Day 6

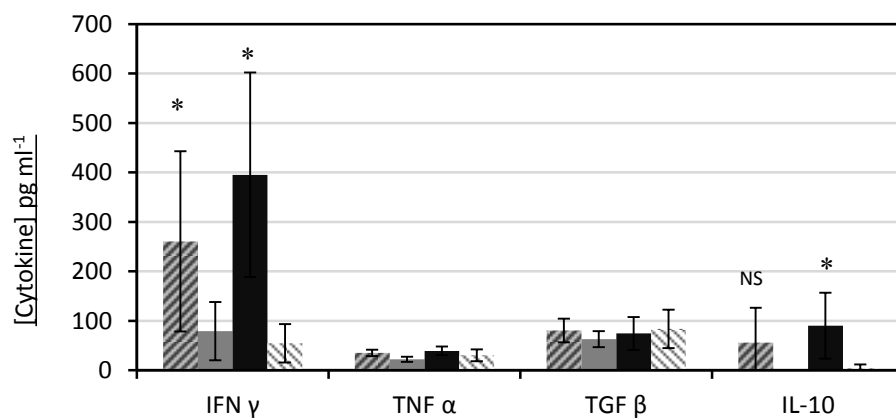


Figure 3.6 Lung homogenates were assayed by ELISA for IFN γ , TNF α , IL-10, TGF β , MIP2, IL-1 β , IL-2 and IFN β cytokines. Results are displayed as mean averages. Error Bars represent ± 1 standard deviation from the mean. **A.** Lung homogenates measured 4 days post infection. N=7, representative of 2 experiments excl. MIP2 / IL-1 β , IL-2 and IFN β where N=4 and is representative of a single experiment. Statistics measured by general linear model. Experimental groups with different letters are significantly different at 95% confidence. **B.** Lung homogenates measured 6 days post infection. Uninfected N=5, All others N=14, 2 experimental repeats. Statistics were measured by Kruskal-Wallis analysis and Mann-Whitney test (*=p<0.05).

IFN β levels at day 4 post infection were much higher than IL-2. All groups expressed ~ 100 pg ml $^{-1}$ of IFN β on average with similar variation within groups of 17-31 pg ml $^{-1}$. Co-infected mice had a subtle trend for increased IFN β with a mean average of 120 pg ml $^{-1}$ however this was again not statistically significant.

At day 6 of the low dose co-infection with MHV-68 and A/WSN/33, IFN γ levels were significantly increased in both co-infected ($p=0.0052$ measured by Kruskal-Wallis and Mann-Whitney test) and singly A/WSN/33 infected mice ($p=0.0006$). IFN γ level in co-infected mice was on average 260.59 pg ml $^{-1}$ compared with 395.00 pg ml $^{-1}$ in the A/WSN/33 infected mice (Figure 3.6B). Uninfected mice and MHV-68 infected mice have similar levels of IFN γ to those recorded at day 4 for these groups, 79.21 ± 53.19 and 54.59 ± 38.88 respectively. The increase in IFN γ is on average much greater in the A/WSN/33 infected mice than the co-infected group however large variation between biological replicates means this trend is not significant.

TGF β and TNF α levels were recorded at similar levels to that at day 4, and again did not show significance between groups (TGF β ~ 75 pg ml $^{-1}$ and TNF α $\sim 30-35$ pg ml $^{-1}$). IL-10 levels in both A/WSN/33 infected groups appear significantly greater than in uninfected and MHV-68 infected mice however the latter two groups contain mostly results below the level of detection. At day 4 IL-10 was detectable in all groups and therefore this difference is treated with caution. Co-infected mice express 55.50 pg ml $^{-1}$ IL-10 and A/WSN/33 infected mice express 90.15 pg ml $^{-1}$ which is similar to that at day 4. The IL-10 ELISA should therefore be repeated to clarify the variability in this result.

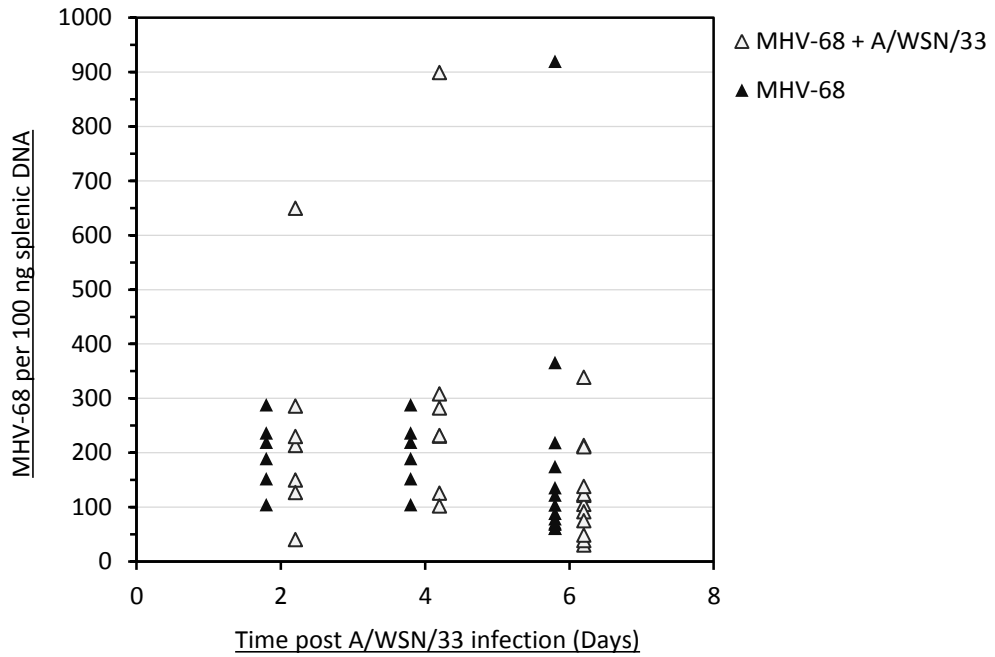
– Effect of A/WSN/33 co-infection on latent MHV-68

Influenza viral titre at day 6 was reduced as a result of co-infection (see Figure 3.3B). MHV-68 preferentially infects B cells of the spleen and lies dormant in a state of latency but also persists in the lung epithelial cells. A/WSN/33 strain of influenza primarily infected epithelial cells of the upper respiratory tract but also spreads out of the lung to other tissues in the mouse. To assess if co-infection impacts the persistent replication of MHV-68 in the lung or causes reactivation of MHV-68 in the spleen, viral load was measured.

MHV-68 is a DNA virus and may therefore be detected by qPCR with primers specific for a gene in the viral genome, (see section 2.10). Using primers designed for the orf 73 gene, MHV-68 viral load was quantified in the lung and spleen to determine the effect of A/WSN/33 induced inflammation on pre-existing MHV-68 latency. At day 2, 4 and 6 post A/WSN/33 infection MHV-68 levels in the spleen were similar, on average between 30 and 300 copies per 100ng of splenic DNA with occasional outliers at greater viral load (Figure 3.7A). Outliers were

Figure 3.7 Latent MHV-68 is not altered by low dose A/WSN/33 infection

A. Spleen MHV-68 viral load



B. Lung MHV-68 viral load

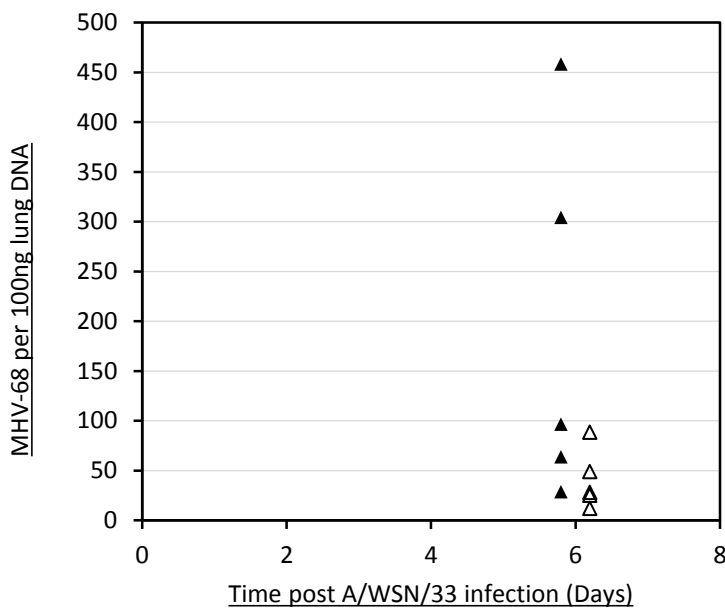


Figure 3.7 DNA was extracted from a segment of the spleen and the left lobe of the lung. Quantitative PCR for orf 73 in the MHV-68 genome was performed on 100 ng of DNA. **A.** MHV-68 viral load in spleen samples 2, 4 and 6 days post A/WSN/33 infection (30, 32 and 34 days post MHV-68 infection). N=7-15, 2 experimental repeats. **B.** MHV-68 viral load in the lung at 6 days post A/WSN/33 infection (34 days post MHV-68 infection), N=5. Results are displayed as individual values. Statistical analysis with two sample student's t test performed on log normalised data.

not specific to one experimental group. Average viral load was 242.2, 311.42 and 127.9 copies in the co-infected group on days 2, 4 and 6 and comparable levels of 198.2, 199.0 and 189.9 copies per 100ng on days 2, 4 and 6 were observed in the MHV-68 singly infected mice. Variation within the two groups was relatively large (between 100 and 200 copies) however this was similar in all groups tested at all time points and is therefore considered highly accurate for such low copy number at a high efficiency.

MHV-68 levels in the lung showed some discrepancy between experimental groups. Co-infected mice showed a trend for decreased lung titre however this was not significant ($p=0.077$, by 2 sample t test, Figure 3.7B). The mean average lung viral load was 40.5 copies with a small standard deviation of 20.6 copies in the co-infected group. The singly MHV-68 infected group varied to a greater degree (164.7) and averaged at 190.1 copies of MHV-68 per 100ng of DNA when measured in a reaction with an efficiency of 1.02.

3.4.2 Co-infection with latent MHV-68 and 5×10^2 A/WSN/33

At this time point the A/WSN/33 stock virus that was used during the co-infection experiments required thawing, aliquoting and re-titrating. Latent MHV-68 infected mice were again infected with 5×10^2 PFU A/WSN/33. In the previous 'low dose' experiments 5×10^2 PFU A/WSN/33 infection caused no weight loss. The re-titred virus caused weight loss and clinical signs. The re-titred virus concentration was verified by two independent plaque assays. It is therefore likely that the previous infections were performed at a dose lower than 5×10^2 PFU due to a miscalculation. The following experiments are therefore referred to as ' 5×10^2 A/WSN/33' infected while the previous experiments are referred to as 'low dose' infections.

– Effect of latent MHV-68 on co-infection with 5×10^2 A/WSN/33

Low dose A/WSN/33 infection did not cause any clinical signs. The increased dose caused moderate evidence of disease in singly A/WSN/33 infected mice. In this higher dose model it was possible to see if MHV-68 co-infection could moderate the pathogenesis of A/WSN/33 infection by alleviating or exacerbating the observable changes to behaviour and weight variation during the experimental time course.

At 5×10^2 dose, A/WSN/33 infection results in moderate clinical signs (Figure 3.8B). Mice showed increased respiratory effort, scored on average above 1 at day 5; decreased mobility, scored at an average of 1.5 by day 5; a staring coat, scored on average at 1.5 on day 5 and hunched appearance scored on average at 1.0 by day 5, accumulating to a sum of 4.9 (moderate severity). On day 6 all categories were scored at 1.5 for each mouse, increasing the sum total to 6 and maintaining the moderate severity threshold. Mice infected with 5×10^2 A/WSN/33 alone

also showed significant weight loss at day 5 (Figure 3.8A), with a reduction of 4.39% ($p<0.01$); at day 6 with a reduction of 11.41% ($p<0.01$) and at day 7 with a reduction of 16.51% ($P<0.001$) compared with their respective starting weights. Standard deviation within this group increased during the time course with 0.84%, 1.32%, 2.28% and 2.60% variability from the mean on days 4, 5, 6 and 7 following A/WSN/33 infection (Figure 3.8A).

Mice co-infected with latent MHV-68 showed less weight loss during the time course. Co-infected mice began to show anorexia at day 6, with a significant decrease of 4.15% compared with MHV-68 infected and uninfected mice ($p<0.05$). Weight loss in the co-infected mice increased to an average of 6.74% at day 7 ($p<0.01$) which was significantly greater than MHV-68 infected and uninfected controls and a significantly lower reduction than singly A/WSN/33 infected mice despite greater variation in weight loss within this group (Figure 3.8A). Standard deviation of the co-infected group was 1.80% and 2.31% on days 6 and 7 respectively.

Clinical signs were also much less severe in the co-infected group. Some, but not all, mice showed mild clinical signs from 5 days post infection, a day later than A/WSN/33 solely infected mice. The mice did not show severe staring coat (scored at 0.5 on average on day 6 and day 7) and incurred only a mild decrease in mobility (on average scored 0.5) by the cull date (Figure 3.8B). Summation of these clinical signs with mild (0.5) average scoring of hunched stature and increased respiratory effort (0.5), means that co-infected mice were scored on average at a severity score of 2 by day 7 and were therefore only showing mild signs of infection compared to the moderate clinical manifestations observed in the singly A/WSN/33 group.

The uninfected and MHV-68 infected mice showed no signs of infection and are not clinically scored. Weights are maintained close to 100% compared with day 0. The uninfected mice were $99.93\pm 0.68\%$ of their original weight on day 7 and MHV-68 infected mice were $102.65\pm 5.50\%$ of their original weight on day 7.

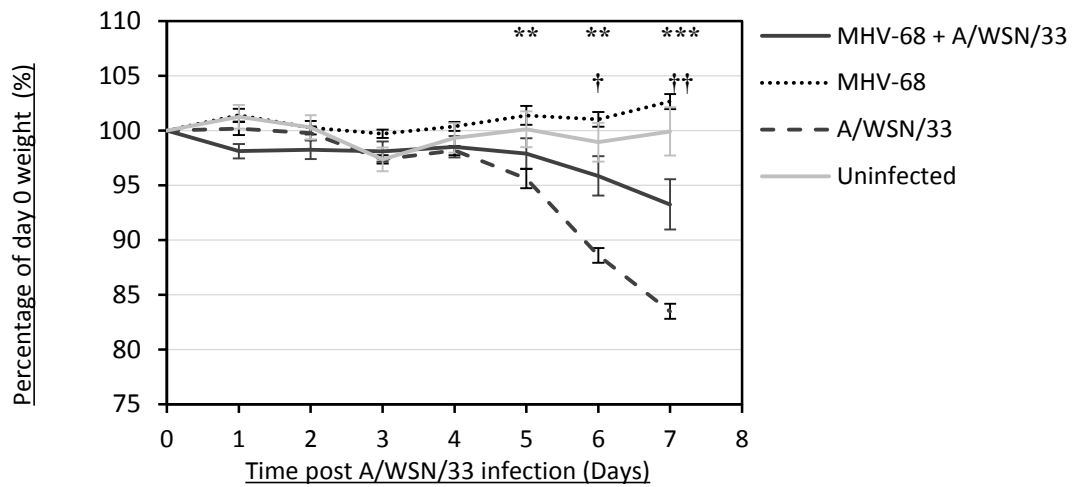
In the low dose infection, there was no change in influenza titre in the lung or weight loss (Figure 3.8C). Therefore to determine if the clinical manifestations and weight loss differences observed during the co-infection with 5×10^2 A/WSN/33, viral titres were measured at the peak of replication, day 4 and during the clearance of infection at day 7. At day 4 and day 7 lungs were excised and influenza titre calculated by plaque assay as described in section 2.4. Normality of the data was tested by probability plot (Anderson Darling test).

At day 4 the data were normally distributed ($p=0.051$) however at day 7 the data were not normally distributed ($p<0.01$). Day 4 has fewer values ($n=7$) and was close to the limit of

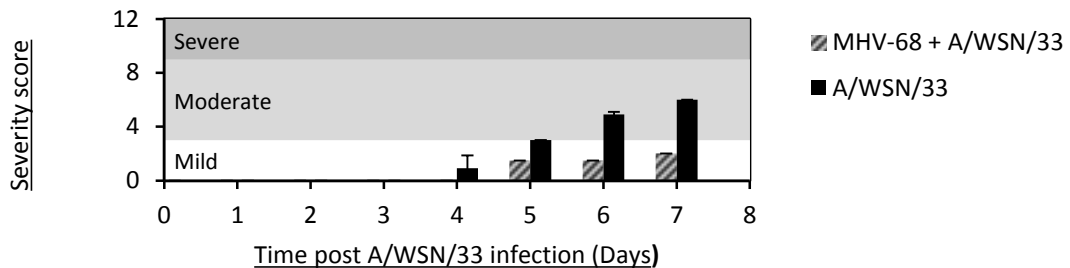
normality testing, therefore all titres were log transformed to produce normal distribution. At day 4 there was no significant difference between co-infected and A/WSN/33 infected mice.

Figure 3.8 Pre-existing latent MHV-68 infection reduces susceptibility to 5×10^2 A/WSN/33 infection

A. Weight loss



B. Clinical severity score



C. Influenza titre

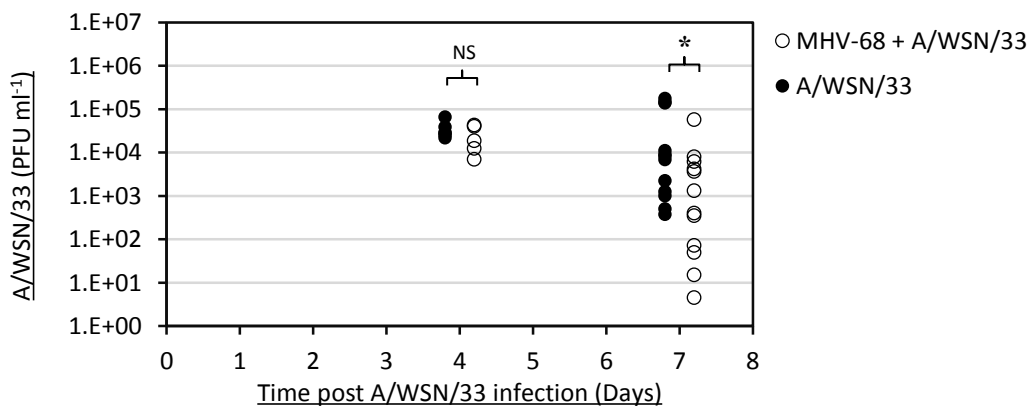


Figure 3.8 – 5-6 week old female BALB/c mice were infected I.N. with 5×10^4 MHV-68 and 28 days later infected I.N. with 5×10^3 A/WSN/33 in 40 μ l Dulbecco's minimum essential medium or medium alone. **A.** Influenza induced weight loss. Error bars represent ± 1 standard deviation of the mean. Significance determined by students two-way ANOVA (\dagger / $*$ = $p < 0.05$, $**$ / $\dagger\dagger$ = $p < 0.01$, $***$ / $\dagger\dagger\dagger$ = $p < 0.001$). **B.** Clinical severity was measured by 4 signs. Each was scored on a scale of 0-3 and the sum reported ± 1 standard deviation as clinical severity score, $N=6$. **C.** Mean A/WSN/33 titre in the lung, $N=7$ at day 4, $N=13$ at day 7, 2 experimental repeats. Significance determined by students 2-sample T test on log transformed data ($*$ = $p < 0.05$)

A/WSN/33 infected mice however showed a trend for a slight increase in mean titre. This group averaged 2.44×10^4 PFU ml⁻¹ of lung homogenate with a standard deviation of $\pm 14,716$ PFU whilst co-infected mice averaged 3.45×10^4 PFU ml⁻¹ with an almost identical standard deviation of $\pm 14,726$ PFU (Figure 3.8C). The two groups were therefore not statistically different. At day 7 the same trend was present. Singly A/WSN/33 infected mice had an average of 4.17×10^4 PFU ml⁻¹ albeit with a greater standard deviation of $\pm 65,000$ PFU. Co-infected mice had a much lower mean average of 6.27×10^3 PFU ml⁻¹; almost a log decrease compared to the singly infected mice. All except a single value were below 1×10^4 PFU, with 4 mice demonstrating infectious titres below 100 PFU ml⁻¹, (n=13 from 2 independent experiments). This difference was therefore statistically significant, (students 2 sample T-test p=0.023).

– Pathology in the lung

The pathology in the lung at this dose of A/WSN/33 infection was more severe. The uninfected mice however had no evidence of pathology. Lungs were inflated in 10% neutral buffered formalin and scored for histological evidence of disease. Uninfected mice (Figure 3.9A-C) had no inflammation or infiltration of cells and clear alveolar spaces (Figure 3.9C).

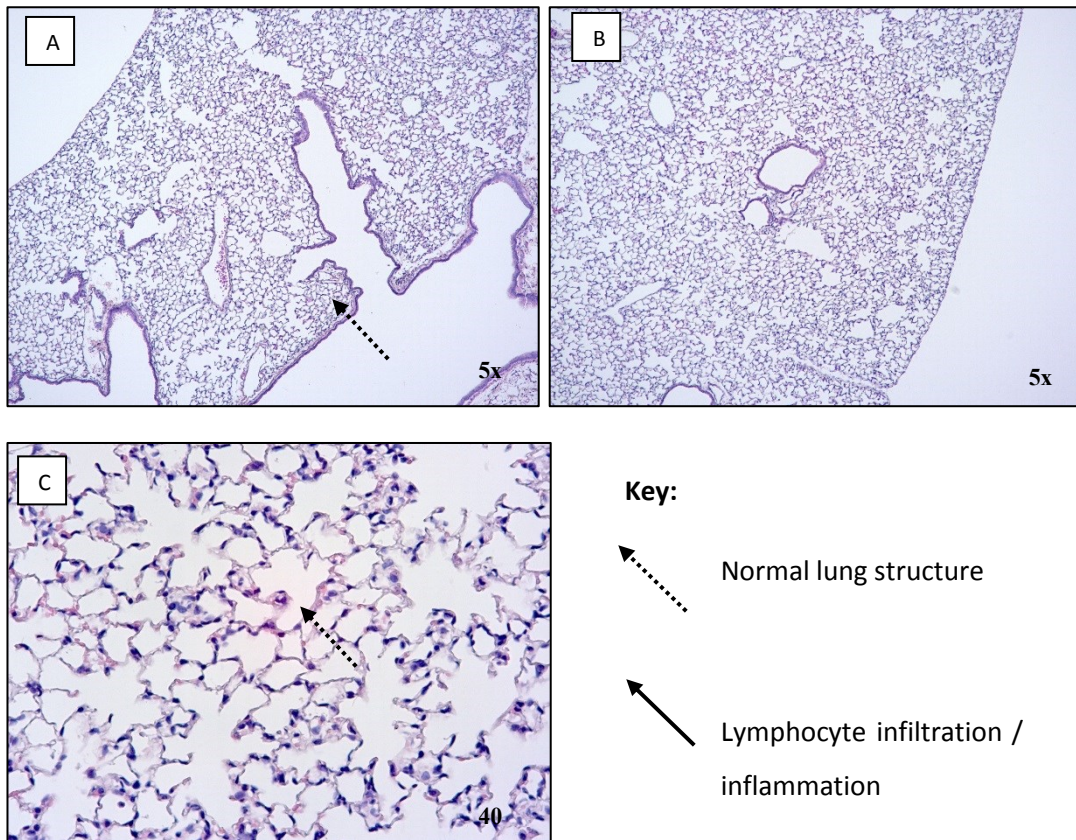
MHV-68 infection had no significant impact on the integrity of the lung (Figure 3.9D and 3.9F) however as discussed in 3.4.1, MHV-68 infection resulted in small, sporadic foci of lymphocyte accumulations in the interstitial spaces in the lung, Figure 3.9D and 3.9E). MHV-68 infection was therefore scored in some cases with very mild pathology in the lung (Figure 3.10) distinguishing this group from the uninfected mice.

5×10^2 A/WSN/33 infection caused moderate pathology in the lungs. Infiltration of lymphocytes into the spaces surrounding the large and small airways (scored at an average of 2.00, Figure 3.10) and blood vessels (scored at 2.30) and subsequent inflammation was evident (Figure 3.9G and 3.9H) alongside more severe epithelial necrosis (scored at 1 in all mice) than was measured in the low dose experiments. Cell infiltration into the alveolar spaces in the lung was also more prevalent in the higher dose infection. Cells including lymphocytes and macrophages were identified in the alveolar spaces (Figure 3.9I).

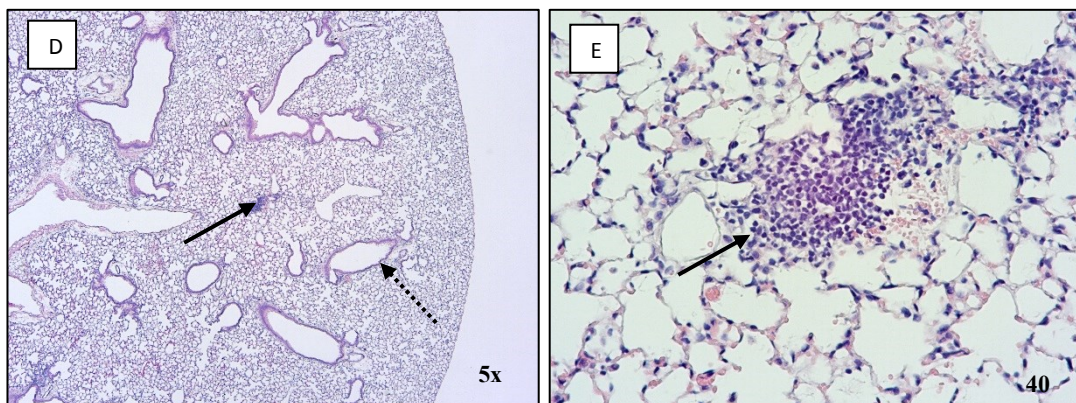
Co-infection with latent MHV-68 reduced the pathology of the A/WSN/33 infection in the lung. Peri-vascular infiltration of lymphocytes was scored at an average of 1.5 for this group and peri-bronchial infiltration of cells was 1.58 on average (Figure 3.9J and 3.9K). While epithelial necrosis did not significantly differ compared with the A/WSN/33 infected mice, there was more variation in the co-infected group, which averaged at a score of 0.75, (Figure 3.10). Cell recruitment into the alveolar spaces was also reduced in these mice, as seen in Figure 3.9L).

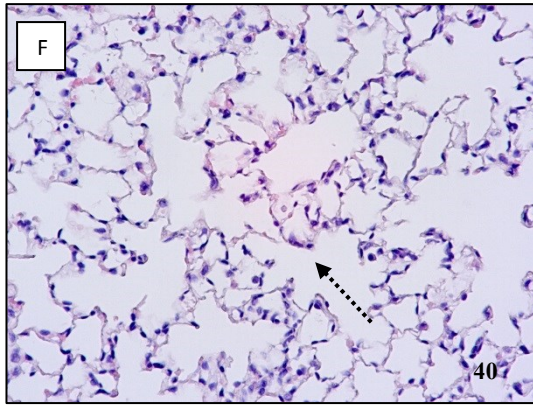
Figure 3.9 MHV-68 latent infection reduces the extent of 5×10^2 A/WSN/33 pathology in the lung

Uninfected

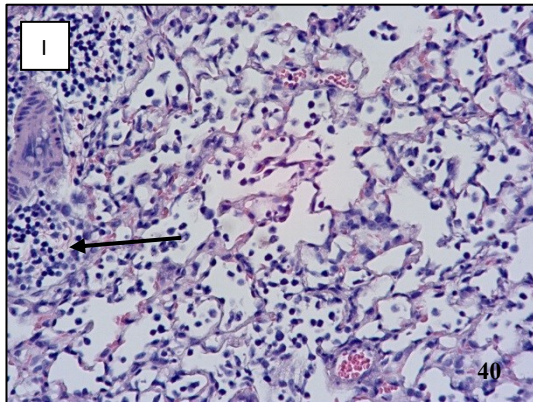
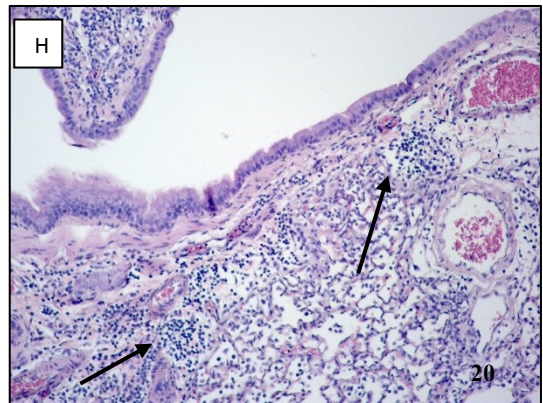
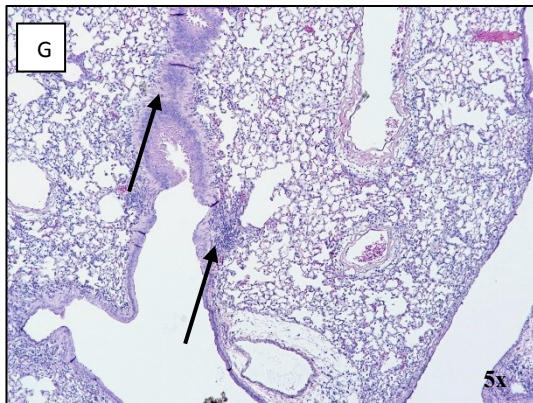


MHV-68 infected

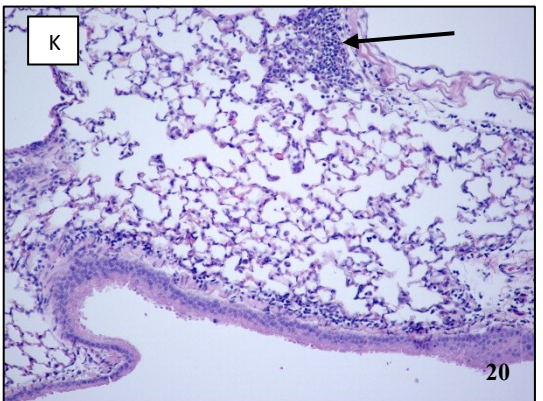
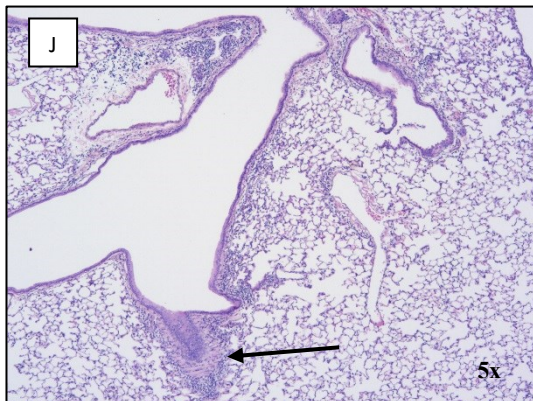




5x10² A/WSN/33 infected



MHV-68 + 5x10² A/WSN/33



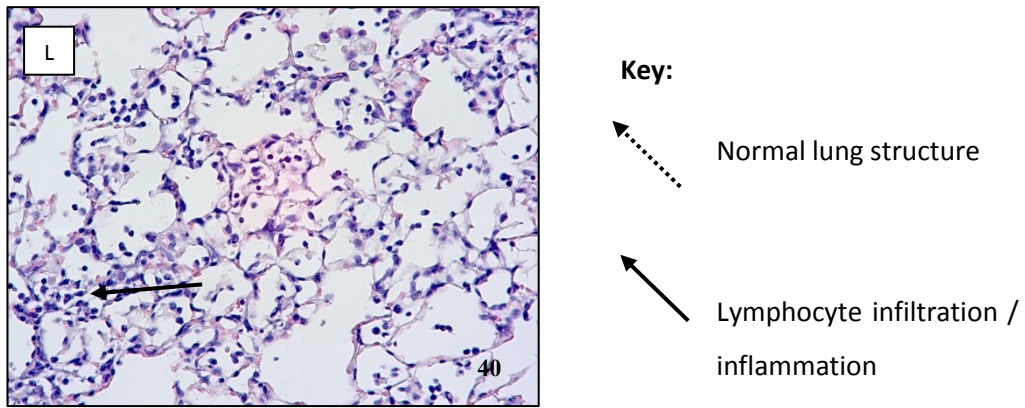


Figure 3.9: The right lung was inflated and fixed with 10% neutral buffered formalin. Lung sections were stained with hematoxylin and eosin. Representative sections are shown. Dashed arrows show areas of unaffected airways and blood vessels. Solid arrows demonstrate regions of lymphocyte infiltration and inflammation. **A-C** Lungs from uninfected mice. **D-F** Lungs from MHV-68 latently infected mice. **G-I** Lungs from A/WSN/33 infected mice. **J-L**. Lungs from MHV-68 + A/WSN/33 infected mice. Images are representative averages from each infection group. Magnification is identified in the bottom right corner of each image.

Figure 3.10 A/WSN/33 pathology score is reduced by latent MHV-68 infection

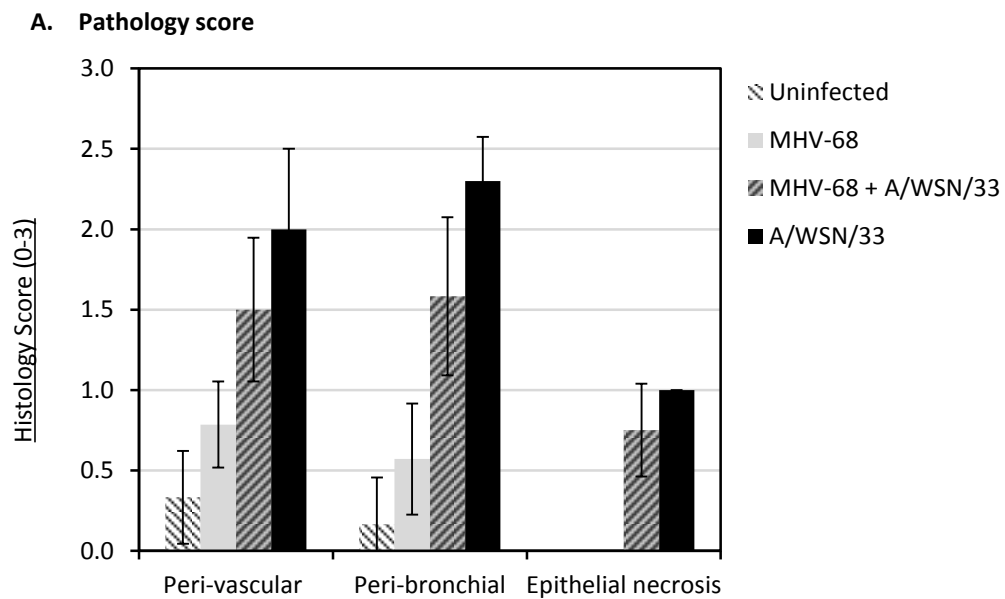


Figure 3.10 A. Complete lung cross-sections were scored for signs of inflammation and cell damage, N=6. Representative of 2 experiments. Results are displayed as mean average per group \pm 1 standard deviation.

– Cytokine environment in the lung

Influenza virus titre is altered at day 7 post infection by pre-existing co-infection with latent MHV-68. Pathology in the lung is also alleviated. To determine if reduced inflammation, or increased regulation of inflammatory viral responses by cytokines were responsible for this attenuation and subsequent reduction in clinical signs, lungs were excised 4 and 7 days post infection and cytokines in lung homogenates measured by ELISA.

At 4 days post infection, all experimental groups had similar levels of inflammatory and regulatory cytokines. The levels of $\text{IFN}\gamma$, $\text{TNF}\alpha$, $\text{TGF}\beta$ and IL-10 were similar to those detected in the low dose infection group. Inflammatory $\text{IFN}\gamma$ showed an increase on average in all infected groups, however this was not significant due to a large variation in all experimental groups infected with A/WSN/33. A low baseline level of $5.68\pm 7.58 \text{ pg ml}^{-1}$ $\text{IFN}\gamma$ was evident in the uninfected group (Figure 3.11A). A slight increase to $32.49\pm 7.91 \text{ pg ml}^{-1}$ was recorded in MHV-68 infected mice and then a large average increase to 60.38 and 40.35 pg ml^{-1} was seen in the co-infected and A/WSN/33 infected mice respectively. These increases however were coupled with an increase in standard deviation of ± 51.69 in the co-infected mice and ± 46.74 in the A/WSN/33 infected mice. Therefore when this was measured statistically, the difference was not significant.

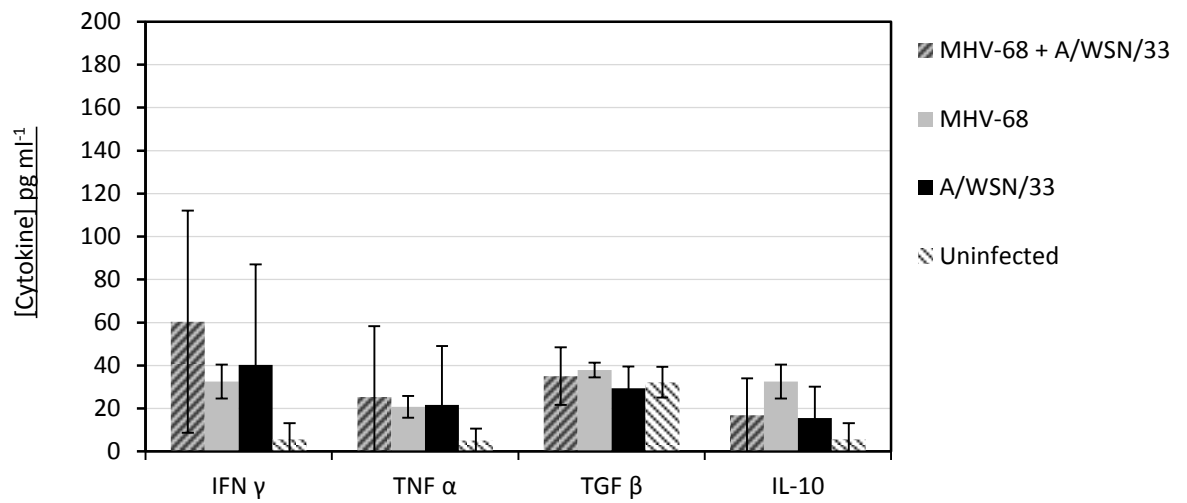
$\text{TNF}\alpha$ levels were shown with a highly similar pattern of detection, with $5.15\pm 5.56 \text{ pg ml}^{-1}$ observed in the uninfected mice, a subtle increase to $20.79\pm 5.09 \text{ pg ml}^{-1}$ and then slightly larger mean averages seen in the co-infected (25.37 pg ml^{-1}) and A/WSN/33 infected (21.60 pg ml^{-1}) groups, again coupled with larger standard deviations of ± 32.93 and ± 27.50 correspondingly. Regulatory cytokine levels were also monitored to determine if variation was due to increased suppression of inflammation.

IL-10 levels in the uninfected mice were $5.68\pm 7.58 \text{ pg ml}^{-1}$ and increased to 32.49 ± 7.49 , 16.87 ± 11.19 and 15.57 ± 14.53 in the MHV-68 infected, A/WSN/33 infected and co-infected mice (Figure 3.11A). There was no statistical significance between group averages. $\text{TGF}\beta$ also showed little variation in averages and standard deviations between groups, with all groups recorded at an average of 30-40 pg ml^{-1} , 4 days post infection.

At 7 days post infection both singly A/WSN/33 infected and co-infected groups demonstrated a significant increase in $\text{IFN}\gamma$ ($p=0.0022$ and 0.0019 respectively by Mann-Whitney test) compared with the uninfected mice. Uninfected mice and MHV-68 infected mice had 14.25 and 14.28 pg ml^{-1} $\text{IFN}\gamma$ present in the lung whilst the co-infected mice increased to a mean average of $305.52 \text{ pg ml}^{-1}$ and A/WSN/33 infected mice increased further to $391.45 \text{ pg ml}^{-1}$ (Figure 3.11B). As with the response of this cytokine at day 4, increased averages were coupled with an

Figure 3.11 5×10^2 A/WSN/33 infection increases IL-10 and IFN γ in the lung 7 days post infection

A. Day 4



B. Day 7

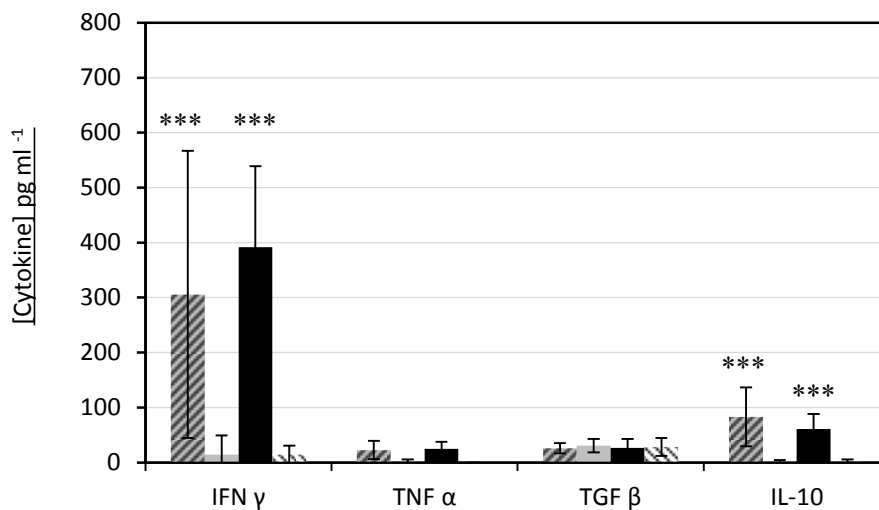


Figure 3.11 Lung homogenates were assayed by ELISA for IFN γ , TNF α , IL-10 and TGF β cytokines. Results are displayed as mean averages. Error Bars represent ± 1 standard deviation from the mean. **A.** Lung homogenates measured 4 days post infection. **B.** Lung homogenates measured 7 days post infection. N=6-14, 2 experimental repeats. Statistics measured by Kruskal-Wallis analysis and Mann-Whitney test. Infected groups were compared with uninfected littermates, (***)= $p < 0.01$).

increase in the standard deviation within these groups of 261.17 and 147.29 pg ml⁻¹ respectively. There was therefore no apparent significant difference due to MHV-68 latent co-infection. A single value (920 pg ml⁻¹) however in the co-infected group was responsible for the high mean value and variation. There was no reason to exclude this value however, so it remained in the analysis.

TNF α was detectable at levels similar to those seen at day 4, however the uninfected group contained samples that were below the level of detection. Averages of 22.72, 1.61 and 24.74 pg ml⁻¹ were recorded in co-infected, MHV-68 infected and A/WSN/33 infected mice. No statistics were performed due to the absence of a detectable uninfected control.

TGF β was detected at similar levels to that seen at day 4. Once again all experimental groups had mean averages of ~30 pg ml⁻¹ in the lung and standard deviations of ~10 observed in all groups.

IL-10 was increased at day 7 in both A/WSN/33 infected groups. MHV-68 and uninfected mice had a baseline level of IL-10 of 1.27 \pm 3.04 and 1.66 \pm 4.06 pg ml⁻¹ (Figure 3.11B). A significant increase to 83.01 \pm 53.53 in the co-infected group (p=0.0014) and 60.96 \pm 27.60 pg ml⁻¹ in the A/WSN/33 infected group (p=0.0015) was in accordance with similar increases in IFN γ in these groups. Many of the ELISA results contained groups with values below the limit of detection. Therefore non-parametric tests were used.

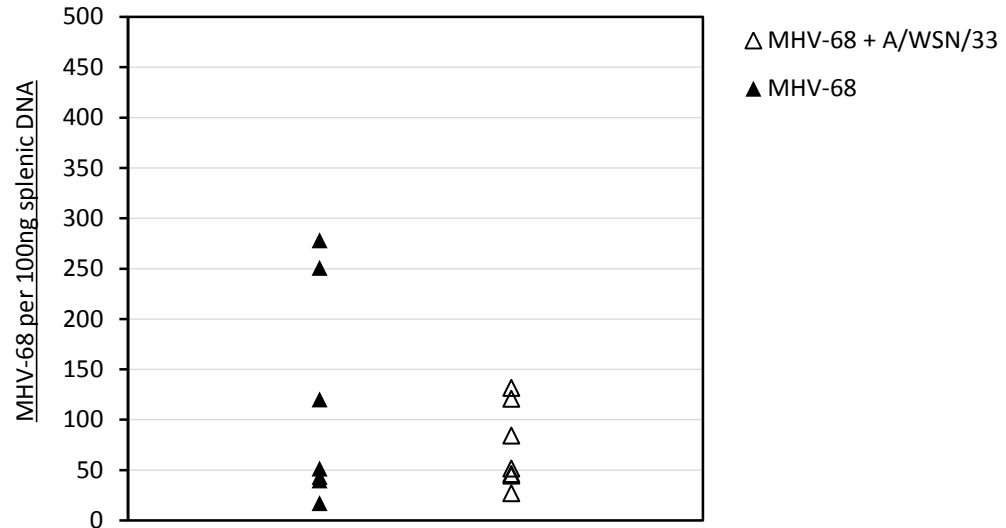
– Effect of A/WSN/33 on latent MHV-68 co-infection

Due to the altered kinetics of A/WSN/33 infection in the co-infected mice, it was hypothesised that MHV-68 latency may also now be affected by the presence of increased inflammatory cytokines in the lung. MHV-68 viral load is unaltered by 5 \times 10² A/WSN/33 infection in the spleen but significantly reduced in the lung. Spleen levels of MHV-68 were measured 7 days post A/WSN/33 infection (35 days post MHV-68 infection). Similar levels were observed to day 34 in the previous experiment infected at the same dose of 5 \times 10⁴ MHV-68 (3.12A). On average 74.12 \pm 37.63 copies per 100ng spleen DNA were detected in the co-infected mice whilst 114.21 \pm 99.60 copies were detected in the MHV-68 infected mice. The two groups were similar in their distribution and are therefore not significantly different.

However, there was a significant decrease in the expression of MHV-68 in the lung following A/WSN/33 infection, p=0.045 by student's t test on log normalised data. Co-infected mice had on average, 73.8 copies of the MHV-68 genome per 100 ng of lung DNA (Figure 3.12B). However this value, along with the large standard deviation of \pm 103.41 was due to a single (clearly outlying) value of 340 copies skewing the results (n=8). With this result included in the analysis there were still significantly lower levels of MHV-68 present in the co-infected mice

Figure 3.12 MHV-68 viral load is unaltered by 5×10^2 A/WSN/33 infection in the spleen but significantly reduced in the lung

A. Spleen MHV-68 viral load - Day 7



B. Lung MHV-68 viral load - Day 7

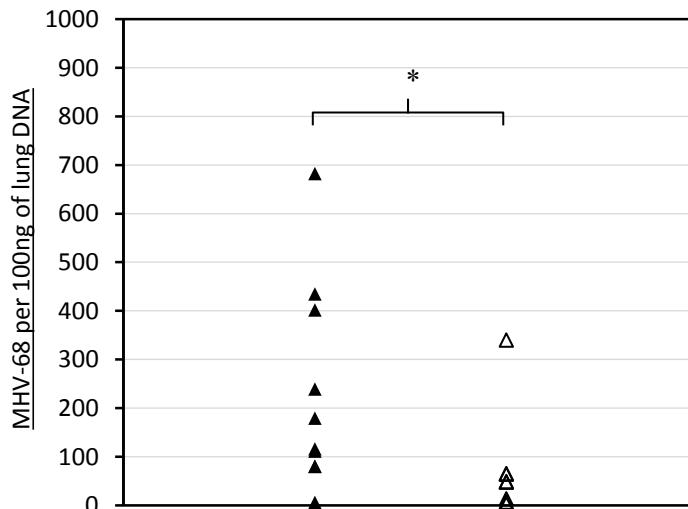


Figure 3.12 DNA was extracted from a segment of the spleen and left lobe of the lung. Quantitative PCR for orf 73 in the MHV-68 genome was performed on 100 ng of DNA. **A.** MHV-68 viral load in spleen samples 7 days post A/WSN/33 infection (35 days post MHV-68 infection). **B.** MHV-68 viral load in the lung at the same time point. N=7-8 representative of 2 experimental repeats. Results are displayed as individual values. Statistical analysis performed by two sample student's t test performed on log normalised data (*= $p < 0.05$).

than in the lungs of solely MHV-68 infected mice, where 233.3 ± 200 copies per 100ng was the average. These results were observed in 2 independent experiments.

– CD4⁺ lymphocyte phenotype in the mediastinal lymph nodes

Alterations to the cytokine environment in the lung and its resulting impact on both pathogens suggest that adaptive immune responses may be modified in response to the A/WSN/33 as a result of MHV-68 co-infection. Day 7 is a critical time point in the response to A/WSN/33, as it coincides with the onset of adaptive immunity. The CD4⁺ and CD8⁺ cells in the lung and lung draining lymph nodes (mediastinal) were stained for intracellular cytokine production.

7 days post infection cells from the lung draining lymph nodes were harvested and analysed by FACS for CD4⁺ intracellular cytokine production. IFN γ , IL-4 and IL-10 production by CD4⁺ cells were raised in mice infected with 5×10^2 A/WSN/33 ($p < 0.01$ for all groups). CD4⁺ cells in uninfected mice were only 1.3% positive for production of IFN γ when stimulated with PMA and ionomycin. Latent MHV-68 infection increased this number to $4.95 \pm 2.89\%$.

IFN γ production was raised in 2 mice in the MHV-68 infected group, and therefore IFN γ was not significantly different between this group and the A/WSN/33 infected and co-infected mice (Figure 3.13A). When comparing these results to the higher dose infection and day 0 mice it was only these 2 mice that appeared to have raised IFN γ levels in the MHV-68 infected group.

The single infection with A/WSN/33 and similarly co-infection increased IFN γ production further to $7.83 \pm 1.10\%$ and $8.69 \pm 2.40\%$ in turn. A/WSN/33 infected groups therefore produced significantly greater amounts of IFN γ than uninfected mice while the increase in MHV-68 infected mice was not significant.

IL-4 production by CD4⁺ cells was also increased by A/WSN/33 infection. IL-4 in uninfected mice was produced in $1.19 \pm 0.86\%$ of cells and to a similar level of $1.04 \pm 0.84\%$ in cells taken from the mediastinal lymph nodes of MHV-68 infected mice (Figure 3.13B). A/WSN/33 infection increased this number to $4.96 \pm 1.66\%$ and co-infected mice show an equally increased percentage of IL-4 production to $3.98 \pm 1.58\%$. The significant increase in IL-4 production in co-infected mice was lower than in the singly A/WSN/33 infected mice, as demonstrated by the reduction in p value, $p < 0.05$.

IL-10 production by CD4⁺ cells followed the same pattern (Figure 3.13C). Uninfected mice and MHV-68 infected mice were $0.70 \pm 0.48\%$ and $1.23 \pm 4.10\%$ positive for IL-10 whilst co-infected mice increased to $4.88 \pm 2.63\%$. This increase was slightly skewed by a single result with 10.20% of CD4⁺ cells producing IL-10, however, this particular mouse also demonstrated a

Figure 3.13 T_H1 $CD4^+$ T cell phenotype in lung draining lymph nodes is the same in A/WSN/33 and co-infected mice

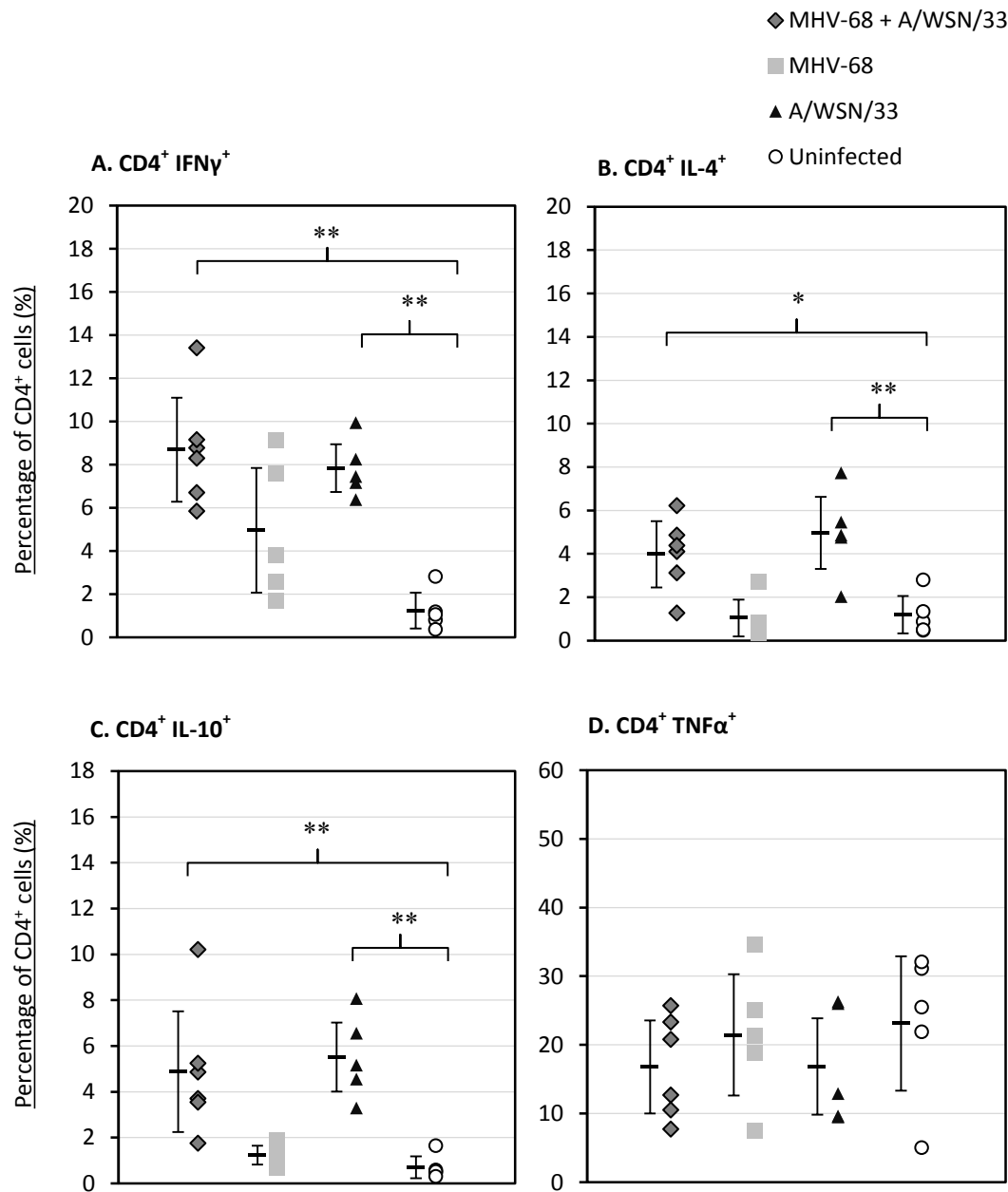


Figure 3.13 Mice were culled 7 days post A/WSN/33 infection. Lung draining lymph nodes were harvested. 1×10^7 cells were stained for $CD4^+$ T cell markers. Samples were run on a BD LSR II Fortessa. Results are displayed as individual percentages and mean per group \pm 1 standard deviation, N=6. Statistics calculated by general linear model on data from a single experiment, (*= $p < 0.05$, **= $p < 0.01$, ***= $p < 0.001$). **A.** $CD4^+$ $IFN\gamma^+$ cells. **B.** $CD4^+$ $IL-4^+$ cells. **C.** $CD4^+$ $IL-10^+$ cells **D.** $CD4^+$ $TNF\alpha^+$ cells.

larger production of IFN γ (13.4%). A/WSN/33 infection alone increased IL-10 production to $5.52\pm 1.51\%$ which was not significantly greater than the co-infected mice.

TNF α production was not significantly raised in any experimental group and was much more variable within groups (Figure 3.13D). The mean averages of CD4 $^+$ TNF α positive cells were between 17 and 23% and varied up to 9.8% which meant that this cytokine was not notably altered by either of the infections.

– CD4 $^+$ and CD8 $^+$ lymphocytes in the lung

While the CD4 $^+$ cell response in the lung was not significantly altered there was evidence of decreased IL-10 and IFN γ production in the co-infected group. To determine if this effect has altered the responses of CD4 $^+$ and CD8 $^+$ cells at the site of infection in the lung, cells from broncho-alveolar lavage (BAL) fluid were analysed by FACS.

Percentages of CD4 $^+$ and CD8 $^+$ cells were not different in the BAL fluid (Figure 3.14A and 3.14C). Co-infected mice had an average of 11.39% CD4 $^+$ lymphocytes and 34.16% CD8 $^+$ lymphocytes. This was comparable to an average of 12.3% CD4 $^+$ and 42.24% CD8 $^+$ lymphocytes recorded in singly A/WSN/33 mice. The variation from the mean was much greater for the CD8 $^+$ lymphocytes in both groups however co-infected mice demonstrated greater variation in both groups of cells. The number of cells in BAL fluid was low and was predominantly composed of macrophages and other non-lymphocyte populations. Therefore uninfected and MHV-68 singly infected mice only had very low numbers of CD4 $^+$ and CD8 $^+$ T cells and are not shown.

While the responding lymphocytes in the lung were composed of similar percentages of CD4 $^+$ and CD8 $^+$ cells, the cytokine production may vary, in reflection of the altered cytokines detected by ELISA and reduced weight loss.

CD4 $^+$ cells did not show differences in their inflammatory cytokine (IFN γ and TNF α) production. CD4 $^+$ cells from co-infected mice were on average $30.87\pm 2.57\%$ positive for IFN γ production whilst A/WSN/33 infected mice were $33.60\pm 5.85\%$ positive. TNF α was produced at much lower levels however this also did not vary between experimental groups with an average of $11.64\pm 4.16\%$ CD4 $^+$ cells in the co-infected mice and $9.90\pm 6.58\%$ in the A/WSN/33 infected mice (Figure 3.14B).

Whilst not statistically significant, the most notable difference in cytokine production was seen as a trend for increased production of inflammatory cytokines IFN γ and TNF α by CD8 $^+$ cells in the co-infected mice. IFN γ was produced by $41.90\pm 12.79\%$ CD8 $^+$ cells in A/WSN/33 infected mice and at a lower percentage of $58.3\pm 9.58\%$ in the CD8 $^+$ cells from co-infected mice. An

Figure 3.14 CD8⁺ cells in the lungs of co-infected mice produce increased levels of inflammatory cytokines 7 days after 5x10² A/WSN/33 infection

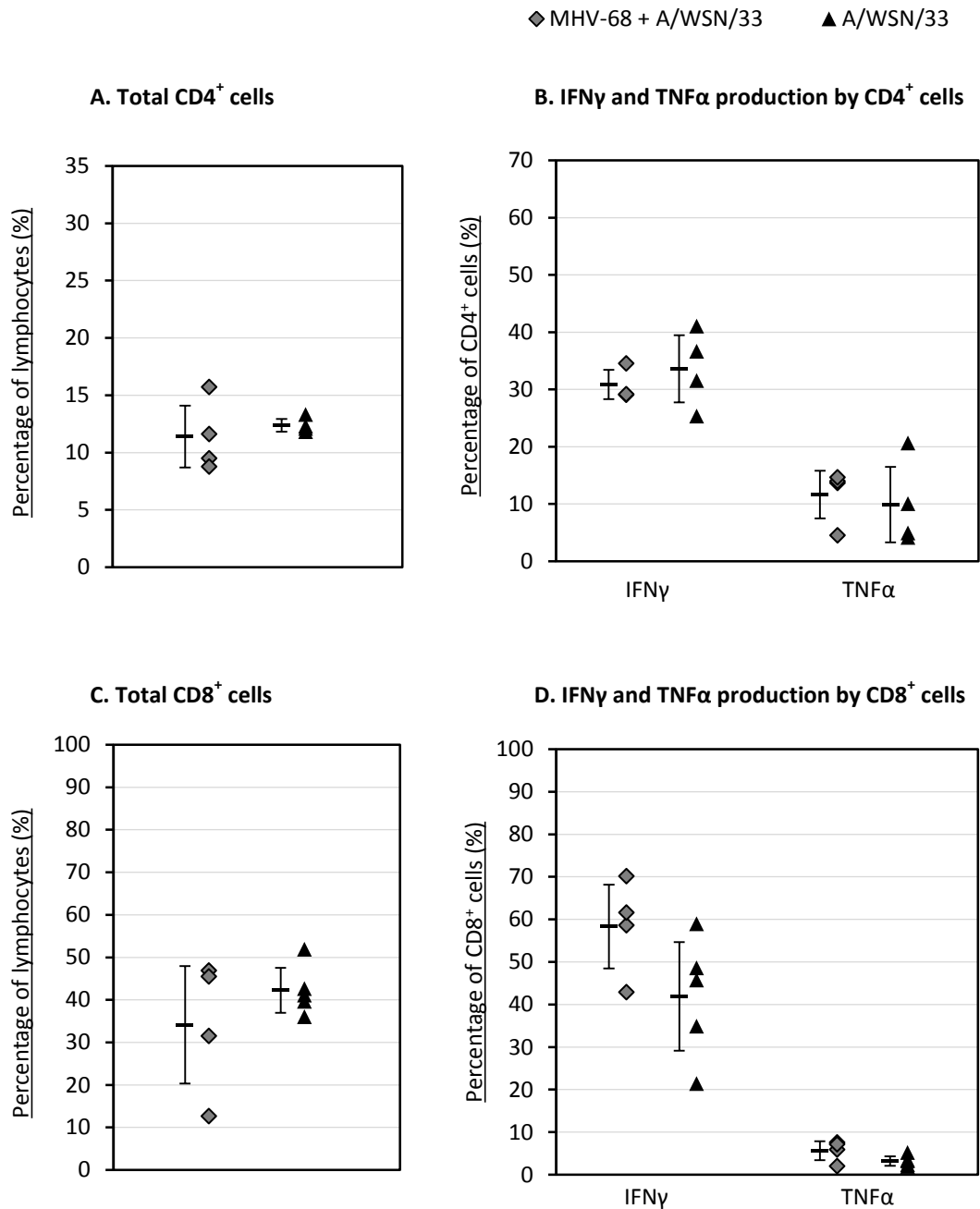


Figure 3.14 Mice were culled 7 days post A/WSN/33 infection and cells in the lung were harvested by bronchoalveolar lavage (BAL). Maximum numbers of cells in the BAL fluid were stained for a range of intracellular CD4⁺ and CD8⁺ T cell markers. The samples were run on a BD LSR II Fortessa. Results displayed as individual percentage per sample and mean average per group \pm 1 standard deviation, N=4-5. All statistics are calculated on data from a single experiment, (*=p<0.05, **=p<0.01, ***=p<0.001). **A.** Total CD4⁺ cells **B.** CD4⁺ IFN γ ⁺ and CD4⁺ TNF α ⁺ cells **C.** Total CD8⁺ cells **D.** CD8⁺ IFN γ ⁺ and CD8⁺ TNF α ⁺ cells.

increase in the number of biological replicates would likely improve the outcome of this difference statistically ($p=0.104$).

As with the $CD4^+$ lymphocytes, $TNF\alpha$ production was detected at a much lower frequency than $IFN\gamma$. $CD8^+$ cells taken from the co-infected mice were $5.66\pm 2.20\%$ positive for $TNF\alpha$ whilst A/WSN/33 infected mice were on average $3.22\pm 1.13\%$ positive for this cytokine (figure 3.14D).

Regulation of inflammation by IL-10 production was also hypothesised to be part of the suppressive mechanism seen during co-infection. IL-10 expression by $CD8^+$ and $CD4^+$ cells was also measured however this cytokine was only expressed in a low number of cells and is therefore not reported.

3.4.3 Co-infection with latent MHV-68 and 5×10^3 A/WSN/33

Increasing the A/WSN/33 dose to a moderate severity increased the observed clinical signs during the course of infection. The co-infected mice were less susceptible to infection with A/WSN/33. To determine whether this protective effect was dose dependent and could still confer protection during a more severe pathogenesis, the dose of influenza A was increased again to 5×10^3 PFU.

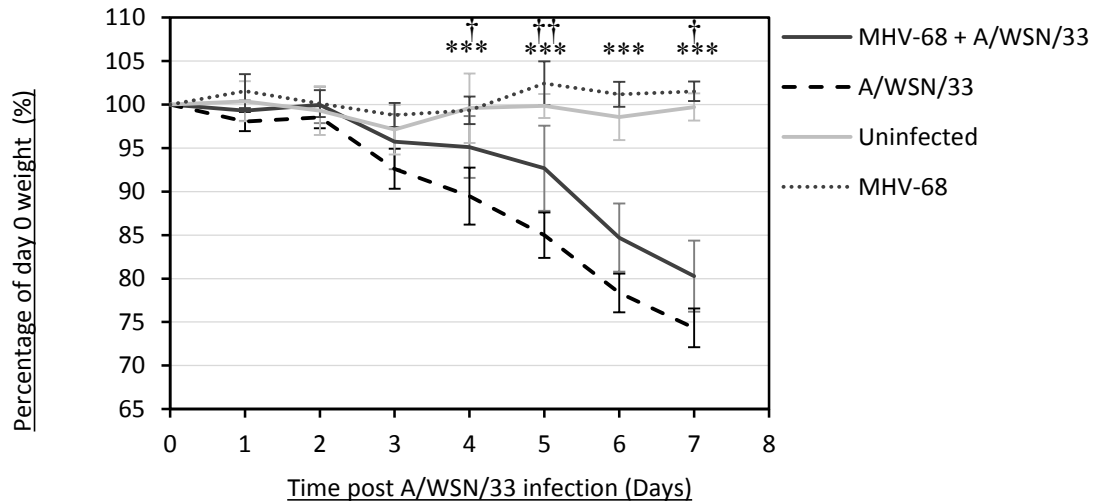
– Effect of latent MHV-68 on co-infection with A/WSN/33

As previously described, mice were scored for clinical signs and weight loss every 24 hours. At the 5×10^3 dose, A/WSN/33 infection resulted in severe clinical signs. At day 4 mice were showing moderate signs of infection. This was a day earlier than in the 5×10^2 infection although there was greater variation within the group. By day 5 increased respiratory effort, staring coat, hunched stature and reduced mobility were all scored above 2 for all animals (Figure 3.15B). The sum therefore reached an average of 9.5 and clinical signs were now consistent amongst all mice in the group. This was maintained through to day 6 and then worsened at day 7 when hunching, staring coat and respiratory effort were scored at 3 and reduced mobility at an average of 2.5. The mean severity rating reached an average of 11.5 on this day.

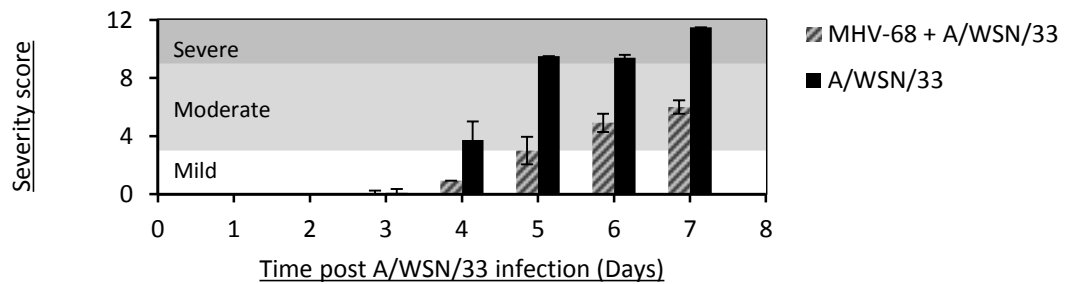
Mice infected with 5×10^3 A/WSN/33 alone also showed significant weight loss compared with uninfected and MHV-68 infected groups from day 4 onwards, ($p<0.05$). At day 4 $7.4\pm 2.3\%$ was the mean weight loss, increasing to 10.53% by day 5 ($p<0.001$) and 15.02% on day 6 ($p<0.001$) (Figure 3.15A). By day 7 A/WSN/33 infected mice had lost a mean average of 22.38% of their weight recorded at day 0 ($p<0.001$). The standard deviation from the mean was less than $\pm 3.0\%$ at all time points measured in this group.

Figure 3.15 MHV-68 latency significantly reduces susceptibility to high dose 5×10^3 A/WSN/33

A. Weight loss



B. Clinical severity score



C. Influenza lung titre

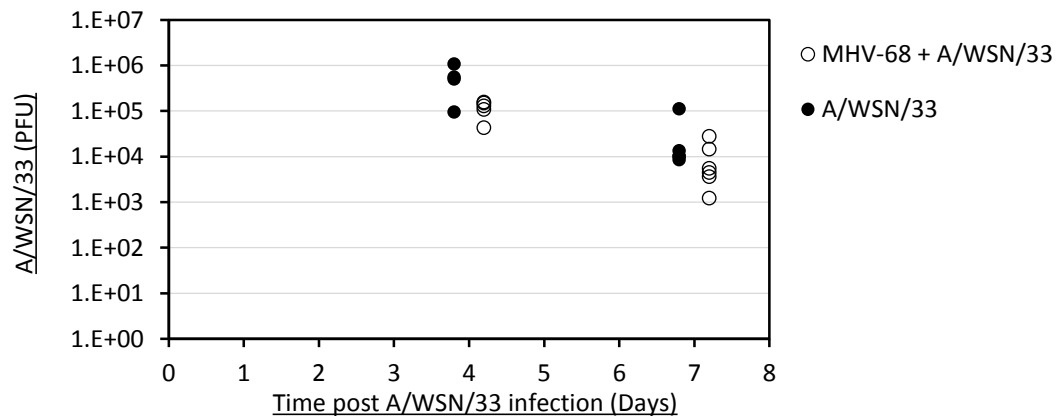


Figure 3.15 – 6 week old female BALB/c mice were infected I.N. with 5×10^4 MHV-68 and 28 days later infected I.N. with 5×10^3 A/WSN/33 in 40 μ l Dulbecco's minimum essential medium or medium alone **A.** Influenza induced weight loss. Error bars represent ± 1 standard deviation of the mean. Significance determined by two-way ANOVA, (\dagger / $*$ = $p < 0.05$, $**$ / $\dagger\dagger$ = $p < 0.01$, $***$ / $\dagger\dagger\dagger$ = $p < 0.001$) * signifies significant difference between A/WSN/33 infected and the uninfected groups. \dagger signifies significant difference between co-infected and A/WSN/33 infected groups. **B.** Clinical severity was measured by 4 signs, each was scored on a scale of 0-3 and the sum reported ± 1 standard deviation as clinical severity score, $N=12$. **C.** Mean A/WSN/33 titre in the lung ± 1 standard deviation, $N=12$.

The co-infected mice now showed much more significant weight loss and clinical signs than was observed in the same group infected with 5×10^2 A/WSN/33 in the previous experiments. A significant decrease in weight occurred at day 5 with a $7.33 \pm 4.9\%$ weight loss compared with day 0, increasing to $15.30 \pm 3.92\%$ at day 6 and $19.72 \pm 4.10\%$ (Figure 3.15A). The variation from the mean was recorded by standard deviation and was much greater within this group and increased over the time course as some mice appeared to be better protected than others.

Weight loss was directly associated with increasingly severe clinical signs. Co-infected mice showed a more gradual increase in severity over the time course than A/WSN/33 alone with an onset of clinical signs in some of the mice as early as 4 days post infection. The hunched stance and slight staring in the coat (averaged at 0.5) was not coupled with an increased respiratory effort or decreased mobility. Day 5 was the onset of increased respiratory effort and slowed movement in some mice, however, at this point clinical signs varied widely within the group, with some mice showing few signs of infection and others scored at 4, in the 'moderate' severity category. Mean scoring increased to 6.8 at day 6 and 8.7 at day 7 when all mice showed an increased respiratory effort (2.5 average), decreased mobility (2.0 average), staring coat (2.3 average) and hunched stature (2.0). The standard deviation at this time point was ± 0.4 (Figure 3.15B). Co-infected mice were still protected from A/WSN/33 at this dose however to a lower degree. Statistical significance was recorded at days, 4, 5 and 7 ($p < 0.05$, $p < 0.01$, $p < 0.05$, tested by general linear model).

The uninfected mice and latent MHV-68 singly infected mice had no significant changes in weight and did not produce any clinical signs of infection. Uninfected mice were on average 101.57% of their original body weight at day 0 and MHV-68 infected mice were 99.70%.

At day 4 and day 7 the lungs were excised and the influenza titre was calculated by plaque assay. At day 4, the peak of viral replication, A/WSN/33 infected mice had a mean titre of 5.57×10^5 PFU ml⁻¹; a log increase compared with the lower dose infection. Co-infected mice had on average, lower replicating virus in the lung (1.18×10^5 PFU ml⁻¹).

In the A/WSN/33 infected group, influenza titre decreased to 3.10×10^4 PFU ml⁻¹ at day 7, which is still a log greater than the virus seen at this time point in the lower dose infection (Figure 3.15C). Similarly co-infected mice still had 9.55×10^3 PFU ml⁻¹ replicating virus in the lungs on average on day 7. At this time point in the lower dose infection these mice were nearing complete clearance. At the day 4 and day 7 time points there was no statistically significant difference in lung A/WSN/33 titres, ($p = 0.242$ and $p = 0.152$ respectively). Students 2 sample T-test, log normalised data). There is again a repeat trend for decreased titres in the co-infected mice however this is less apparent than at the lower dose infection.

– Pathology in the lung

The effect of 5×10^3 A/WSN/33 infection is recorded in Figure 3.16. Uninfected mice once again showed no signs of disease, with clear alveolar spaces and no changes to peri-bronchial and peri-vascular inflammation. MHV-68 infected mice also maintained lung integrity however the small foci of lymphocyte accumulations described in previous experiments were once again evident in the interstitial spaces. These results are therefore not shown.

Infection with 5×10^3 A/WSN/33 caused severe inflammation around the large and small airways and around the blood vessels in the lung. Infiltration of lymphocytes was scored at an average of 2.4 at both the peri-vascular and peri-bronchial surfaces. This inflammation is evident in Figure 3.16A and 3.16B. Epithelial necrosis was scored at an average of 1.8, which is a small increase from the previous dose of infection (see Figure 3.16F for pathology scores).

Co-infected mice showed a trend for less severe inflammation. The inflammation in these mice was more prevalent than at the lower dose of infection (Figure 3.16C-F). Peri-vascular infiltration of lymphocytes was scored at 1.8 and peri-bronchial infiltration of cells was also scored at an average of 1.8 (Figure 3.16F). Epithelial necrosis however was scored at a similar extent to that scored in the A/WSN/33 infected group (mean average of 1.9).

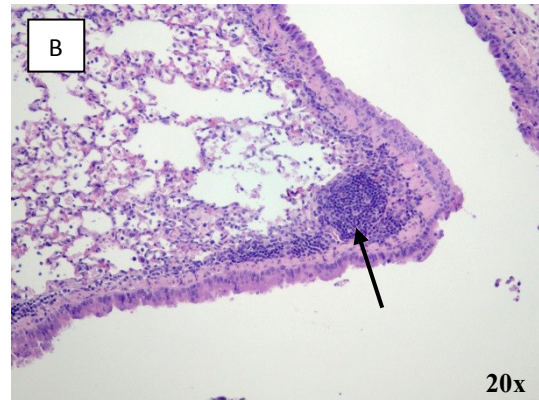
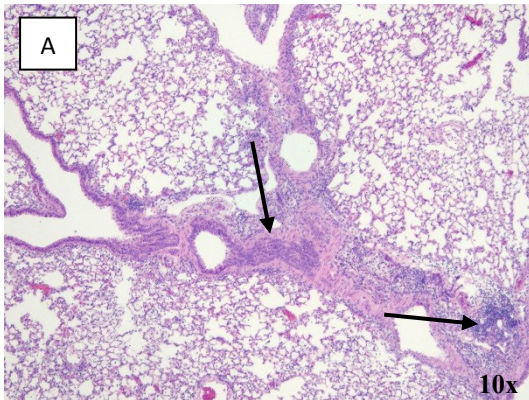
– Cytokine environment in the lung

Hypercytokinemia in the lung, associated with fatality in influenza A infection appears after the peak viral replication when the virus is starting to clear. In the mouse model of infection this is around day 6-8 post infection. Inflammatory $\text{IFN}\gamma$ and regulatory IL-10 levels appeared to be attenuated in the lungs by co-infection with MHV-68 in the lower dose infections and so a cytokine array of cytokines and chemokines with key roles in different pathways of the immune response to infection was used to identify individual targets that may be crucial to the protective effect conferred by co-infection.

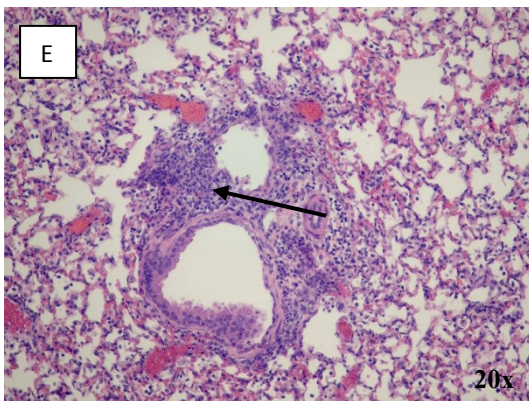
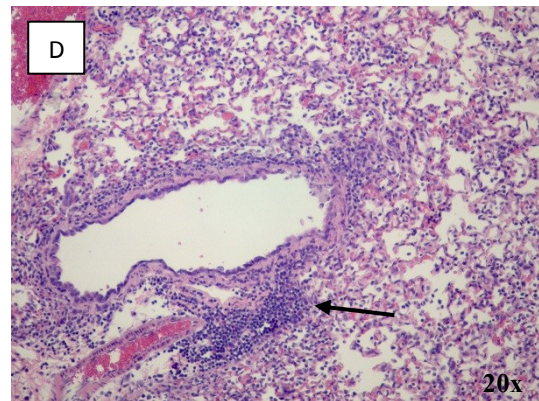
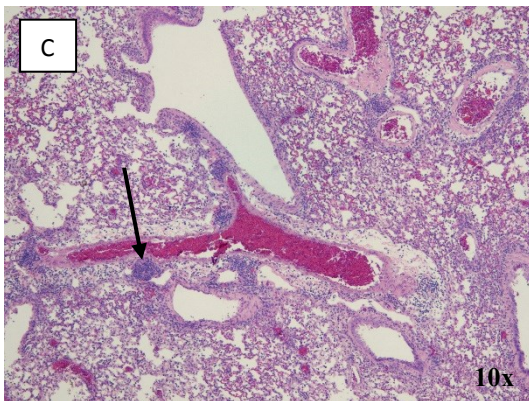
The cytokines and chemokines in the array may be divided into four broad groups relating to inflammation observed during influenza A infection. All cytokines associated with the cytokine storm (Figure 3.17A) in human infections were significantly increased in A/WSN/33 infected mice. $\text{TNF}\alpha$, IL-1 α , IL-1 β and IL-6 were all significantly ($p < 0.01$) increased in A/WSN/33 infected mice compared with the co-infected group after normalisation to the uninfected controls. Of interest in this group were $\text{TNF}\alpha$ and IL-6. $\text{TNF}\alpha$ was also not elevated significantly in MHV-68 mice or co-infected mice however this cytokine was highly increased in the presence of A/WSN/33 alone ($p < 0.001$). In the A/WSN/33 infected mice, $\text{TNF}\alpha$

Figure 3.16 Co-infection with latent MHV-68 does not significantly reduce pathology of 5×10^3 A/WSN/33 infection

5×10^3 A/WSN/33 infected



MHV-68 + 5×10^3 A/WSN/33 infected



Key:



Normal lung structure



Lymphocyte infiltration /
inflammation

F. Histology scoring

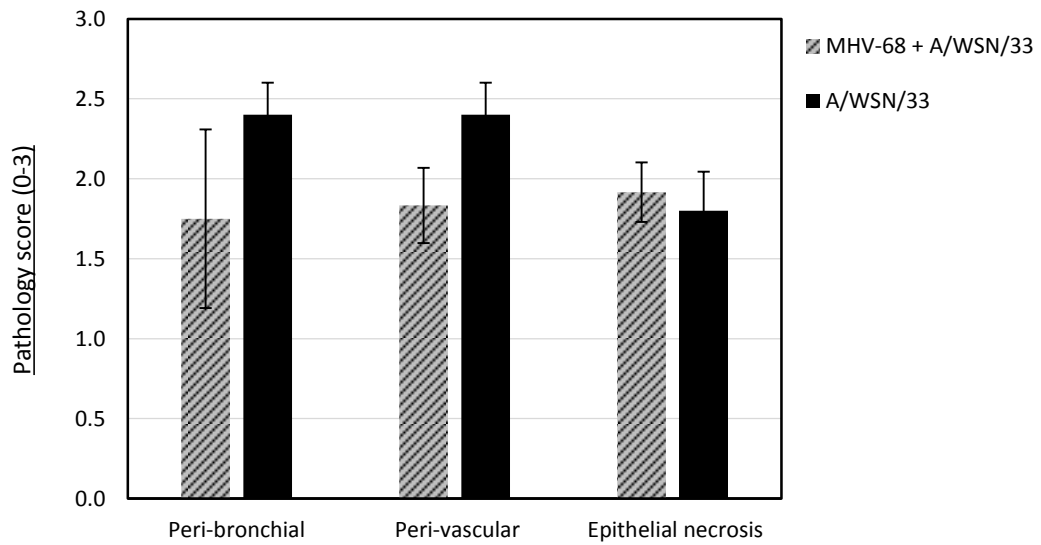
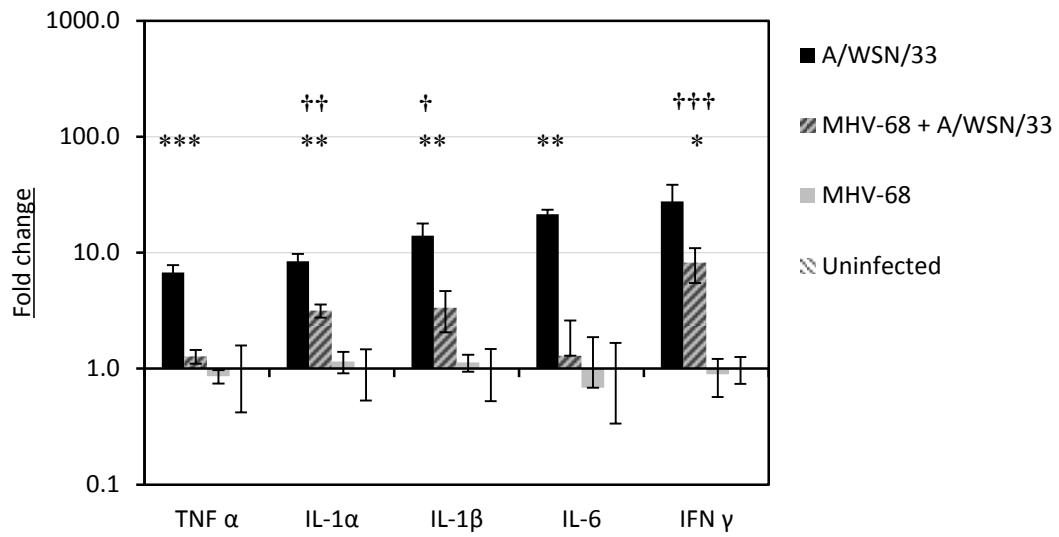


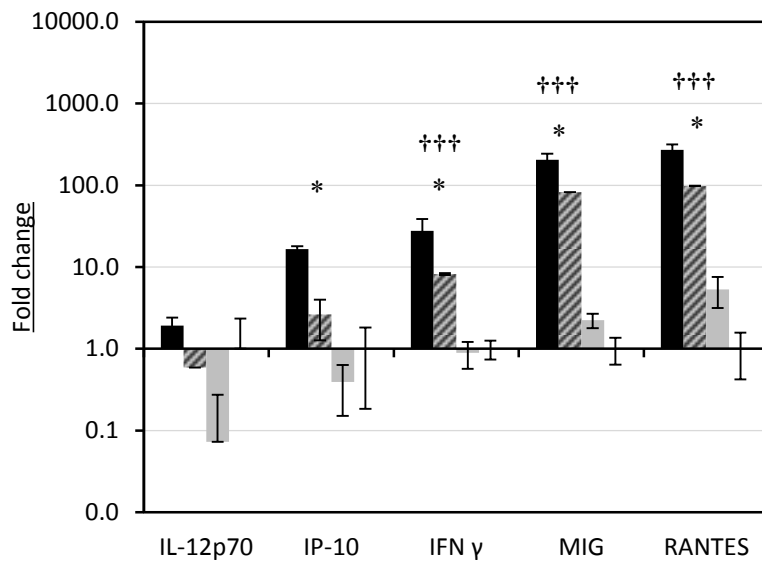
Figure 3.16 The right lung was inflated and fixed with 10% neutral buffered formalin. Lung sections were stained for hematoxylin and eosin. Representative sections are shown. Dashed arrows show areas of unaffected airways and blood vessels. Solid arrows demonstrate regions of lymphocytes infiltration and inflammation. **A-B** Lungs from A/WSN/33 infected mice. **C-E**. Lungs from MHV-68 + A/WSN/33 infected mice. Images represent averages from each infection group. Magnification is identified in the bottom right corner of each image. **F**. Complete lung cross-sections were scored for signs of inflammation and cell damage, N=6. Representative of 2 experiments. Results are displayed as mean average per group \pm 1 standard deviation. Uninfected and MHV-68 infected groups are not shown.

Figure 3.17 The cytokine environment following 5×10^3 A/WSN/33 is significantly ameliorated by pre-existing latent MHV-68 infection

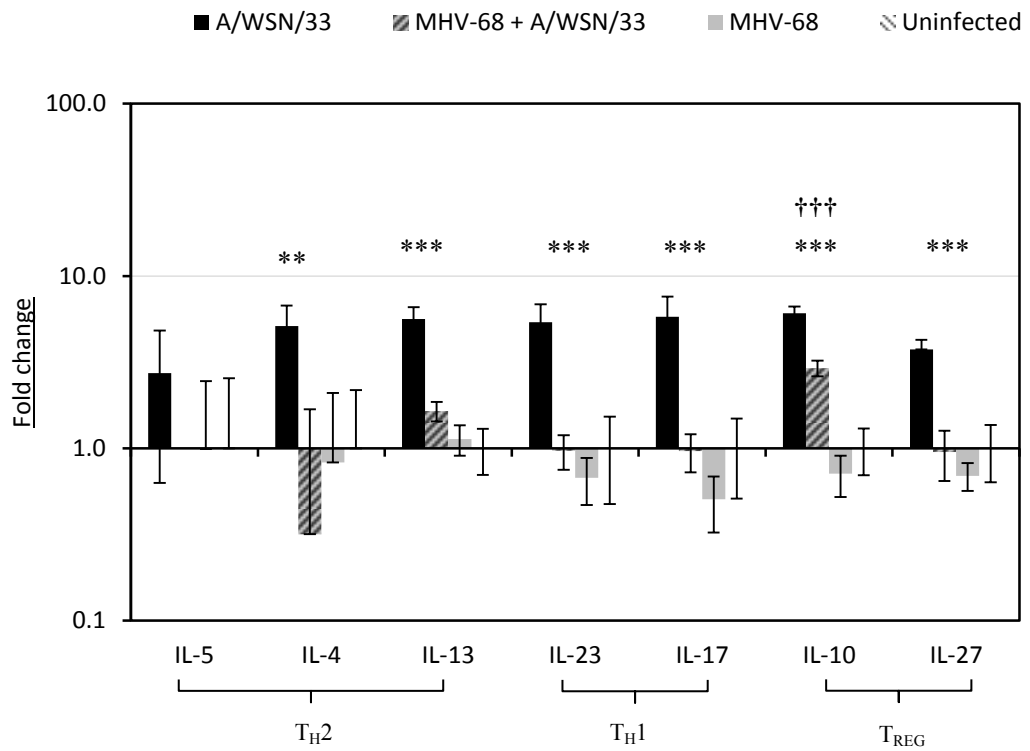
A. 'Cytokine storm' cytokines



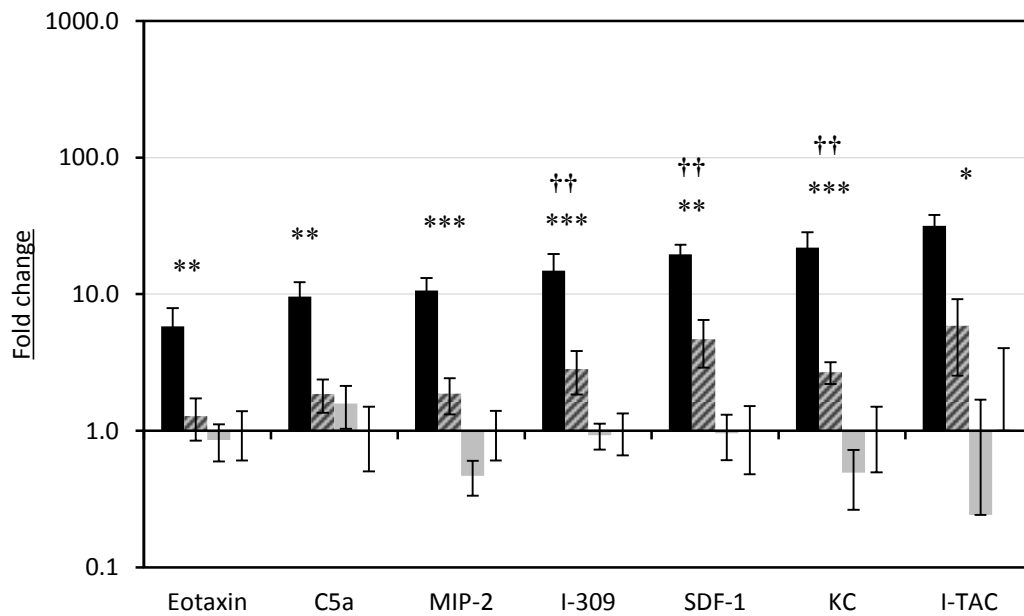
B. IFN γ inducible cytokines



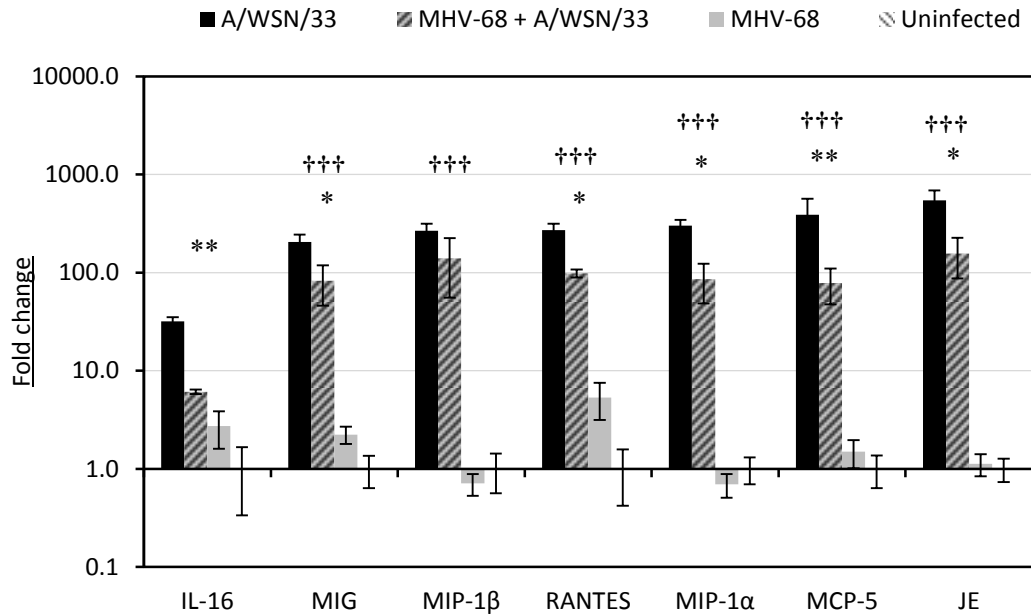
C. T_H2, T_H17 and T_{REG} cytokines



D. Chemokines 1.



E. Chemokines 2.



F. Adhesion, stimulation and proliferation cytokines

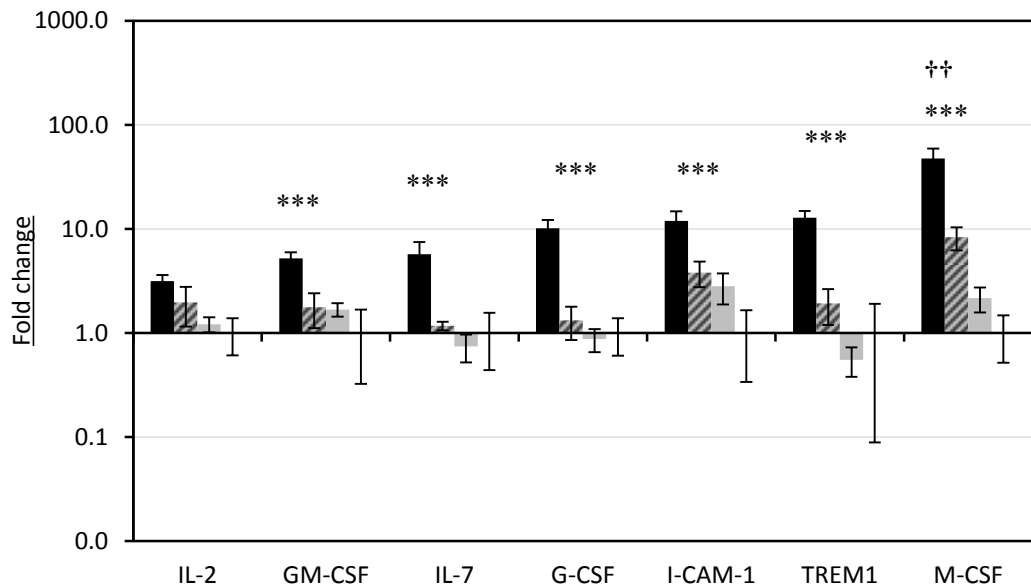


Figure 3.17 Cytokine environment in the lung was measured by protein array on lung homogenates 6 days post 5×10^3 A/WSN/33 infection. Results represented as mean fold change per experimental group compared to expression in the uninfected mice. Error bars are ± 1 standard deviation, N=4. Statistics are conducted by general linear model on raw or log transformed (normalised) data. Otherwise by Kruskal-Wallis and Mann-Whitney non-parametric tests, (*/+ = $p < 0.05$, **/+ $p < 0.01$, ***/+ $p < 0.001$). Asterisks, (*) display significant differences between co-infected and singly A/WSN/33 infected groups. Crosses, (+) display significant differences between co-infected and solely MHV-68 infected groups.

increased by 6.7 fold ($p < 0.001$) on average compared with uninfected mice, whereas co-infected mice only show a 1.5 fold increase and was not significantly increased. MHV-68 infection alone did not differ significantly from the uninfected mice. IL-6 followed a similar pattern; A/WSN/33 infected mice produced around 21.5 times the amount of IL-6 compared with uninfected mice. There was no significant change in the other experimental groups however.

IFN γ ($p < 0.05$) was also significantly increased in the A/WSN/33 infected mice compared with the co-infected group. The A/WSN/33 mice had an increase of 26.5 fold compared with the uninfected mice and 8.19 fold increase compared with the co-infected animals. The cytokine array is more sensitive than previous detection with ELISA and may therefore validate the trend observed at lower doses of infection. IFN γ was not significantly elevated in latently MHV-68 infected mice alone by this method of detection and therefore the co-infected mice had significantly higher ($p < 0.001$) levels than MHV-68 infected and uninfected mice.

The cytokines that are subsequently altered by IFN γ signalling (Figure 3.17B) were also increased in A/WSN/33 infected mice. IP-10, MIG and RANTES are all significantly increased by A/WSN/33 infection. Pre-existing co-infection with MHV-68 however reduced the levels of these cytokines significantly compared with A/WSN/33 singly infected mice, ($p < 0.01$, $p < 0.001$ and $p < 0.001$ respectively). IP-10 levels increased significantly 16 fold whilst levels in co-infected mice increased by 2.6 fold and therefore were not significantly different when compared with uninfected mice. MHV-68 infected mice also showed similarity to the uninfected group. RANTES however was increased in co-infected mice (98 times) and in A/WSN/33 infected mice (271 fold). MHV-68 infection alone also increased expression of this chemokine as discussed later. The pattern and levels of MIG expression were very similar to RANTES in each experimental group. IL-12p70 was the exception to this group of cytokines and did not significantly increase compared with MHV-68 and uninfected mice. This may in part be due to the large variation in these two groups (E.g. measured pixel density on the array varies from 107 to 131,424 in the uninfected mice whereas A/WSN/33 infected mice were measured within the range of 2,000-4,500).

Influenza virus induced hypercytokinemia induces type 1 and 2 cytokines. Three cytokines associated with 'T_H2 immunity' were measured (Figure 3.17C). A/WSN/33 infection alone increased IL-4 ($p < 0.01$) 5.1 fold and IL-13 ($p < 0.001$) significantly to 5.6 fold compared to the uninfected mice. All other experimental groups had similar levels of these cytokines to the uninfected mice, MHV-68 showed a 0.8 and 1.1 fold difference and co-infected mice were altered by 0.8 and 1.6 for IL-4 and IL-13 respectively. IL-5 did not alter significantly for any group. Expression was highly variable for IL-5 levels in the uninfected group which may explain this lack in variation.

Two cytokines associated with T_H17 immunity were also measured. As with the type 2 cytokines, A/WSN/33 infection alone increased the levels of IL-23 and IL-17 significantly higher ($p < 0.001$) than the co-infected or MHV-68 infected mice. IL-23 increased by 5.4 times and IL-17 by 5.8, demonstrating the mixed phenotypic response in influenza infection. Co-infected mice had similar levels of these cytokines to the MHV-68 singly infected group. IL-23 was expressed at 0.6 and 0.9 fold change to the uninfected mice for MHV-68 and co-infected mice and IL-17 varied by 0.5 and 0.9 fold compared with the uninfected mice. This was not statistically significant.

The regulatory cytokine IL-27 was also significantly increased by A/WSN/33 infection alone ($p < 0.001$) to 3.75 times the amount detected in uninfected mice but was not increased during co-infection (0.95). Similarly IL-10 expression was up-regulated by A/WSN/33 infection by 6.08 fold to a significantly higher level ($p < 0.001$) than seen in co-infected mice which only increased by 2.92 fold. This cytokine did increase significantly ($p < 0.001$) in the co-infected group when compared with solely MHV-68 infected and uninfected mice. This is the only cytokine in this group to increase significantly during co-infection.

All chemokines tested (Figure 3.17D and 3.17E) were at significantly higher levels in the A/WSN/33 singly infected mice compared with the co-infected mice at day 7 post infection, with the exception of MIP-1 β which increased to a similar degree in co-infected mice.

I-309 (CCL1), SDF-1 (CXCL12), KC (CXCL1), MIP-1 α (CCL3), MIP-1 β (CCL4), MCP-5 (CCL12) and JE (CCL2) all increased significantly in the co-infected mice as well whilst the other chemokines in this group did not significantly differ from uninfected mice during co-infection. MCP-5 (CCL12) showed the greatest increase of 390 fold compared with uninfected animals during A/WSN/33 infection and co-infected mice increased by 78.6 fold. A 5.8 fold increase in eotaxin (CCL11) in the A/WSN/33 infected mice however was equally significant ($p < 0.01$). Larger increases were hence more variable between mice of the same experimental group.

Cytokines associated with adhesion, stimulation and proliferation of immune cells (Figure 3.17F) were all significantly increased in the singly A/WSN/33 infected mice but only M-CSF increased significantly in the co-infected group, ($p < 0.01$). GM-CSF, for example, increased by 5.2 fold in the A/WSN/33 infected mice, however, MHV-68 infection and co-infection did not significantly alter its expression (1.60 and 1.75 fold difference). M-CSF increased by 47.5 times due to the influenza infection compared with uninfected mice while the co-infected mice only increased by 8.3 fold. IL-2 was also an exception in this group and was surprisingly not significantly increased in any of the experimental groups.

– Effect of A/WSN/33 on co-infection with latent MHV-68

Persistent MHV-68 was reduced in the lung by co-infection with 5×10^2 A/WSN/33. A/WSN/33 pathogenesis was reduced in mice co-infected at both 5×10^2 and 5×10^3 doses although protection was less apparent at the high dose. To determine if this protective effect was less efficient due to an increased suppression of MHV-68 by the second infection, MHV-68 viral load was calculated in the lung and spleen.

Seven days after 5×10^3 A/WSN/33 infection, (35 days after MHV-68 infection), the levels of MHV-68 in the spleen, detected by QPCR for ORF 73 were similar in both MHV-68 and co-infected mice (Figure 3.18A). In both groups the viral load was variable although the majority of results were below 1000 copies. The mean copy number in MHV-68 infected mice was 780.2 whilst co-infected mice had a much lower average of 386.7 copies however variation within the groups meant that this was not significantly different. These results were also in line with viral loads observed in the spleens in previous experiments.

In the lung, co-infected mice had significantly decreased levels of MHV-68 compared to singly infected mice ($p=0.002$, measured by 2 sample t test) as with the lower dose experiments (Figure 3.18B). MHV-68 infected mice averaged 69.8 ± 28.6 copies per 100ng of lung DNA. The co-infected mice had 13.2 ± 10.2 copies. A single sample in this group had no detectable MHV-68 in the lung.

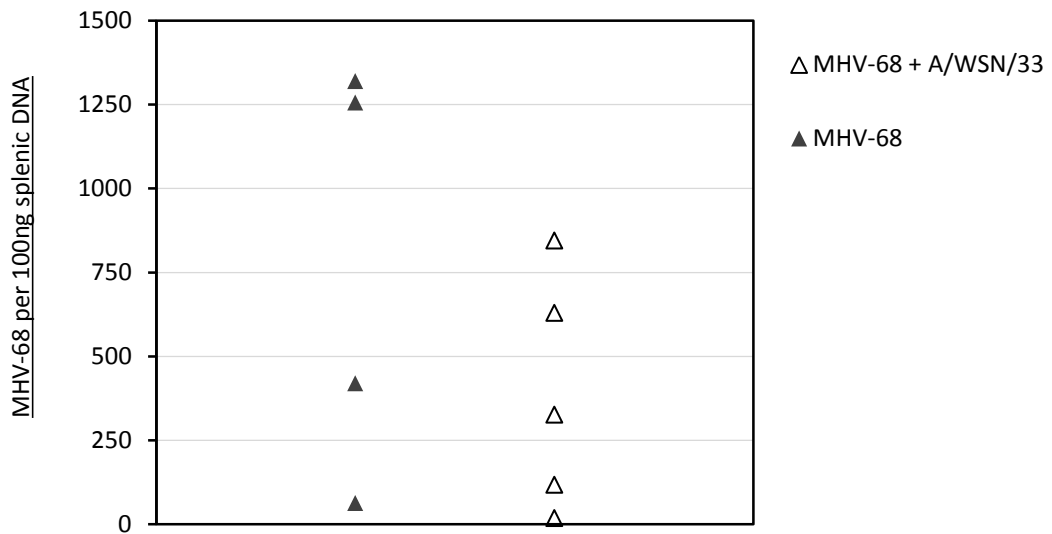
– CD4⁺ lymphocytes in the mediastinal lymph nodes

T_H1 cytokine production was unaltered in the mediastinal lymph node at the low dose of infection. To confirm normal function in the CD4⁺ cells in the lymph node, cells were harvested and stained for intracellular cytokines 7 days post infection.

IFN γ and IL-4 production by CD4⁺ cells was significantly raised in mice infected with 5×10^3 A/WSN/33 ($p < 0.05$ for all groups). In uninfected mice $1.12 \pm 0.59\%$ of CD4⁺ lymphocytes were producing IFN γ and $0.71 \pm 0.73\%$ were producing IL-4. A/WSN/33 infection increased IFN γ producing cells to $8.71 \pm 2.09\%$ of the total CD4⁺ lymphocytes and IL-4 producers increased to $4.69 \pm 3.33\%$. The MHV-68 latently infected mice show similar levels of IFN γ and IL-4 production to the uninfected mice (2.63% IFN γ positive and 0.41% IL-4 producing cells). CD4⁺ lymphocytes in the mediastinal lymph nodes of co-infected mice were also significantly raised in their production of IFN γ and IL-4, with an average of $6.99 \pm 3.07\%$ IFN γ positive and $2.26 \pm 1.76\%$ IL-4 producing cells (Figure 3.19A and 3.19B). The standard deviation within this group was greater than the A/WSN/33 singly infected mice due to a single mouse with

Figure 3.18 Infection with 5x10³ A/WSN/33 reduces the MHV-68 viral load in the lung

A. Spleen MHV-68 titre– Day 7



B. Lung MHV-68 titre – Day 7

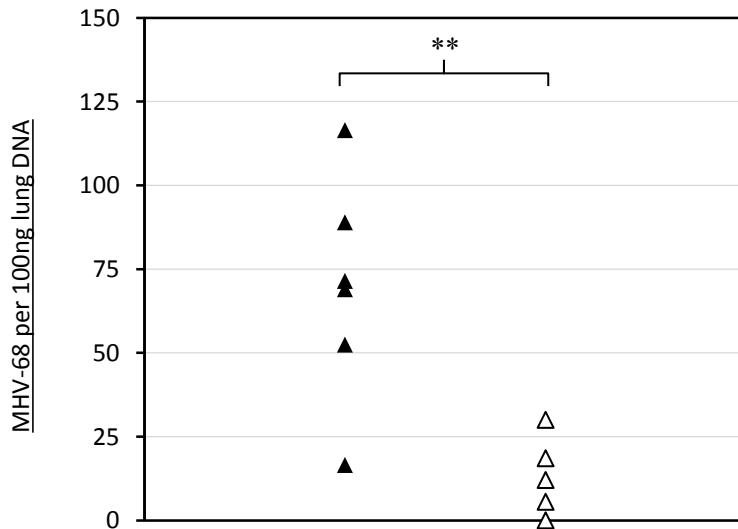


Figure 3.18 DNA was extracted from a segment of the spleen and the left lobe of the lung. Quantitative PCR for orf 73 in the MHV-68 genome was performed on 100 ng of DNA. **A.** MHV-68 viral load in spleen samples 7 days post A/WSN/33 infection (35 days post MHV-68 infection), N=5. **B.** MHV-68 viral load in the lung at the same time point. N=6. Results are displayed as individual values. Statistical analysis performed by two sample student's t test (** = p<0.01) representative of a single experiment.

Figure 3.19 TH1 CD4+ T cell phenotype in lung draining lymph nodes is the same in 5x10³ A/WSN/33 and co-infected mice

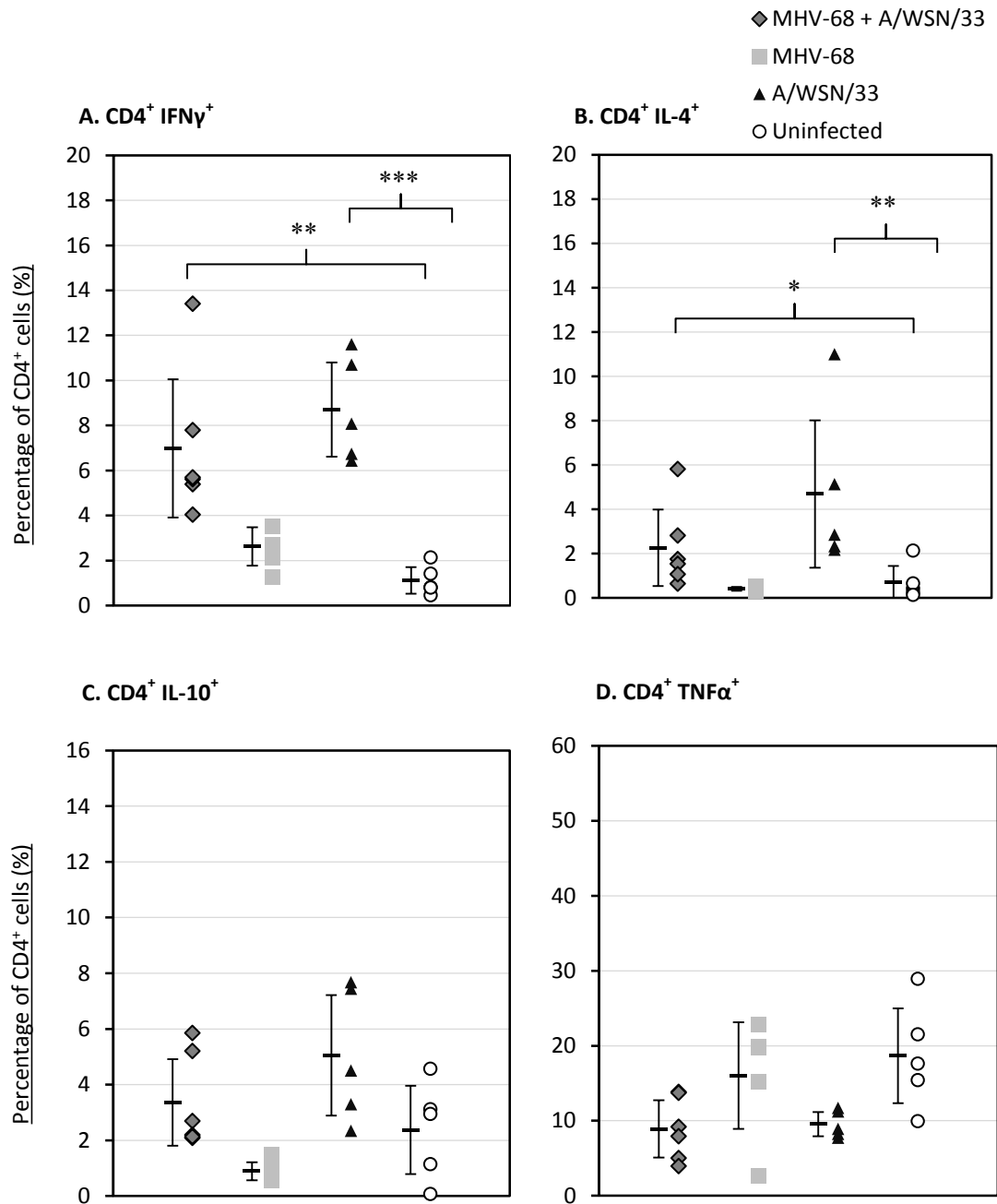


Figure 3.19 Mice were culled 7 days post A/WSN/33 infection. Lung draining lymph nodes were harvested. 1×10^7 cells were stained for CD4⁺ T cell markers. Samples were run on a BD LSR II Fortessa. Results are displayed as percentages and mean per group \pm 1 standard deviation. N=6. (*=p<0.05, **=p<0.01, ***=p<0.001 general linear model). **A.** CD4⁺ IFN γ ⁺ cells. **B.** CD4⁺ IL-4⁺ cells. **C.** CD4⁺ IL-10⁺ cells **D.** CD4⁺ TNF α ⁺ cells.

increased IFN γ (13.4%) and IL-4 (5.81%) production. In the absence of this result there would have been a strong trend for decreased production of both cytokines in the co-infected mice compared with the A/WSN/33 singly infected group.

IL-10 and TNF α production by CD4⁺ T cells, were not significantly raised at this dose in any experimental group (Figure 3.19C and 3.19D) however there was greater variation within the uninfected group (2.37 \pm 1.58% and 18.67 \pm 6.34% for IL-10 and TNF α respectively). There were no significant differences between the singly A/WSN/33 infected and co-infected mice. TNF α was produced at an average of 3.36 \pm 1.56% in the co-infected mice and 5.05 \pm 2.16% in the A/WSN/33 infected mice. IL-10 was expressed by 8.91 \pm 3.83% of CD4⁺ lymphocytes in the co-infected mice and 9.54 \pm 1.91% in the A/WSN/33 infected mice. While the results were not significant, similar patterns of expression could be seen in all cytokines, with A/WSN/33 infected mice always averaging a greater production of IL-10, TNF α , IFN γ and IL-4 by CD4⁺ lymphocytes than the co-infected mice.

– CD4⁺ and CD8⁺ lymphocytes in the lung

Differences in the pathology were less evident in the lungs of co-infected and A/WSN/33 infected mice at this dose. To determine if this was reflected in the adaptive immune response in the lung at this time point cells from BAL fluid were stained for CD4, CD8 and intracellular inflammatory cytokines.

Numbers of lymphocytes in lavage samples from uninfected and MHV-68 infected mice were too low to report and are therefore not shown. There were no significant differences in the proportions of responding CD4⁺ and CD8⁺ cells in the lung between co-infected and A/WSN/33 infected mice (Figure 3.20A and 3.20C). Co-infected mice had 14.24 \pm 4.40% CD4⁺ lymphocytes and A/WSN/33 infected mice had 12.38 \pm 0.56% CD4⁺ cells. Production of cytokines by these cells was significantly different between experimental groups. Co-infected mice had a significantly increased production of TNF α , (p=0.009) with 15.83 \pm 4.12 positive CD4⁺ cells compared to 8.42 \pm 1.86% in the A/WSN/33 infected group (Figure 3.20B). IFN γ production was similar in these cells with 26.20 \pm 5.13% in the co-infected and 22.30 \pm 4.90% in the A/WSN/33 infected mice.

The proportion of CD8⁺ lymphocytes in the lungs did not differ between co-infected mice (46.57 \pm 6.57%) and A/WSN/33 infected mice (38.46 \pm 3.97%). However, production of cytokines by these cells was significantly different. IFN γ production was observed in 58.30 \pm 9.84% of CD8⁺ lymphocytes in co-infected mice (Figure 3.20D) whilst CD8⁺ lymphocytes from A/WSN/33 infected mice averaged 41.90 \pm 12.79% (p=0.001). Similarly TNF α production was apparent in a greater percentage (p=0.001) of CD8⁺ cells in the co-infected mice (5.66 \pm 2.20%)

Figure 3.20 CD8⁺ cells in the lungs of co-infected mice produce significantly increased levels of inflammatory cytokines 7 days after 5x10³ A/WSN/33 infection

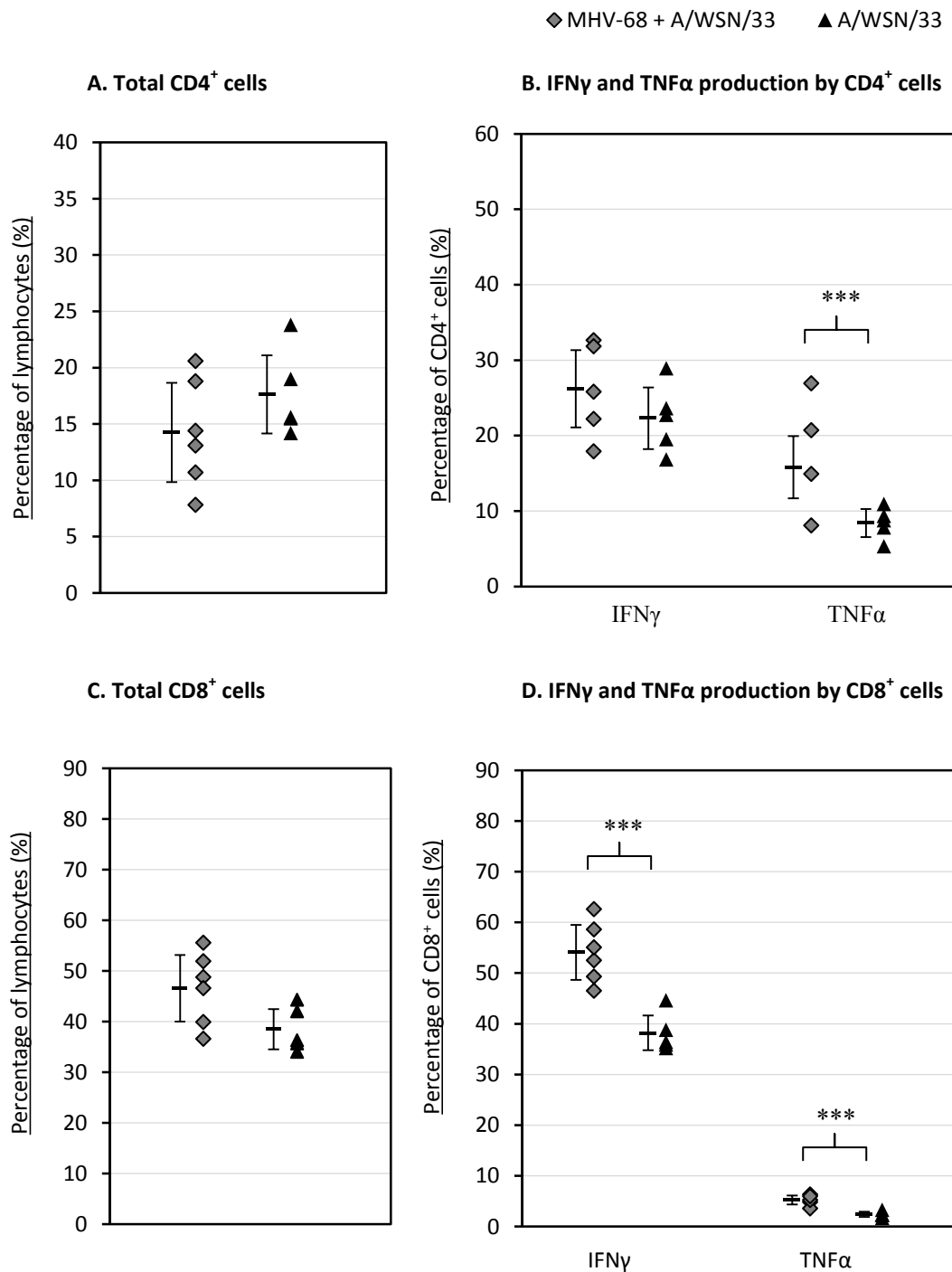


Figure 3.20 Mice were culled 7 days post A/WSN/33 infection and cells in the lung were harvested by bronchoalveolar lavage (BAL). Maximum numbers of cells in the BAL fluid were stained for a range of intracellular CD4⁺ and CD8⁺ T cell markers. The samples were run on a BD LSR II Fortessa. Results displayed as individual percentage per sample and mean average per group \pm 1 standard deviation, N=5-6. All statistics are calculated on data from a single experiment, (*=p<0.05, **=p<0.01, ***=p<0.001). **A.** Total CD4⁺ cells **B.** CD4⁺ IFN γ ⁺ and CD4⁺ TNF α ⁺ cells **C.** Total CD8⁺ cells **D.** CD8⁺ IFN γ ⁺ and CD8⁺ TNF α ⁺ cells.

compared with singly A/WSN/33 infected mice ($3.22 \pm 1.13\%$). As in previous experiments IFN γ levels exceeded TNF α production in both cell types.

3.4.4 Co-infection with latent MHV-68 and 5×10^3 A/WSN/33 in WT 129

Sv/Ev mice

Changes to IFN γ levels and cytokines and chemokines induced by IFN γ in the co-infected mice suggested that this cytokine may be integral to the reduction in susceptibility seen in this group. It was hypothesised that an IFN γ R^{-/-} mouse would therefore lose this phenotype. The IFN γ R^{-/-} mice are on a 129Sv/Ev background and so a repeat of the 5×10^3 experiment was undertaken in WT 129 Sv/Ev mice to determine the effect of co-infection in this particular background strain prior to the 'removal' of IFN γ signalling from the system.

As before, 5-6 week old female mice were infected with 5×10^4 MHV-68 and 28 days later with 5×10^3 A/WSN/33 intranasally and compared with uninfected and singly infected controls. As with BALB/c mice, latent MHV-68 infection caused no clinical signs or weight loss.

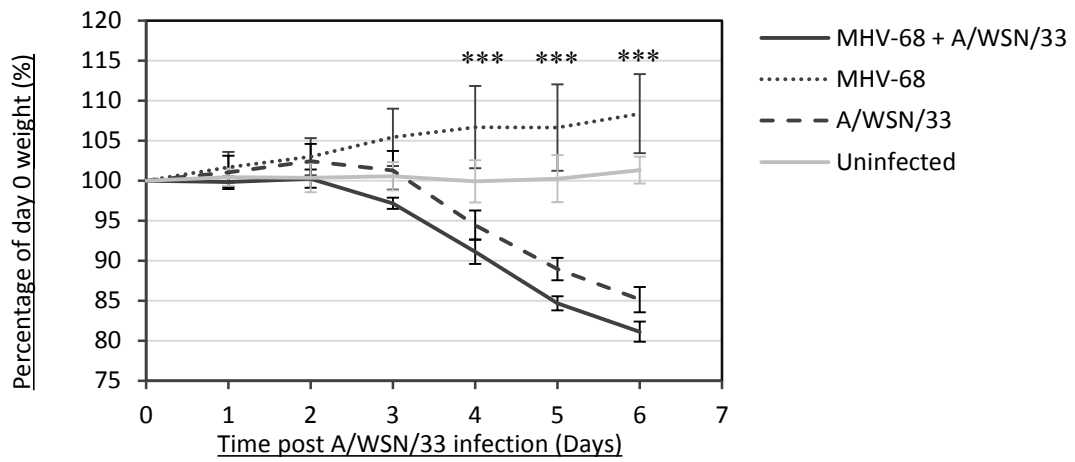
– Effect of latent MHV-68 on co-infection with A/WSN/33

Infection of these mice with A/WSN/33 resulted in less severe presentation of clinical signs and weight loss progression compared to the BALB/c mice. Significant weight loss occurred at day 4 with a $5.56 \pm 1.83\%$ ($p < 0.01$) decrease, a day later than in the BALB/c counterparts. Weight loss increased at day 5 to an average of $11.05 \pm 1.41\%$ ($p < 0.001$) and a peak total weight loss of $14.87 \pm 1.59\%$ ($p < 0.001$) was observed in A/WSN/33 infected mice at day 6 post infection (Figure 3.21A). Standard deviation was very low within this group and did not reach any higher than 2%.

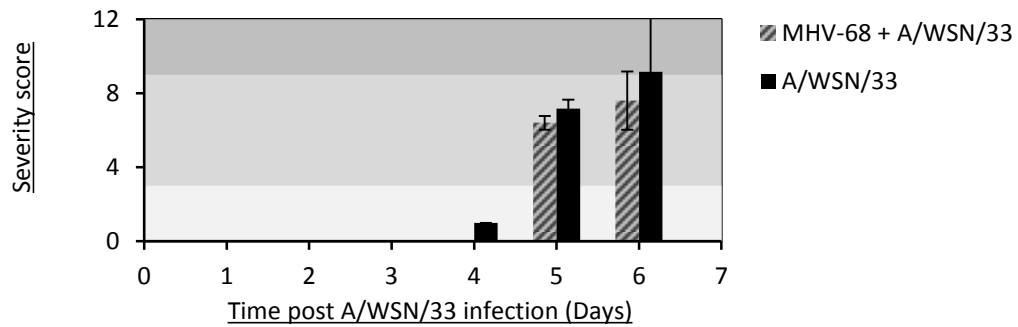
Clinical signs were slightly different compared with the BALB/c mice. The first sign of infection was a hunched stature recorded at day 4 (average score of 1). By day 5 hunching score averaged 2 and was coupled with increased respiratory effort and decreased mobility, both scored at 1. This combination gave an overall 'moderate' severity to this group (Figure 3.21B). By the final day, some mice were scored at 3 in the hunched category and varied greatly in clinical score for respiratory effort, reduced mobility and increased respiratory effort, unlike the BALB/c mice which had previously shown cohesive symptom severity within the same group. A final severity score was 9.16, however, this varied from 7-12 from mouse to mouse. In this mouse strain co-infection led to an increased weight loss (Figure 3.21A). A reduction of

Figure 3.21 Effect of MHV-68 latency co-infection on pathogenesis of 5×10^3 A/WSN/33 (129Sv/Ev)

A. Weight loss



B. Clinical severity score



C. Influenza lung titre

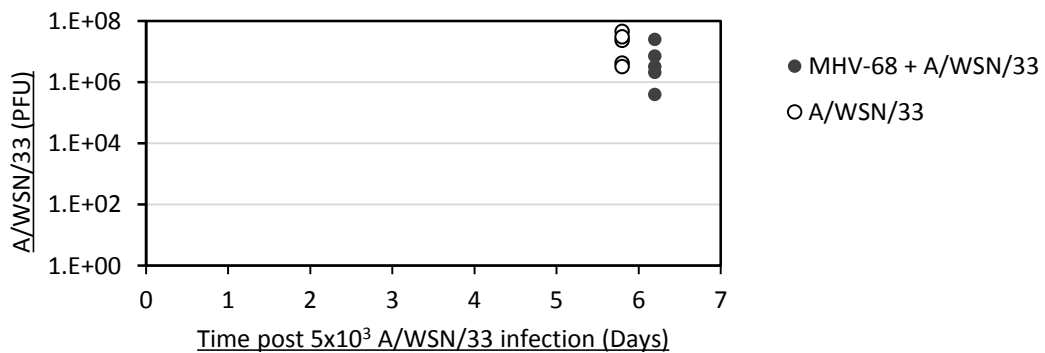


Figure 3.21 5-6 week old 129 Sv/Ev female mice were infected I.N. with 5×10^4 MHV-68 and 28 days later infected I.N. with 5×10^3 A/WSN/33 in 40 μ l Dulbecco's minimum essential medium or medium alone. **A.** Influenza induced weight loss. Error bars represent ± 1 standard deviation of the mean. Significance determined by students two-way ANOVA (+/= $p < 0.05$, **/++ = $p < 0.01$, ***/+++ = $p < 0.001$). * represents significant difference between A/WSN/33 infected and uninfected groups. **B.** Clinical severity was measured by 4 signs. Each was scored on a scale of 0-3 and the sum reported ± 1 standard deviation as clinical severity score, N=6. **C.** Mean A/WSN/33 titre in the lung, N=6 at day 6.

8.91±1.76% was seen by day 4, increasing to 15.38±0.89% by day 5 and 18.88±1.27% at the final time point. Variation from the mean was again very low within this group. A significant difference compared with the A/WSN/33 infected group was seen at day 5 and 6 post infection ($p < 0.01$). Clinical signs followed the same progression as A/WSN/33 infected mice, however, did not appear until day 5 (a day later than singly infected mice) and reached similar average severity scores of 6.4 and 7.6 on days 5 and 6 respectively (Figure 3.21B). Clinical signs therefore they did not appear to be directly correlated to weight loss in these mice as has been seen previously in BALB/c mice.

Uninfected mice maintained similar weights to that measured on day 0 with an average of 101.31±1.17% by day 6. Unexpectedly 3/5 mice solely infected with MHV-68 began to increase in body weight over the course of the experiment. These mice began to gain weight at day 3 skewing the average weights in this group up to 108.37±5.03%. This was not coupled with any signs of disease and the remaining 2 mice in the cage remained at 102% and 103% by day 6. This increase was significant compared with uninfected mice ($p > 0.01$) which is completely unanticipated.

An important consideration for this experiment became apparent after the cull date. During this experiment mice were unknowingly housed in abnormal lighting conditions, extending the light period beyond the normal biphasic light cycle. This may have contributed to the unexpected increase in weight seen in the MHV-68 infected mice although all mice were housed in the same conditions. A repeat of this experiment is therefore required to interpret data from all experimental groups accurately.

(A comparison of differences in A/WSN/33 induced weight loss between strains can be seen in Appendix 6.1)

Influenza titre was measured in the lung to determine if the apparent loss of protective phenotype in this mouse strain had any bearing on A/WSN/33 viral load. A/WSN/33 infection led to very high titres of infectious virus at 6 days post infection. A/WSN/33 singly infected mice had on average 1.83×10^7 PFU ml⁻¹ in lung homogenate samples. (In comparison to BALB/c mice this appears much higher however these measurements are made at day 6 instead of day 7. Figure 3.21C). Similar high levels were observed in co-infected mice however once again there was a subtle trend for a decrease in average titre (7.53×10^6 PFU ml⁻¹) compared with singly infected mice but this was not significant.

– Pathology in the lung

The pathology of A/WSN/33 infection was analysed in the 129Sv/Ev strain to determine differences from the BALB/c mice of comparable age.

Uninfected mice showed no signs of infection or inflammation (Figure 3.22A-B). Latent MHV-68 infection in these mice caused similar pathology to that seen in the BALB/c strain. Small, sporadic foci of lymphocyte accumulations were evident in the interstitial spaces of the lung (Figure 3.22C).

5×10^3 A/WSN/33 infection in these mice caused similar pathology to the comparable infection in the lungs of BALB/c mice however the severity of the pathology was scored much lower and there was greater variation within groups (Figure 3.22K). Infiltration of lymphocytes around the bronchioles (Figure 3.22D and 3.22F) was scored at an average of 1.38. This was the same for peri-vascular inflammation (score of 0.88). Epithelial necrosis was reduced compared with the BALB/c mice and alveolar spaces appeared to contain less infiltrating cells than in the other mouse strain (Figure 3.22E and 3.22G).

Co-infected mice were scored on average at a greater level of inflammation for peri-vascular and peri-bronchial infiltration of cells (1.6 and 1.6 respectively, Figure 3.22H and I). There was also greater variation in this group than was seen in the BALB/c infected mice. Epithelial necrosis was scored at a similar level to the singly A/WSN/33 infected mice (0.4 mean average) and recruitment of immune cells into the alveolar cells was at a comparably low amount (Figure 3.22).

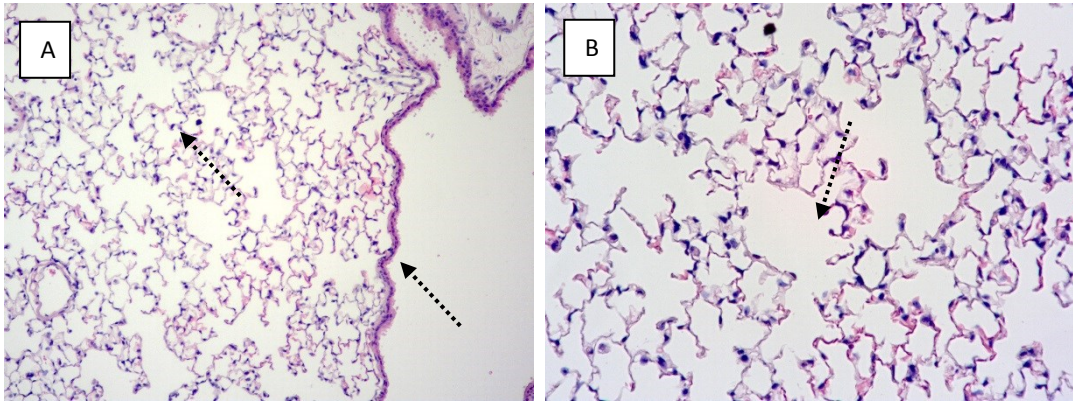
– Cytokine environment in the lung

A loss of protective phenotype in the co-infected mice of this strain was surprising. As such cytokine environment in the lung was measured in these samples to determine if a different cytokine response was present in response to any of the infections due to strain differences. Lungs were removed and homogenised 6 days post infection with A/WSN/33. As with BALB/c mice at a similar time point, TNF α levels were not significantly altered in the lung homogenates by either infection, however, base levels of TNF α were much higher in these mice, as seen in the mean levels in uninfected mice which averaged at 415.18 pg ml⁻¹ (Figure 3.23).

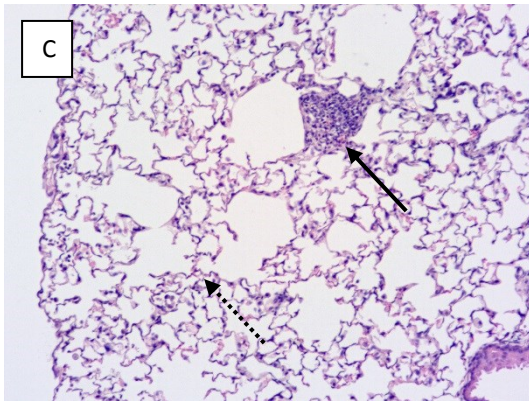
IFN γ levels were 12.36 pg ml⁻¹ in the uninfected mice and 5.70 pg ml⁻¹ in the MHV-68 infected mice. An increase in IFN γ , to a mean value of 157.70 \pm 67.31 pg ml⁻¹ (p=0.072) was observed in the co-infected mice and an even greater increase to an average of 439.18 pg ml⁻¹ (p=0.007, Mann-Whitney test) in the A/WSN/33 infected mice. Variation from the mean is large within

Figure 3.22 Co-infection with latent MHV-68 does not alter pathology caused by A/WSN/33 infection in 129Sv/Ev mice

Uninfected



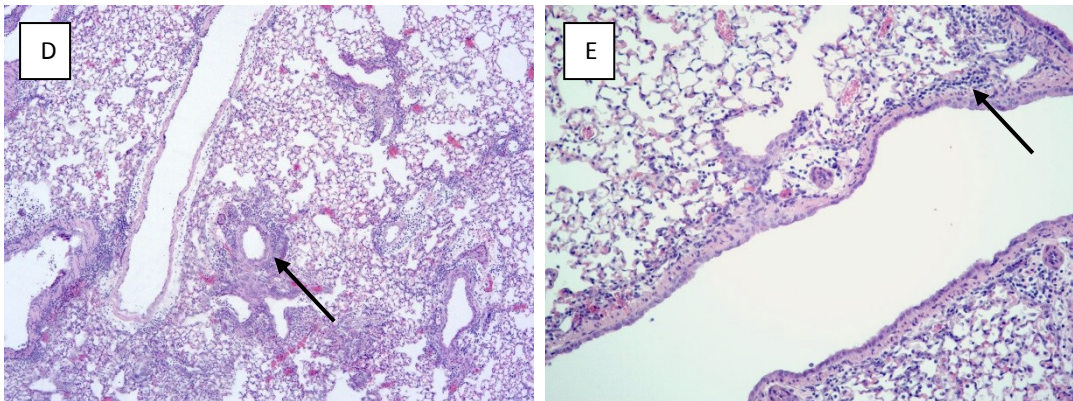
MHV-68 infected

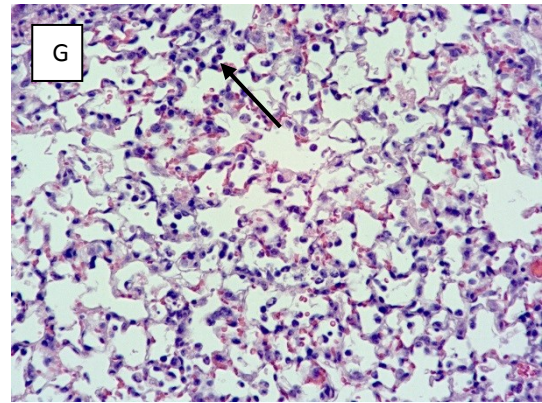
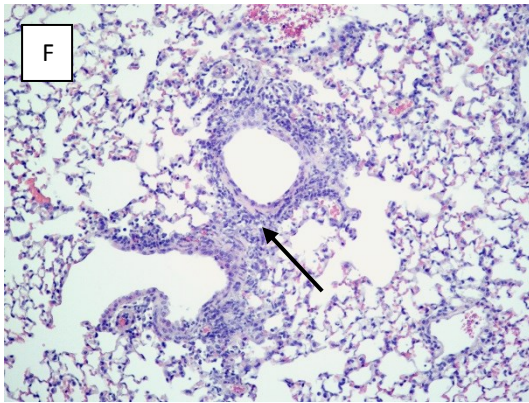


Key:

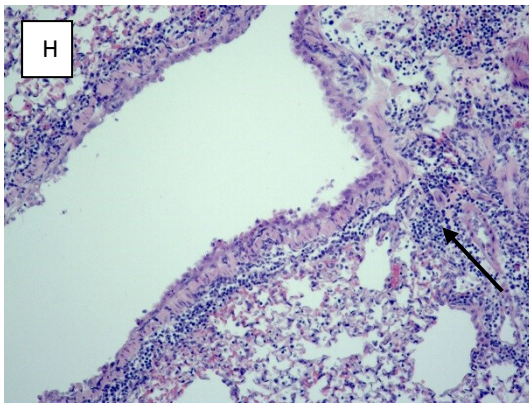
- Normal lung structure
- Lymphocyte infiltration / inflammation

5x10³ A/WSN/33 infected





MHV-68 + 5×10^3 A/WSN/33



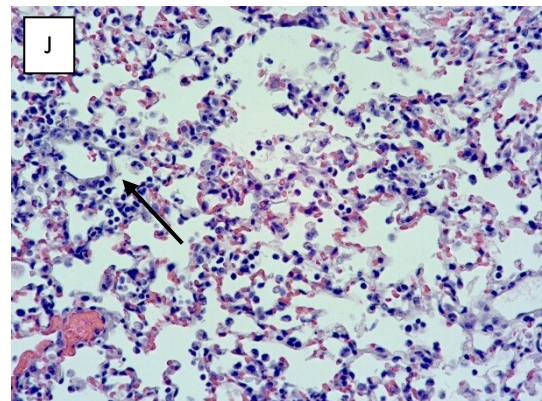
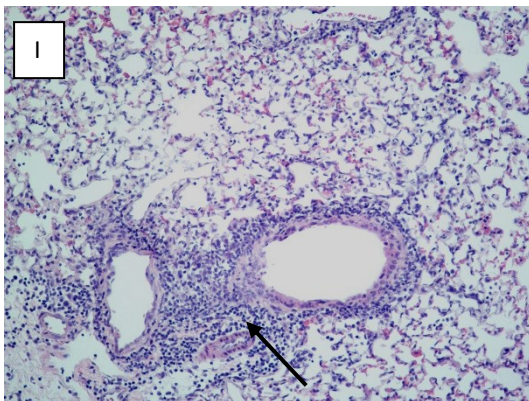
Key:



Normal lung structure



Lymphocyte infiltration /
inflammation



K. Pathology score

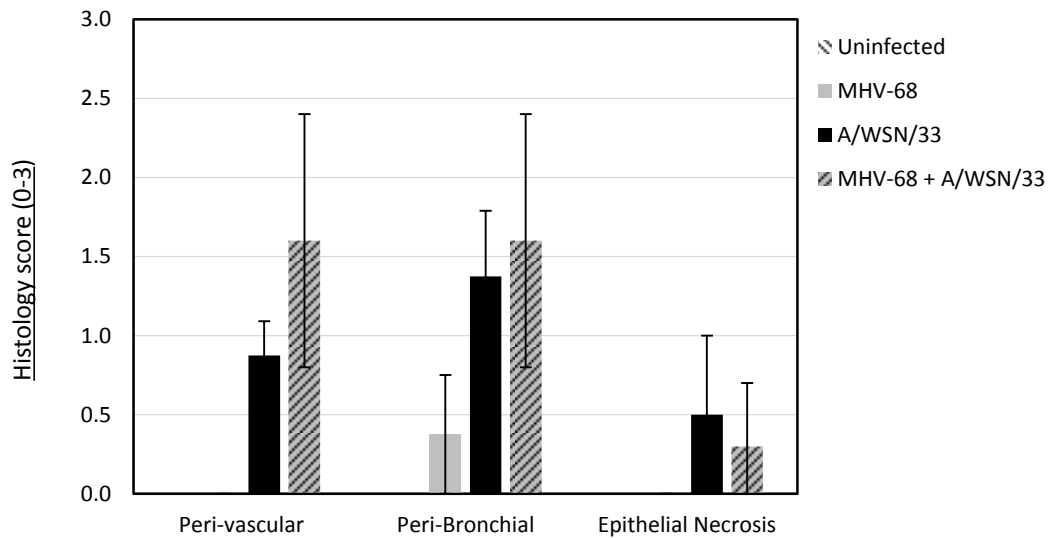


Figure 3.22 The right lung was inflated and fixed with 10% neutral buffered formalin. Lung sections were stained for hematoxylin and eosin. Representative sections are shown. Dashed arrows show areas of unaffected airways and blood vessels. Solid arrows demonstrate regions of lymphocyte infiltration and inflammation. **A-B** Lungs from uninfected mice. **C** Lungs from MHV-68 latently infected mice. **D-G** Lungs from A/WSN/33 infected mice. **H-J** Lungs from MHV-68 + A/WSN/33 infected mice. Images represent averages from each infection group. Magnification is identified in the bottom right corner of each image. **K**. Complete lung cross-sections were scored for signs of inflammation and cell damage, N=6. Representative of 1 experiment. Results are displayed as mean average per group \pm 1 standard deviation.

Figure 3.23 Co-infection has no significant impact on cytokine environment in WT 129Sv/Ev mice

A. Lung cytokine environment

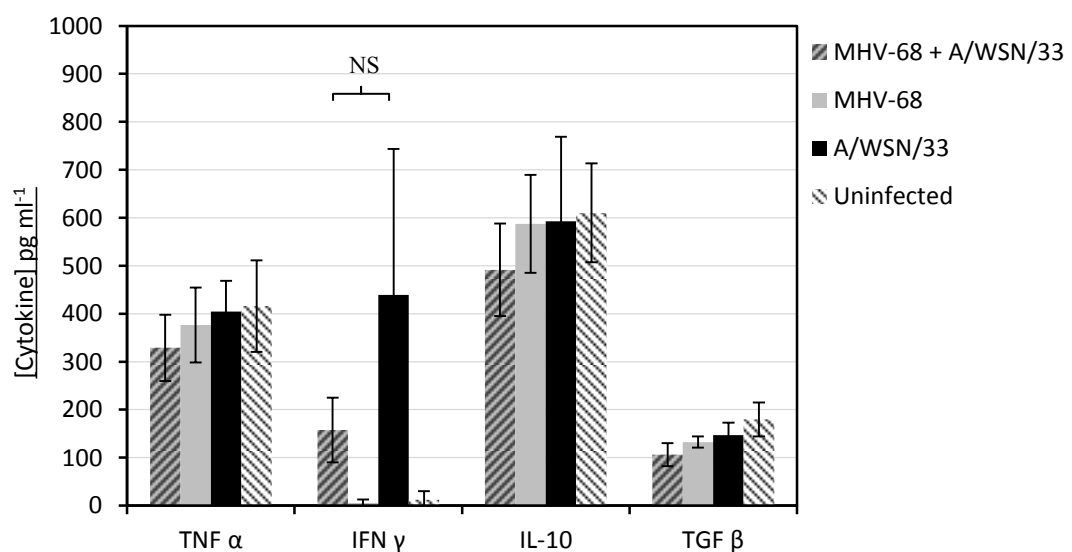


Figure 3.23 6 days post A/WSN/33 infection, the left lung was homogenised in Dulbecco's minimum essential medium and the homogenate used for ELISA detection of cytokines TNF α , IFN γ , IL-10 and TGF β . Results are displayed as mean averages per experimental group \pm 1 standard deviation, N=6.

this group (304.38) and therefore despite the large difference in means the change does not reach significance ($p=0.055$).

IL-10 was not altered significantly by either infection. This was in contrast to the response in BALB/c mice where A/WSN/33 infection caused a robust increase in IL-10 regardless of co-infection with MHV-68. As is the case with TNF α , IL-10 was detected at relatively high levels compared with BALB/c mice (Figure 2.23). For example the level of IL-10 in uninfected mice was on average 610 pg ml⁻¹. Similarly TGF β was unaltered by either infection, however, this cytokine was present at much lower amounts than IL-10. Uninfected mice had an average of 179.94 pg ml⁻¹ TGF β and no other group had significantly more or less than this amount.

– Effect of A/WSN/33 on co-infection with latent MHV-68

In the BALB/c mice, A/WSN/33 infection resulted in significantly reduced MHV-68 loads in the lung but not the spleen. To determine if this effect still occurred when A/WSN/33 pathogenesis was exacerbated by co-infection, levels of MHV-68 were measured in lung and spleen samples for comparison.

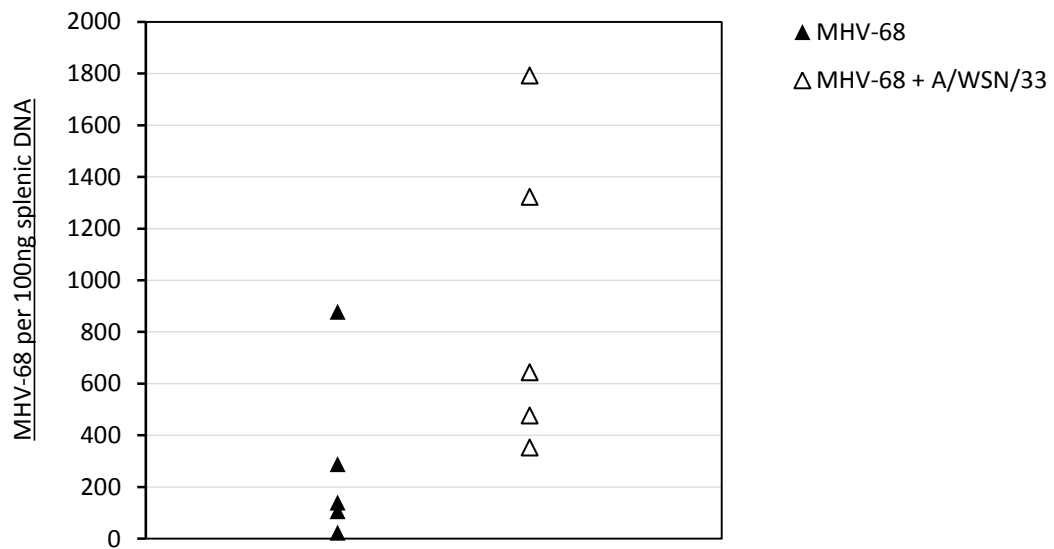
Whilst copy numbers were detectable at similar amounts in both organs when compared to BALB/c mice there was no decrease in MHV-68 viral load in the spleen and (more importantly) in the lungs of co-infected 129 Sv/Ev mice (Figure 3.24A and 3.24B). Mean spleen copy numbers of MHV-68 were 918 per 100ng DNA in co-infected mice and 287 per 100ng DNA in the singly MHV-68 infected mice. Whilst not significant, MHV-68 in the spleen shows an increased presence in the co-infected mice. In the lung MHV-68 copy number averaged 220 copies per 100ng DNA in the co-infected mice and a similar copy number of 120 in the MHV-68 infected mice. The reduction in MHV-68 viral load was therefore not apparent in this co-infection.

3.4.5 Co-infection with latent MHV-68 and 5×10^3 A/WSN/33 in IFN γ ^{-/-} 129Sv/Ev mice

In the BALB/c mice, IFN γ expression was decreased in the co-infected mice at all doses of A/WSN/33 co-infection. In the 129 Sv/Ev mice, where protection due to co-infection was not observed, IFN γ levels still appeared to be regulated by co-infection with MHV-68. To determine the effect of the inflammatory cytokine IFN γ and factors induced by IFN γ , female 5-6 week old 129Sv/Ev mice lacking the IFN γ receptor were infected with 5×10^4 MHV-68 and after 28 days were infected intranasally with 5×10^3 A/WSN/33.

Figure 3.24 A/WSN/33 infection does not alter MHV-68 viral load in 129Sv/Ev mice

A. Spleen – Day 6



B. Lung – Day 6

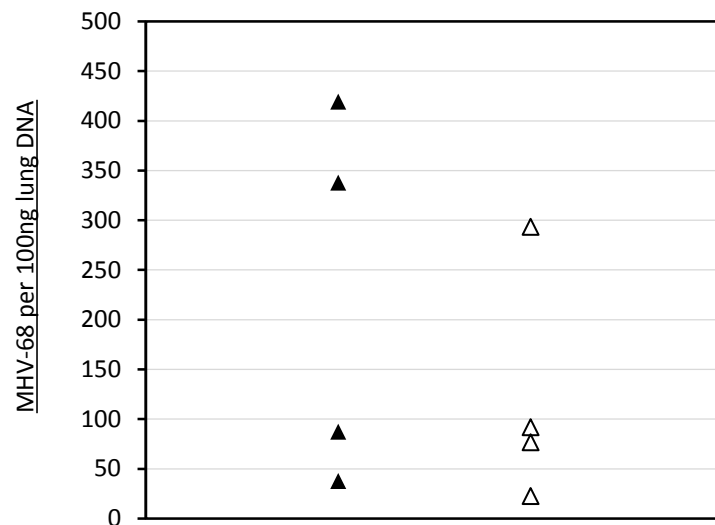


Figure 3.24 DNA was extracted from a segment of the spleen and left lobe of the lung. Quantitative PCR for orf 73 in the MHV-68 genome was performed on 100 ng of DNA. **A.** MHV-68 viral load in spleen samples 6 days post A/WSN/33 infection (34 days post MHV-68 infection), N=5. **B.** MHV-68 viral load in the lung at the same time point. N=4. Results are displayed as individual values. Statistical analysis performed by two sample student's t test.

– Effect of MHV-68 on co-infection with A/WSN/33

Weight loss and clinical signs of infection were compared to singly infected and uninfected controls. MHV-68 and uninfected controls showed no significant difference in weight throughout the time course. Uninfected mice were on average 102.94% of their original weight at day 0 by day 6 (Figure 3.25A). MHV-68 infected mice were similarly 100.70% of their original weight on day 0 by day 6.

A/WSN/33 infected IFN γ R^{-/-} mice lost more weight than their WT 129Sv/Ev counterparts following 5×10^3 PFU infection (see Appendix 6.1). Significant weight loss appeared at day 3 post infection ($p < 0.01$) with a reduction of $4.99 \pm 3.17\%$, increasing to $9.73 \pm 3.3\%$ on day 4 ($p < 0.001$), $15.79 \pm 2.3\%$ on day 5 ($p < 0.001$) and $20.09 \pm 2.68\%$ by day 6 ($p < 0.001$).

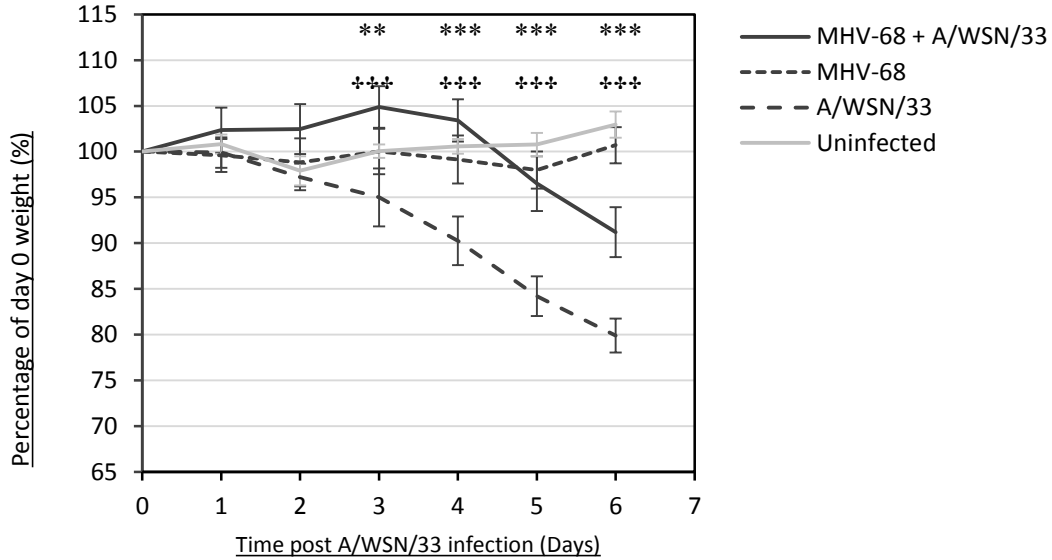
Clinical signs were also evident by day 3 post infection, (Figure 3.25B) with decreased mobility scored at an average of 1 for this group. On day 4, mobility was scored at an increased severity of 2 on average and is coupled with signs of hunching (0.5 average). On day 5 pointed face was identifiable (score of 1 on average), raising the severity score to an average of 4.5 overall. On day 6, mice were scored around 3 for decreased mobility, 2 for hunching and 1.5 for pointed face, raising the total score to 7 on average which is an overall ‘moderate’ severity.

Co-infected mice demonstrated a highly attenuated response in the absence of IFN γ . Weight loss was not observed as a result of A/WSN/33 until 5 days post infection. An average reduction in weight of $3.49 \pm 3.42\%$ increased to a total of $8.79 \pm 3.4\%$ on day 6 (Figure 3.25A) which was the only day that a reduction in weight in the co-infected mice was significantly different to the uninfected group ($p < 0.01$). Therefore significant reduction in weight loss, afforded by co-infection was evident from day 3 to 6 at a confidence level of 99.9%. Clinical signs in these mice were also highly reduced. Co-infected mice began to show decreased mobility on day 5 (average score of 1.5) and reached a total severity score of 4.5 on day 6, (Figure 3.25B), similar to that of the A/WSN/33 infected group.

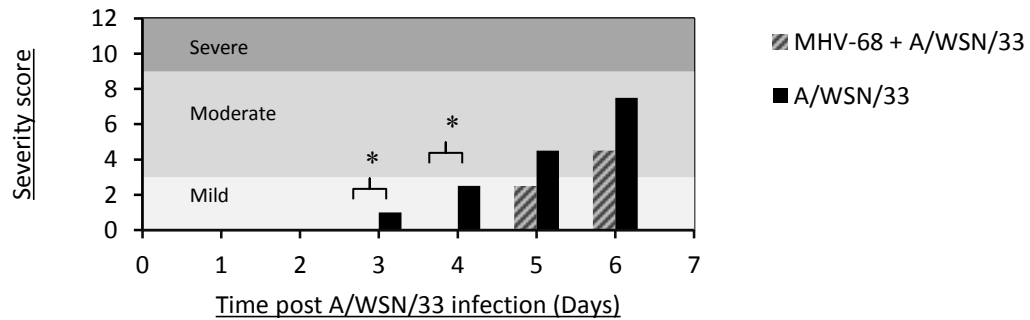
Influenza replication has thus far been unhindered by co-infection. To verify this in the IFN γ R^{-/-} mice, which had shown the most attenuated phenotype during co-infection, mice were culled at day 4 and day 7 post A/WSN/33 infection and lung viral load was calculated by plaque assay (Figure 3.25C). At both time points, similar levels of infectious A/WSN/33 were present in the lung and there was no significant difference detected between A/WSN/33 and co-infected mice. (2-sample Student’s T test on log transformed data). At day 4, singly A/WSN/33 infected mice had a mean influenza titre of 3×10^5 PFU ml⁻¹ lung homogenate reducing slightly to 2.09×10^5 PFU ml⁻¹ at day 7. Co-infected mice had a similar average titre of 5.0×10^5 PFU at day 4 and an equally high titre of 6.07×10^5 PFU in the lung at day 7 post infection. Both time points are

Figure 3.25 Effect of latent MHV-68 co-infection on pathogenesis of A/WSN/33 in an IFN γ R $^{-/-}$ model

A. Weight loss



B. Clinical severity score



C. Influenza lung titre

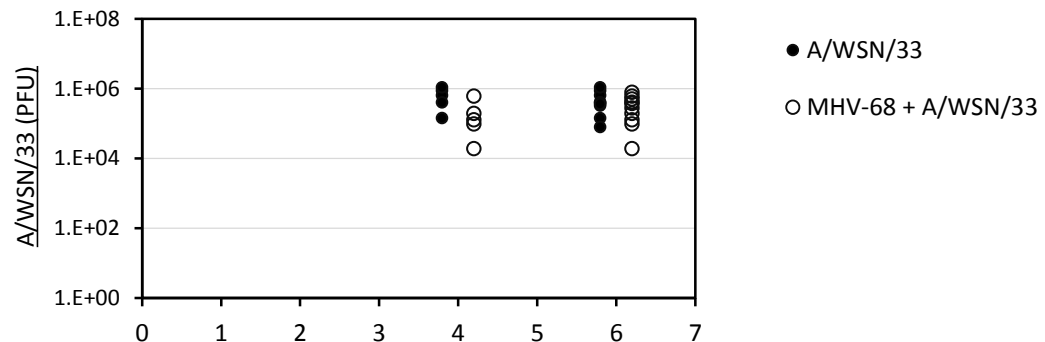


Figure 3.25 5-6 week old 129Sv/Ev IFN γ R $^{-/-}$ female mice were infected I.N. with 5×10^4 MHV-68 and 28 days later infected I.N. with 5×10^3 A/WSN/33. **A.** Influenza induced weight loss. Error bars represent ± 1 standard deviation of the mean. Significance determined by students two-way ANOVA (\dagger / \ast = $p < 0.05$, $\ast\ast$ / $\dagger\dagger$ = $p < 0.01$, $\ast\ast\ast$ / $\dagger\dagger\dagger$ = $p < 0.001$). \ast signifies significant difference between A/WSN/33 infected and uninfected groups. \dagger signifies a significant difference between co-infected and A/WSN/33 infected mice. **B.** Clinical severity was measured by 4 signs. Each was scored on a scale of 0-3 and the sum reported ± 1 standard deviation as clinical severity score, N=12. **C.** Mean A/WSN/33 titre in the lung, N=12 at day 4, N=6 at day 6.

therefore not significantly altered by co-infection however an interesting observation was that these titres in the singly A/WSN/33 infected mice were once again reduced compared with the 129Sv/Ev (more resistant) mice and shared greater similarity with the BALB/c (more susceptible) mice.

– Pathology in the lung

The pathology in the lung, in the absence of IFN γ was markedly different to that of the WT infections. Uninfected mice displayed no significant signs of pathology or disease (Figure 3.26A-C).

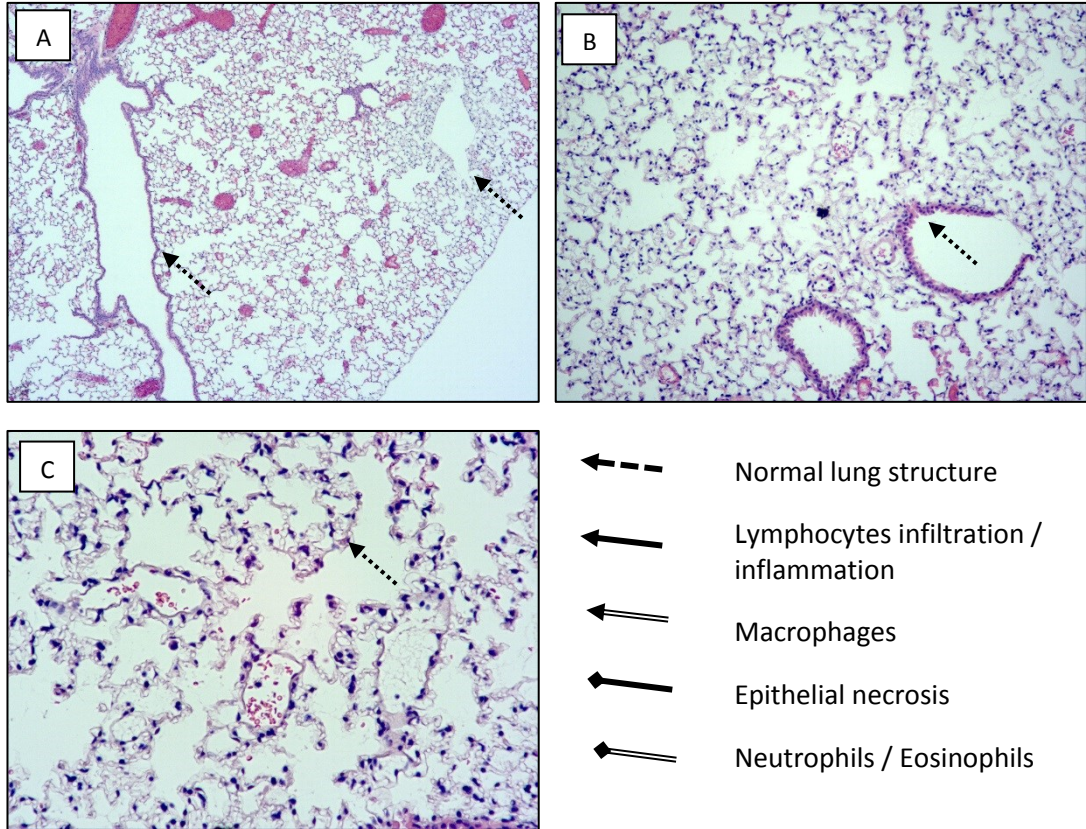
Latent MHV-68 infection however had a drastic and complex effect in the lungs of IFN γ R^{-/-} mice. Inflammation and infiltration of cells around the large airway vessels was severe and widespread throughout each lung cross section. Large areas of lymphocytic infiltration (Figure 3.26D-F) were coupled with areas of macrophage infiltration (Figure 3.26G-I). These macrophage cells were enlarged and contained crystal like structures that have been observed by others as alternatively activated macrophages in fibrotic lungs following MHV-68 infection of IFN γ R^{-/-} mice (Mora, Torres-Gonzalez et al. 2006). Peri-vascular infiltration was scored at 1.5 and peri-bronchial inflammation was scored at a mean average of 1.75. This is much greater than the mild pathology observed in the wild type mice.

A/WSN/33 infection of these mice lead to similar pathology to that in the wild type mice. Peri-bronchial and peri-vascular infiltration of lymphocytes was scored at an average of 1.9 and 2.0 respectively (Figure 3.26V). Variation within this group was also minimal (Figure 3.26 J-L) however some areas of inflammation were more severe and more focal than in the wild type mice. There was also extensive epithelial necrosis, apoptotic debris and infiltration of macrophages in these mice (Figure 3.26N-P).

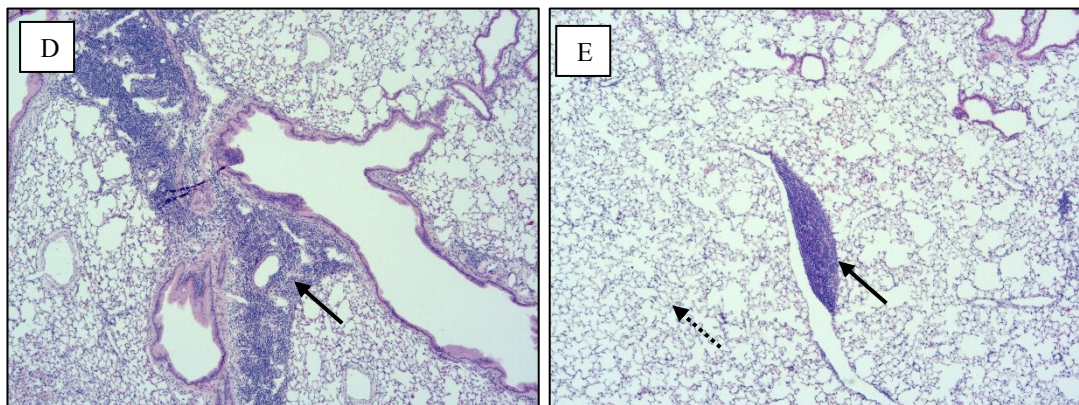
Co-infected mice were scored slightly higher than either of the singly infected groups. Peri-vascular inflammation was 2.17 and peri-bronchial inflammation was 2.00 on average for these mice. The severity of the pathology was extensive and areas of lymphocyte infiltration were vast within the interstitial spaces (Figure 3.26Q-U). It was difficult to assess the contributions of each infection to the extensive pathology, as both single infections caused severe disease in the lungs of these mice (Figure 3.26V).

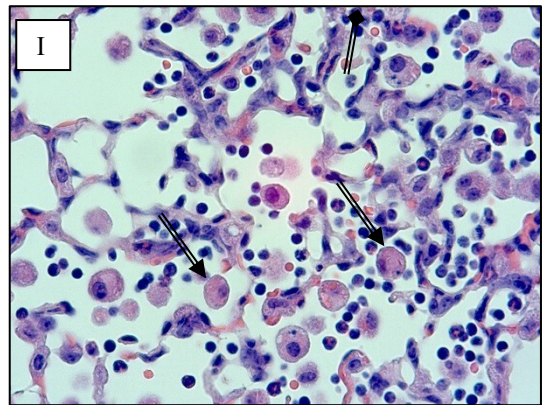
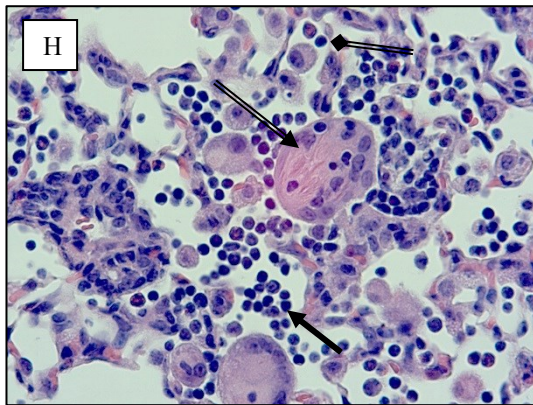
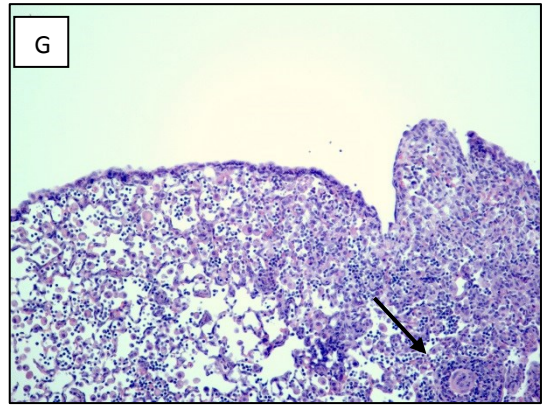
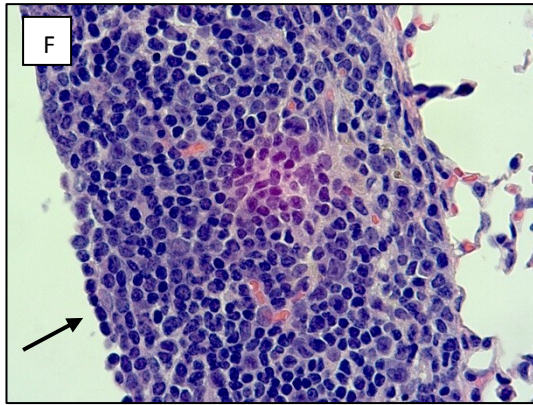
Figure 3.26 Latent MHV-68 infection causes severe pathology in the lung but is not exacerbated by co-infection with A/WSN/33

Uninfected

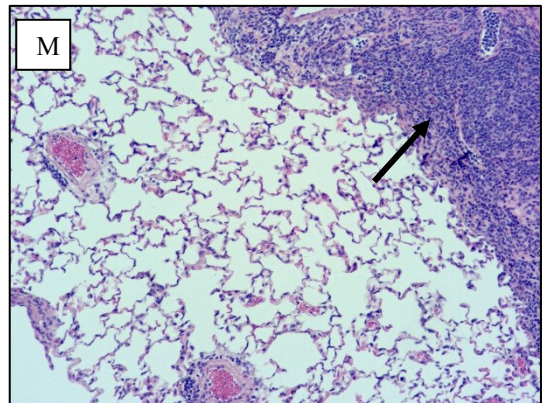
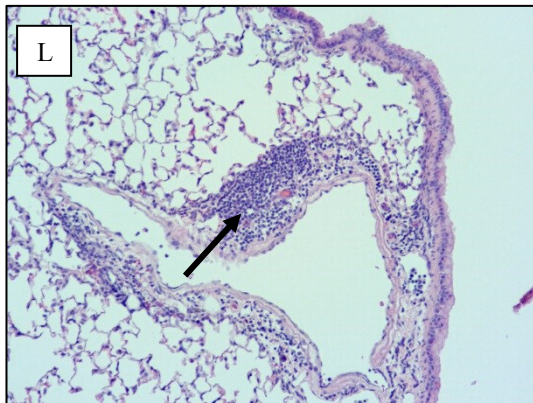
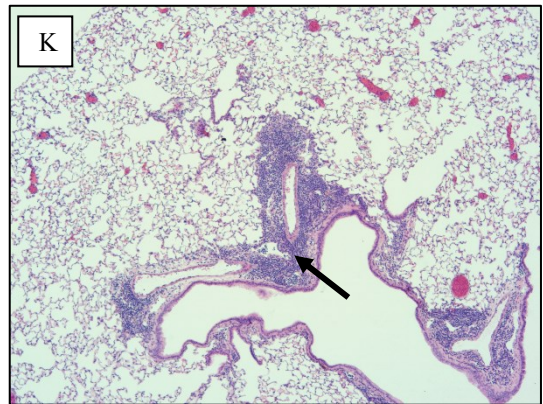
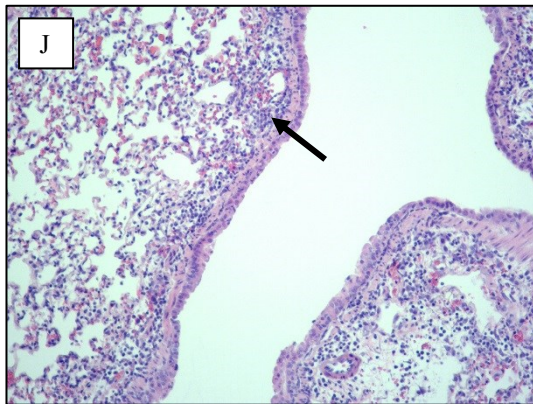


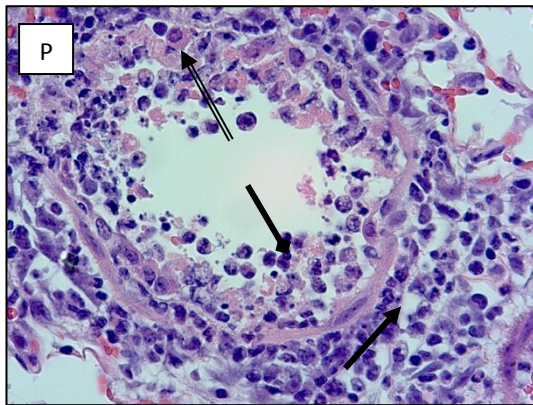
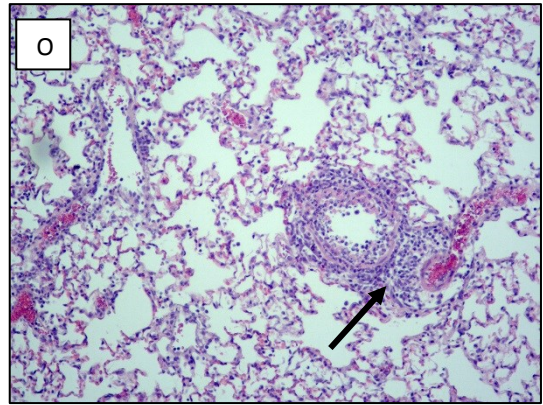
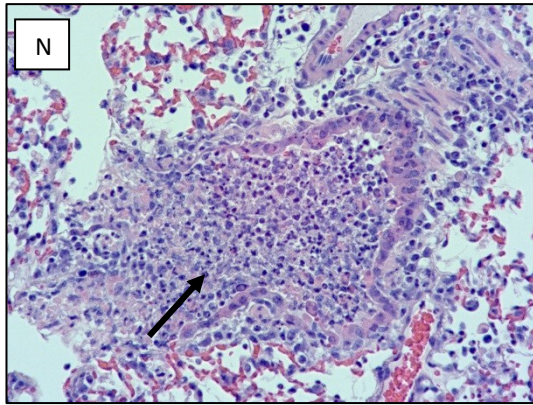
MHV-68 infected





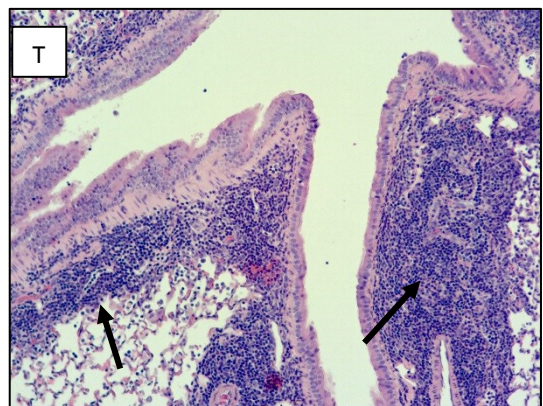
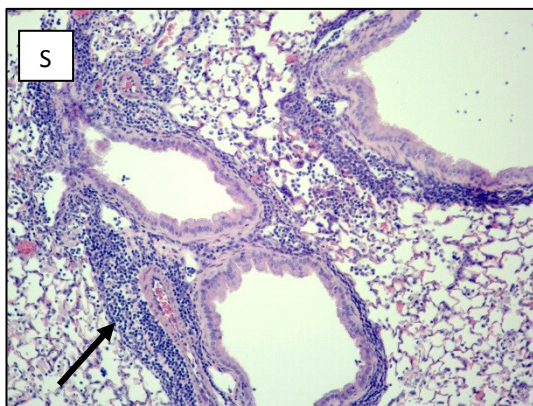
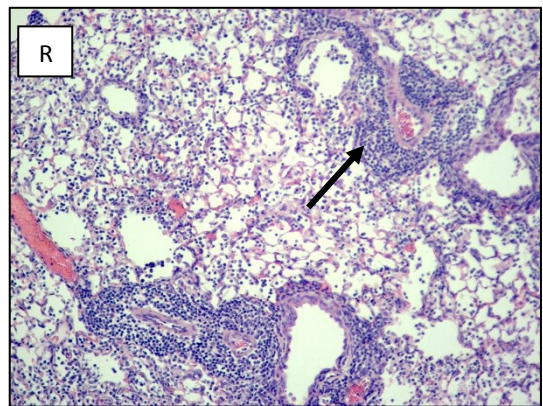
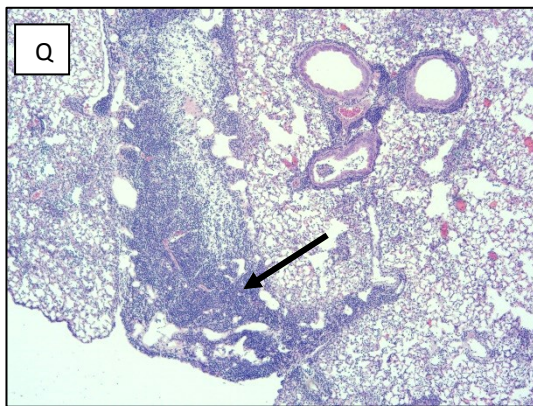
5×10^3 A/WSN/33 infected

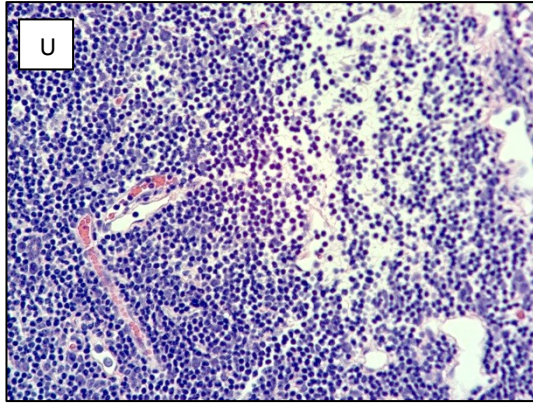




- ← Normal lung structure
- ← Lymphocytes infiltration / inflammation
- ← Macrophages
- ← Epithelial necrosis
- ← Neutrophils / Eosinophils

MHV-68 + 5×10^3 A/WSN/33 infected





V. Pathology score

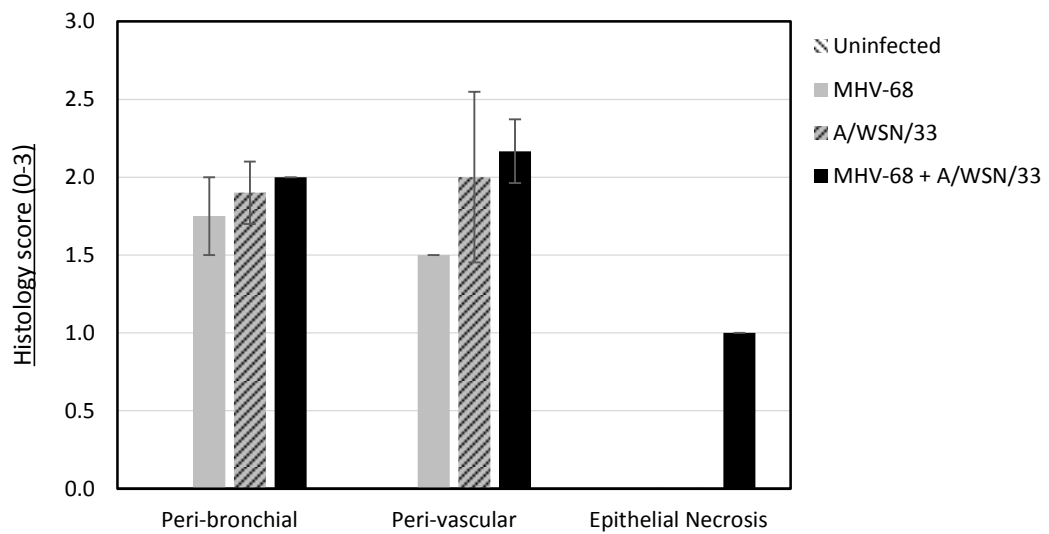


Figure 3.26 The right lung was inflated and fixed with 10% neutral buffered formalin. Lung sections were stained for hematoxylin and eosin. Representative sections are shown. **A-C** Lungs from uninfected mice. **D-I** Lungs from MHV-68 latently infected mice. **J-P** Lungs from A/WSN/33 infected mice. **Q-U** Lungs from co-infected mice. Images represent averages from each infection group. Magnification is identified in the bottom right corner of each image. **V.** Complete lung cross-sections were scored for signs of inflammation and cell damage, N=6. Representative of 1 experiment. Results are displayed as mean average per group \pm 1 standard deviation.

– Cytokine environment in the lung

In the absence of IFN γ , the protective effect is enhanced in the co-infected mice. To determine if this tempering in response was due to redundancy or overlap with other inflammatory cytokines, lung homogenates from IFN γ R^{-/-} 129 Sv/Ev mice were analysed for TNF α by ELISA at 4 and 6 days post infection with 5x10³ A/WSN/33. In the absence of IFN γ signalling, TNF α levels were not altered in any experimental group measured. At day 4 TNF α was detected at an average of 7.58 pg ml⁻¹ in the co-infected mice and 8.36 pg ml⁻¹ in the A/WSN/33 infected mice (Figure 3.27B). At day 7, levels of TNF α were very similar, with co-infected mice expressing an average of 9.92 pg ml⁻¹ and A/WSN/33 infected mice expressing 7.67 pg ml⁻¹. Uninfected and MHV-68 infected controls were also measured to ensure that these levels were not increased or reduced due to either infection. Both groups expressed very similar levels of TNF α , 4.79pg ml⁻¹ in uninfected mice and 19.72 pg ml⁻¹ (larger due to a single outlier) in MHV-68 infected mice.

IFN β production in lung homogenates from co-infected and A/WSN/33 infected mice was also measured at day 4 during the peak of viral replication. This type 1 inflammatory cytokine was not detected at significant levels, however there was a general trend for an increase in IFN β in co-infected mice (24.54 pg ml⁻¹) compared with A/WSN/33 singly infected mice (3.21 pg ml⁻¹) 4 days post infection (Figure 3.27A). This difference between these groups was not statistically significant.

– Effect of A/WSN/33 on co-infection with latent MHV-68

Considering that the protective effect of co-infection is restored in 129 Sv/Ev mice in the absence of the IFN γ receptor it was of interest to determine if the reciprocal suppression of latent MHV-68 by A/WSN/33 infection in the lung was also evident.

Lung and spleen DNA was analysed by qPCR for ORF73. As in BALB/c mice but unlike WT 129 Sv/Ev mice, MHV-68 viral load in the lung appears to decrease 6 days after A/WSN/33 infection of IFN γ R^{-/-} 129 Sv/Ev mice (Figure 3.28B). Co-infected mice had on average 39.5 copies of the MHV-68 genome per 100ng DNA. MHV-68 infected mice however had 155 copies per 100ng DNA. This decrease is not significant, (p=0.068, Mann-Whitney test) likely due to the low number of replicates which could be strengthened with a repeat experiment at the same day 6 time point. In the spleen there is no reduction in MHV-68 frequency in the co-infected mice. Both groups harbour similar levels of MHV-68. Co-infected mice have an average of 685 copies whilst singly MHV-68 infected mice have 402 copies per 100ng splenic DNA (Figure 3.28A). This result is therefore also not significant.

Figure 3.27 Inflammatory environment is not altered in IFN γ R $^{-/-}$ S129Sv/Ev mice

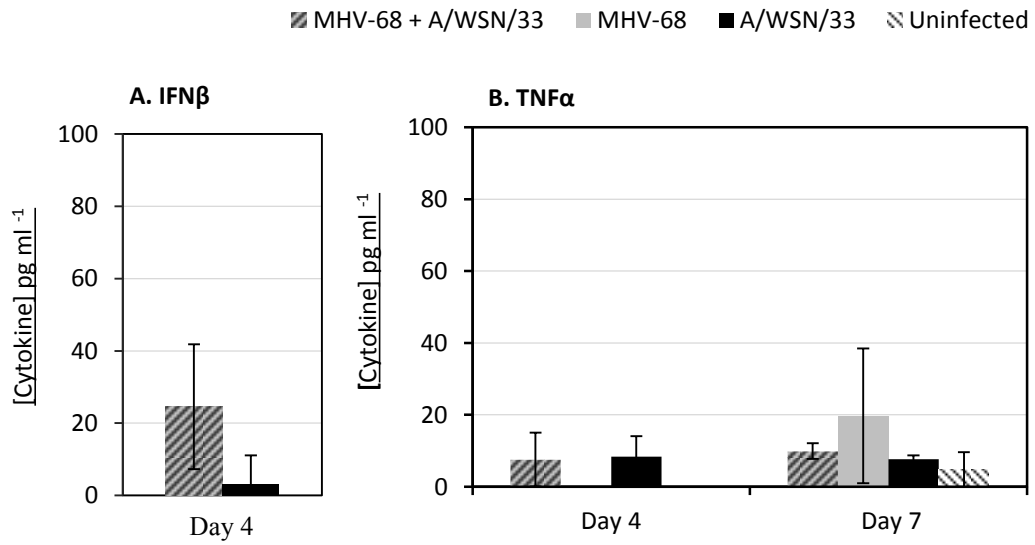


Figure 3.27 ELISA analysis of lung homogenates in IFN γ R $^{-/-}$ 129 Sv/Ev mice were performed at day 4 and day 6 post infection with 5×10^3 A/WSN/33. **A.** Mean IFN β level ± 1 standard deviation. **B.** Mean TNF α levels ± 1 standard deviation N=6.

Figure 3.28 A/WSN/33 infection in IFN γ R $^{-/-}$ 129Sv/Ev mice reduces MHV-68 in the lung

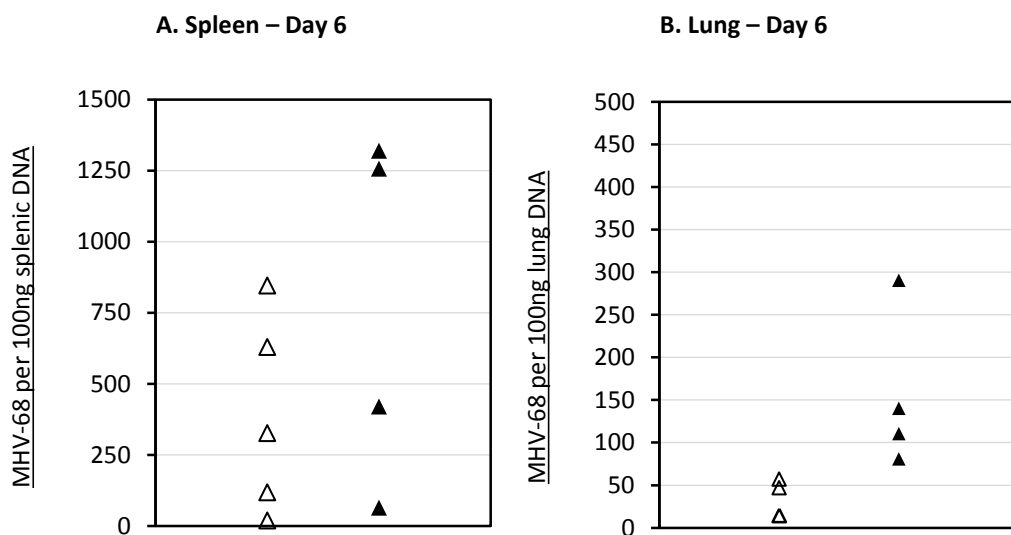


Figure 3.28 DNA was extracted from a segment of the spleen and left lobe of the lung. Quantitative PCR for ORF 73 in the MHV-68 genome was performed on 100 ng of DNA. **A.** MHV-68 viral load in spleen samples 6 days post A/WSN/33 infection (34 days post MHV-68 infection), N=5. **B.** MHV-68 viral load in the lung at the same time point. N=4. Results are displayed as individual values. Statistical analysis performed by two sample student's t test.

3.4.6 Latent MHV-68 infection

Co-infection with latent MHV-68 infection causes attenuation to the pathogenesis of A/WSN/33. Likewise, infection with A/WSN/33 decreases the viral load of MHV-68 in the lungs of co-infected mice. MHV-68 latency has been shown to increase the circulating inflammatory cytokines in the blood and subsequently offset the immune response to bacterial pathogens (Barton, White et al. 2009). To determine how MHV-68 alters the lung environment prior to A/WSN/33 co-infection, latently infected mice were analysed for cytokine production, changes to resident macrophages in the lung and alterations to the CD4⁺ cell responses in the lung draining lymph nodes.

The lytic phase of the MHV-68 life cycle is resolved 21 days after infection. The majority of the MHV-68 lytic infection is cleared from the lungs after 10 days although some virus persists for much longer (Stewart, Usherwood et al. 1998).

Latency is established in the spleen around 20 days post infection. Splenomegaly, caused by acute infection is resolved by 21 days post infection. MHV-68 infection causes no observable clinical disease or associated signs in female BALB/c mice during the latent stage of infection. MHV-68 infected mice 28 days post-infected are considered to be harbouring a latent MHV-68 infection. This time point was used in all co-infection experiments as the point of influenza infection. Prior to infection with influenza A/WSN/33 mice were weighed. At this age the mice were between 18 and 22 g. There was no difference in weight between mice infected with MHV-68 for 28 days and uninfected mice of the same age.

Mice infected for 28 days with MHV-68 were culled and compared with uninfected litter mates.

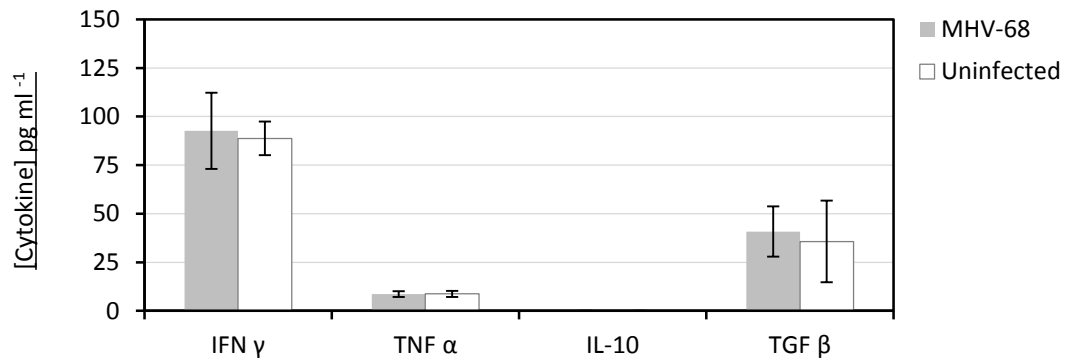
– Cytokine environment

The cytokine environment in the lung was not altered due to MHV-68 latency (Figure 3.29A). Pro-inflammatory cytokines, IFN γ and TNF α were not different between groups. IFN γ was measured at 92.65 \pm 19.63 pg ml⁻¹ in the MHV-68 infected mice and 88.73 \pm 8.61 pg ml⁻¹ in the lungs of uninfected mice. TNF α was much lower at 8.65 \pm 1.42 pg ml⁻¹ in MHV-68 infected mice and 8.73 \pm 1.55 pg ml⁻¹ in the uninfected mice.

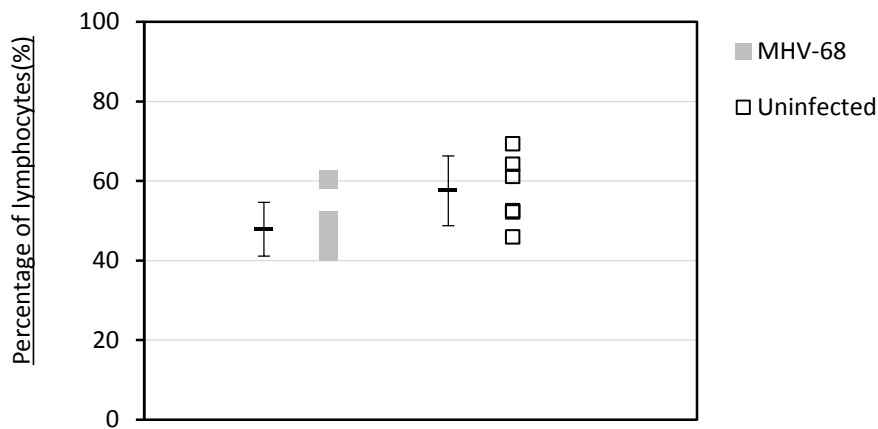
Likewise, regulatory cytokines IL-10 and TGF β were not differentially expressed due to latent MHV-68 infection. IL-10 was undetectable in the lungs of both uninfected and MHV-68 infected mice while TGF β was expressed at 35.72 \pm 20.96 pg ml⁻¹ in uninfected and 40.83 \pm 12.93 pg ml⁻¹ in MHV-68 infected mice.

Figure 3.29 Lung cytokine environment and CD4⁺ cells in the draining lymph node are not altered by latent MHV-68 infection

A. Lung cytokines



B. Total CD4⁺ cells in the lung draining lymph nodes



C. Production of cytokines by CD4⁺ cells in the lung draining lymph nodes

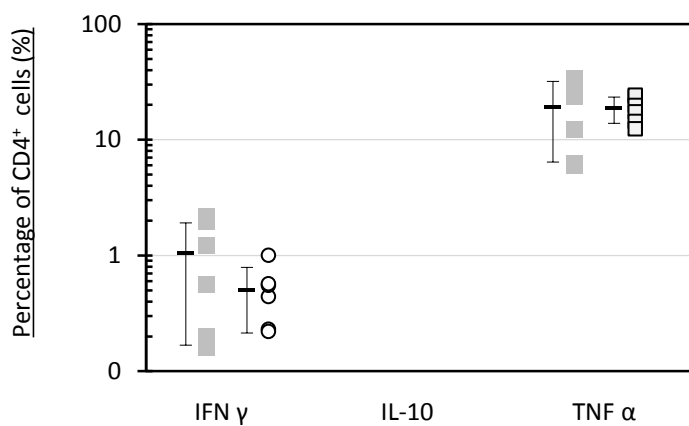


Figure 3.29 Female BALB/c mice were culled 28 days post MHV-68 infection. **A.** lung homogenates were analysed for cytokines by ELISA. Results are mean averages \pm 1 standard deviation, N=6. **B/C.** Cells from the lung draining lymph nodes were harvested and 1×10^7 cells were stained for CD4⁺ and cytokine production. Samples were run on a BD LSR II Fortessa. Results are displayed as percentages and mean per group \pm 1 standard deviation. N=6.

Further information on the cytokine environment could be determined from the protein array discussed later.

– Lymph nodes

Mediastinal lymph nodes are also a site of latent MHV-68 infection. To determine if there was any effect of MHV-68 latency on responding CD4⁺ T cells in the lung draining lymph node, cells of the lymph nodes were analysed by FACS. There was no detectable difference in the percentage of CD4⁺ cells in the lymph node or in the production of cytokines by these cells when stimulated with PMA and ionomycin (Figure 3.29B).

Uninfected mice had on average 57.53±8.77 % of CD4⁺ lymphocytes in the mediastinal lymph node. 0.5% of these cells produced IFN γ and 18.6% produced TNF α . In the MHV-68 latently infected mice 47.88±6.74 % of total lymphocytes were CD4⁺ and within this population 1.0% produced IFN γ and 19.13% produced TNF α . IFN γ and TNF α levels were therefore not significantly different between MHV-68 and uninfected mice (Figure 3.29B). IL-10 expression by CD4⁺ cells could not be detected in either group. Results were not analysed statistically.

– Macrophages

Lung cells were retrieved by broncho-alveolar lavage 28 days post MHV-68 infection. Adherent cells were lysed and cDNA was made using the maximum RNA available. Quantitative PCRs for macrophage polarisation markers were undertaken and normalised relative to SDHA, a cellular house-keeping gene. Macrophages in MHV-68 latently infected mice did not demonstrate increased M1 associated markers iNOS and TNF α compared with uninfected mice. On average iNOS was 73.08 fold more abundant than SDHA in uninfected mice and the standard variation within this group was ±67.01 (Figure 3.30D). The reason for the large mean average was a single value 188.5 fold the copy number of SDHA detected. Results from this same mouse skew the mean within the uninfected group for all markers tested. The SDHA level detected in this mouse was particularly low (2 copies in both replicates) and therefore all other markers were normalised by a small number which often led to high fold change compared with other mice within the same group. Analysis of the raw data gave no reason to exclude the sample and therefore it was not excluded. Median was not used as a measure of experimental group average due to the low number of animals per group, (n=6). The mice infected with MHV-68 for 28 days had an average fold increase of 9.08 iNOS verses the SDHA copy number and a smaller standard deviation of 11.2. Therefore despite differences in the mean averages, iNOS was not significantly different due to MHV-68 infection (Figure 3.30D). TNF α levels showed a similar pattern to iNOS (Figure 3.30C). On average there was an

Figure 3.30 Latent MHV-68 infection increases SOCS-1 expression in lung macrophages

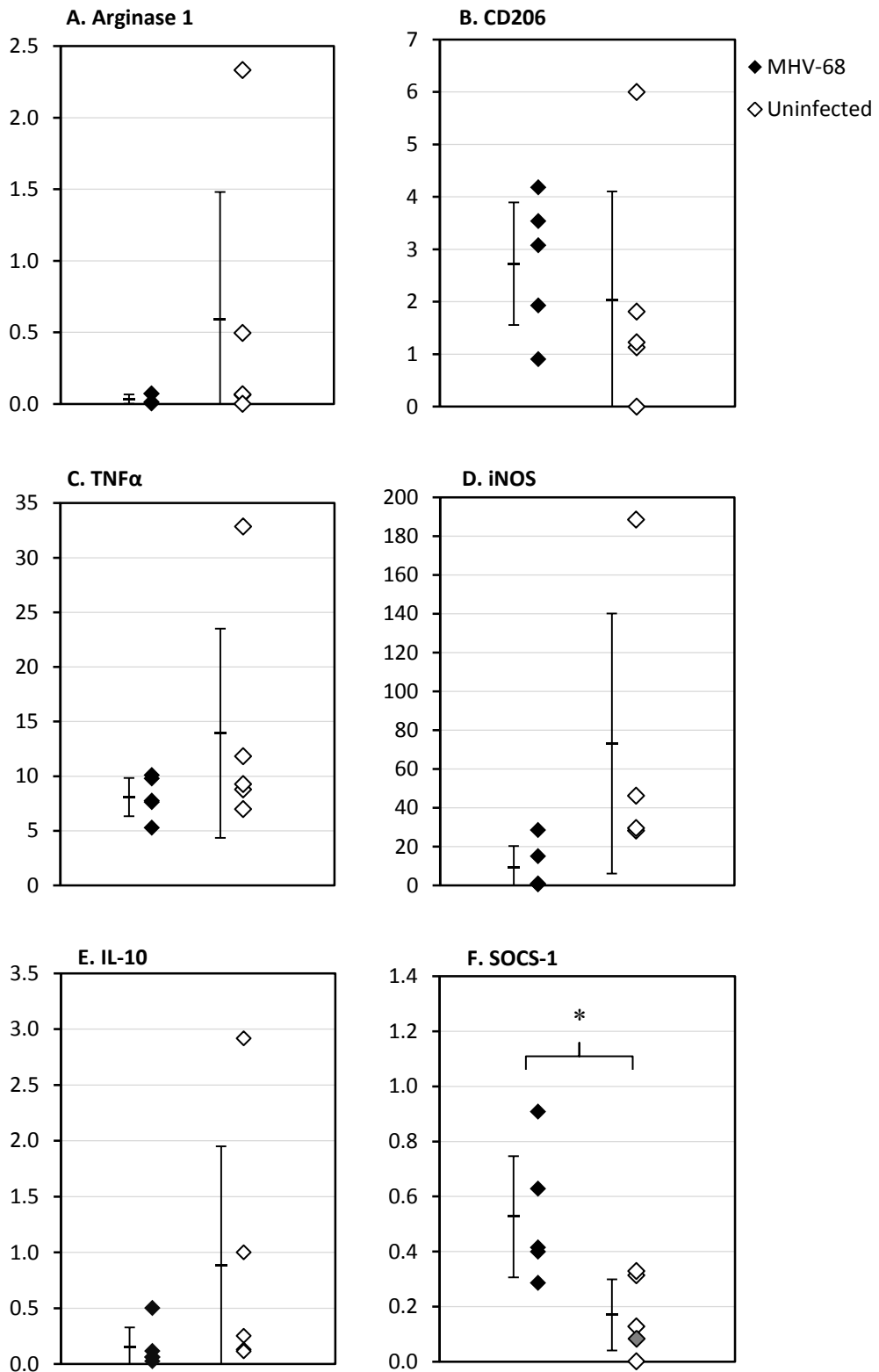


Figure 3.30 Adherent cells from broncho-alveolar lavage fluid of mice 28 days post MHV-68 infection were analysed for M1 and M2 macrophage markers by QPCR. Results are shown as individual values per copy of the house-keeping gene SDHA and means \pm 1 standard deviation. N=5, results from a single experiment. Statistical analysis by 2 sample t test, *p =0.03. A. Arginase-1 expression B. CD206 expression C. TNF α expression

8.08±1.74 and 13.92±9.58 fold more TNF α compared with SDHA copy number in the MHV-68 infected and uninfected mice respectively (Figure 3.4C). A single outlier was again detected in the uninfected group with 32.82 fold more TNF α than SDHA. This is the same problematic sample identified in the iNOS group and is evident as an outlier on the graph. The levels of TNF α are therefore not different between experimental groups.

M2 markers CD206, IL-10 and arginase 1 were similar between experimental groups (Figures 3.30B, 3.30E and 3.30A). CD206 had an average 2.72±1.71 and 2.07±2.03 fold increase compared with SDHA in the MHV-68 and uninfected mice respectively. In this instance the outlier mouse (6 fold increase versus SDHA) appears to increase the mean average in the uninfected group. Overall there is a trend for slightly more CD206 expression in MHV-68 infected mice than uninfected. This is again not significant. IL-10 levels are low in both experimental groups and all samples contained less IL-10 than SDHA, therefore results are lower than 1. Mean IL-10 fold change is 0.15±0.18 in the MHV-68 infected and 0.88±1.06. Despite the skew due to a single sample, the effect of MHV-68 infection was not significant on IL-10 production in adherent cells from the lung. The final M2 marker, arginase 1 was also detected at low levels and was expressed below that of SDHA level, 0.03±0.03 for MHV-68 infected and 0.59±0.89 for uninfected mice. This was not significantly different between groups.

SOCS1 expression (Figure 3.30F) was significantly ($p=0.03$) increased in the MHV-68 infected mice despite low expression in both experimental groups. Uninfected mice expressed 0.53±0.22 SOCS1 normalised to SDHA whilst uninfected mice expressed 0.17±0.13; significantly lower. A second house-keeping gene expressed at low numbers in macrophages could be used to validate this result. The outlier from previous markers is highlighted although it does not seem to alter the response for this marker. Latent MHV-68 infection does not alter macrophage polarisation markers however SOCS1 is decreased in adherent cells from the lungs in mice 28 days after MHV-68 infection.

– Protein array

During the MHV-68 + 5x10³ A/WSN33 co-infection experiments in BALB/c mice (see Figure 3.17), lungs from each experimental group, 6 days post A/WSN/33 or A/WSN/33 mock infection were homogenised and protein arrays were performed. Differences between the MHV-68 and uninfected groups show the effect of MHV-68 latency on protein levels in the lung and provide further evidence of changes to the immune environment in the lung caused by MHV-68 persistence.

Latent MHV-68 infection alone resulted in 5 cytokines increasing to significantly higher expression levels than the uninfected group. These cytokines may provide examples of

responses caused by MHV-68 latent infection that protect and alter the immune response to A/WSN/33 co-infection. GM-CSF increased significantly ($p < 0.05$) by 1.68 fold, MIG (CXCL9) by 2.24 fold ($p = 0.014$), M-CSF increased by 2.16 times ($p < 0.05$), ICAM-1 by 2.8 fold ($p < 0.05$), and RANTES (CCL5) showed the largest significant increase to 5.6 fold the levels seen in uninfected mice ($P < 0.001$).

3.5 Discussion

3.5.1 Co-infection with latent MHV-68 and 'low dose' influenza A/WSN/33

The influenza viral dose was chosen as 5×10^2 PFU due to the unknown effect of co-infection, albeit the dose used in initial experiments was lower still, (see section 3.4.1). As the latent MHV-68 did not significantly alter the lung environment (Figure 3.29A) then subtle changes to the progression of influenza infection were more likely detectable in lower dose infections. At this initial dose, however, there were no clinical signs and no effect on weight during the time course (Figure 3.3A and 3.3B). Simultaneously, although the low dose was sufficient to cause cellular infiltration around the airways and blood vessels as well as minor epithelial necrosis, (Figure 3.5), it was not evident that pre-existing co-infection with MHV-68 was capable of mediating this minor pathological outcome of A/WSN/33 infection.

The lung cytokine environment at this dose was monitored in lung homogenates 4 and 6 days post A/WSN/33 infection by ELISA. Four days post infection IL-1 β is raised in the A/WSN/33 infected groups (Figure 3.6A). IL-1 β is an early pro-inflammatory cytokine activated by the inflammasome, associated with lung immunopathology and activation of CD4⁺ T cell responses to influenza (Schmitz, Kurrer et al. 2005). The co-infection, however, did not alter early inflammatory signalling via IL-1 β production. (Influenza NS1 can inhibit inflammasome cleavage of pro-IL-1 β).

MIP2 (CXCL-2) was significantly increased in co-infected mice compared with uninfected mice. However, singly MHV-68 or A/WSN/33 infected mice also show evidence of increases in MIP2 but not to a significant level. MIP2 is a chemokine responsible for macrophage and neutrophil recruitment to the lung during low dose influenza infection (Wareing, Lyon et al. 2007), however the histological results from day 6 (Figure 3.4F-H) do not show obvious differences in the number of macrophages or neutrophils in the alveolar spaces or co-infected mice. While this difference does not appear to alter the influenza response, chemokine dysregulation has often been implicated in contributing to bacterial susceptibility and super-infection post influenza A infection (Zavitz, Bauer et al. 2010) and it is possible that underlying infection prior to influenza infection could alter an individual's susceptibility to super-infection.

At day 4, interferons gamma and beta and inflammatory markers IL-2 and TNF α have not significantly increased in any group. Regulatory cytokines IL-10 and TGF β have also not altered by either infection at this time point (Figure 3.6). Six days post infection however IFN γ and IL-10 levels are increased in all A/WSN/33 infected groups. IFN γ and IL-10 have counter regulatory roles in the other's expression (Ito, Ansari et al. 1999; Hu, Paik et al. 2006) and are expected to peak during influenza infection at day 6 (Sun, Madan et al. 2009) thus their elevation is consistent with the peak in weight loss and significant inflammation in the lung pathology.

Mean averages in IFN γ levels showed that there was a trend for increased expression in A/WSN/33 infected mice compared with co-infected mice and the same was seen in IL-10 expression, however, this was not significant. In combination with this, the influenza titre at this final time point was significantly reduced in the co-infected mice (Figure 3.3C).

The mean titre of the A/WSN/33 infected group was double that of the co-infected mice 6 days post infection. More rapid clearance of the virus would correlate well with increased presence of macrophages and inflammatory cells brought into the lung by the increase in chemokines such as MIP2 however this was not visible in the histology (discussed earlier) and epithelial necrosis was very similar in co-infected and singly A/WSN/33 infected mice suggesting replication of the virus was unhindered by the underlying MHV-68 infection. There was therefore no clear evidence that chemokine signalling as a result of co-infection can alter the kinetics of influenza pathogenesis.

Spleen MHV-68 DNA load was measured by qPCR every 2 days post infection (Figure 3.7A). A/WSN/33 infection had no effect on latency of MHV-68 in the spleen. In the lung at day 6 there was a general trend for a decrease in the levels of MHV-68 present during co-infection (Figure 3.7B). However this would need to be repeated with greater numbers of samples to clarify if a subtle decrease in MHV-68 load is due to the latent MHV-68 co-infection.

3.5.2 Co-infection with latent MHV-68 and 5×10^2 influenza A/WSN/33

Heterologous immunity as discussed in the introduction (section 1.4) has been observed in human herpesvirus infections. CD8⁺ T cells specific to Epstein Barr virus and human cytomegalovirus have been shown to attenuate subsequent unrelated infections such as hepatitis B (Sandalova, Laccabue et al. 2010).

There were no changes in the percentages of total CD8⁺ cells in the lung following A/WSN/33 co-infection however it is possible that the antigen specificity of these cells is different to that of the A/WSN/33 singly infected mice. The CD8⁺ cells in the co-infected mice have, on average,

increased levels of IFN γ and TNF α (Figure 3.14C and 3.14D) although this was not statistically significant. The increased production of cytokines other than IFN γ by CD8⁺ T cells is generally associated with a switch towards a memory phenotype (Kristensen, Madsen et al. 2004). This may suggest a contribution of memory cells specific for the herpes virus within the total population of responding cells or simply suggest a subtle change in the kinetics of the T cell response to A/WSN/33 due to underlying influence of the co-infection.

In a co-infection with *Trichinella spiralis*, CD8⁺ lymphocyte infiltration was reduced when compared with influenza infection alone, leading to a more rapid recovery. Although total percentages were similar, extending the time course of the co-infection may give greater insight into whether alterations to cytokine production and potentially activation state in the CD8⁺ T cell population can change the resolution of inflammation.

The reduced influenza viral titre at this time point (Figure 3.8C) would suggest alteration to the kinetics of the infection, however, CD8⁺ T cells, although integral for an acute response are not inversely correlated with viral load. Instead macrophage and neutrophil populations seen in the lung at early and late phases of the acute infection are more closely related to a reduction in influenza titre (Lv, Hua et al. 2014). Macrophages and neutrophil numbers in the lungs of infected and co-infected mice were not noticeably different in the pathology (Figure 3.9).

The most significant change in the co-infected group is an absence of clinical signs (Figure 3.8B). A/WSN/33 infected mice show increasing clinical severity from 4 days post infection. Co-infected mice begin to show signs of infection at day 5 but signs do not increase over the time course. These changes are not reflected in the peak viral titres measured at day 4 which are not different in the lung between co-infected and singly A/WSN/33 infected mice. However, a decrease is evident at day 7 in co-infected animals. An earlier 24 or 48 hour time point may show differences in the initial stages of viral replication however, ultimately both experimental groups reach the same peak viral titre (Figure 3.8C). It could be important to understand if the initial stages of replication differ between experimental groups in order to determine if the decreased viral titre in the co-infected mice at day 7 was a result of increased clearance and therefore changes to adaptive immunity or was a result of altered kinetics in viral replication, point of infection and the decrease at day 7 is because viral replication occurred faster in the co-infected mice.

In human viral challenge experiments, a H3N2 derivative showed a direct association between clinical signs and viral shedding in the upper respiratory tract. It is well known that influenza will replicate in the nasal tissues of mice (Iida & Bang, 1963) and is predominantly an upper respiratory tract infection in humans. The upper respiratory tract may be an interesting site to monitor for changes to influenza titre caused by co-infection, as MHV-68 will also replicate in

the nose and salivary glands (Hwang, Wu et al. 2008) and the upper respiratory tract ultimately is the initial site of infection through natural transmission.

Early production of increased IFN γ by CD8 $^+$ cells and NK cells is usually associated with the development of strong T_H1 CD4 $^+$ T cell responses (Teixeira, Fonseca et al. 2005). CD4 $^+$ T cells are vital for polarisation of the immune response, governing CD8 $^+$ T cells and differentiating B cells during viral infection. In the lung they are also producers of cytokines at the site of infection and have been shown to harness direct cytolytic function in influenza infection (Brown 2010). CD4 $^+$ T cells and their cytokine production were therefore hypothesised to play a pivotal role in the protective effect observed during co-infection and may be a potential source of the long term production of IFN γ and TNF α seen in latent MHV-68 infection.

Therefore CD4 $^+$ T cells were characterised in both the lung and lymph nodes. CD4 $^+$ T cells do not appear to be altered in the lung (Figure 3.13) or the draining lymph nodes (Figure 3.14) in the co-infected group compared with the singly A/WSN/33 infected mice. CD4 $^+$ T cells show a predominantly T_H1 phenotype with high production of IFN γ , however IL-4 and IL-10 production is also increased during A/WSN/33 infection. The increase in production of IFN γ by CD4 $^+$ T cells in the lung will contribute to increased levels measured in lung homogenates in Figure 3.11. Simultaneously, increased levels of IFN γ are likely responsible for the decrease in MHV-68 viral load seen in the lung and not the spleen (Figure 3.12).

IFN γ actively suppresses the gene 50 promoter, controlling the switch from lytic to latent gene expression profiles (Goodwin, Molleston et al. 2010). Interestingly the opposite effect has recently been reported in helminth and MHV-68 co-infected mice, where IL-4 production by gastro-intestinal nematode infection encourages reactivation from latency (Reese, Wakeman et al. 2014). Co-infection therefore affects the prognosis of both pre-existing chronic and acute infections. Influenza virus may actively suppress reactivation of the latent MHV-68 or alternatively, as persistent MHV-68 virus in the lung is still replicating at low levels, influenza infection could cause an increase in IFN γ production and indirectly suppresses replication of the persistent virus. It would be interesting to understand the long-term effect following the resolution of the A/WSN/33 response and determine if the latent herpesvirus load was significantly changed. It would also be of interest to determine if changes to the expression of MHV-68 latency and lytic genes occurs in co-infected animals as a result of influenza infection.

3.5.3 Co-infection with latent MHV-68 and 5×10^3 influenza A/WSN/33

Subtle changes in the immune responses due to co-infection were identified more easily at the lower dose infections. This is also the case for changes in viral clearance seen at day 6 and 7.

Case-fatality statistics during the outbreak of the 1918 pandemic virus, (from which A/WSN/33 is distantly derived from), demonstrate that there is a direct correlation with 'infectious dose' and hypercytokinemia. To determine if MHV-68 can still provide the same protective effect against a potentially severe 'high dose' A/WSN/33 infection another set of experiments was performed at 5×10^3 PFU, (10 fold higher infection).

As with the lower dose of infection, weight loss was reduced in the co-infected mice. However, the variation in weight loss in the co-infected mice following the 5×10^3 dose was greater than that observed at the lower dose. As such, significant changes are observed at 4, 5 and 7 days post infection but not day 6. The co-infected mice are also subject to a second variable in the system due to the two separate viral infections and may therefore differ from one another to a greater extent than the individuals in the singly infected group.

The level of statistical significance is also lower than in the lower dose experiments, suggesting that the protective effect afforded by co-infection with MHV-68 is less capable of attenuating high doses of influenza and its subsequent pathology. The pattern of clinical signs is similar, with clinical effects occurring a day earlier in both groups, (3 days post infection) but increasing in severity much more rapidly in the singly A/WSN/33 infected mice than the co-infected mice.

Herpesviruses employ an arsenal of immune evasion strategies during lytic and latent infection. To understand the individual changes to cytokines and chemokines in the inflammatory environment, lung homogenates were used in a cytokine array. Cytokine storm associated cytokines, TNF α , IL-1 β , IL-1 α , IFN γ and IL-6 are all significantly reduced at day 6 post infection in the co-infected mice compared with singly A/WSN/33 infected mice. IL-6 is of particular interest within this panel of cytokines, as it was reported to have close association with progression of disease in patients during the 2009 H1N1 pandemic (Yu, Zhang et al. 2011). IL-6 is a necessary cytokine in mice however as it promotes neutrophil mediated viral clearance and in its absence sub-lethal infection leads to fatality (Dienz, Rud et al. 2012). A delicate balance in control of infection is therefore required by this cytokine. IFN γ at this dose is also significantly reduced in co-infected mice along with a number of IFN γ inducible cytokines, IL-12p70, IP-10, MIG and RANTES. This was a trend seen at the lower dose infection but did not quite reach significance due to a single result within the co-infected group, (Figure 3.11A). The results from the protein arrays are likely more sensitive than the ELISAs performed at other time points.

A T_H17 secondary response following influenza vaccination has recently been identified as detrimental to influenza prognosis, increasing weight loss and clinical severity in mice (Maroof, Yorgensen et al. 2014). Therefore a significant decrease in IL-17 and IL-23 are likely contributing factors to the decrease in clinical signs seen in the co-infected mice. In IL-17R

knock-out studies, neutrophil mediated immunopathology and weight loss were greatly reduced during influenza infection. Both of these were decreased during the latent MHV-68 co-infection (Figure 3.17C). These changes occurred without an impact on recruitment of CD8⁺ T cell populations. Equal percentages of CD8⁺ T cells were identified in the lung in both singly A/WSN/33 infected and co-infected mice, increasing the likelihood that decreased T_H17 responses may be a critical difference in co-infected mice. IL-17 knock-out mice however can exhibit reduced B cell recruitment to the lung during influenza A infection (Wang, Chan et al. 2011). Consideration of the long term implications of co-infection and experiments to determine whether appropriate antibody responses are made to provide protection from re-infection with influenza may be required to determine if co-infection reduces secondary immunity due to mediated primary responses.

Type 2 cytokines have a similar pattern of expression, with co-infected mice expressing much lower IL-4, IL-5 and IL-13 levels than singly A/WSN/33 infected mice (Figure 3.17C). IFN γ production is known to be increased in serum during MHV-68 latency (Barton, White et al. 2009) however this was not evident in the lungs of BALB/c mice 28 days post infection (Figure 3.29A). IL-4 has recently been identified as capable of reactivating MHV-68 into a lytic replication cycle, (Reese, Wakeman et al. 2014) therefore underlying inflammatory cytokine or suppression of type 2 cytokine production in order to maintain MHV-68 latency appears to mitigate an increase in the T_H2 cytokines during influenza infection. The source of the additional IL-4 in the lungs of singly A/WSN/33 infected mice is unknown. CD4⁺ cells in the draining lymph nodes appear to have a similar T_H1 phenotype in both singly and co-infected mice. There is limited description of type 2 cytokine production in influenza A infection, however in TLR7^{-/-} mice there is a shift towards T_H2 cell phenotype in the lung and production of more IgG1 than IgG2a during the adaptive response (Jeisy-Scott, Davis et al. 2011). These mice are less resistant to infection despite not showing differences in the influenza titre in the lung. This may therefore contribute to the alleviated clinical effects seen in the co-infected mice which produce IL-4, IL-5 and IL-13 to similar levels to the uninfected mice.

In an experiment with transgenic expression of IL-4 in the lung, secondary but not primary responses were impacted and viral clearance was delayed (Bot, Holz et al. 2000). It is therefore unlikely the type 2 cytokines are fundamentally required for protection from influenza. In the absence of CD4⁺ T cells, however, cytokines signalling via the IL-4R α can compensate for an absence of IL-2 mediated 'help' from CD4⁺ T cells required to activate cytotoxic function in CD8⁺ T cells (Marsland, Schmitz et al. 2005). The CD4⁺ T cell population is intact in this model, however, the influence of type 2 cytokines could hypothetically contribute to the subtle variations in CD8⁺ T cells discussed previously at the lower dose infection and later at this dose of influenza A infection.

Identifying the mechanism by which MHV-68 infection reduces inflammatory cytokine and chemokine activation could identify useful therapeutic targets for hypercytokinemia during human infection. For example MHV-68 and the human gammaherpesvirus Kaposi's sarcoma associated virus (KSHV) have been shown to down regulate TLR signalling in macrophages and abrogate responses to TLR 2,4,7 and 9 stimulants (Bussey, Reimer et al. 2014). Such changes to fundamental innate immunity would certainly impact the production of cytokines and chemokines in response to influenza co-infection. These changes are not evident in the macrophage profiling seen in Figure 3.30, where macrophages do not appear to be impaired in production of iNOS, CD206, Arginase 1 or cytokines IL-10 or TNF α , however, do show increased levels of SOCS-1 suggesting a more suppressed phenotype.

Modification of the immune response during infection may be a realistic approach to treatment, as severe influenza only becomes clinically evident days after infection when the virus has already reached peak replication and the immune response is underway. A number of strategies to target the excessive inflammatory response have been previously discussed here: (D'Elia, Harrison et al. 2013). To determine which of the cytokines and chemokines are altered in the first 24 hours of co-infection, levels of TLRs and anti-viral surveillance molecules such as NOD-like receptors and retinoic acid inducible genes and RIG-I like helicase receptors would be useful in order to interpret the results from the later time point and delimitate the initiating factors and inflammatory signalling at the site of infection.

CD4⁺ and CD8⁺ cells follow the same pattern of expression as in the 5x10² infection with no significant changes between co-infected and A/WSN/33 infected mice in regards to CD4⁺ responses in the lung and draining lymph nodes. CD8⁺ cells in the lung produce increased percentages of IFN γ and TNF α however are not increased in total percentage. This phenotype is associated with memory CD8⁺ responses and TNF α in particular is associated with a contraction in the CD8⁺ T cell response, usually observed around day 9 as discussed in the lower dose experiment. Co-infection decreases the extent of inflammation and therefore these responses may be seen earlier than in the singly infected mice. Future experiments, incorporating markers of activation would be useful to conclude how these cells may contribute to the mediated immune response.

3.5.4 Co-infection with latent MHV-68 and 5x10³ influenza A/WSN/33 in wild type 129 Sv/Ev mice

Due to the inhibited cytokine and chemokine environment in co-infected mice, it was hypothesised that removal of signalling by the highly inflammatory and prototypic T_H1 cytokine IFN γ would diminish the immunophenotypic skewing and subsequent immune suppression

caused by pre-existing MHV-68 infection. In order to test this theory $\text{IFN}\gamma\text{R}^{-/-}$ mice on a 129Sv/Ev background were co-infected with 5×10^4 MHV-68 for 28 days followed by 5×10^3 A/WSN/33 for a further 6 days (see 3.4.6). Therefore age matched female WT 129Sv/Ev mice were also co-infected to quantify baseline responses in this strain.

A/WSN/33 infection was less severe in this strain than in the BALB/c mice. Weight loss reached a maximum of 14.9% 6 days post infection compared with 21.7% in BALB/c mice at the same time point. Differences in severity of infection are attributed to mouse strain genetics, absence of Mx genes (Staeheli, Grob et al. 1988) and class I MHC molecules (Taylor, Davey et al. 1987). DBA/2J and A/J mice have a more severe inflammatory response and disease severity than other strains and are also susceptible to non-attenuated influenza strains (Alberts, Srivastava et al. 2010). Similar changes can be seen in human infections, for example the recently described IFITM3 alleles that can account for severe attenuation of influenza A prognosis (Everitt, Clare et al. 2012). Influenza titre was much higher in the 129Sv/Ev mice despite a lower clinical score.

The pathology in the lungs of the 129Sv/Ev mice was also different to the BALB/c mice. Co-infected mice appeared to have increased pathology in lungs on average although this was never significant (Figure 3.20K). There was no change in the lung due to MHV-68 infection alone, aside from the small foci of lymphocyte accumulations seen in the BALB/c infected mice. The A/WSN/33 infection was mediated however average lung scores were lower than that seen in the BALB/c mice, supporting the resistant phenotype present in the weight loss and clinical signs.

Sixty percent (3/5) of the MHV-68 infected mice unexpectedly gained weight during the influenza time course of this experiment. While strain dependent differences in MHV-68 infection have also been reported, both in lytic (Weinberg, Lutzke et al. 2004) and latent infection (Tsai, Hu et al. 2011) it is unlikely that this is responsible for the seemingly unstable weight changes in this experiment. After the time course it was discovered that the light cycle had been disturbed during the experiment and mice had been subject to longer light periods than in a normal cycle. This may account for some of the unusual feeding patterns in these mice and therefore other results are interpreted with caution.

There was no significant difference in weight loss, clinical signs or influenza viral titre between co-infected and singly A/WSN/33 infected mice. Similarly MHV-68 viral load was not reduced by co-infection in the lung as seen in the BALB/c experiments. Levels of $\text{TNF}\alpha$ and IL-10 were much higher in these mice but not different between experimental group. Interferon gamma production follows the same expression on average as in the BALB/c mice, however, there was high variation within the co-infected group and this is therefore not statistically significant. A

repeat of this experiment is required to interpret these results accurately but this was not possible within the time available.

3.5.5 Co-infection with latent MHV-68 and 5×10^3 influenza A/WSN/33 in $\text{IFN}\gamma\text{R}^{-/}$ 129 Sv/Ev mice

Interferon gamma and inflammatory mediators up regulated in response to $\text{IFN}\gamma$ signalling were elevated in singly A/WSN/33 infected mice compared with co-infected mice. Experiments were repeated in the absence of $\text{IFN}\gamma$ to determine if an absence of inflammation due to MHV-68 infection abrogates the protective effect against influenza A.

The role of $\text{IFN}\gamma$ in influenza infection is debatable. Influenza actively interferes with $\text{IFN}\gamma$ signalling via the JAK/STAT pathway in epithelial cells (Uetani, Hiroi et al. 2008). This is a common tactic employed by viruses to avoid host up regulation of interferon stimulated genes (ISGs), anti-viral immune molecules and receptors. Such molecules target and limit viral replication however viral titres in the WT 129Sv/Ev mice and $\text{IFN}\gamma\text{R}^{-/}$ mice are not significantly different between any of the A/WSN/33 infected experimental groups, suggesting a limited effect of $\text{IFN}\gamma$ on viral replication.

Weight loss in the A/WSN/33 singly infected mice is significantly increased in the absence of $\text{IFN}\gamma$. This is evident at the onset of clinical signs 3-4 days post influenza infection. $\text{IFN}\gamma$ is not only inflammatory but also has a critical reciprocal role in the resolution of inflammation. Mice lacking $\text{IFN}\gamma$ demonstrate accelerated autoimmune disease, (Feuerer, Eulenburg et al. 2006) including asthma (Teixeira, Fonseca et al. 2005) and $\text{IFN}\gamma$ is required for resolution of listeria infection, (Buchmeier and Schreiber 1985) herpes simplex virus, (Milligan and Bernstein 1997) chlamydia (Lampe, Wilson et al. 1998) and contraction of CD8^+ T cell responses to influenza as well as regulating the extent of lung immunopathology (Prabhu, Ho et al. 2013). This appears to be evident in the reduced infiltration of cells in co-infected mice from the BALB/c experiments where CD8^+ T cells show an altered phenotype in production of intracellular cytokines.

Interestingly, co-infected mice still show a significant reduction in severity compared with singly A/WSN/33 infected mice in the absence of $\text{IFN}\gamma$. Weight loss is significantly reduced in co-infected mice in the absence of $\text{IFN}\gamma$. Clinical signs are also reduced, although still reach moderate severity as in the WT 129 Sv/Ev mice. $\text{IFN}\gamma$ induction by MHV-68 was hypothesised to increase anti-viral immune surveillance and therefore reduce the extent of further inflammation by A/WSN/33 infection. $\text{IFN}\gamma$ regulates antigen processing, MHC-I is induced as a result of both $\text{IFN}\alpha/\beta$ and $\text{IFN}\gamma$ expression however MHC-II expression is solely up regulated

by IFN γ signalling (Schroder et al. 2004) and similarly MHC class II transactivator (CIITA), a regulator of MHC-II expression (Muhlethaler-Mottet et al. 1998). Therefore it was expected that the absence of IFN γ would repeal protection. During other viral infections, removal of the IFN γ R can even lead to exacerbated disease. Mice lacking the IFN γ R are more susceptible to infection with vaccinia virus due to ameliorated antigen specific IgG2a responses (Cantin et al. 1999) and herpes simplex virus in the trigeminal ganglia, where IFN γ usually acts to suppress reactivation from latency (Cantin et al. 1995).

During the co-infection experiments the absence of IFN γ had a significant effect on MHV-68 latency. Histological analysis showed that MHV-68 infected mice appear to maintain a persistent infection that caused severe pathology in the lung. Fibrosis was present as were macrophages containing crystal structures associated with chronic lung pathology, Figure 3.26.

The protective phenotype observed in the absence of IFN γ suggests that either IFN γ is not required or there is a redundant pathway compensating for its absence. Similarly MHV-68 viral load was again significantly reduced in the lung but not the spleen, suggesting that the suppressive effect of influenza co-infection in the lung is still present in the absence of IFN γ . The overall viral loads were on average much higher in the spleen but maintain similar levels in the lung. This is surprising as the inflammatory response observed in the histology is much more severe in these mice than in the WT 129Sv/Ev mice. To account for this, the cytokine environment in the lung was measured for TNF α and IFN β to determine if an absence of IFN γ altered the inflammatory pathways in the lung, IFN β acts through a different receptor and is quite distinct from IFN γ however the two pathways have overlapping activation of other cytokines and immune responses. The level of IFN β was increased in the co-infected mice at day 4, but not significantly and TNF α was only present at low levels in all groups at days 4 and 7 post A/WSN/33 infection. The levels of type 2 and T_H17 cytokines would be of interest. These cytokines show significant mediation by co-infection in the BALB/c mice and may provide a mechanism for protection still evident in the absence of IFN γ .

Influenza virus replicates at tenfold lower levels in the 129Sv/Ev IFN γ R^{-/-} mice than in the WT 129Sv/Ev mice suggesting that IFN γ may even exacerbate the ability of A/WSN/33 to replicate in the lung. This is evident in both co-infected and singly A/WSN/33 infected mice which do not differ in viral titre.

3.5.6 Latent MHV-68 infection

MHV-68 preferentially establishes latent infection in B cells in the spleen (Flano, Husain et al. 2000). Persistent infection has also been recorded at a high titre in lung epithelial cells (Stewart, Usherwood et al. 1998). The effect of MHV-68 latency on immune responses in the lung has

not been recorded, however, MHV-68 is known to cause an increase in serum levels of IFN γ and TNF α , even during the latent phase of infection (Barton, White et al. 2009). Due to this systemic change it was hypothesised that latent MHV-68 infection would alter the immune response in the lung to heterologous infection with the acute respiratory virus influenza A.

Fatality following human influenza A infection is often associated with severe cytokine dysregulation and inflammation. To determine the potential impact of latent MHV-68 on inflammatory responses in the lung mice were culled 28 days post MHV-68 infection.

ELISAs on lung homogenates (Figure 3.29A) demonstrated no significant changes in inflammatory cytokines IFN γ and TNF α . Similarly there was no increase in regulation by TGF β and IL-10 suggesting that the systemic changes observed by Barton *et al* 2009 in the serum were not significantly altering the lung immune environment directly. Based on observations discussed in later experiments, it may be useful in a repeat experiment to measure the amounts of these cytokines in broncho-alveolar lavage samples instead of whole lung to see the direct influence of MHV-68 infection at the alveolar epithelial cell barrier; the site of influenza A infection.

While day 28 is considered a latent stage of MHV-68 infection, persistent virus in the lung epithelial cells is still present and virus is easily detectable in the spleen by quantitative PCR (Figure 3.7A). Published data suggest that latency transcripts are detectable to some degree throughout infection while gene expression associated with all stages of lytic infection is detectable in the spleen (K3, M3, M8 and M9 genes) from 10-16 days post infection and in the mediastinal lymph node (K3, M3, M8, M9 and M11 genes) from 2-16 days post infection (Rochford, Lutzke et al. 2001).

Lung draining lymph nodes (including the mediastinal) were taken 28 days post infection and examined by FACS to determine if CD4⁺ T cells were still proliferating in response to infection (Figure 3.29B and 3.29C). The percentage of CD4⁺ cells was not increased compared with uninfected litter mates and cytokine production by these cells was not significantly altered. Therefore at the point of influenza A/WSN/33 co-infection, 28 days after intranasal MHV-68 infection, MHV-68 persists in the lung, (Stewart, Usherwood et al. 1998) is latent in the spleen and has no apparent immune response in the lung draining lymph nodes (Figure 3.18 and 3.29C). Co-infection therefore occurs during latent MHV-68 infection when the immune response to lytic MHV-68 replication is cleared.

Lavage samples from the lungs of MHV-68 infected mice and uninfected mice contain a high percentage of macrophages. By incubating lavage samples for 1 hour at 37°C macrophages and other adherent cells can be isolated. These cells were lysed and the expression of markers

associated with M1 / M2 macrophage polarisation was measured by qPCR. None of the markers utilised were increased or decreased in this adherent population as a result of MHV-68 infection. SOCS1 (suppressor of cytokine signalling 1) expression was however significantly increased in these cells. In influenza A infection, SOCS1 is induced and has been shown to regulate IFN β expression and act as negative feedback regulators in early innate immunity to viral infection (Pothlichet, Chignard et al. 2008). Virus induced SOCS1 is produced in a cytokine independent manner and binds to STAT1 reducing IFN λ receptor signalling *in vivo*. SOCS-1 forms part of a negative feedback loop downstream of cytokine signalling and modulate IFN γ action (Alexander et al. 1999). IFN λ has anti-viral function in epithelial cells and many overlapping characteristics with the type 1 interferons during influenza infection (Mordstein, Kochs et al. 2008). However, reduction of STAT1 in turn induces NF κ B expression and increases expression of IFN λ (Wei, Wang et al. 2014). This understanding may contribute to the protective effect observed following MHV-68 infection if SOCS1 is already at an increased level in macrophages and is therefore produced pre-emptive of influenza infection. This would also suggest a change to inflammatory signalling that is unrelated to IFN γ and TNF α production. These cytokines were not detected at a higher level in the lung of latent MHV-68 infected mice and therefore the protective effect observed in the co-infected mice might be a result of more subtle changes to the immune cells and epithelial barrier already present in the lung prior to influenza infection.

Chapter 4 - Persistent *Litomosoides sigmodontis* and influenza A co-infection

4.1 Introduction

Infections with persistent filarial helminths are widespread and as such present a common background in which co-infection can occur. Lymphatic filariasis poses a significant threat to human health. There are three human lymphatic filarial nematodes (roundworms) of the family filariodidea; *Wuchereria bancrofti*, *Brugia malayi* and *Brugia timori*. These parasites can cause lymphedema and elephantiasis and are endemic in tropical and subtropical regions of Africa, Asia, Central and Southern Americas and many Pacific Isles (Taylor, Hoerauf et al. 2010). Filarial infection causes substantial morbidity and mortality through physical debilitation and damage to the lymphatic system, kidneys and immune system. Socio-economic problems often occur as a result of stigmatisation, loss of income and cost of medical bills contributing to an individual's isolation and poverty (Ramaiah, Das et al. 2000; Babu and Nayak 2003). The severity of filariasis can be seen by its high disability adjusted life years (DALY) rating which determines the impact of disease on life expectancy and debilitation during the sufferer's life time (Fenwick 2012). With 1.3 billion people at risk, ~120 million people across 83 countries already infected and around one third of that number disfigured or incapacitated by the resulting disease (WHO, 2014), understanding the immune responses to filarial nematode infection is critical to produce novel therapies and reduce morbidity due to infection or subsequent co-infection. Incidence of infection is subject to increase above current estimations with better testing in endemic regions (Gyapong, Kyelem et al. 2002).

– Filarial nematode life cycles

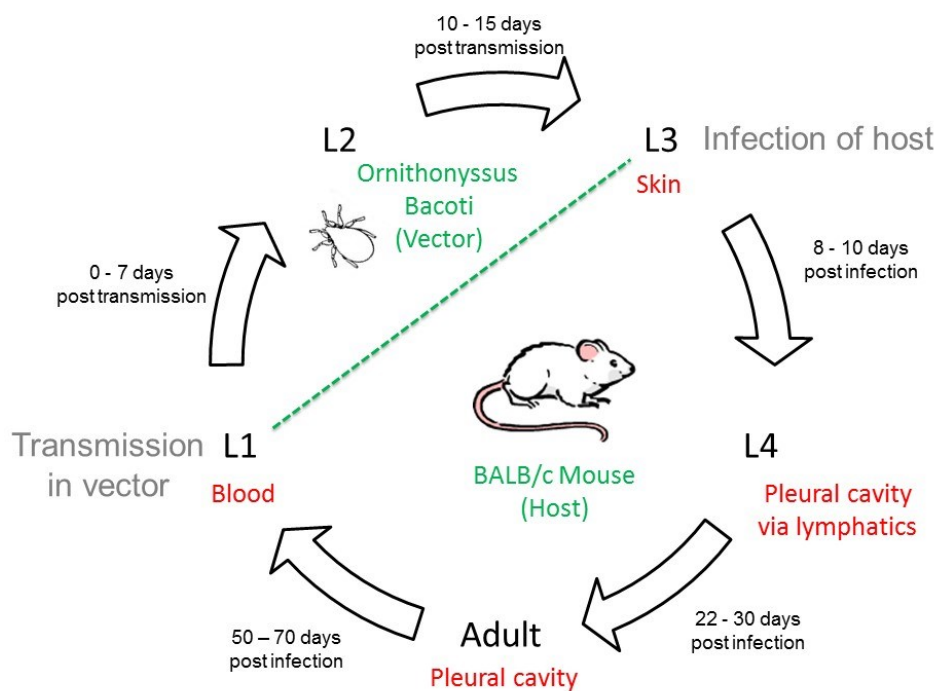
Filarial nematodes are transmitted via blood feeding insects, specifically mosquitoes; *Anopheles* in Africa, *Culex* in the Americas and *Aedes* mosquitoes in human infections of Pacific and Asian regions (CDC, 2014). Microfilaria are ingested into the mosquito proventriculus and mesenteron from an infected individual during a blood meal. Upon losing their protective sheath they migrate to the thoracic muscles and develop to L3 stage larvae. This takes around 7-12 days. Upon maturation, the L3 larvae migrate to the hemocoel of the proboscis, where they are subsequently transferred back into a susceptible human host as the mosquito takes another blood meal (Cross 1996). Transmission requires repeat exposure and risk of infection is therefore increased for those living in endemic areas. Transmission efficiency can also vary between vector species (de Souza, Koudou et al. 2012). Understanding the natural factors

limiting transmission within the vector can be used to isolate strategies of treatment and predict epidemiology (Chandra 2008).

- Human filarial nematode infections

Brugia malayi is an example of a filarial nematode responsible for lymphatic filariasis in humans. The life cycle within the human host can be complex. After established infection it may still take years to develop symptoms of disease and some will remain entirely asymptomatic. L3 larvae migrate from the site of infection to the lymphatics where they undergo further developmental stages to adulthood and eventually produce sheathed microfilaria (L1) which enter the blood stream and peripheral tissues (CDC, 2014). Impact of infection upon the immune system likely differs between symptomatic and asymptomatic individuals and microfilaremic and amicrofilaremic infections.

- *Litomosoides sigmodontis*



Litomosoides sigmodontis provides a rodent model of filarial nematode infection. It is capable of infecting some inbred laboratory mouse strains to full patency (presence of L1 larvae). (Hoffmann, Pfaff et al. 2001) All stages of the *L. sigmodontis* life cycle may be acquired from infected jirds, (*Meriones unguiculatus*). L3 larvae acquired from infected jirds are subcutaneously injected into a murine host to mimic the vector transmission observed in human infection. In 3-4 days, migration through the lymphatics to the pleural cavity is observed. Within 8 days, L3 have moulted to L4 stage larvae. After 25 days, adult worms are found in the pleural cavity and by around 50 days, microfilaria are present in the blood of patently infected

mice. The infection model follows similar progression to an asymptomatic human infection. *L. sigmodontis* is also host to the endosymbiotic alpha protobacteria *wolbachia* (*Rickettsiales*). (Ferri, Bain et al. 2011)

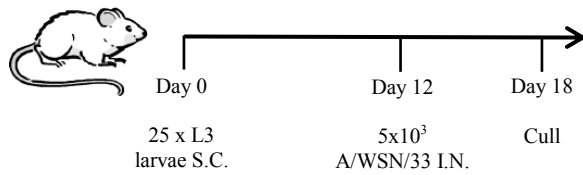
4.1.1 Strain and sex specificity

Elimination of the infection varies between mouse strains. BALB/c females show greater susceptibility to infection than males of the same strain or C57BL/6 mice. There is greater survival of L3 larvae to L4 and adult stages of infection in BALB/c females while C57BL/6 mice never develop circulating microfilaria and are therefore considered resistant (Graham, Taylor et al. 2005). Resistance in C57BL/6 is associated with increased production of CXCL-12 by pleural mesothelial cells and subsequent increase of CD4⁺ and CD8⁺ lymphocyte recruitment to the pleural cavity 30 days post infection (Babayan, Ungeheuer et al. 2003; Bouchery, Denece et al. 2012). Migration of worms to the pleural cavity by day 4 post infection, development to adulthood and production of IgG1 and IgG2a specific antibody responses are similar in both strains, however, 10-30 days post infection production of IL-5 and IL-6 by ex vivo stimulated lymphocytes from the draining lymph nodes is greater in C57BL/6 mice (Babayan, Ungeheuer et al. 2003). B10D2 and BALB/c mice share the same MHC haplotype H-2^d but differ in resistance. In resistant female B10D2 mice, worm burden in the initial month following infection is comparable with susceptible BALB/c females, however, *L. sigmodontis* life span is half that in BALB/c females and female worms recovered showed greatly decreased fecundity and size and were often covered with inflammatory cells including neutrophils and eosinophils (Marechal, Le Goff et al. 1996). Genetic variation between these strains may reflect disease and outcome of infection seen in human infections. While some individuals manage to mount an appropriate immune response and clear a filarial infection or remain asymptomatic, others succumb to disease with apparent signs of infection.

4.2 Co-infection model

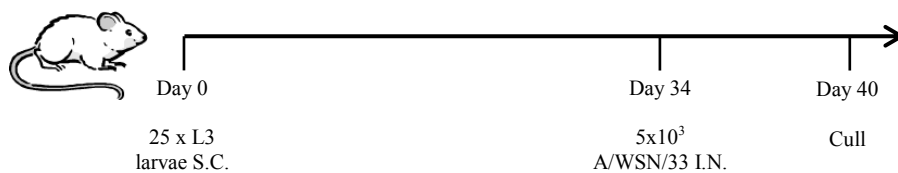
Co-infections with *Litomosoides sigmodontis* and A/WSN/33 have not been performed before. The filarial nematode undergoes multiple stages of development inside the host which results in variations in the immune response. As such, 3 time points were chosen for co-infection experiments with 5x10³ PFU A/WSN/33. The dose of A/WSN/33 was chosen in order to cause moderate pathology within the 6 day co-infection time course. *L. sigmodontis* produces no clinical signs in a susceptible female BALB/c model. The following co-infection model was therefore produced:

A. L4 (immature) *Litomosoides sigmodontis* + A/WSN/33 co-infection



Female 5-6 week old BALB/c mice were sub-cutaneously infected with 25 x L3 *L. sigmodontis* larvae. After 12 days, larvae have developed to L4 immature stage and have migrated via the lymphatics to the pleural cavity. Mice were then co-infected with 5x10³ A/WSN/33 for 6 days and compared with singly infected or uninfected controls.

B. Adult (pre-patent) *Litomosoides sigmodontis* + A/WSN/33 co-infection



Sub-cutaneously injected *L. sigmodontis* L3 larvae reach the adult stage of development at ~25 days post infection in female BALB/c mice. At day 34 post infection mice were co-infected with 5x10³ A/WSN/33 and compared with singly infected and uninfected controls.

C. Adult (patent stage ± microfilaria) *Litomosoides sigmodontis* + A/WSN/33 co-infection



L. sigmodontis larvae develop to patency at ~50-60 days post L3 infection. At day 68 BALB/c mice were infected with 5x10³ A/WSN/33 and compared with singly infected and uninfected controls.

Upon A/WSN/33 infection, all mice were monitored for clinical signs and weight loss every 24 hours. Mice were culled 6 days after A/WSN/33 infection. Groups of singly infected and uninfected mice were used as controls.

4.3 Hypothesis

Filarial nematode infection is associated with increased type 2 and regulatory immune responses. These infections are persistent and therefore have an on-going influence on the immune system. Mortality in human influenza infection is often associated with an overwhelming type 1 inflammatory immune response. It is therefore hypothesised that co-infection during persistent filarial nematode infection will impact the outcome of acute influenza virus infection.

- Persistent *Litomosoides sigmodontis* infection impairs the immune response to acute infection with influenza virus by suppressing appropriate inflammatory responses required to eliminate the infection.

4.4 Results

4.4.1 Pathology associated with *Litomosoides sigmodontis* infection at each developmental stage

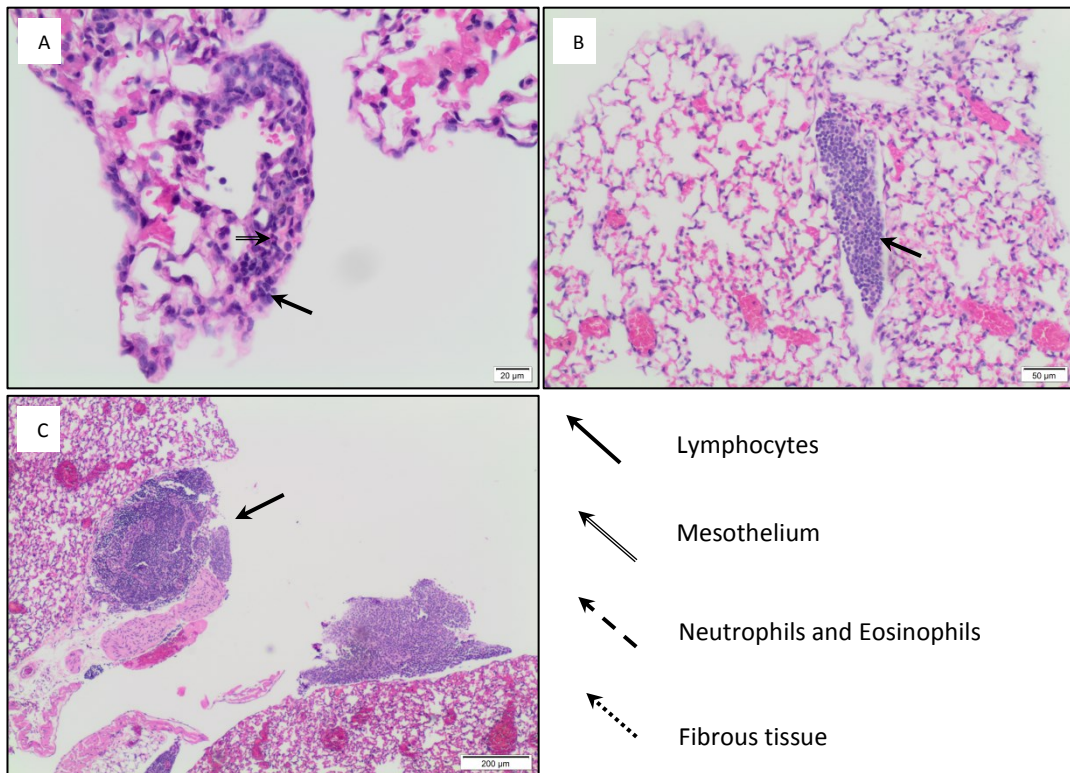
The effect of *L. sigmodontis* on lung pathology has not been reported. Current publications focus mainly on the cells recruited to the pleural cavity and those involved in granuloma formation on the pleural surface (Attout, Martin et al. 2008). Therefore, we determined the *L. sigmodontis* induced pathology at all 3 developmental stages of infection.

Understanding the on-going pathological changes in the lung caused solely by *L. sigmodontis* infection allows us to determine how changes to lung integrity can moderate influenza induced pathology during co-infection.

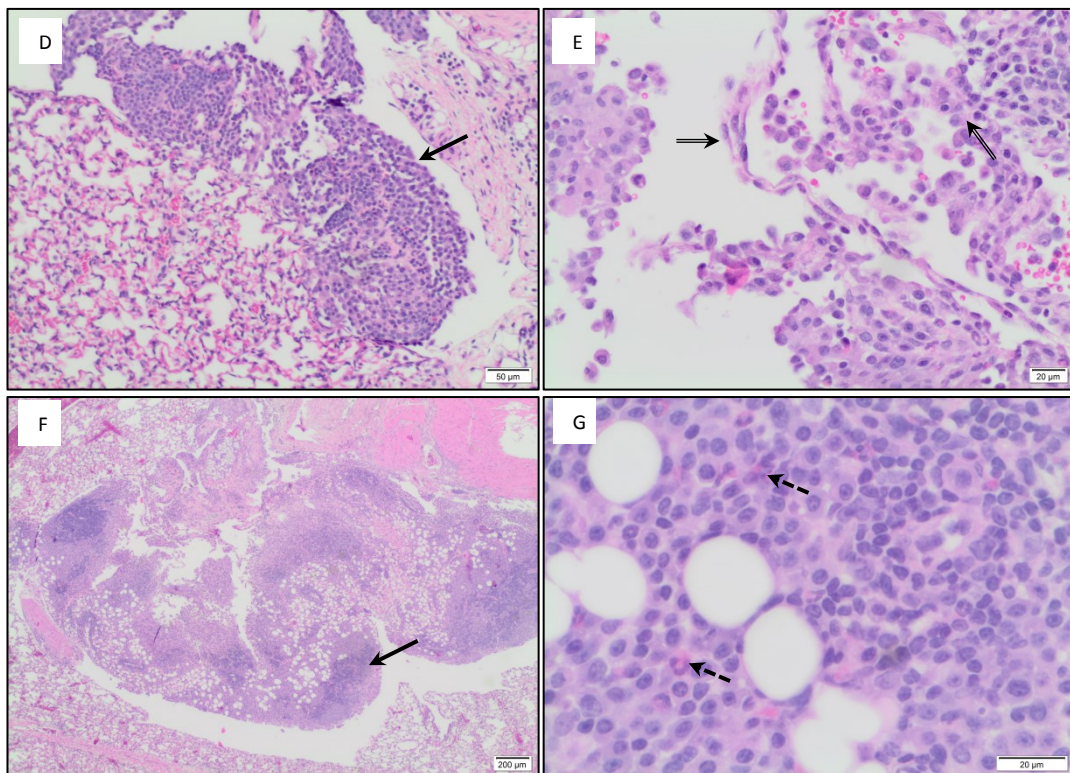
At the immature stage (L4) of infection, (Figure 4.1A-C) solid black arrows depict the infiltrating lymphocyte populations that were seen in the sub-pleural spaces. At this stage of infection, pathology from *L. sigmodontis* infection was subtle and focused in small areas around the lung surface and pleural cavity.

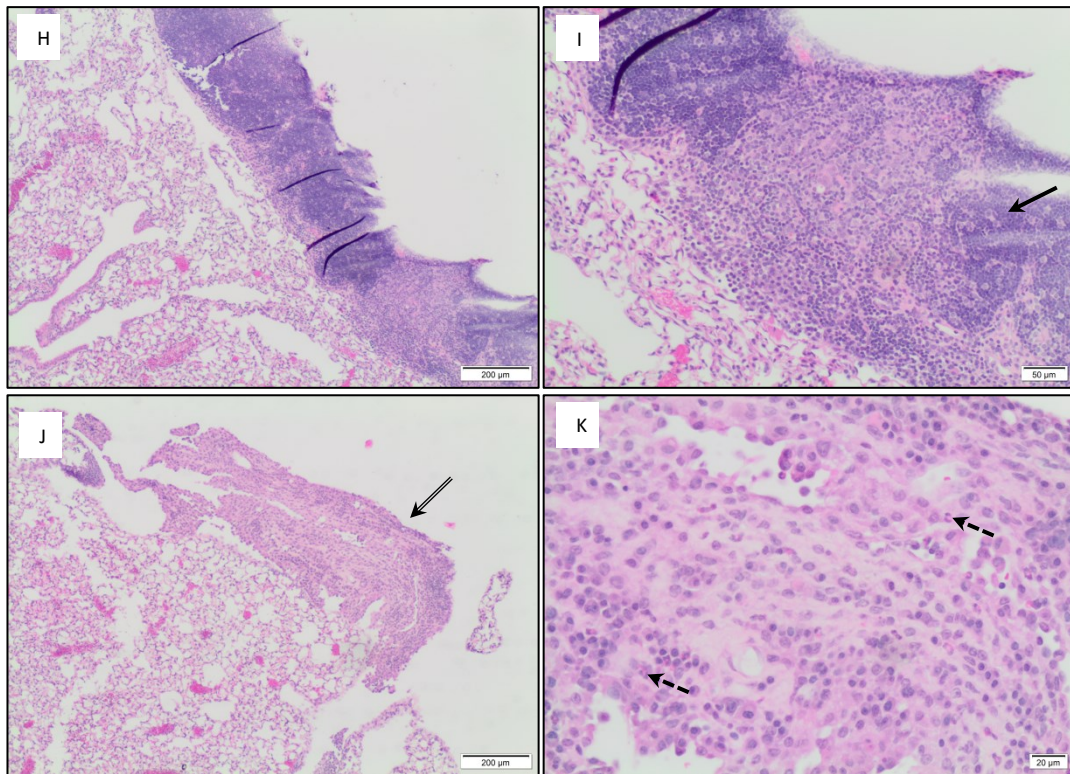
Figure 4.1 Lung pathology caused by *Litomosoides sigmodontis* infection

Immature (L4) - 18 days post infection



Pre-patent (adult) – 40 days post infection





Patent (adult ± mf) – 74 days post infection

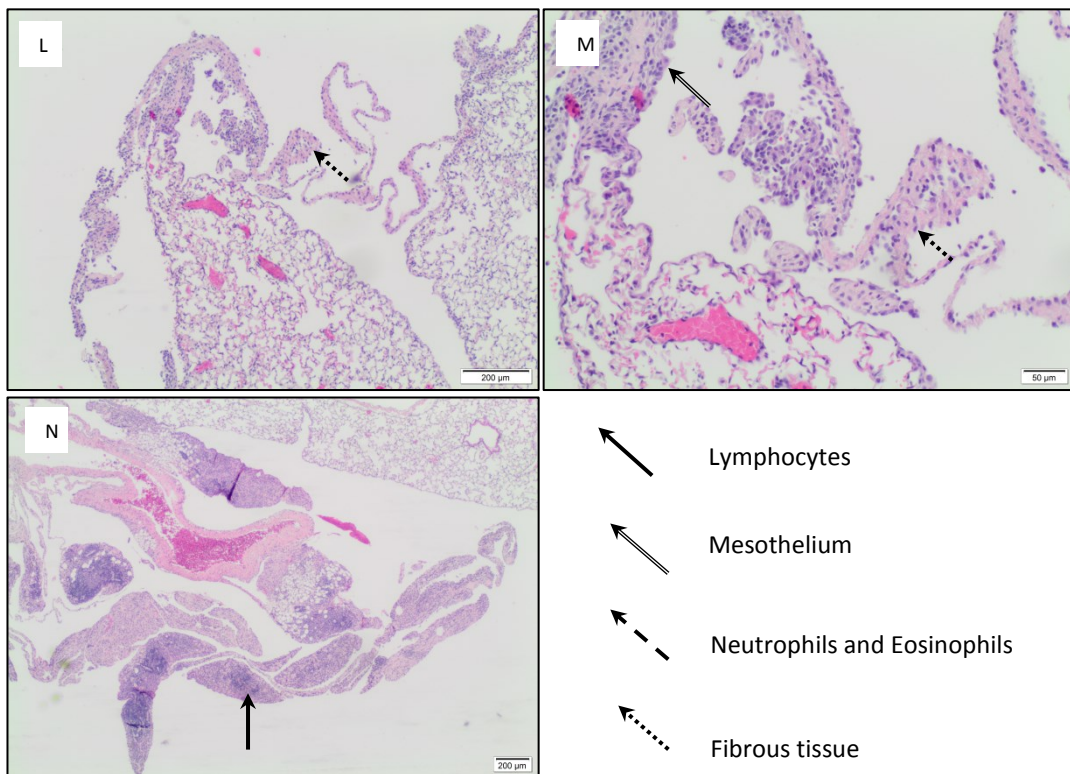


Figure 4.1 Lungs from infected mice were fixed, cut and stained with hemoxilyn and eosin 6 days post infection. Slides were assessed for a number of pathological features of *L. sigmodontis* infection at each time point of infection. (A-C) Immature L4 infection (D-K) Adult pre-patent infection (L-N) Patent adult ± mf infection. Results demonstrate typical signs of *L. sigmodontis* infection and cell types present in the infected lung and mesothelium. Images were taken by Dr.P Beard. The Roslin Institute, University of Edinburgh, 2013.

At the (pre-patent) adult stage of infection, (Figure 4.1 D-K) *L. sigmodontis* infection was more evident. Lymphocyte infiltrations were more extensive in the mesothelium layer (see Figure 4.1D and 4.1H). Polymorphonuclear granulocytes were also identified within these infiltrations (the dashed arrows in Figure 4.1G and 4.1K). These mainly consisted of neutrophils but also eosinophils. *L. sigmodontis* at this time point had caused mechanical damage to the mesothelium cell layer, particularly around the hilus of the lung where many of the adult worms are recovered.

In the patent (adult \pm microfilaria) stage of infection there was similar pathology to that seen at earlier time points. In addition, this was now coupled with signs of chronic infection including hypertrophic and hyperplastic cells at the pleural surface which extended into exophytic frond-like structures. These are identified by the hollow arrows in Figure 4.1J and 4.1M. Due to the chronic nature of *L. sigmodontis* infection later stages of infection lead to fibrosis within the hyperplastic mesothelium. (Dotted arrow, Figure 4.1M).

In Figures 4.1J and 4.1L it is evident that the interstitial spaces of the lung were completely unaltered by the presence of *L. sigmodontis* worms. This was evident in all mice infected solely with *L. sigmodontis* and is an important observation for influenza co-infection, as damage from this pathogen largely impacts the alveolar epithelial cell surfaces surrounding the airways and blood vessels.

The damage caused by the filarial nematode infection at each developmental stage is varied. Each stage is also considered during co-infection in Figures 4.3B, 4.7B and 4.14B.

4.4.2 Co-infection with immature (L4) *Litomosoides sigmodontis* and 5×10^3 A/WSN/33

An early time point of *L. sigmodontis* infection (L4 stage of development) was chosen to determine the impact of co-infection before filarial nematode infection has skewed the host immune response towards a robust T_H2 and regulatory phenotype.

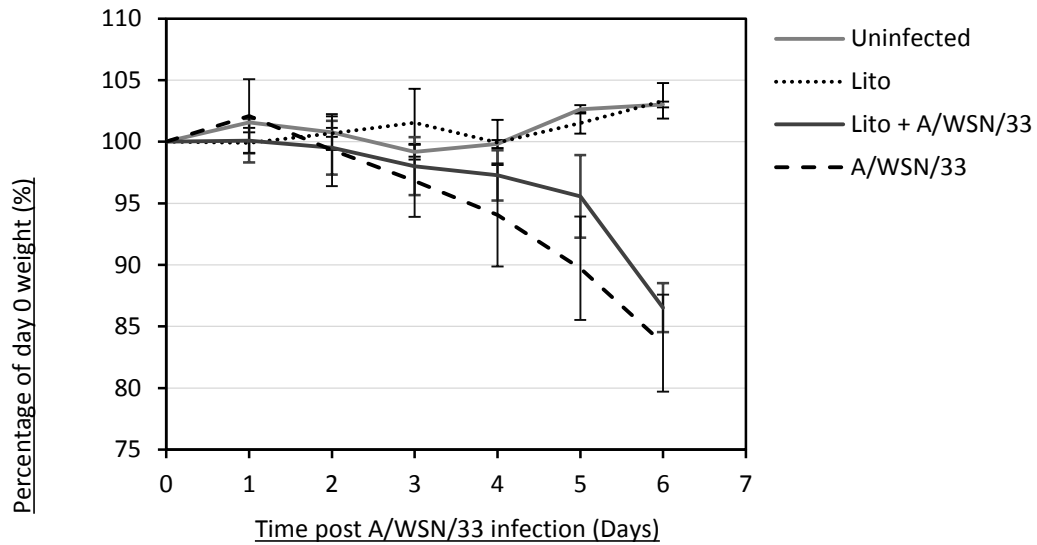
- Effect of immature (L4) *Litomosoides sigmodontis* on 5×10^3 A/WSN/33 co-infection

Weight loss, clinical signs and influenza virus titre in the lung were measured to determine the effect of co-infection on the pathogenesis and outcome of influenza infection.

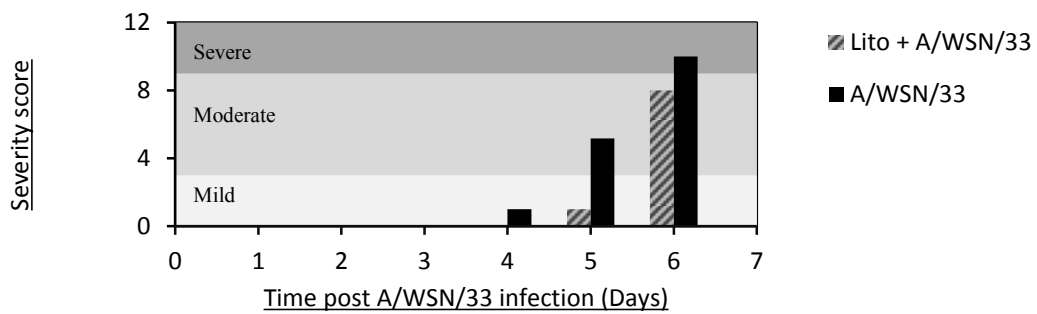
Uninfected and L4 infected mice showed no change in weight during the experimental time course (Figure 4.2A). The final mean percentage weight changes were 103.32% and 103.03% respectively at day 6.

Figure 4.2 – Co-infection with immature (L4) *Litomosoides sigmodontis* has no effect on A/WSN/33 pathogenesis

A. Weight loss



B. Clinical severity score



C. Influenza lung titre – Day 6



Figure 4.2 5-6 week old female BALB/c mice were infected S.C. with 25 x *Litomosoides sigmodontis* L3 larvae and 12 days later infected I.N. with 5×10^3 A/WSN/33 in 40 μ l Dulbecco's minimum essential medium or medium alone. **A.** Weight loss post A/WSN/33 infection. Weight loss is calculated as percentage of weight at day 0 prior to infection. Mean weight loss is shown \pm 1 standard deviation, N=6. **B.** Clinical severity was measured by 4 signs. Each was scored on a scale of 0-3 and the average sum reported \pm 1 standard deviation as clinical severity score, N=6. **C.** Left lung homogenate was measured by dilution series plaque assay on MDCK cells for levels of infectious virus. Individual values are plotted in PFU, N=6.

The A/WSN/33 infected mice began to show clinical signs of infection at day 4 (Figure 4.2B). All mice in the singly infected group were scored 1 for decreased mobility. This increased to an average score of 2 by day 5 and was coupled with staring coat, increased respiratory effort and hunched stature all scored at an average close to 1. Multiple signs therefore meant that these mice were scored at a moderate severity with an average severity score of 5.17 ± 1.42 . This increased further at day 6 to 10.00 ± 1.41 and all mice were scored between 2 and 3 for all signs of severity measured. This response was reflected in the weight loss. Weight loss in the A/WSN/33 singly infected mice was apparent by day 4 with a mean average decrease of $5.95 \pm 4.19\%$ (Figure 4.2A). The variation in this group was a result of a single outlying mouse (N=12) with 14.46% weight loss at this time point. At day 5 the mean weight loss was $10.27 \pm 4.2\%$ and this was increased to a final average of $16.34 \pm 3.90\%$ by day 6.

Co-infected mice showed moderately reduced clinical signs from A/WSN/33 infection. Clinical signs became apparent at day 5 with a mild decrease in mobility (average score of 1). On day 6 clinical effects were increased. All mice in this group were scored at 2 for decreased mobility, increased respiratory effort, hunched stature and staring coat. Therefore, the final severity score was 'moderate' for this group at day 6. The mean severity score was 8.0 ± 0.0 . Mean weight loss was slightly reduced in co-infected mice compared with singly A/WSN/33 infected mice. This was most notable at 5 days post infection. The mean weight of these mice was subtly decreased by an average of $2.73 \pm 2.56\%$ on day 4 and this increased to $4.44 \pm 2.2\%$ on day 5, (much lower than the 10.27% average decrease in the A/WSN/33 infected group). By day 6 however, weight loss increased more drastically to a mean average of $13.47 \pm 2.48\%$ which is more consistent with the singly A/WSN/33 infected mice. The difference in weight loss between groups at day 5 was not significant ($p > 0.05$) when measured by 2 way ANOVA.

There was no effect of co-infection with L4 *L. sigmodontis* on the replication of A/WSN/33 detected in the left lobe of the lung by plaque assay on MDCK cells (Figure 4.2C). Viral load in the lung was on average 2.4×10^4 PFU ml⁻¹ in co-infected animals and 2.2×10^4 PFU ml⁻¹ in singly A/WSN/33 infected animals. The standard deviation for each group was almost identical, $\pm 10,800$ and $\pm 11,700$ PFU respectively.

- Pathology in the lung

As the outcome of the influenza infection and viral replication appear to be unaltered by co-infection at this stage of *L. sigmodontis* co-infection, the underlying lung pathology was scored to determine if the two infections cause overlapping or compartmentalised pathology in the lungs.

As described in section 4.3, *L. sigmodontis* infection is associated with lung pathology at the mesothelium. Infection with immature L4 larvae has a subtle pathology on the lung. At this stage the L4 larvae are located in the pleural cavity. Mild infiltration of inflammatory cells, including lymphocytes, neutrophils and multi-nucleated giant cells (MNGC) are observed in the sub pleural layer of the lung (Figure 4.1A-C). Hyperplasia is also evident in the broncho-alveolar associated lymphoid (BALT) tissues.

To determine if influenza infection could alter *L. sigmodontis* induced pathology in the mesothelium, these pathologies were scored in each experimental group to determine the impact of co-infection.

BALT hyperplasia was consistent between all groups with mean average scores of ~0.7-1 for all groups (Figure 4.3B). Infiltration of cells into the sub pleural space varied slightly between infections. Neutrophils were only present in the *L. sigmodontis* infected mice (mean score of 0.17) and co-infected mice (mean score of 0.33), however, there was no significant difference between the two groups and not all mice in each group demonstrated neutrophil infiltrations in the sub pleural space.

Lymphocyte infiltrations in these groups were also scored at a similar level, 0.5 and 0.5 mean averages for co-infected and *L. sigmodontis* groups respectively. A/WSN/33 infected mice had an average score of 0.4 whilst uninfected mice showed zero lymphocyte infiltration. This was the same for BALT hyperplasia which was present at minimal levels (~0.5) in all infected groups.

Sub-pleural infiltration of MNGC was minimal at this time point and only present in a single A/WSN/33 infected mouse (see Figure 4.3B). A/WSN/33 therefore has no significant impact on the pathology caused by *L. sigmodontis* during the 6 day co-infection.

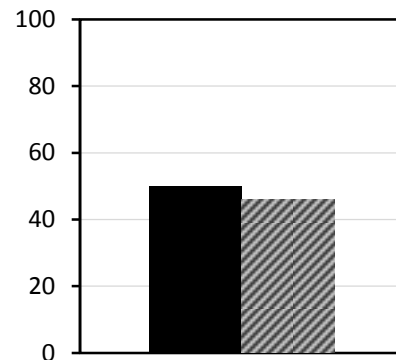
Influenza infection causes distinct pathology 6 days post infection. This includes epithelial cell and interstitial necrosis, inflammation and infiltration of cells around airways and blood vessels. To determine the effect of presiding *L. sigmodontis* infection on influenza induced pathology these effects were scored and compared between experimental groups.

Interstitial pathology was scored at similar levels in co-infected and A/WSN/33 infected mice. A/WSN/33 singly infected animals had a mean score of 2.10 for interstitial inflammation and co-infected mice were scored at 2.17. Interstitial necrosis was scored at 1.5 and 1.4 on average in the A/WSN/33 infected and co-infected mice respectively. There were no signs of interstitial pathology in *L. sigmodontis* infected and uninfected mice (As discussed in section 4.3). Epithelial necrosis around the airways was also absent in the *L. sigmodontis* and uninfected

Figure 4.3 Co-infection with immature (L4) *Litomosoides sigmodontis* does not alter pathology caused by A/WSN/33

A. Percentage of lung affected

- ▨ Uninfected
- Lito
- ▨ Lito + A/WSN/33
- A/WSN/33



B. Pathological scoring

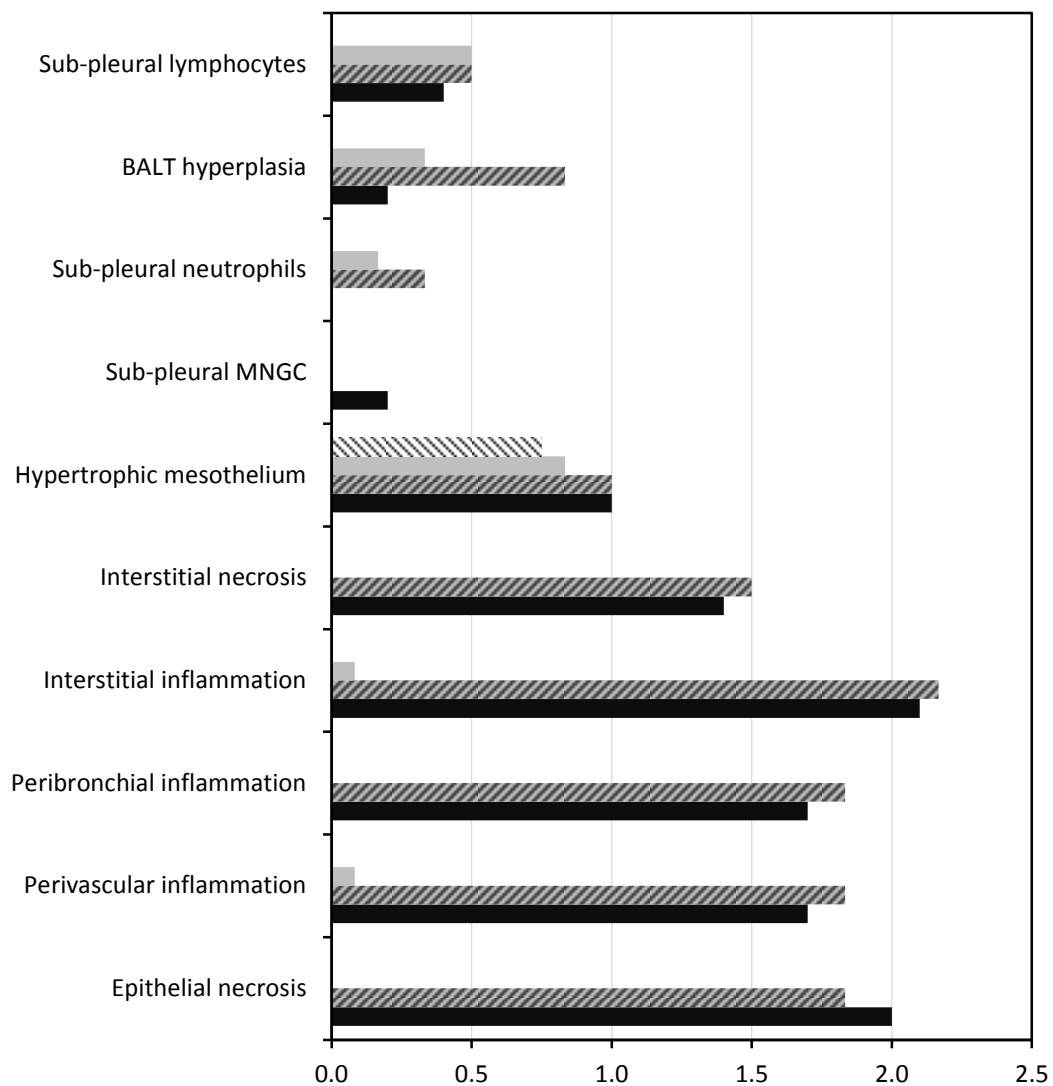


Figure 4.3 The left lobes of lungs from co-infected, singly infected and uninfected mice were harvested, fixed, cut into sections and stained by hematoxylin and eosin 6 days post infection with A/WSN/33. **A.** The extent of lung damage was assessed as 0%, 25%, 50%, 75% or 100% per lung. **B.** Pathology and infiltration of immune cells was

scored on a scale from 0-3 for each lung. All results are presented as mean average for each group. N=6. Error bars are not displayed due to the ranked nature of the data.

mice. In A/WSN/33 infected mice the mean score was 2.0 and co-infected mice showed similar pathology, scored at 1.8 on average (see Figure 4.3B).

Infiltration of cells around the airways and blood vessels were scored at 1.83 and 1.83 in the co-infected mice. This was very similar to the A/WSN/33 singly infected group, which averaged 1.70 and 1.70 for these pathologies. Scores for all influenza-associated pathologies were therefore generally very consistent within the A/WSN/33 infected and co-infected mice.

The extent of pathology was also similar between co-infected and A/WSN/33 infected experimental groups with a mean average of 45-50% damage to the right lung of each mouse in both groups when histologically scored (see Figure 4.3A).

- Cytokine environment

While the pathology of influenza infection was unchanged by co-infection, *L. sigmodontis* was in the early stages of infection at the point of co-infection and therefore it was of interest to determine if the overall cytokine environment in the lung had already been altered by this stage of infection. It was also of importance to determine if such a change could impact the immune environment following influenza infection.

The left lobe of each lung was homogenised and levels of inflammatory cytokines, TNF α and IFN γ along with regulatory cytokines, IL-10 and TGF β were measured by ELISA (Figure 4.4A). Due to the high polarisation in cytokine levels between experimental groups, a standard curve of known concentration could not be used accurately at both low and high concentrations and therefore all cytokines were normalised to the levels found in the uninfected control group, and reported as fold change.

TNF α and TGF β levels were not significantly altered by either infection, when measured in the total lung homogenate. TNF α was detected at 0.81 ± 0.17 and TGF β was detected at 0.73 ± 1.06 fold differences (on average) in the A/WSN/33 infected group compared with the uninfected mice. Similarly, co-infected mice had 0.80 ± 0.16 and 0.70 ± 0.12 fold variations for these two cytokines. *L. sigmodontis* infection led to fold changes of 1.05 ± 0.27 and 1.05 ± 0.39 for TNF α and TGF β respectively.

The regulatory cytokine IL-10 was significantly increased in mice co-infected with L4 larvae and A/WSN/33, ($p < 0.001$ general linear model). There was a 1.73 fold increase on average compared with the uninfected group. Individual infections did not significantly increase the levels of IL-10. *L. sigmodontis* and A/WSN/33 infections had 0.94 and 0.97 times the amount of

IL-10 in uninfected mice respectively. Variation within these groups was also minimal (~0.2 in both cases), see Figure 4.4A.

Figure 4.4 IL-10 level is increased in mice co-infected with immature (L4) *Litomosoides sigmodontis* and A/WSN/33

A. Lung homogenate

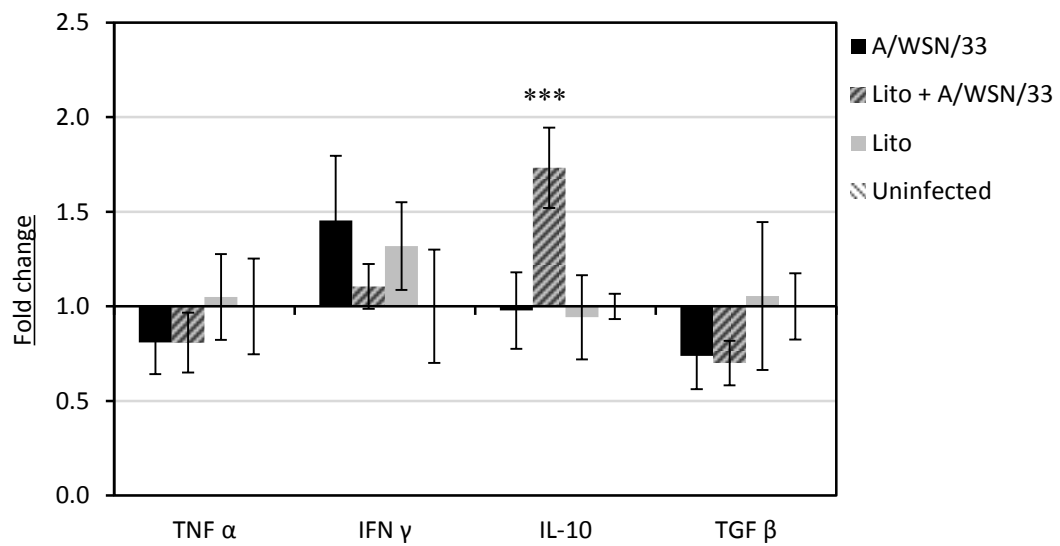


Figure 4.4 A. 6 days post A/WSN/33 infection, the left lung was homogenised in Dulbecco's minimum essential medium. ELISA was used for detection of cytokines. Each group is represented as mean average fold change \pm 1 standard deviation. All results are normalised to the expression in the uninfected group. N=6.

IFN γ was increased in singly A/WSN/33 infected mice as expected however co-infected mice had on average a 1.16 \pm 0.11 fold IFN γ compared with the uninfected group. A/WSN/33 singly infected mice were 1.45 \pm 0.34 fold higher. This increase was not significant due to variation in the uninfected mice. *L. sigmodontis* infected mice were similar to the A/WSN/33 infected group with a surprising increase of 1.39 \pm 0.23 fold IFN γ .

- T cell responses in the lung and lung draining lymph nodes

The cytokine environment within the whole lung and pathology within the interstitial spaces and airways within the lung were predominantly modulated by the influenza infection. Pathology in the pleural cavity was solely due to *L. sigmodontis* infection. The immune response to *L. sigmodontis* and A/WSN/33 infections however will both require T cells to traffic to the lung and pleural cavity draining lymph nodes. As such it was hypothesised that changes to adaptive T cell responses to both infections may occur in the lymph nodes during co-infection.

Six days after A/WSN/33 infection, cells from the thoracic and lung draining lymph nodes were harvested and stained for CD4 and CD8 intracellular cytokines. Total CD4⁺ and CD8⁺ T cell counts were not significantly changed by either infection (Figures 4.5A and 4.5B). CD4⁺ T cells were detected at a higher overall level in all infected groups with mean averages of 31.18 \pm 4.27% reported in the co-infected mice, 27.38 \pm 2.91% in the A/WSN/33 singly infected mice, 31.28 \pm 5.34% in the *L. sigmodontis* infected mice and 16.29 \pm 12.34% on average in the uninfected group.

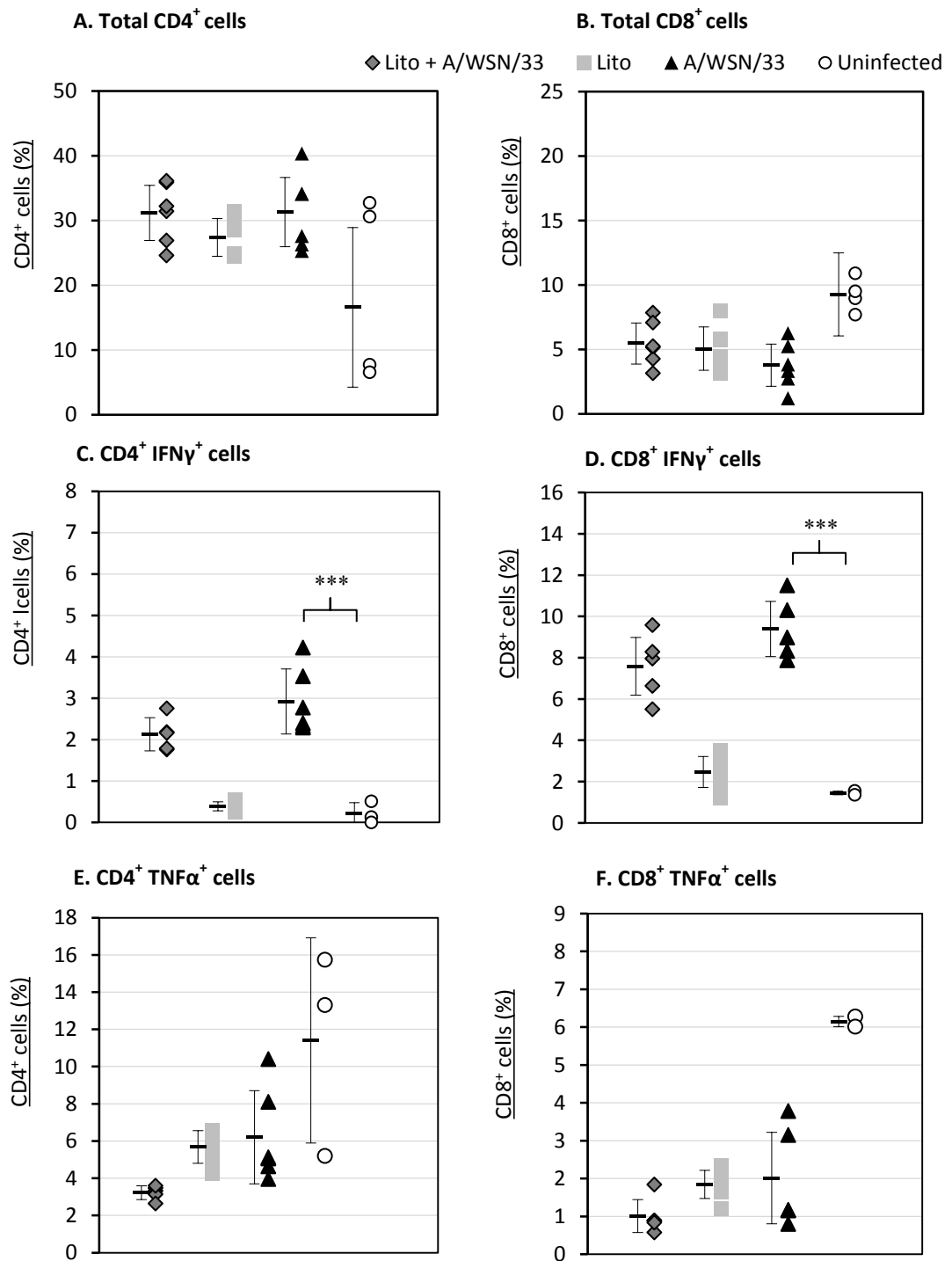
The A/WSN/33 infection polarised CD4⁺ and CD8⁺ T cells to produce the inflammatory cytokine IFN γ at significantly higher levels than in uninfected and *L. sigmodontis* infected counterparts ($p < 0.001$ calculated by general linear model).

IFN γ was produced by 7.59 \pm 1.40% of CD8⁺ cells in the co-infected mice and 9.39 \pm 1.33% in the A/WSN/33 infected mice (Figure 4.5D). This was greater than the mean average amount of IFN γ produced in the uninfected (1.55 \pm 0.09%) and *L. sigmodontis* infected (2.47 \pm 0.75%) groups.

IFN γ was produced by 2.32 \pm 0.31% of CD4⁺ cells in the co-infected mice and 3.04 \pm 0.88% in the A/WSN/33 infected mice (Figure 4.5C). This was greater than the mean average amount of IFN γ produced in uninfected (0.43 \pm 0.14%) and *L. sigmodontis* infected (0.55 \pm 0.06%) groups, however, was not significantly different between co-infected and A/WSN/33 infected mice, despite a subtle trend for a greater increase in the singly infected group.

The highest production of TNF α was found in the uninfected group, in both CD4⁺ (11.41 \pm 5.52%) and CD8⁺ (6.05 \pm 0.14%) cells, (Figures 4.5E and 4.5F). A/WSN/33 infected

Figure 4.5 Co-infection with immature (L4) *Litmosoides sigmodontis* has a subtle impact on T cell responses in the lung and thoracic draining lymph nodes



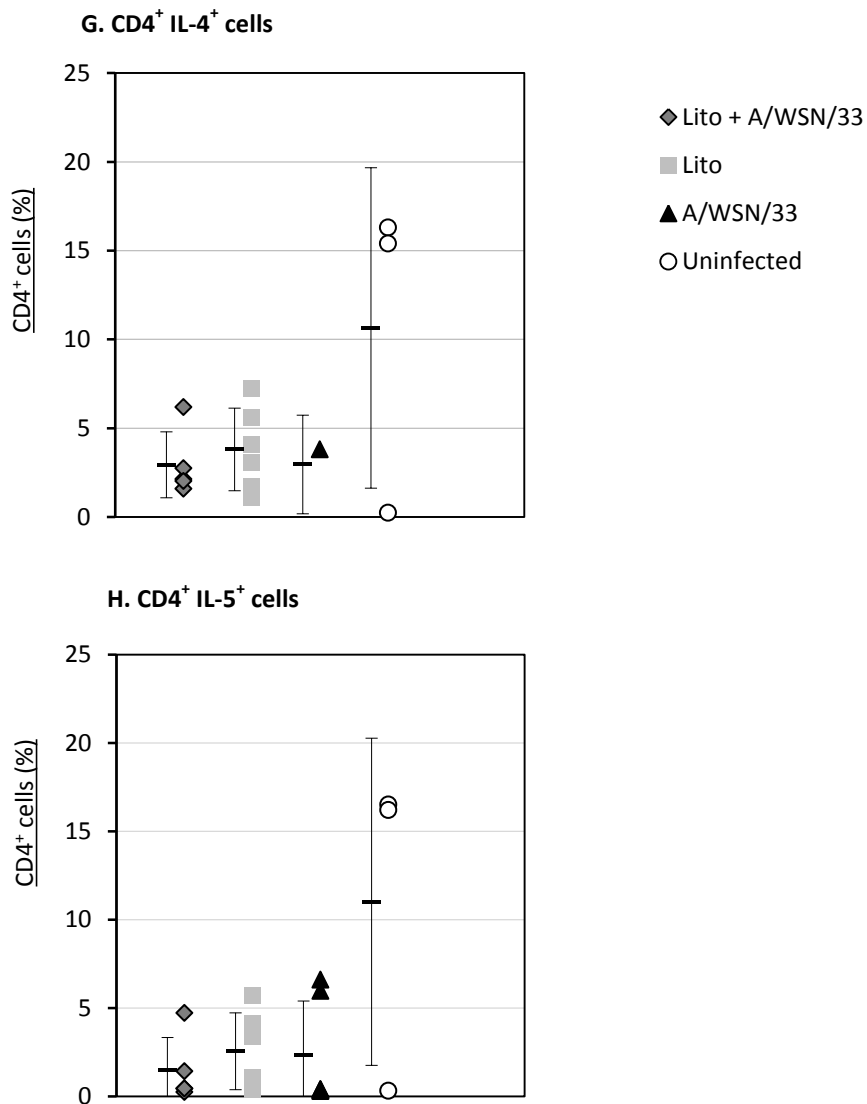


Figure 4.5 Mice were culled 6 days post A/WSN/33 infection. Lung draining and thoracic lymph nodes were harvested. 1×10^7 cells were stained for CD4⁺ and CD8⁺ T cell markers. Samples were run on a BD LSR II Fortessa. Results are displayed as percentages (scatter plot) and mean per group \pm 1 standard deviation (whisker plot). N=6, Uninfected N=3. Statistics calculated on 2 independent experiments, (*=p<0.05, **=p<0.01, ***=p<0.001 general linear model). **A.** CD4⁺ lymphocytes **B.** CD8⁺ lymphocytes **C.** CD4⁺ IFN γ ⁺ cells **D.** CD8⁺ IFN γ ⁺ cells **E.** CD4⁺ TNF α ⁺ cells **F.** CD8⁺ TNF α ⁺ cells **G.** CD4⁺ IL-4⁺ cells **H.** CD4⁺ IL-5⁺

mice had $6.21 \pm 2.15\%$ $CD4^+ TNF\alpha^+$ cells and $2.01 \pm 1.21\%$ of $CD8^+$ cells producing $TNF\alpha$ while *L. sigmodontis* had similar $TNF\alpha$ production of $5.68 \pm 0.88\%$ and $1.85 \pm 0.37\%$ in the CD4 and CD8 populations correspondingly. Co-infected mice produced the least $TNF\alpha$ in both cell types. Co-infected mice were $3.23 \pm 0.37\%$ positive for $TNF\alpha$ in the CD4 population and $1.01 \pm 0.43\%$ in the CD8 population. These results were unexpected. $TNF\alpha$ was not expected to increase in the uninfected mice.

IL-4 and IL-5 cytokines were produced in very low numbers of $CD4^+$ T cells in all groups, with no notable differences in expression. Uninfected mice however had unusually increased production of IL-4 and IL-5 ($10.65 \pm 9.05\%$ and $11.00 \pm 9.26\%$ correspondingly). Although these results were highly variable, the absolute cell numbers recovered were high and therefore the results could not be discounted (Figures 4.5G and 4.5H). IL-4 and IL-5 production in other groups were more cohesive, with the *L. sigmodontis* infected group producing $3.81 \pm 2.33\%$ IL-4 and $2.54 \pm 2.18\%$ IL-5, A/WSN/33 infected mice producing $2.97 \pm 2.77\%$ and $3.07 \pm 2.33\%$ and co-infected mice producing $2.95 \pm 1.86\%$ and $1.45 \pm 1.88\%$ respectively.

IL-10 production was minimal in all groups, with expression undetectable in some individuals. These results are therefore not presented.

- *Litomosoides sigmodontis* L4 worm burden

Pre-existing L4 stage *L. sigmodontis* infection did not appear to alter influenza pathogenesis or replication. To determine if influenza co-infection alters the course of *L. sigmodontis* infection, the number of worms that could be recovered from the pleural cavity was measured in the co-infected and singly infected groups. The number of L4 worms recovered from the pleural cavity at the L4 developmental stage are recorded in Table 4.1

The number of L4 worms recovered from the pleural cavity of mice infected with *L. sigmodontis* was not altered by the presence of a 6 day co-infection with 5×10^3 A/WSN/33.

At the L4 stage, the male to female ratio of *L. sigmodontis* larvae is undeterminable and therefore total numbers are reported (Table 4.1, end column). Singly *L. sigmodontis* infected mice had a mean worm burden 3.16 and ranged from 0-6. The single mouse with 0 recovered worms had no distinct characteristics compared with others within the group, perhaps suggesting recent clearance of the *L. sigmodontis* infection as opposed to an unsuccessful infection or early clearance at the site of infection in the skin. Co-infected mice had a mean average of 5.16 and ranged from 1 and 9. There is therefore no significant difference between the two groups.

Table 4.1 *Litomosoides sigmodontis* L4 worm burden

Mouse	Day	<i>L.sigmodontis</i>	A/WSN/33	Male	Female	Total
3392	18	+	+			1
3393	18	+	+			0
3394	18	+	+			4
3395	18	+	+			6
3396	18	+	+			2
3397	18	+	+			6
3398	18	+	-			1
3399	18	+	-			8
3400	18	+	-			9
3401	18	+	-			2
3402	18	+	-			7
3403	18	+	-			4

4.4.3 Co-infection with pre-patent (adult) *Litomosoides sigmodontis* and 5×10^3 A/WSN/33

At this developmental stage of *L. sigmodontis* infection, the now adult larvae have a more significant impact on lung integrity (Figure 4.1D-K). The underlying infection also skews the local immune response towards a type 2 and regulatory phenotype. Co-infection at this time point was therefore used to determine the outcome of influenza infection in a host with an ongoing type 2 polarised immune response.

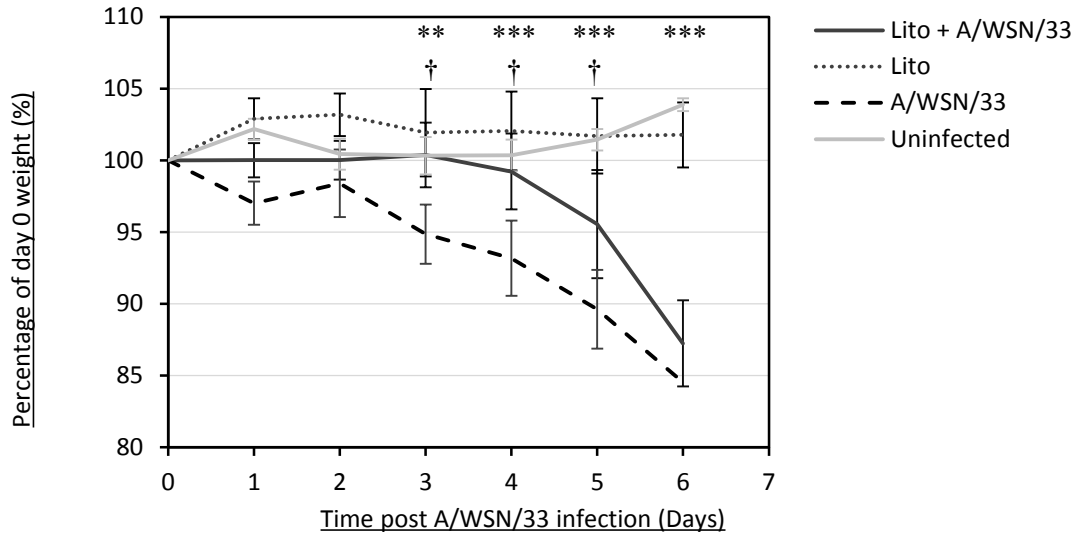
- Effect of adult (pre-patent) *Litomosoides sigmodontis* infection on A/WSN/33 co-infection.

Weight loss, clinical scoring and influenza titre were once again used to determine the overall change in outcome of influenza infection caused by the underlying *L. sigmodontis* co-infection.

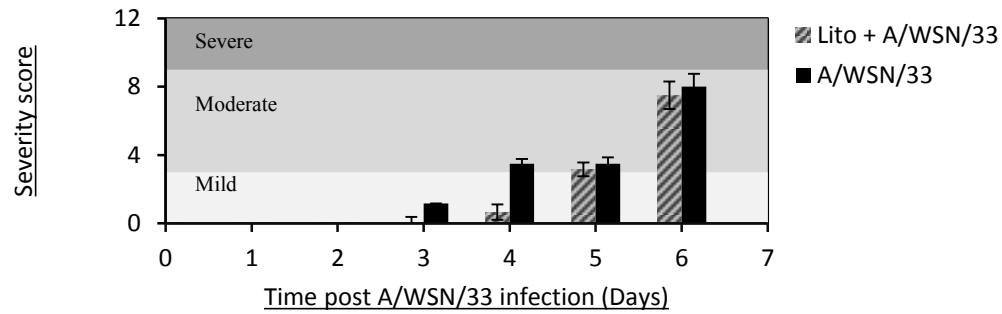
A/WSN/33 induced weight loss was evident in singly infected mice at day 3 with a mean reduction in weight of $7.2 \pm 1.97\%$ (Figure 4.6A). This increases to $8.8 \pm 2.5\%$ by day 4 and further to $10.66 \pm 2.61\%$ by day 5. Weight loss progressed to a mean average of $15.46 \pm 3.13\%$ by day 6 post infection. This is identical to the weight loss seen in the younger mice infected at the earlier *L. sigmodontis* time point (see Figure 4.2A). All mice in the A/WSN/33 singly infected group displayed decreased mobility at day 3, with a mean score of 1.17 (Figure 4.6B). At day 4, decreased mobility was scored the same however mice in this group were also showing increased respiratory effort, mild staring coat and hunching (both scored at a mean of 1) resulting in a mean overall clinical score for this group of 3.5, placing them in the ‘moderate’

Figure 4.6 Co-infection with pre-patent (Adult) *Litomosoides sigmodontis* has a protective effect against A/WSN/33 pathogenesis

A. Weight loss



B. Clinical severity score



C. Influenza lung titre – Day 6

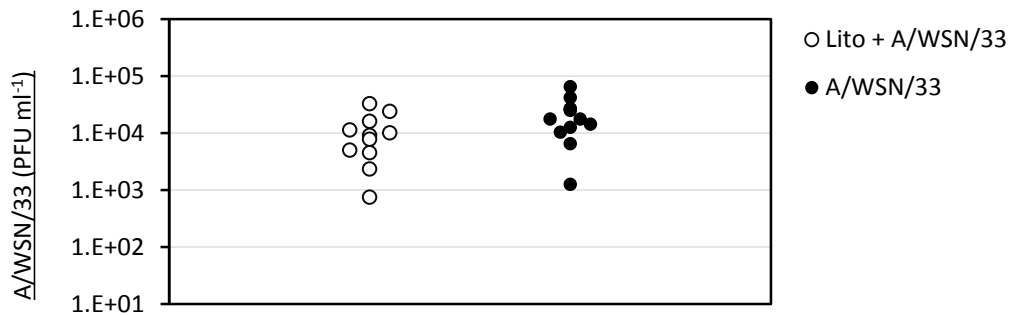


Figure 4.6 A. Weight loss post A/WSN/33 infection. Results displayed as percentage of weight at day 0 prior to infection. Mean weight loss is shown \pm 1 standard deviation, N=6, representative of 2 experiments. Significance determined by general linear model (*/+ = $p < 0.05$, **/+ = $p < 0.01$ ***/+++ = $p < 0.001$). * denotes significance of A/WSN/33 vs. uninfected. † denotes significance between co-infected and A/WSN/33 infected groups. **B.** Clinical severity was measured by 4 signs, each was scored on a scale of 0-3 and the average sum reported \pm 1 standard deviation as clinical severity score, N=12, 2 experimental repeats. **C.** Left lung homogenate was measured by dilution series plaque assay on MDCK cells for levels of infectious virus. Individual values are plotted as PFU per ml of lung homogenate, N=12 from 2 experimental repeats.

severity category. This moderate phenotype continued to day 5 and then increased in severity on day 6 when each mouse in the group was scored at ~2 in all categories, increasing the severity score to an overall average of 8.

Co-infected mice show significantly less weight loss than singly infected mice (Figure 4.6A). A significant decrease in weight was only seen from day 5, when a mean decrease in weight of $4.43 \pm 3.58\%$ was recorded. At day 6 this mean value was increased rapidly to $12.75 \pm 2.55\%$ mean average weight loss. When compared with A/WSN/33 mice, a significant difference was detected at days 3, 4 and 5 ($p < 0.05$ by general linear model) post infection.

This effect was also seen in the clinical severity of co-infected mice (Figure 4.6B). Clinical signs of infection did not appear until day 4, a day later than A/WSN/33 infected controls. Half of the co-infected mice at day 4 were showing mild signs of increased respiratory effort (scored at 0.67) but this was not coupled with decreased mobility and hunching until day 5 when all mice began to show signs of infection. Mean overall severity score on day 5 was 3.17 which was a similar severity level to the A/WSN/33 infected group. Similarly at day 6 the severity score increased to 7.5 on average. All mice showed signs of increased respiratory effort, decreased mobility, hunching and staring coat, which were all scored individually at ~2.

Uninfected and *L. sigmodontis* infected mice did not show clinical signs and did not undergo any weight loss. At day 6 post infection the uninfected mice were 103.88% of their original weight and *L. sigmodontis* infected mice were on average 101.78% of their original weight at the point of mock influenza infection.

Influenza virus titre was measured in the lungs of infected mice at day 6 (Figure 4.6C). Co-infected and singly A/WSN/33 infected mice had near identical viral loads in the lung. Co-infected mice had an average of 1.07×10^4 PFU ml⁻¹ and singly A/WSN/33 mice averaged 1.12×10^4 PFU ml⁻¹. Variation from the mean was also very similar within the two groups (10,700 PFU and 11,300 PFU respectively).

– Pathology

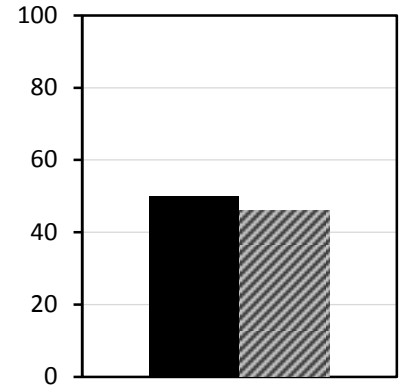
At this stage, co-infection can alter the outcome of influenza infection. To determine if co-infection can also alleviate influenza induced pathology, the lungs were investigated for histological changes.

Infection with adult worms showed similar pathology in the lung to the immature L4 infection (see Figure 4.1 D-K). The adult worms remain located in the pleural cavity, however are now much larger after undergoing a moulting stage (from L4 to adult). A/WSN/33 had no significant impact on the pathology caused by *L. sigmodontis* during the 6 day co-infection.

Figure 4.7 Co-infection with pre-patent (Adult) *Litomosoides sigmodontis* does not alter pathology caused by A/WSN/33

A. Percentage of lung affected

- Uninfected
- Lito
- ▨ Lito + A/WSN/33
- A/WSN/33



B. Pathological scoring

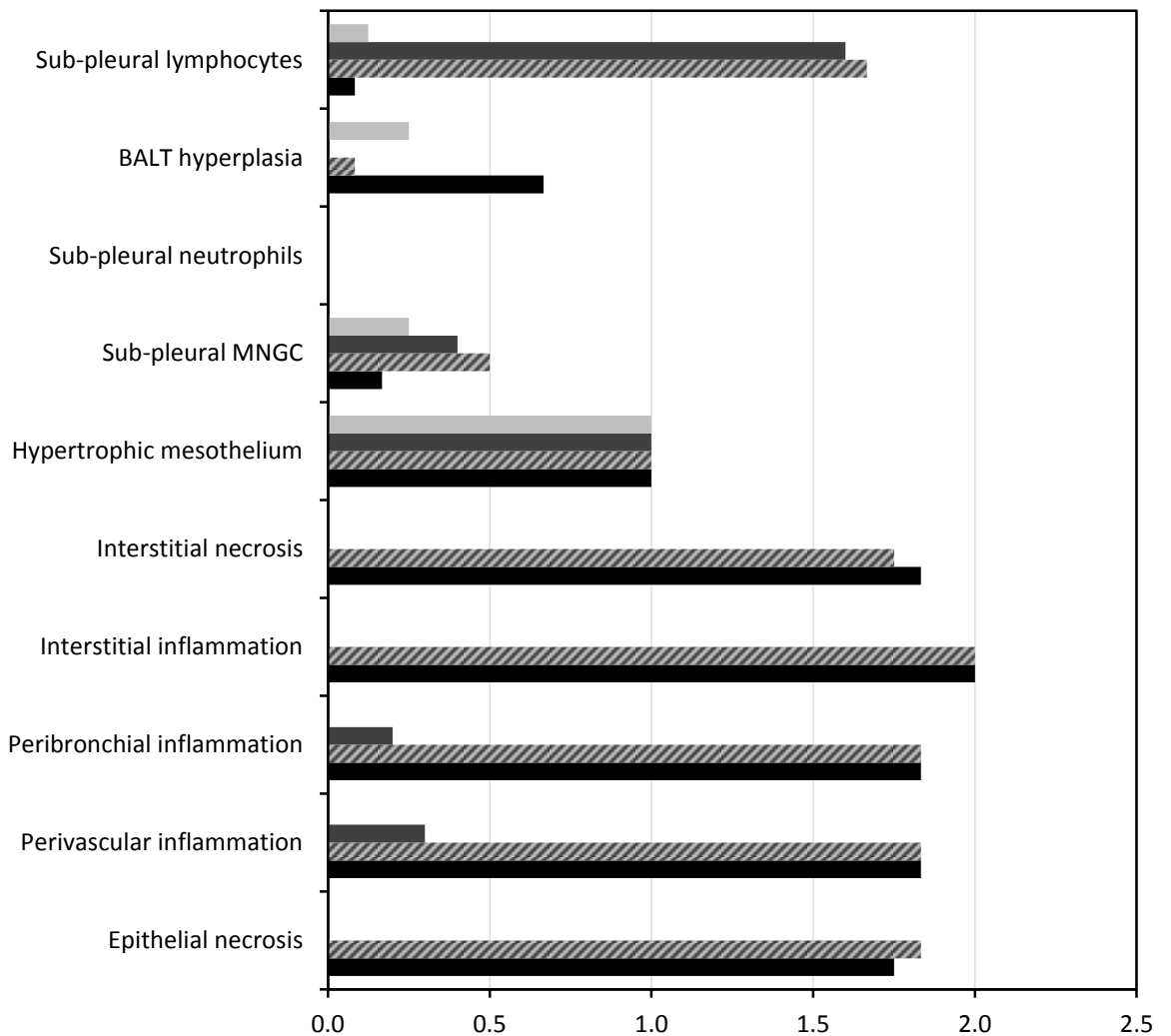


Figure 4.7 The left lobes of lungs from co-infected, singly infected and uninfected mice were harvested, fixed, cut into sections and stained by hematoxylin and eosin 6 days post infection with A/WSN/33. **A.** The extent of lung damage was assessed as 0%, 25%, 50%, 75% or 100% per lung. **B.** Pathology and infiltration of immune cells was scored on a scale from 0-3 for each lung. All results are presented as mean average for each group. N=6. Error bars are not displayed due to the ranked nature of the data.

Infiltration of inflammatory cells into the sub pleural layer was evident in all infected mice (Figure 4.7B). At this time point neutrophil infiltration was not evident in any group, however, lymphocytes were at similar levels (0.50, 0.40, 0.17 and 0.25 in the co-infected, *L. sigmodontis* infected, A/WSN/33 infected and uninfected). Similarly hypertrophic mesothelium was not specific to *L. sigmodontis* infected groups with all groups averaging a score of 1 for this pathology.

BALT hyperplasia was evident at a greater level in A/WSN/33 mice than any other group at this time point. A/WSN/33 infected mice were scored at 0.67 on average. Co-infected mice were scored at 0.25 but this pathology was not present in the uninfected and *L. sigmodontis* infected mice. The most notable difference at this time point was the increased presence of exophytic frond-like structures extending into the pleural space in mice infected with *L. sigmodontis*. Co-infection had little effect on this pathology with both *L. sigmodontis* groups scored at ~1.6 on average. These structures were seen in particular at the hilum of each lung in mice infected with the adult nematodes.

Influenza pathology was also unaffected by co-infection (Figure 4.7B). Levels of influenza induced pathology were similar to that seen in the younger mice (see Figure 4.3B) for both A/WSN/33 infected groups. Interstitial necrosis was scored at 1.75 in the co-infected and 1.83 on average in the A/WSN/33 singly infected mice. Similar levels of cell inflammation were also recorded, with both groups scoring a mean average of 2 (Figure 4.6B). Peri-bronchial and peri-vascular inflammation were also recorded at similar levels in the singly A/WSN/33 infected and co-infected mice. Both groups scored an average of 1.83 for both peri-vascular and peri-bronchial inflammation and the variation within each group was minimal (all mice were scored 1.5 or 2 for this pathology). Both peri-bronchial (0.2) and peri-vascular inflammation (0.3) are now more evident in the *L. sigmodontis* infected group than was recorded at the previous time point. These pathologies are not present in the uninfected mice. Epithelial necrosis was similar between A/WSN/33 infected and co-infected mice with recorded scores of 1.75 and 1.83 respectively.

The extent of influenza induced pathology was also similar to the previous time point (see Figure 4.3A) with a mean average of 45-50% damage to the right lung of each mouse histologically scored (Figure 4.7A).

– Lung cytokine environment

While pathogenesis of influenza infection was less aggressive in co-infected mice, the pathology in the lung is compartmentalised and one infection does not appear impact the site of infection of the other pathogen. To determine if this is also true for the overall immune

responses to each infection, the inflammatory and regulatory cytokine environment was assayed.

The inflammatory environment in the lung was measured by ELISA in two samples from each mouse at this time point. There were no cytokines in the lung homogenate found to show statistically significant differences between experimental groups (Figure 4.8A) when compared with the co-infected mice. IFN γ , a pro-inflammatory cytokine is increased by A/WSN/33 infection (1.90 ± 1.08 fold) and is increased to a lesser (but not significantly lower) degree in the homogenate of co-infected mice (1.34 ± 0.67 fold). *L. sigmodontis* infected mice were measured at a 0.62 ± 0.40 fold reduction in IFN γ level.

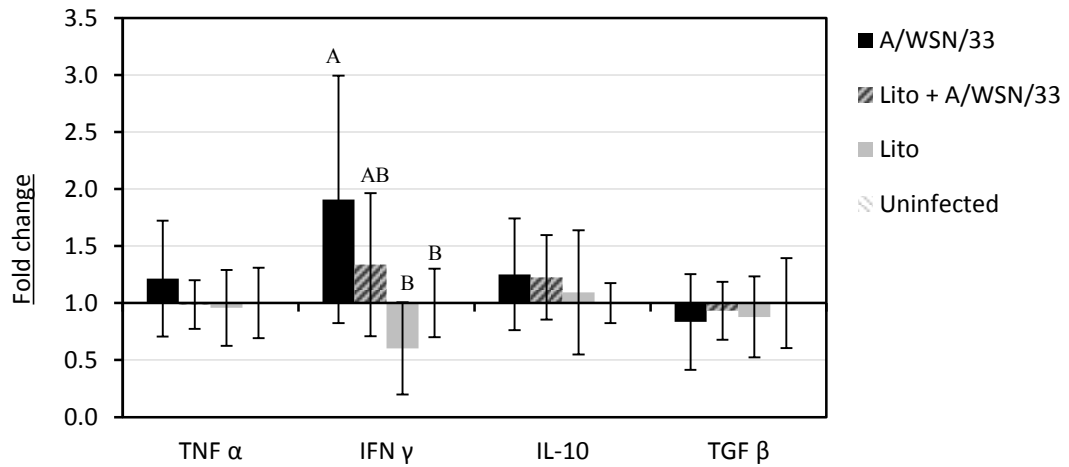
TNF α , IL-10 and TGF β were all unaltered by any infection (Figure 4.8A) in the lung homogenates. TNF α was present at 0.98 ± 0.21 , 0.96 ± 0.33 and 1.22 ± 0.51 fold concentrations in the co-infected, *L. sigmodontis* infected and A/WSN/33 infected groups respectively when compared with the uninfected mice. Levels of IL-10 were 1.23 ± 0.37 , 1.09 ± 0.54 and 1.25 ± 0.48 times that of the uninfected mice and TGF β levels were 0.93 ± 0.25 , 0.87 ± 0.35 and 0.84 ± 0.42 that of the uninfected mice for the co-infected, *L. sigmodontis* infected and A/WSN/33 infected experimental groups.

IFN γ was detectable at ~ 50 fold greater concentrations in all A/WSN/33 infected mice in the BALF samples compared with uninfected mice (Figure 4.8B). Co-infected mice had 41.9 ± 11.6 fold greater IFN γ and A/WSN/33 infected mice had 49.7 ± 13.0 fold greater than the uninfected mice. These two groups are not significantly different from one another. *L. sigmodontis* infection did not elevate the levels of IFN γ .

A coinciding increase in IL-10 (33.6 ± 8.0 fold) was also evident in A/WSN/33 infected mice. Co-infection IL-10 levels were 26.3 ± 12.4 fold higher than uninfected mice. Again *L. sigmodontis* infection did not appear to significantly increase the levels of IL-10 present, however, a single mouse within this group did show a 7 fold increase in IL-10; increasing the standard deviation. This data follows a bimodal distribution and cannot be normalised, therefore experimental groups were examined by Kruskal-Wallis non-parametric test for IFN γ and IL-10. Significance was identified at $p < 0.001$ for both cytokines. Based on the average rank scores and z values for each experimental group, *L. sigmodontis* infected, uninfected, co-infected and A/WSN/33 infected groups were individually compared by Mann-Witney test to determine if co-infected differed from singly A/WSN/33 infected and whether *L. sigmodontis* has a significant effect on IFN γ or IL-10 compared with uninfected mice. These tests showed there were no significant differences between the groups. The increase in IL-10 and IFN γ , however,

Figure 4.8 Cytokine environment is not significantly altered in mice co-infected with pre-patent (*Adult*) *Litomosoides sigmodontis* and A/WSN/33

A. Lung homogenate



B. Broncho-alveolar lavage fluid

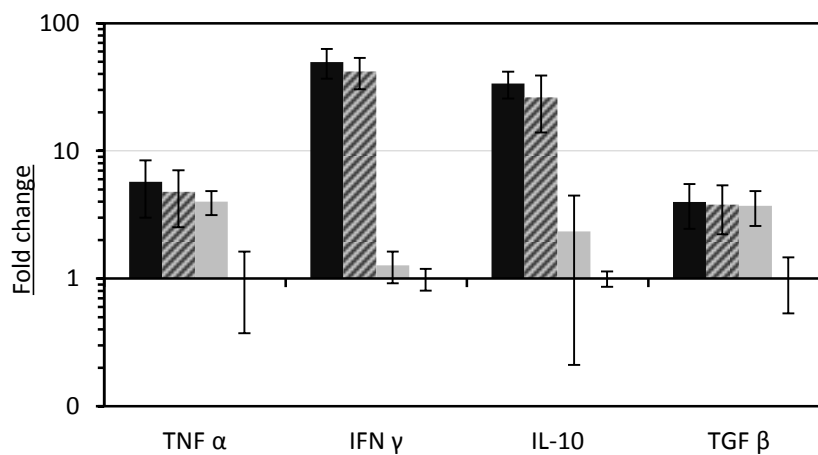


Figure 4.8 A. 6 days post A/WSN/33 infection, the left lung was homogenised in Dulbecco's minimum essential medium and the homogenate used for ELISA detection of cytokines. Representative of 2 independent experiments. N=12. **B.** Lungs were lavaged with 2mls HBSS + 3mM EDTA, cells were removed and the broncho-alveolar lavage fluid (BALF) used to detect cytokines in the interstitial/alveolar environment. Single experiment, N=6. Each group is represented as mean average fold change \pm 1 standard deviation compared to the mean level of expression in the uninfected group. Statistics were performed by general linear model. Groups that do not share the same letter are significantly different at a 95% confidence level.

had a very strong positive Pearson's correlation co-efficient of 0.884 (when all samples were aligned).

TNF α and TGF β were moderately increased in all infected experimental groups (Figure 4.8B). A/WSN/33 infected mice had a 5.7 ± 2.7 mean fold increase in TNF α and 3.9 ± 1.5 fold increase in TGF β . Co-infected mice had a 4.8 ± 2.2 fold increase in TNF α and 3.8 ± 1.5 fold increase in TGF β . *L. sigmodontis* infected mice had a 4.0 ± 0.8 fold increase in TNF α and 3.7 ± 1.1 fold increase in TGF β . TNF α and TGF- β were highly correlated in the BALF samples, (0.846 Pearson correlation on all samples). These cytokines were significantly increased in all infected experimental groups compared with the uninfected mice.

– CD8⁺ cell response in the lymph nodes

The lymph nodes draining the lungs and pleural cavity are the site of antigen presentation during the adaptive immune response for both infections. As the pathology in the lung is not altered by co-infection, the change in outcome to influenza infection due to pre-existing *L. sigmodontis* co-infection may be a result of an altered adaptive response in the draining lymph nodes.

Six days after A/WSN/33 infection, cells from the thoracic and lung draining lymph nodes were harvested and stained for CD8 and intracellular cytokines. The total CD8⁺ cell frequency (Figure 4.9A) was highest in the *L. sigmodontis* infected group (2.41%), however, this was not statistically significant when compared with all other groups. Overall the number of CD8⁺ T cells in the draining lymph node was very low with a mean average of ~2% of total cells recorded in all groups.

CD8⁺ cells from mice infected with A/WSN/33 produced higher levels of IFN γ ($53.73\pm 6.52\%$, $p<0.001$ general linear model) compared with uninfected ($21.96\pm 5.18\%$) and *L. sigmodontis* infected mice ($16.04\pm 6.04\%$). IFN γ levels were also significantly increased to a mean average of $29.52\pm 13.52\%$ (Figure 4.9B). The co-infected mice produced significantly less IFN γ than their A/WSN/33 singly infected counterparts, ($p<0.01$) and showed much greater variation in IFN γ levels than the singly infected mice and uninfected controls.

TNF α production by CD8⁺ cells was also increased in A/WSN/33 infected mice (Figure 4.9C) to a mean average of $9.08\pm 2.89\%$ ($p<0.001$) compared with uninfected mice $6.76\pm 2.06\%$. This did not vary significantly from the co-infected group (mean $4.44\pm 1.67\%$) or *L. sigmodontis* singly infected mice (mean of $3.68\pm 2.47\%$) despite a similar trend.

Figure 4.9 Pre-patent (Adult) *Litomosoides sigmodontis* co-infection alters the CD8⁺ T cell profile in the lung draining lymph nodes following A/WSN/33 infection.

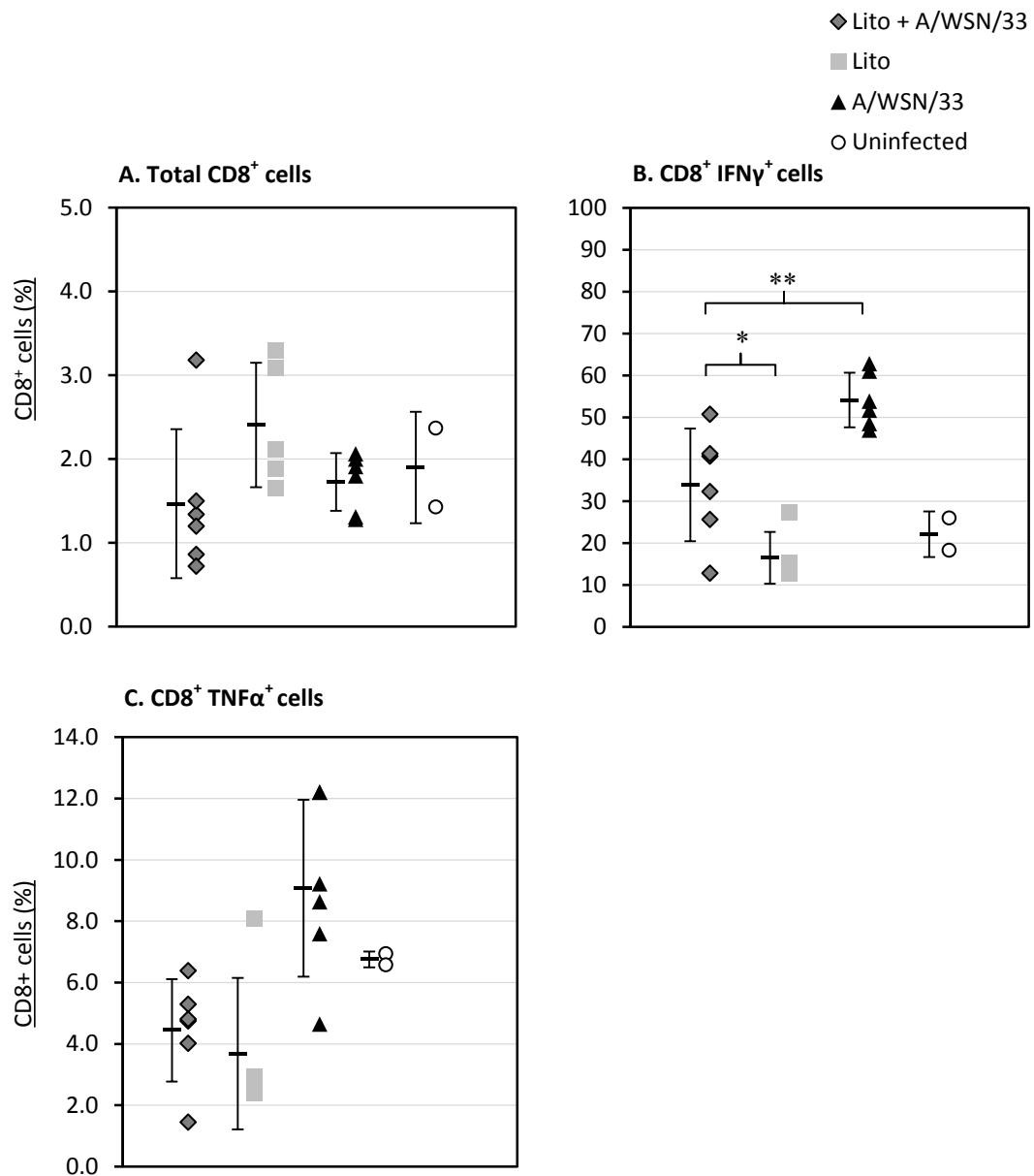


Figure 4.9 Mice were culled 6 days post A/WSN/33 infection and draining lymph nodes of the thoracic cavity and lung were harvested. 1×10^7 cells from the lymph nodes were stained for a range of intracellular CD8⁺ T cell markers. The samples were run on a BD LSR II Fortessa. Results displayed as individual percentages (scatter plot) and mean per group \pm 1 standard deviation (whisker plot). N=6 except for uninfected mice where N=2. All statistics are calculated on data from 2 independent experiments by general linear model, (*=p<0.05, **=p<0.01). **A.** CD8⁺ lymphocytes **B.** CD8⁺ IFN γ ⁺ cells **C.** CD8⁺ TNF α ⁺ cells.

These two inflammatory cytokines showed positive correlation in their expression in CD8⁺ cells (0.733 Pearson's correlation co-efficient). IL-10 production by CD8⁺ cells was limited (~1%) and did not vary between experimental groups. Data is therefore not shown due to low numbers.

– CD8⁺ response in the lung

Six days after influenza infection, cells of the adaptive immune response are present in the lungs. To determine if the alterations to the immune environment in the CD4⁺ cells in the lymph nodes affects the responding CD8⁺ T cells in the lung, cells harvested by lavage were intracellularly stained for inflammatory cytokine production.

Six days post infection with A/WSN/33, the number of CD8⁺ cells in the broncho-alveolar lavage fluid (BALF) accounted on average for 37.03±5.16% of the lymphocytes recovered from co-infected mice (Figure 4.10A) and 23.20±2.00% in the A/WSN/33 infected mice. Uninfected and *L. sigmodontis* infected mice had a significantly lower percentage (p<0.001, 2 way ANOVA) of CD8⁺ cells, (9.09 and 11.35% mean averages respectively).

Co-infected mice have a greater proportion of CD8⁺ cells than singly A/WSN/33 infected mice. The CD8⁺ cells in co-infected mice showed similar characteristics to those in A/WSN/33 infected. IFN γ production (Figure 4.10B) in A/WSN/33 infected mice was present in 30.68±4.01% of CD8⁺ cells. Similarly in co-infected mice 33.17±0.24% CD8⁺ cells were producing IFN γ . 4.18±2.66% of CD8⁺ cells in uninfected mice produce IFN γ and 8.76±6.29% of CD8⁺ cells in the *L. sigmodontis* infected mice produce IFN γ . TNF α production by these cells did not follow the same pattern (Figure 4.10C). CD8⁺ cells from uninfected, *L. sigmodontis* infected, A/WSN/33 infected and co-infected mice produced similar levels of TNF α (3.54, 4.14, 5.37 and 6.34% respectively with 2-3% standard deviation in all groups). The absolute numbers of CD8⁺ cells producing IL-10 was minimal in all groups and is therefore not reported.

– CD4⁺ T cell response in the lymph nodes

Six days after A/WSN/33 infection, cells from the thoracic and lung draining lymph nodes were harvested and stained for CD4 and intracellular cytokines. Mice that were singly infected with A/WSN/33 showed a T_H1 phenotype in the CD4⁺ T cell population. IFN γ was produced by 8.80±0.95% of CD4⁺ cells (Figure 4.11A), which is significantly higher (p<0.001, general linear model) than in the co-infected (5.71±1.20%, p<0.001), *L. sigmodontis* infected (1.85±0.95% p<0.001) and uninfected control mice (1.98±1.47% p<0.001). While TNF α production by CD4⁺ T cells was not significantly increased in A/WSN/33 infected mice (29.48±4.14%), compared with the uninfected animals (26.24±7.14%) there was a significant decrease (p<0.001) in TNF α production in the group infected solely with *L. sigmodontis* (14.48±1.16%) and in the co-

Figure 4.10 Pre-patent (Adult) *Litomosoides sigmodontis* co-infection leads to an increased inflammatory CD8⁺ T cell population in the lung following A/WSN/33 infection.

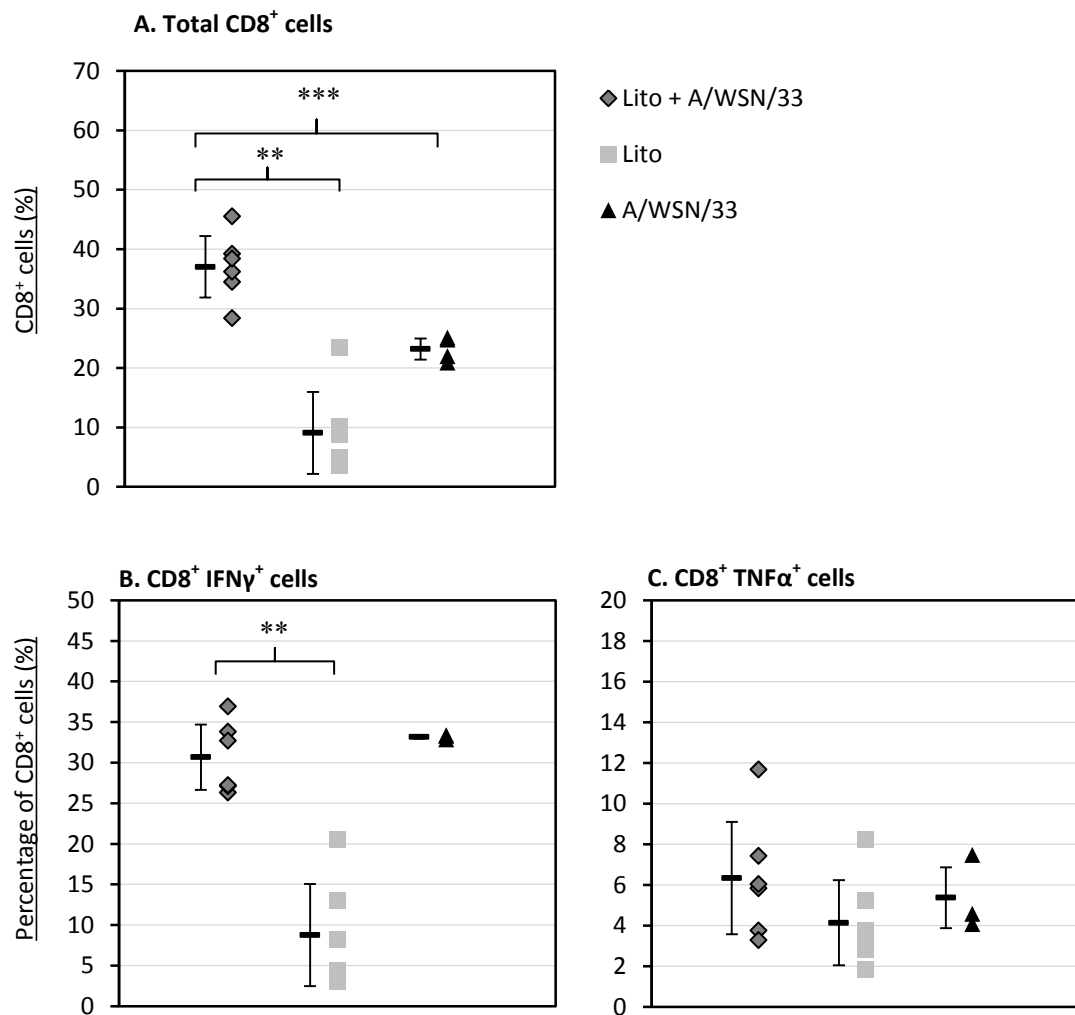
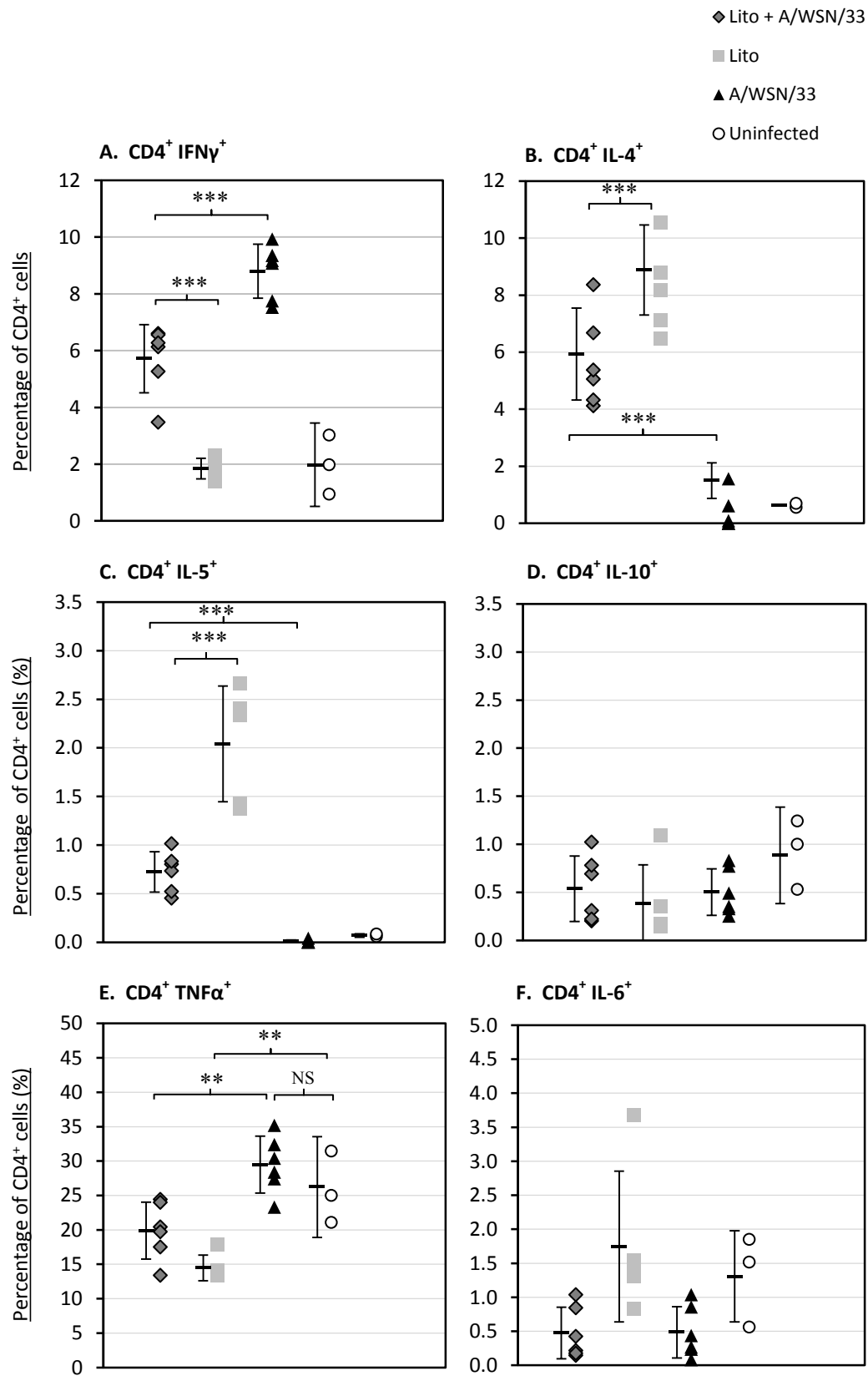


Figure 4.10 Mice were culled 6 days post A/WSN/33 infection and cells in the lung were harvested by bronchoalveolar lavage (BAL). Maximum numbers of cells in the BAL fluid were stained for a range of intracellular CD8⁺ T cell markers. The samples were run on a BD LSR II Fortessa. Results are displayed as individual percentage (scatter plot) and mean fluorescence intensity per group \pm 1 standard deviation (whisker plot). N=6 except for uninfected mice where N=3. All statistics are calculated on data from a single experiment, (**=p<0.01, ***=p<0.001 general linear model). **A.** Total CD8⁺ T cells. **B.** CD8⁺ IFN γ ⁺ cells **C.** CD8⁺ TNF α ⁺ cells

Figure 4.11 Pre-patent (Adult) *Litomosoides sigmodontis* co-infection alters the CD4⁺ T cell profile in the lung draining lymph nodes following A/WSN/33 infection



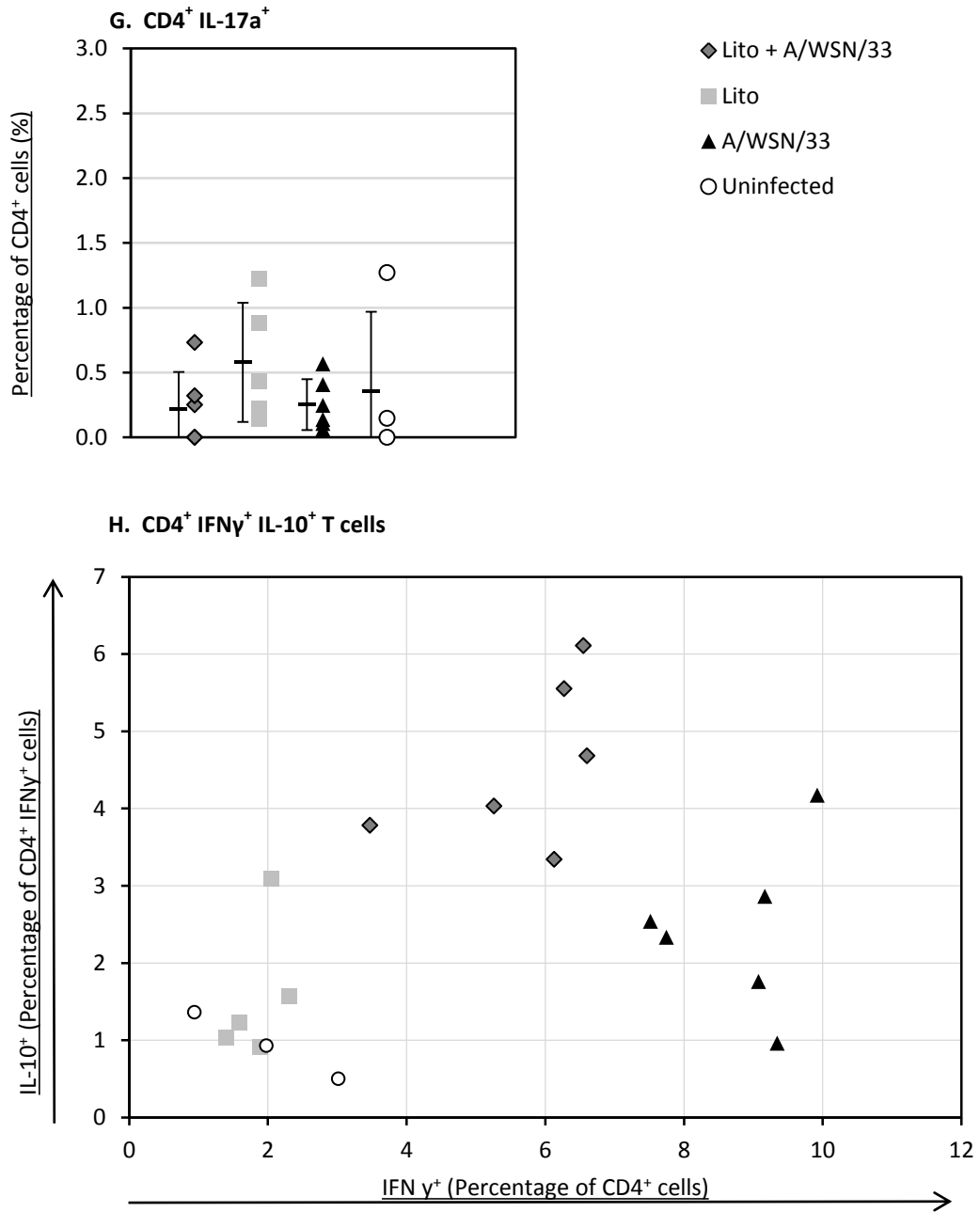


Figure 4.11 5-6 week old female BALB/c mice were infected with 25 x *L3 Litomosoides sigmodontis* larvae S.C. and 34 days later with 5×10^3 A/WSN/33 I.N. Mice were culled 6 days post A/WSN/33 infection and draining lymph nodes of the thoracic cavity and lung were harvested. 1×10^7 cells from the lymph nodes were stained for a range of intracellular CD4⁺ T cell markers. The samples were run on a BD LSR II Fortessa. Results displayed as individual percentage positive (scatter plot) and mean per group \pm 1 standard deviation (whisker plot). N=6 except for uninfected mice where N=3. These were compared with singly infected and uninfected controls. All statistics are calculated on data from a single experiment, (*=p<0.05, **=p<0.01, ***=p<0.001 general linear model). **A.** CD4⁺ IFN γ ⁺ cells **B.** CD4⁺ IL-4⁺ cells **C.** CD4⁺ IL-5⁺ cells **D.** CD4⁺ IL-10⁺ cells **E.** CD4⁺ TNF α ⁺ cells **F.** CD4⁺ IL-6⁺ cells **G.** CD4⁺ IL-17a⁺ cells **H.** CD4⁺ IFN γ ⁺ cells co-expressing IL-10.

infected mice ($19.88 \pm 4.33\%$). See Figure 4.11E. $\text{TNF}\alpha$ and $\text{IFN}\gamma$ cytokines showed only a weak Pearson's correlation co-efficient of 0.616.

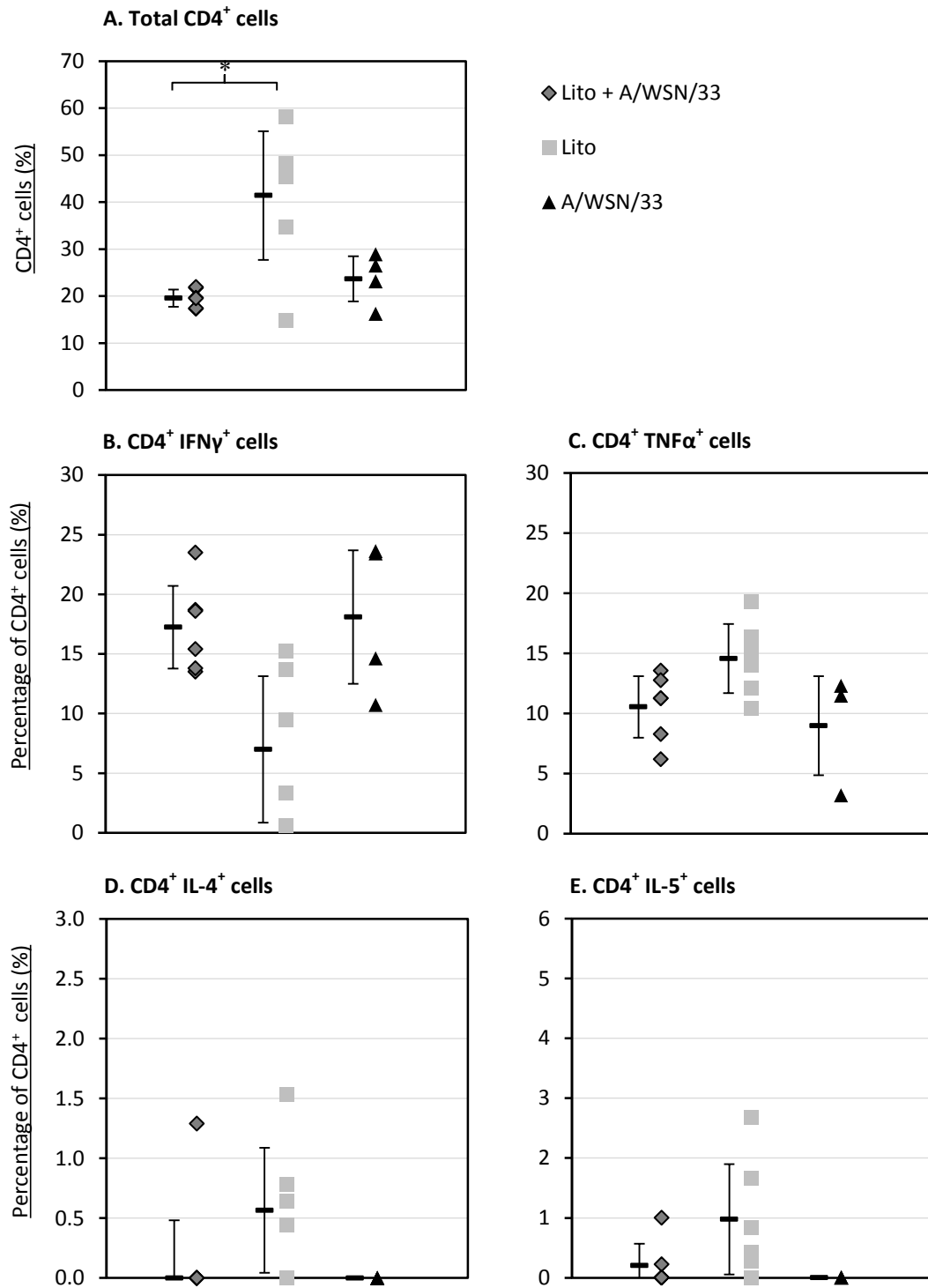
Infection with *L. sigmodontis* resulted in a $\text{T}_{\text{H}2}$ phenotype in the CD4^+ T cells. IL-4 and IL-5 production (Figure 4.11B and 4.11C) was higher in this group ($8.21 \pm 1.58\%$ and $2.04 \pm 0.60\%$ respectively) compared with A/WSN/33 infected mice, ($0.37 \pm 0.62\%$ and $0.01 \pm 0.02\%$), uninfected mice, ($0.10 \pm 0.01\%$ and $0.07 \pm 0.02\%$) and the co-infected group ($5.65 \pm 1.61\%$ and $0.72 \pm 0.10\%$). IL-4 and IL-5 cytokines did not display normal distribution and could not be transformed and were therefore analysed by non-parametric tests. IL-4 and IL-5 both demonstrated significant differences between groups when evaluated by Kruskal-Wallis, ($p=0.0048$ for both). From the rank averages and z values, experimental groups were identified for comparison.

IL-4 and IL-5 were both significantly increased in the A/WSN/33 infected groups. The increase was significantly reduced by pre-existing co-infection with *L. sigmodontis* ($p<0.001$, Mann-Whitney test). These cytokines were highly correlated in all groups, with a Pearson's correlation coefficient of 0.893.

The other cytokines, IL-10 (Figure 4.11D), IL-6 (Figure 4.11F) and IL-17a (Figure 4.11G) displayed some trends in mean differences between experimental groups but none were significantly changed by either infection. IL-6 and IL-17a were also not normally distributed. IL-6 showed suggestion of significant differences between groups ($p=0.022$) however Mann-Whitney analysis demonstrated no significant decrease in A/WSN/33 singly infected mice compared with the uninfected controls ($p=0.09$). IL-17a production was not assessed for significance.

Co-infected mice produced lower levels of $\text{IFN}\gamma$ than A/WSN/33 singly infected mice and had (surprisingly) an unaltered production of IL-10. Within the $\text{IFN}\gamma$ producing CD4^+ T cells however, there was a significant increase ($p<0.01$, general linear model) in the levels of IL-10 co-expression (Figure 4.11H). CD4^+ cells from co-infected mice were $4.58 \pm 1.07\%$ $\text{IFN}\gamma^+$ and IL-10^+ whilst A/WSN/33 infected mice were $2.44 \pm 1.08\%$ positive for this cell population due to an increased expression of $\text{IFN}\gamma$ producing cells and reduced co-expression of IL-10. Although the number of cells in this population are low, the variation in the groups is evident in Figure 4.11H. Uninfected and *L. sigmodontis* infected mice however had almost zero cells with this phenotype.

Figure 4.12 Co-infection with A/WSN/33 reduces the number of CD4⁺ T cells in the lung during pre-patent (Adult) *Litomosoides sigmodontis* infection



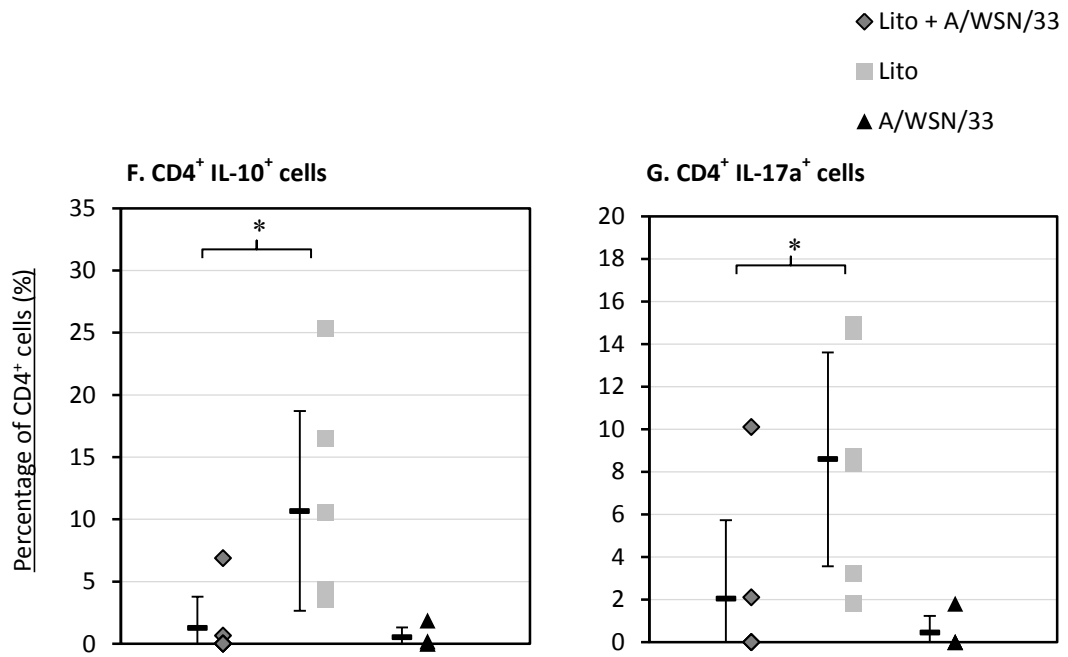


Figure 4.12 Mice were culled 6 days post A/WSN/33 infection and cells in the lung were harvested by bronchoalveolar lavage (BAL). Maximum numbers of cells in the BAL fluid were stained for a range of intracellular CD4⁺ T cell markers. The samples were run on a BD LSR II Fortessa. Results displayed as individual percentage (scatter plot) and mean per group \pm 1 standard deviation (whisker plot). N=6, A/WSN/33 N=4 and uninfected N=3. All statistics are calculated on data from a single experiment, (*=p<0.05, **=p<0.01, ***=p<0.001 Kruskal Wallis and Mann-Whitney tests). **A.** Total CD4⁺ T cells **B.** CD4⁺ IFN γ ⁺ cells **C.** CD4⁺ TNF α ⁺ cells **D.** CD4⁺ IL-4⁺ cells **E.** CD4⁺ IL-5⁺ cells **F.** CD4⁺ IL-10⁺ cells **G.** CD4⁺ IL-17a⁺ cells.

– CD4⁺ T cell responses in the lung

To determine if the changes to lymph node CD4⁺ cells were also evident in the lung by day 6, cells were harvested by lavage.

The number of CD4⁺ T cells in the lungs of *L. sigmodontis* infected mice (measured in BALF) was variable but averaged 41.4±13.71%. The co-infected and A/WSN/33 groups showed significantly reduced ($p < 0.05$) levels of CD4⁺ T cells. Lymphocytes from the A/WSN/33 infected mice were 23.68±4.57% CD4⁺ and lymphocytes from the co-infected mice were 19.57±1.07% CD4⁺ (Figure 4.12A). There was low recovery of CD4⁺ cells in the uninfected group and therefore the data are not shown.

L. sigmodontis infected mice showed a T_H2 phenotype, with increased but not significantly higher mean levels of IL-4 and IL-5 production (0.57% and 0.98% respectively) compared with almost absent expression in A/WSN/33 infected mice (0.00% and 0.02%) and co-infected mice, (0.00% and 0.07%) see Figures 4.12D and 4.12E.

A similar relationship was observed in the proportions of IL-10 (Figure 4.12F) and IL-17a (Figure 4.12G) producing CD4⁺ cells. Careful assessment of the contribution of such cell populations was therefore an important consideration. *L. sigmodontis* infected mice produced significantly more IL-10 ($p < 0.0181$, Mann-Whitney, following Kruskal Wallis analysis) and IL-17a ($p = 0.0416$) however these cytokines were in some cases not detected at all in A/WSN/33 and co-infected animals and are therefore not discussed further.

The pro-inflammatory IFN γ production by CD4⁺ cells was increased in A/WSN/33 infected (18.08±5.60%) and co-infected mice (17.24±3.47%) however not significantly (Figure 4.12B). TNF α did not follow the same expression pattern (Figure 4.12C) and on average was increased in the *L. sigmodontis* infected mice (14.57%) compared with the A/WSN/33 infected group (10.55%) and the co-infected mice (8.98%), however this difference was also not significant.

– *Litomosoides sigmodontis* worm burden

The number of adult worms recovered from the pleural cavity at each developmental stage are recorded in Table 4.2 below.

Table 4.2 *Litomosoides sigmodontis* adult worm burden

Mouse	Day	<i>L.sigmodontis</i>	A/WSN/33	Male	Female	Total
3414	40	+	+	1	2	3
3415	40	+	+	3	1	4
3416	40	+	+	6	6	12
3417	40	+	+	4	4	8
3418	40	+	+	2	3	5
3419	40	+	+	2	3	5
4574	40	+	+	0	0	0
4575	40	+	+	9	8	17
4576	40	+	+	6	9	15
4577	40	+	+	0	1	1
4578	40	+	+	1	2	3
4579	40	+	+	8	6	14
3420	40	+	-	2	4	6
3421	40	+	-	4	2	6
3422	40	+	-	2	4	6
3423	40	+	-	2	3	5
3424	40	+	-	8	4	12
4580	40	+	-	2	3	5
4581	40	+	-	5	5	10
4582	40	+	-	5	11	16
4583	40	+	-	2	3	5
4584	40	+	-	3	2	5
4585	40	+	-	7	8	15

The number of adult worms recovered from the pleural cavity of mice infected with *L. sigmodontis* was not altered by the presence of a 6 day co-infection with 5×10^3 A/WSN/33. At the adult stage, male to female ratio of *L. sigmodontis* worms can be determined. As expected, co-infection did not alter the male to female ratio of adult worms which are reported alongside total numbers (see Table 4.2). Singly *L. sigmodontis* infected mice had a mean adult worm burden of 3.5 males and 3.75 females (7.25 total) and ranged from 0-17 worms. The mouse with 0 worms recovered did not appear to act differently to the other mice in the group in terms of weight loss, clinical effects or cytokine production and is therefore included in the analysis. Co-infected mice had a mean average of 3.8 males and 4.45 females (8.27 total) and ranged between 5 and 16. There is, therefore, no significant difference between the two groups.

4.4.4 Co-infection with patent (adult \pm mf) *Litomosoides sigmodontis* on co-infection with 5×10^3 A/WSN/33.

The outcome of the pre-patent co-infection was a temporarily reduced susceptibility to influenza infection. At the microfilaraemic stage of *L. sigmodontis* infection, L1 larvae are present in the tissues leading to a change in the immune response to a partially inflammatory phenotype from the established chronic type 2 and regulatory phenotype. Co-infection with influenza at this time point was therefore expected to produce a different outcome.

- Effect of patent (adult \pm mf) *Litomosoides sigmodontis* infection on A/WSN/33 co-infection.

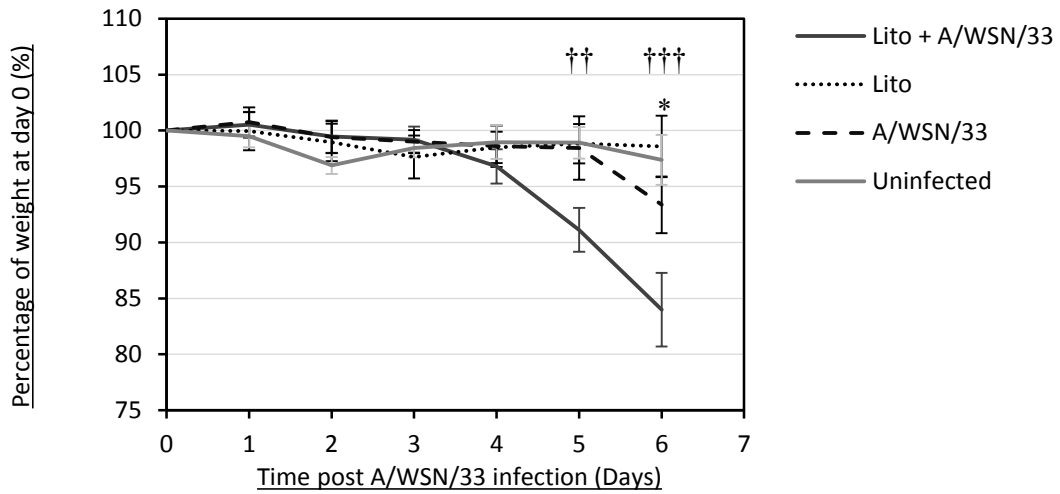
Mice infected with A/WSN/33 were 13-14 weeks old due to the developmental stage of the nematode infection. As such, the adult mice were less susceptible to A/WSN/33 clinical signs and weight loss (see Figures 4.2A and 4.7A).

Singly A/WSN/33 infected mice showed no weight loss until day 6 post infection (Figure 4.13A) at which point this group had lost only a mean average of $6.64 \pm 3.3\%$ in weight. A single mouse in this group even remained at 99.98% of its original weight. There are also limited clinical signs of infection (Figure 4.13B). At day 6, half of the mice in this group began to show mild signs of reduced mobility (scored at an average of 0.5) and respiratory effort (also scored at 0.5), giving a clinical score of ‘mild’ overall.

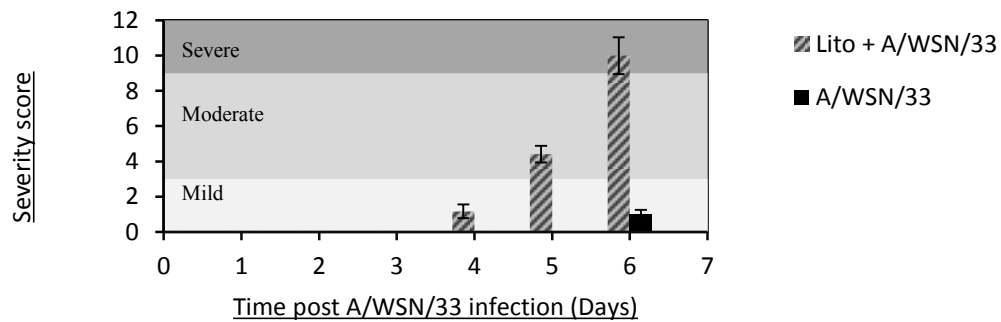
Co-infected mice at this time point however showed significantly increased weight loss ($p < 0.01$) when compared with singly infected controls (Figure 4.13A). Weight loss became statistically significant at 5 days post-infection, with an overall mean loss of $8.88 \pm 4.0\%$ at day 6 this increased to $16.00 \pm 2.52\%$ ($p < 0.001$, general linear model). These mice also displayed heavily exacerbated clinical signs beginning at day 4 with mildly increased respiratory effort (observed in some but not all) but rapidly increasing in severity. At day 5 the increased respiratory effort (mean score of 0.92) was coupled with a staring coat (1.25), and a hunched stature (1.33) as well as reduced mobility (0.92) which meant that most of the mice were now scored as having moderate signs. A ‘severe’ score was recorded by day 6, consistent with the extensive weight loss (Figure 4.13B). Respiratory effort was scored at 2.82 along with a hunched stature (2.82), a staring coat (2.86) and decreased mobility of 2.00. The overall severity score was therefore an average of 10 by the final time point and had increased rapidly over days 4 to 6.

Figure 4.13 Co-infection with patent (Adult \pm Mf) *Litomosoides sigmodontis* has a deleterious effect on A/WSN/33 pathogenesis

A. Weight loss



B. Clinical severity score



C. Influenza lung titre – Day 6

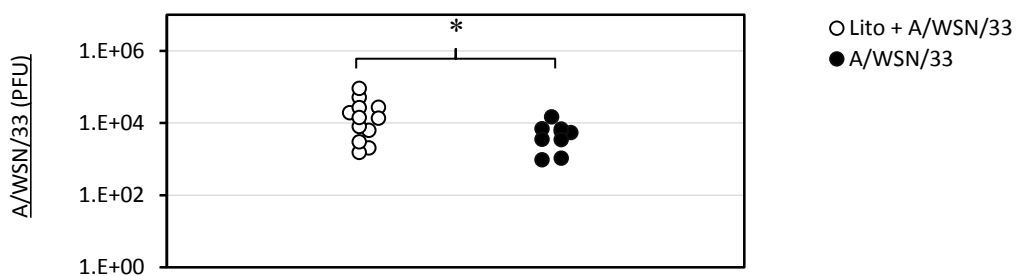


Figure 4.13 A. Mice were weighed every 24 hours post A/WSN/33 infection. Weight loss is calculated as percentage of weight at day 0 prior to infection. Mean weight loss is shown \pm 1 standard deviation, N=6, representative of 2 experiments. Significance determined by general linear model (*/+ = $p < 0.05$, **/+ = $p < 0.01$ ***/+++ = $p < 0.001$). * denotes significance of A/WSN/33 vs. uninfected. + denotes significance between co-infected and A/WSN/33 infected groups. **B.** Clinical severity was measured by 4 signs scored on a scale of 0-3 and the sum is reported \pm 1 standard deviation as clinical severity score, N=12, 2 experimental repeats. **C.** Left lung homogenate was measured by dilution series plaque assay on MDCK cells for levels of infectious virus. Individual values are plotted, N=12 from 2 experimental repeats. Significance is determined by 2 sample T-test on log normalised data, (* = $p < 0.05$).

Influenza titre in the lungs of co-infected animals was also significantly increased compared with A/WSN/33 infected mice, ($p=0.027$, 2-sample Student's T test on log normalised data) at this time point (Figure 4.13C). A/WSN/33 infected mice had a mean average of 5.3×10^3 PFU ml⁻¹ whilst the co-infected group had a mean average of 2.0×10^4 PFU ml⁻¹ in the lung homogenates.

– Pathology

The lungs were analysed for changes to pathology. This was of particular interest due to the increased resistance of the older mice to the influenza infection and the apparent deleterious effect of *L. sigmodontis* co-infection at this time point.

The histopathology associated with influenza infection had a similar severity to mice infected with A/WSN/33 at the earlier time point (see Figures 4.1 L-N), despite the increased resistance to infection in these older mice. Evidence of epithelial necrosis was apparent at a similar score of 1.5. This was the same score in the co-infected mice despite their exacerbated weight loss. Similarly, interstitial necrosis, scored at 1.33 and interstitial inflammation, scored at 1.50 in A/WSN/33 infected mice was like that in co-infected mice (1.45 and 1.75 respectively). Peri-bronchial and peri-vascular inflammation, were scored at an average of 1.50 and 1.58 in both A/WSN/33 infected mice and co-infected mice. The uninfected mice did not display any significant changes to lung integrity or signs of influenza-associated pathology. The *L. sigmodontis* group did show mild peri-vascular inflammation (0.42 mean average) and peri-bronchial inflammation (0.42 mean average) as was the case in the previous co-infection time point.

Pathology associated with the *L. sigmodontis* infection mirrored that of the pre-patent (adult) time point (Figure 4.14B). Evidence of chronic infection was now also identifiable, including fibrotic formations within the hypertrophic mesothelium extensions and some areas now exhibited extensive hyperplasia within the mesothelium and evidence of proliferation (see Figure 4.1L-M). Hypertrophy in the mesothelium in the singly *L. sigmodontis* infected mice was scored at 1.92. In the co-infected group this was slightly reduced to an average of 1.42, while uninfected and A/WSN/33 infected mice were scored at 1.00. The presence of lymphocytes in the sub-pleural space was increased in the *L. sigmodontis* infected groups (Mean score of 1.2 in both groups) compared with A/WSN/33 infected (0.2) and uninfected mice (0.0). The presence of exophytic-frond like structures, a pathology associated with chronic mechanical damage to the mesothelium, was also scored at this time point. *L. sigmodontis* infected mice were scored at 1.17 and co-infected mice were scored at 1.00. A/WSN/33 infected and uninfected mice did not show this pathology.

Figure 4.14 Effect of patent *Litomosoides sigmodontis* co-infection on pathology caused by A/WSN/33.

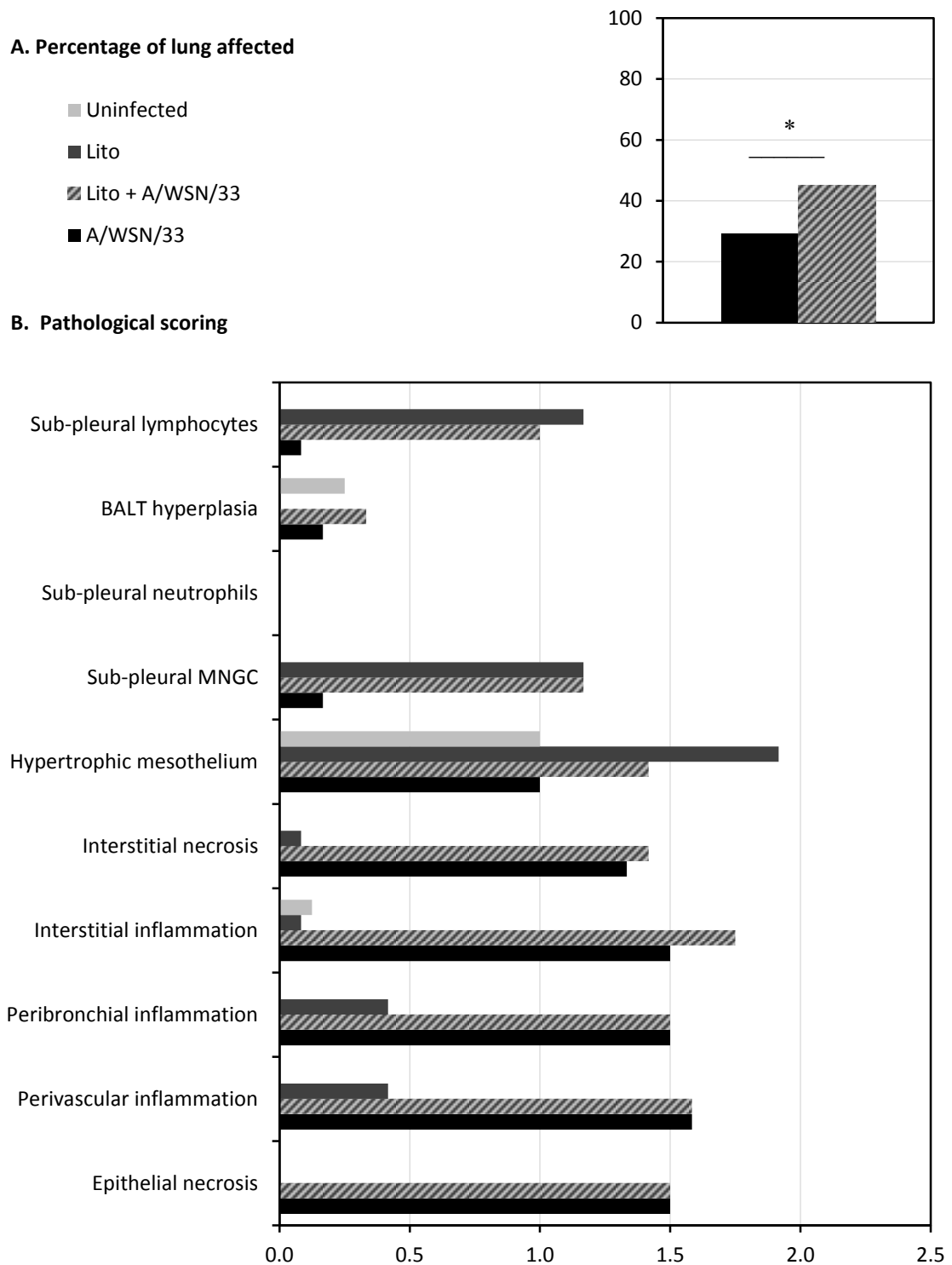


Figure 4.14 The left lobes of lungs from co-infected, singly infected and uninfected mice were harvested, fixed, cut into sections and stained by hematoxylin and eosin 6 days post infection with A/WSN/33. **A.** The extent of lung damage was assessed as 0%, 25%, 50%, 75% or 100% per lung. **B.** Pathology and infiltration of immune cells was scored on a scale from 0-3 for each lung. All results are presented as mean average for each group. N=6. Error bars are not displayed due to the ranked nature of the data. Statistics performed by mann whitney test. *=p<0.05.

One significant difference at this time point was the extent of damage in the co-infected lungs (Figure 4.14A). While severity of each pathology was similar, A/WSN/33 infected mice had much less damage (~25% less) than at the previous time points, perhaps due to the increased age of the mice. Co-infected mice had around 50% of the lung affected by influenza associated pathology as was the case at the previous time point. This difference was significant ($p=0.034$) when the ranked data was analysed by Mann-Whitney test.

- Lung cytokine environment

Lung pathology was more widespread in the co-infected mice. To determine if this was due to a change in the inflammatory environment in the lung, cytokine responses were investigated.

The inflammatory environment in the lung was measured by ELISA in two samples from each mouse at this time point. Cytokines were detected in homogenate from the left lobe of the lungs and in broncho-alveolar lavage fluid, collected prior to fixation of the right lobes of the lung.

IFN γ levels were significantly increased in lung homogenate in all groups infected with A/WSN/33 (Figure 4.15A) compared with *Litomosoides sigmodontis* infected mice and uninfected controls. IFN γ was significantly higher in the singly A/WSN/33 infected (2.63 fold) than in the co-infected mice (1.67 fold, $p<0.05$ general linear model).

IL-10 was also increased in these two groups compared with the uninfected mice. The A/WSN/33 infected mice had a 2.38 fold increase in IL-10 and co-infected mice had on average 1.96 fold more IL-10 than uninfected mice. There was no significant difference between the two groups however.

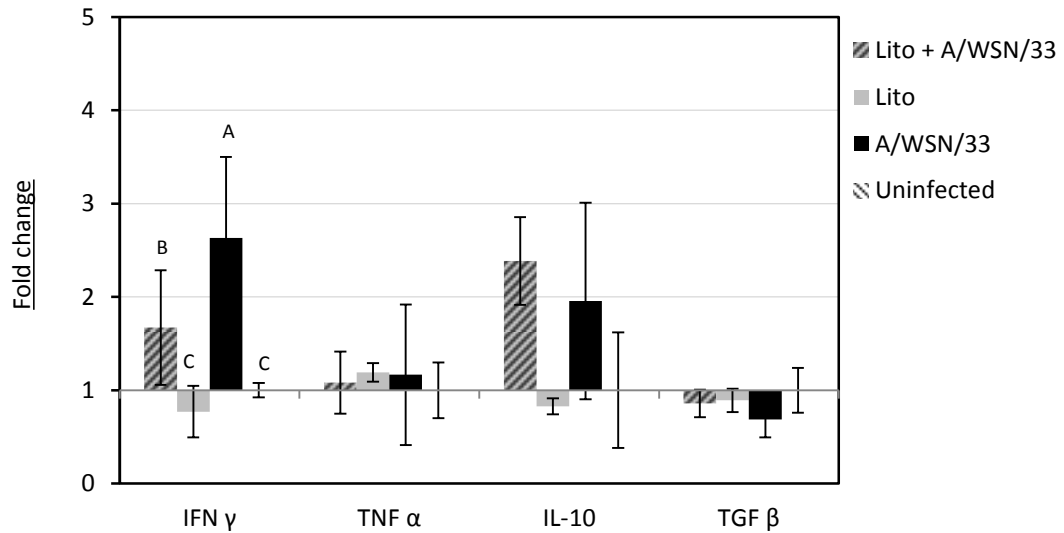
As with previous time points, TGF β and TNF α were both unaffected by either infection when measured in the lung homogenates (Figure 4.15A). Co-infected mice, *L. sigmodontis* infected mice and A/WSN/33 infected mice produced 1.08, 1.19 and 1.17 fold increase in TNF α respectively and 0.86, 0.89 and 0.69 fold difference in TGF β compared with uninfected mice.

In the lavage samples (Figure 4.15B), IFN γ was significantly increased by 12.55 fold due to A/WSN/33 infection. This is much lower than at the previous time point. The co-infected group also showed a 6.75 fold increase in IFN γ while *L.sigmodontis* infected mice did not produce an increased amount of IFN γ in comparison with uninfected mice. There was no significant difference between singly A/WSN/33 and co-infected mice.

IL-10 levels showed only a moderate increase in the A/WSN/33 infected groups which is much lower than observed at the earlier time point. IL-10 was recorded at a mean fold increase of 1.89 fold in the co-infected group and 1.27 fold in the A/WSN/33 singly infected mice.

Figure 4.15 Cytokine environment is not significantly altered in mice co-infected with patent (adult \pm mf) *Litomosoides sigmodontis* and A/WSN/33

A. Lung homogenate



B. Broncho-alveolar lavage fluid

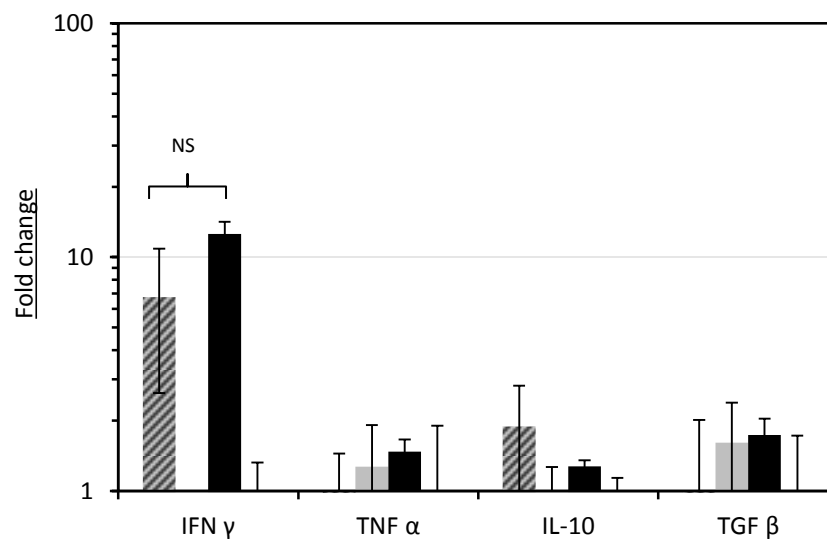


Figure 4.15 A. 6 days post A/WSN/33 infection, the left lung was homogenised in Dulbecco's minimum essential medium and the homogenate used for ELISA detection of cytokines. Representative of 2 independent experiments. N=12. **B.** Lungs were lavaged with 2ml HBSS + 3mM EDTA, cells were removed and the broncho-alveolar lavage fluid (BALF) used to detect cytokines in the interstitial environment. Single experiment, N=6. Each group is represented as mean average fold change \pm 1 standard deviation compared to the mean level of expression in the uninfected group. Statistics were performed by general linear model. Groups that do not share the same letter are significantly different at a 99% confidence level.

TGF β and TNF α levels were not increased in any experimental group. In some instances these cytokines were undetectable. TNF α was present at 0.67, 1.27 and 1.47 fold differences in the co-infected, *L.sigmodontis* infected and A/WSN/33 infected mice when compared with the uninfected group. TGF β was present at 0.93, 1.61 and 1.97 fold difference compared with the uninfected.

To determine if changes in the T cell populations in the lymph nodes were again contributing to an amended response to influenza, CD4 $^+$ and CD8 $^+$ cells were analysed by flow cytometry.

- CD8 $^+$ T cell responses in the lymph node

After 6 days A/WSN/33 infection, cells from the thoracic and lung draining lymph nodes were harvested and stained for CD8 and intracellular cytokines. Total CD8 $^+$ cell frequency was highest in both *L. sigmodontis* infected groups however this was not statistically significant. Overall the number of CD8 $^+$ T cells in the draining lymph node was very low (Figure 4.16A) with a mean of 2-4%. Lymphocytes from *L. sigmodontis* infected mice were 4.25 \pm 2.25% CD8 $^+$. Co-infected mice had 3.92 \pm 1.14%. The A/WSN/33 infected mice had 2.41 \pm 0.78% CD8 $^+$ lymphocytes and uninfected mice had 1.41 \pm 0.14% CD8 $^+$ lymphocytes in the draining lymph nodes.

CD8 $^+$ cells from *L. sigmodontis* infected mice were producing increased levels of IFN γ $^+$ cells (33.26 \pm 11.00%) compared with the previous time point (Figure 4.16B). This coincides with the release of microfilaria by adult worms. IFN γ production by CD8 $^+$ cells was not significantly different from the A/WSN/33 singly infected group (44.14 \pm 5.30%) or co-infected mice (37.56 \pm 6.16%). Uninfected mice did not produce high percentages of CD8 $^+$ IFN γ $^+$ cells (9.41 \pm 4.17%).

Therefore CD8 $^+$ T cells from all infected groups were producing increased IFN γ compared with uninfected controls. Levels of TNF α and IL-10 production in CD8 $^+$ T cells were very low and so these results are not shown and were not analysed further.

- CD8 $^+$ T cell responses in the lung

CD8 $^+$ T cells in the lavage were at very low numbers in the uninfected group and are therefore absent from the analysis (Figure 4.17A). The numbers of CD8 $^+$ cells in the lung were increased due to A/WSN/33 infection and significantly elevated further in the co-infected mice ($p=0.0077$ Mann-Whitney).

Figure 4.16 CD8⁺ T cells in the lymph node are producing IFN γ in all infected groups and therefore co-infection has no significant impact.

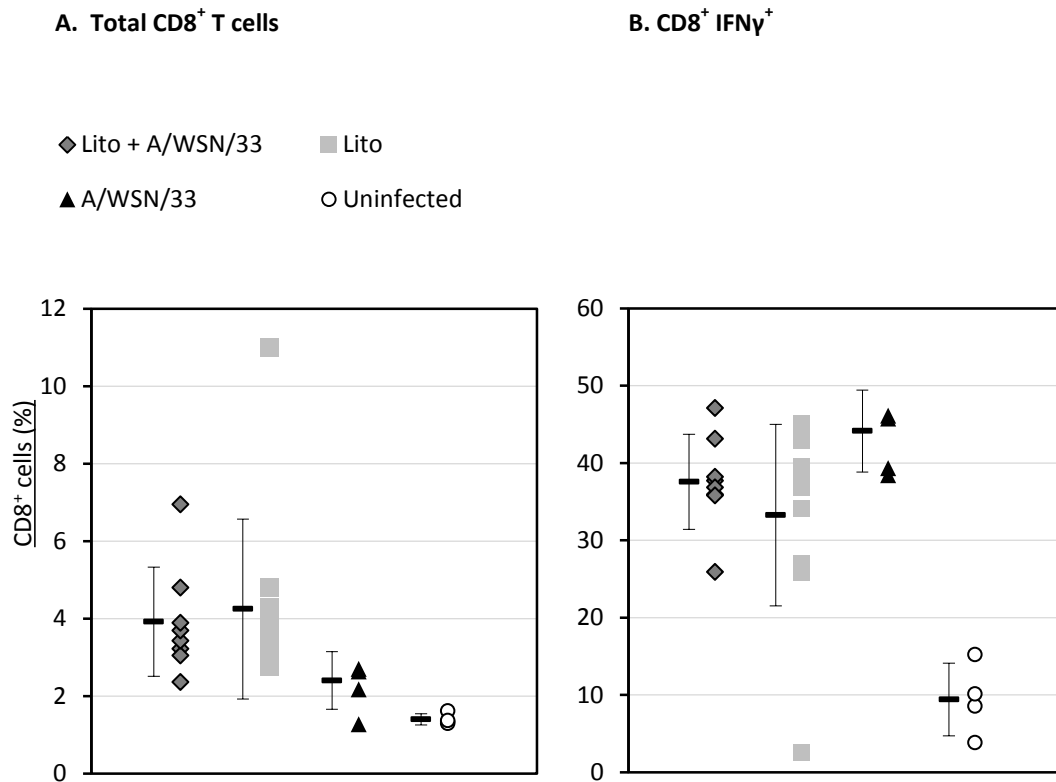


Figure 4.16 5-6 week old female BALB/c mice were infected with 25 x *L3 Litomosoides sigmodontis* larvae S.C. and 34 days later with 5×10^3 A/WSN/33 I.N. These were compared with singly infected and uninfected controls. Mice were culled 6 days post A/WSN/33 infection and draining lymph nodes of the thoracic cavity and lung were harvested. 1×10^7 cells from the lymph nodes were stained for a range of intracellular CD8⁺ T cell markers. The samples were run on a BD LSR II Fortessa. Results displayed as individual percentages per sample and mean per group \pm 1 standard deviation. N=4-9. All statistics are calculated on data from 2 independent experiments, (*= $p < 0.05$, **= $p < 0.01$, ***= $p < 0.001$ general linear model). **A.** CD8⁺ lymphocytes **B.** CD8⁺ IFN γ ⁺ cells.

Figure 4.17 Patent (adult \pm mf) *Litomosoides sigmodontis* co-infection leads to an increased inflammatory CD8⁺ T cell population in the lung following A/WSN/33 infection

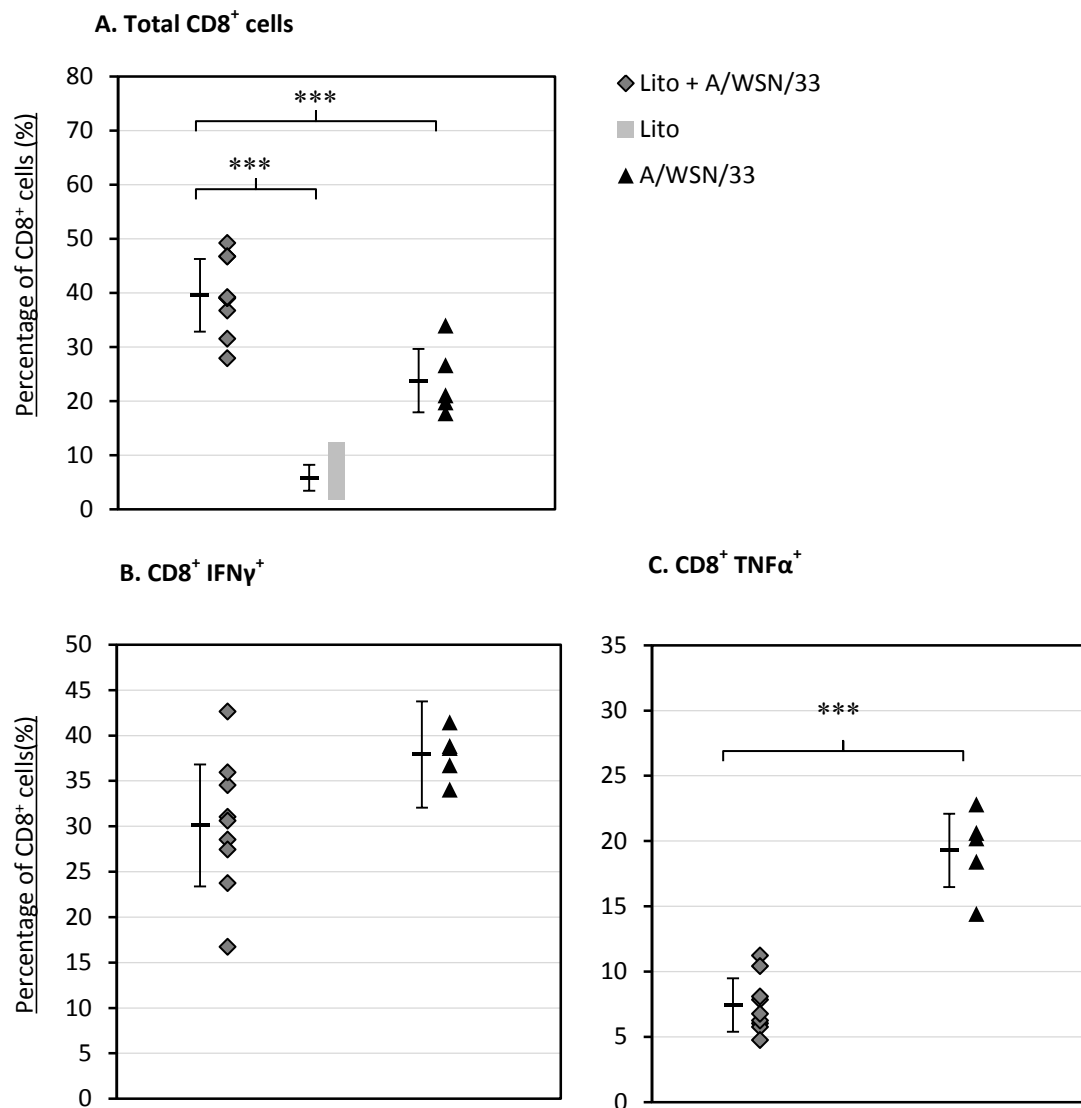


Figure 4.17 5-6 week old female BALB/c mice were infected with 25 x *L3 Litomosoides sigmodontis* larvae S.C. and 68 days later with 5×10^3 A/WSN/33 I.N. These were compared with singly infected and uninfected controls. Mice were culled 6 days post A/WSN/33 infection and cells in the lung were harvested by broncho-alveolar lavage (BAL). Maximum numbers of cells in the BAL fluid were stained for a range of intracellular CD8⁺ T cell markers. The samples were run on a BD LSR II Fortessa. Results displayed as individual percentage (scatter plot) and mean per group \pm 1 standard deviation (whisker plot). N=6 except for co-infected mice where N=9. Uninfected mice did not have sufficient numbers of cells to be included. All statistics are calculated on data from a single experiment, (***)= $p < 0.001$ Mann-Whitney test). **A.** Total CD8⁺ T cells. **B.** CD8⁺ IFN γ ⁺ cells **C.** CD8⁺ TNF α ⁺ cells

CD8⁺ IFN γ ⁺ cells in *L. sigmodontis* infected mice were largely undetectable. A/WSN/33 infected mice had 30.1 \pm 6.99% CD8⁺ cells producing IFN γ and co-infected mice were higher on average at 37.9 \pm 2.45% (Figure 4.17B). Unlike the previous time point TNF α production by CD8⁺ cells was elevated in A/WSN/33 to 19.28 \pm 2.81% (Figure 4.17C). This was significantly higher than in co-infected mice which had a similar level to the previous time point of 7.43 \pm 4.30% (p=0.0075). Once again uninfected mice and *L. sigmodontis* infected mice had low (close to undetectable) levels of CD8⁺ IL-10⁺ cells in the BAL fluid.

– CD4⁺ T cell responses in the lymph nodes

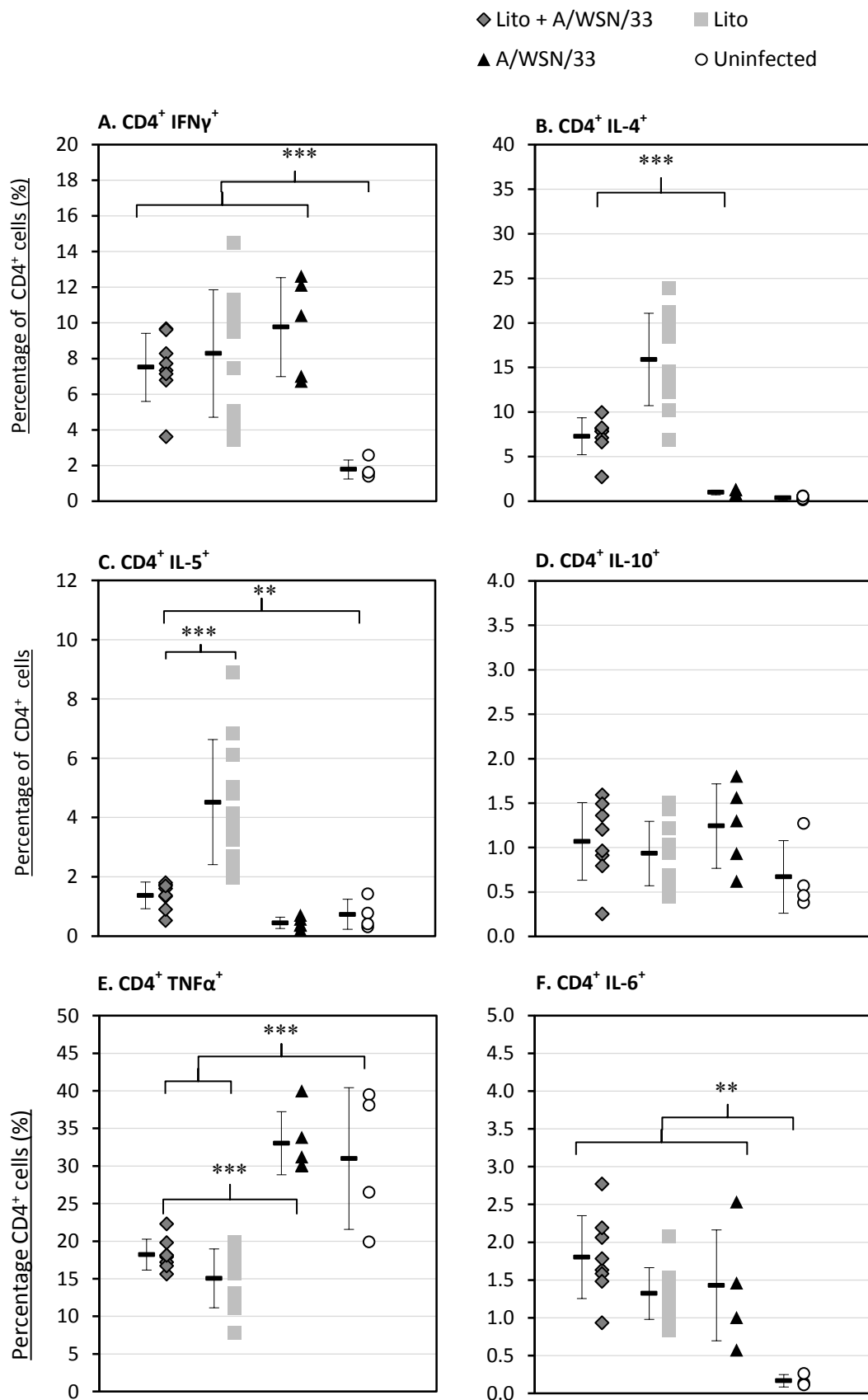
After 6 days A/WSN/33 infection cells from the thoracic and lung draining lymph nodes were harvested and stained for CD4 and intracellular cytokines. At this time point, *L. sigmodontis* infected mice showed an increase in IFN γ production by CD4⁺ T cells (Figure. 4.18A). Therefore all infected groups had a significant (p<0.001, general linear model) increase in comparison to uninfected controls. IFN γ production by CD4⁺ cells was on average 7.51 \pm 1.91% in the co-infected group, 8.28 \pm 3.57% in the *L. sigmodontis* infected group and 9.76 \pm 2.16% in the A/WSN/33 infected mice. The uninfected group were 1.78 \pm 1.04% IFN γ positive.

TNF α showed a significant decrease in production in both *L. sigmodontis* infected groups (Figure 4.18E). CD8⁺ cells in the co-infected mice were 18.21 \pm 2.05% TNF α positive and in the *L. sigmodontis* group, 15.06 \pm 3.01% of CD8⁺ cells were producing TNF α . This was in comparison to 33.0 \pm 24.19% in the A/WSN/33 infected mice and 31.0 \pm 9.01% in the uninfected mice, when non-specifically stimulated with PMA and ionomycin. There was therefore only a very weak inverse correlation between the inflammatory cytokines IFN γ and TNF α , (-0.462) at this time point.

The IL-4 distribution was not normally distributed. Mann-Whitney analysis demonstrated a significant increase in IL-4 as a result of *L. sigmodontis* infection. 15.89 \pm 5.18% CD8⁺ cells from *L. sigmodontis* mice were producing IL-4 and 7.28 \pm 2.09% of CD8⁺ cells from co-infected mice were IL-4 positive (Figure 4.18B). The combined p value for the co-infected group compared with singly *L. sigmodontis* infected mice was 0.0713. This shows a very strong trend (but not significance) for a smaller increase in IL-4 in co-infected mice than in the *L. sigmodontis* only group.

IL-5 was significantly (p<0.001) raised in *L. sigmodontis* infected mice (4.52 \pm 2.11%) compared with all other experimental groups (1.37 \pm 0.45% in co-infected, 0.45 \pm 0.19% in A/WSN/33 infected and 0.73 \pm 0.15% in the uninfected group). While levels were far lower in co-infected mice, IL-5 was increased significantly in these mice compared with uninfected and

Figure 4.18 Patent (Adult \pm Mf) *Litomosoides sigmodontis* co-infection alters the CD4⁺ T cell profile in the lung draining lymph nodes following A/WSN/33 infection.



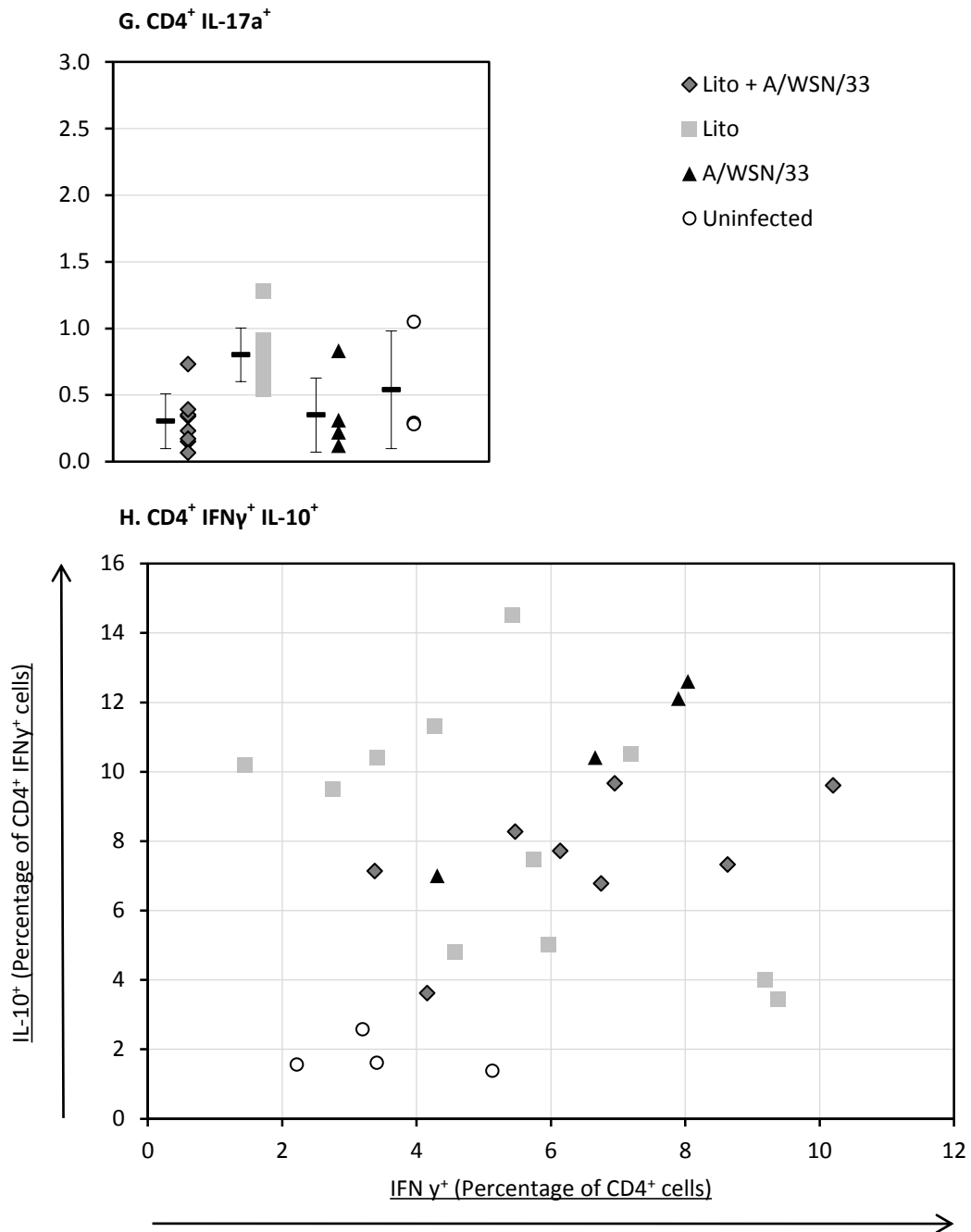


Figure 4.18 5-6 week old female BALB/c mice were infected with 25 x *L3 Litomosoides sigmodontis* larvae S.C. and 68 days later with 5×10^3 A/WSN/33 I.N. Mice were culled 6 days post A/WSN/33 infection and draining lymph nodes of the thoracic cavity and lung were harvested. 1×10^7 cells from the lymph nodes were stained for a range of intracellular CD4⁺ T cell markers. These were compared to singly infected and uninfected mice. The samples were run on a BD LSR II Fortessa. Results are displayed as percentage of positive cells per sample (scatter plot) as well as mean per group \pm 1 standard deviation (whisker plot). N=12 for *L. sigmodontis* infected groups, N=6 for A/WSN/33 singly infected and N=4 for uninfected mice. All statistics are calculated on data from 2 independent experiments, (*= $p < 0.05$, **= $p < 0.01$, ***= $p < 0.001$ general linear model). **A.** CD4⁺ IFN γ ⁺ cells **B.** CD4⁺ IL-4⁺ cells **C.** CD4⁺ IL-5⁺ cells **D.** CD4⁺ IL-10⁺ cells **E.** CD4⁺ TNF α ⁺ cells **F.** CD4⁺ IL-6⁺ cells **G.** CD4⁺ IL-17a⁺ cells **H.** CD4⁺ IFN γ ⁺ cells co-expressing IL-10.

A/WSN/33 singly infected mice (Figure 4.18C). The T_H2 cytokines, IL-4 and IL-5 strongly correlate in their production, (Pearson's co-efficient 0.927).

IL-10 was produced at low levels in CD4⁺ cells and infection produced no significant modulation (figure 4.18D). IL-6 production by CD4⁺ T cells (Figure 4.18F) was significantly lower ($p < 0.01$) in the uninfected group ($0.17 \pm 0.08\%$) however there were no differences between the infection groups (1.32 ± 0.04 in the co-infected, $1.43 \pm 0.70\%$ in the *L. sigmodontis* infected and $1.80 \pm 0.55\%$ in the A/WSN/33 infected mice). IL-17a was moderately raised in singly *L. sigmodontis* infected mice (at $p < 0.05$ significance level) to 0.80% on average compared with an average of 0.30% in the co-infected group and 0.35% in the A/WSN/33 infected however due to variation in the uninfected group the most significant difference was between *L. sigmodontis* and co-infected mice, ($p < 0.01$ Figure 4.18G).

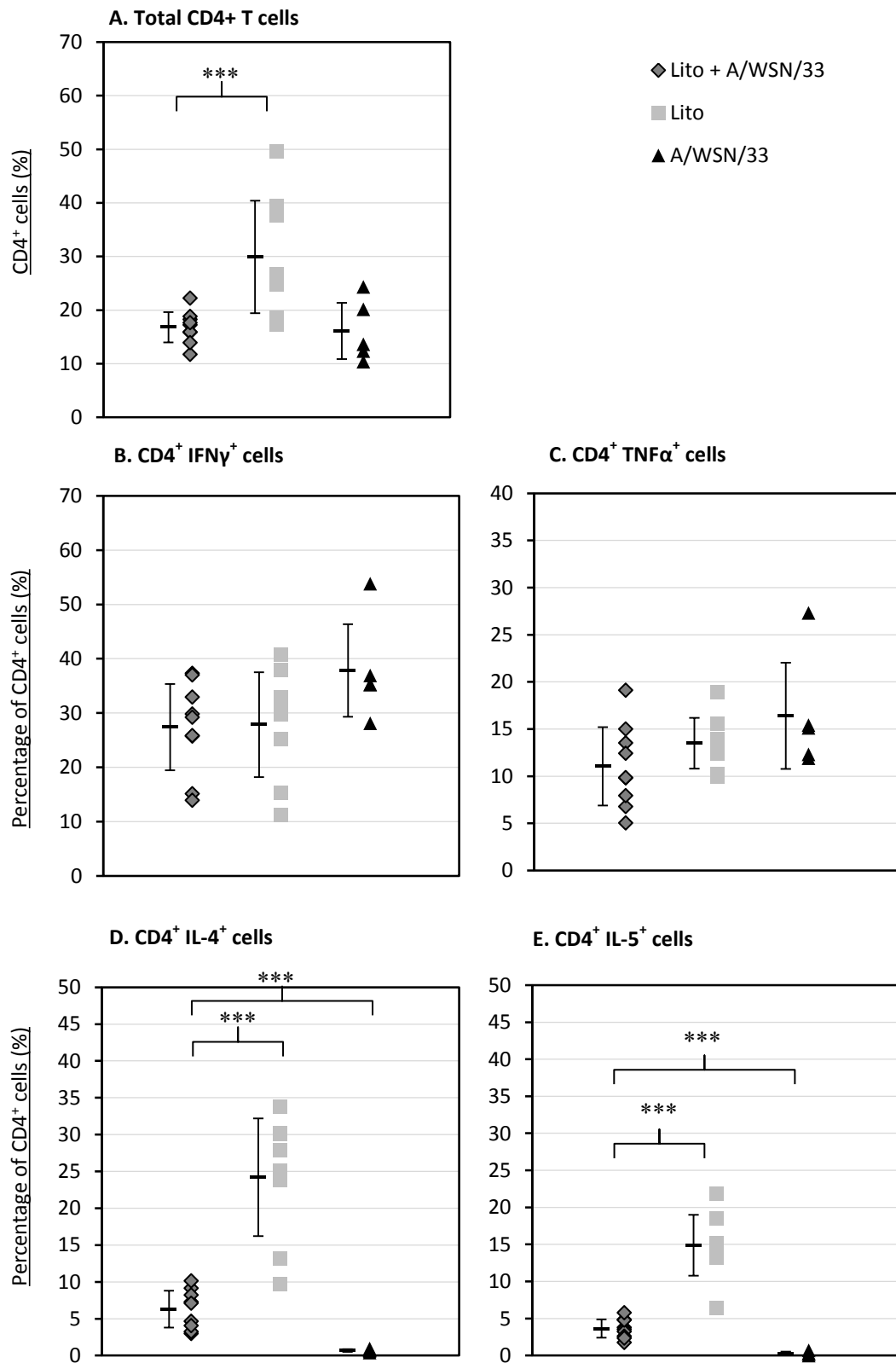
The population of CD4⁺ IFN γ ⁺ IL-10⁺ cells identified at the previous time point was less clearly defined at this time point. Expression of IFN γ in *L. sigmodontis* infected mice has increased on average but varies within the group (Figure 4.18H). Co-expression of IL-10 in these cells is much higher than at the previous time point which may contribute to the variation. Co-expression of IL-10 and IFN γ in the co-infected mice and A/WSN/33 infected group are less easily distinguishable, as both groups appear to be producing IL-10 and IFN γ in equal measures in this cell population.

– CD4⁺ T cell responses in the lung

74 days post *L. sigmodontis* infection the proportion of CD4⁺ cells in the lung is increased in the *L. sigmodontis* infected group compared to the A/WSN/33 infected and co-infected groups ($p = 0.00054$). *L. sigmodontis* infected mice had $29.9 \pm 10.4\%$ CD4 positive cells whilst cells from co-infected mice were $16.8 \pm 2.3\%$ positive for CD4 and $16.12 \pm 5.12\%$ positive in the A/WSN/33 infected mice (figure 4.19A). Uninfected mice had very low numbers of CD4⁺ lymphocytes in the lung and are therefore excluded from the analysis.

The levels of IFN γ and TNF α production by lung CD4⁺ cells were increased in all infected groups. Co-infected mice were $27.41 \pm 7.11\%$ and $11.04 \pm 4.15\%$ positive for IFN γ and TNF α respectively, A/WSN/33 infected mice were $37.848.53\%$ and $16.45.63\%$ positive and *L. sigmodontis* infected mice were $27.86 \pm 9.65\%$ and $13.49 \pm 2.69\%$ positive on average for these two inflammatory cytokines (figure 4.19B and 4.19C). There were too few CD4⁺ cells in the lungs of uninfected mice to record accurately. The increase in expression of inflammatory cytokines in the infected groups was therefore not compared with the uninfected mice or

Figure 4.19 Patent (Adult \pm Mf) infection with *Litomosoides sigmodontis* results in a mixed T_H1/T_H2 phenotype in the lung but does not alter cytokine production by $CD4^+$ during A/WSN/33 co-infection



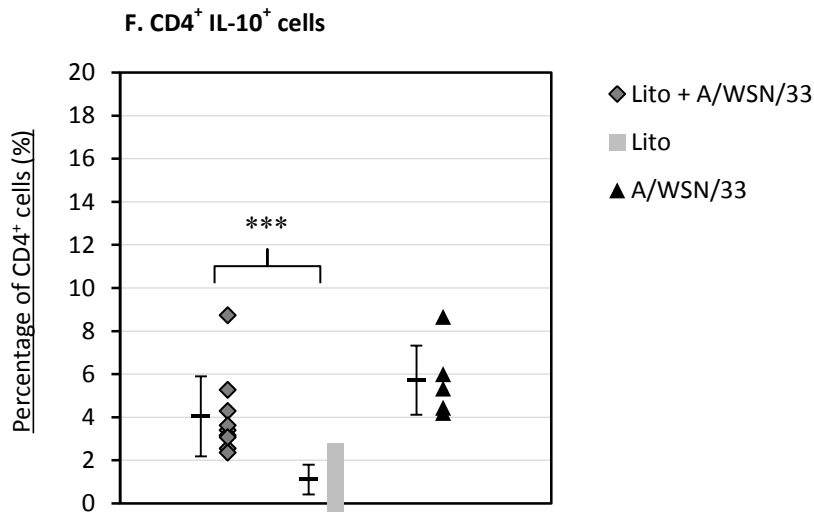


Figure 4.19 Mice were culled 6 days post A/WSN/33 infection and cells in the lung were harvested by bronchoalveolar lavage (BAL). Maximum numbers of cells in the BAL fluid were stained for a range of intracellular CD4⁺ T cell markers. The samples were run on a BD LSR II Fortessa. Results displayed as individual percentage (scatter plots) and mean per group \pm 1 standard deviation (whisker plots). N=9, A/WSN/33 N=5 and uninfected were at insufficient numbers and are not reported. All statistics are calculated on data from a single experiment, (*=p<0.05, **=p<0.01, ***=p<0.001 Kruskal Wallis and Mann-Whitney tests). **A.** Total CD4⁺ T cells. **B.** CD4⁺ IFN γ ⁺ cells **C.** CD4⁺ TNF α ⁺ cells **D.** CD4⁺ IL-4⁺ cells **E.** CD4⁺ IL-5⁺ cells **F.** CD4⁺ IL-10⁺ cells.

analysed statistically. There was no difference in inflammatory cytokine production between infected groups.

T_H2 cytokines, IL-4 and IL-5 were significantly raised in *L. sigmodontis* infected mice (to 24.20±7.98% and 14.89±4.11%, Mann-Whitney p=0.0009 and p=0.0006 respectively when compared with the co-infected mice). Co-infected mice have small increases in IL-4 and IL-5 to 6.29±2.45% and 3.65±1.21% when compared with the influenza infected mice (Figure 4.19D and 4.19E).

These two cytokines were once again very highly correlated in their production, IL-10 was significantly raised in the A/WSN/33 infected mice (p=0.0009) to 5.72±1.59% and in the co-infected mice to 4.04±1.85% when compared with the uninfected mice but there was no difference between co-infected and singly A/WSN/33infected groups (Figure 4.19F).

– *Litomosoides sigmodontis* worm burden

Once the mice had been autopsied, both adult worms and microfilaria (L1 larvae) were enumerated. There was no significant differences between the number of adult males or females in either group infected with *L. sigmodontis*. There was also no significant difference in the number of mice to reach patent infection or the incidence of microfilaria in the blood. Co-infection with influenza did not lead to an increase or decrease in the number of microfilaria in the blood or granuloma formation in the pleural cavity. Table 4.3 below shows the number of adult and L1 worms recovered.

Table 4.3 *Litomosoides sigmodontis* adult and microfilaria worm burden

Mouse	Day	<i>L.sigmodontis</i>	A/WSN/33	Worm Recovery					
				Male	Female	Granuloma count	Mf 68	Mf 74	Total
3437	74	+	+	1	0	1	19		1
3438	74	+	+	3	2		X		5
3439	74	+	+	1	1	2	2		2
3440	74	+	+	2	2		57		4
3441	74	+	+	2	1		6		3
3442	74	+	+	0	2	1	0		2
3444	74	+	+	1	2	*	22		3
3445	74	+	+	1	0	2	5		1
3446	74	+	+	1	4		2		5
3447	74	+	+	4	3		134		7
4593	74	+	+	1	1	1	0	2	2
4597	74	+	+	2	0	0	17	0	2
4598	74	+	+	0	2	2	15	12	2
4599	74	+	+	4	3	0	2	217	7
4600	74	+	+	1	3	0	3	0	4
4601	74	+	+	2	1	1	14	150	3
3448	74	+	-	2	3	1	101		5
3449	74	+	-	0	1	2	0		1
3450	74	+	-	2	0	1	116		2
3451	74	+	-	2	1		553		3
3452	74	+	-	2	2		501		4
3453	74	+	-	3	2		323		5
3454	74	+	-	3	4	1	23		7
3456	74	+	-	8	6		2		14
3457	74	+	-	3	2		51		5
3458	74	+	-	1	2		13		3
3459	74	+	-	2	6		0		8
4602	74	+	-	5	1	1	5	4	6
4603	74	+	-	2	1	1	2	0	3
4604	74	+	-	1	1	1	0	0	2
4605	74	+	-	4	2	0	355	269	6
4606	74	+	-	3	0	1	31	25	3
4607	74	+	-	3	5	1	5	2	8

* = partial worm in granuloma x = undetermined / clotted sample

Mf 68 = number of L1 larvae (microfilaria / mf) measured on day 68 post infection.

Mf 74 = number of L1 larvae (microfilaria / mf) measured on day 74 post infection.

4.5 Discussion

4.5.1 Co-infection with immature (L4) *Litomosoides sigmodontis* had no significant impact on A/WSN/33 pathogenesis

The early stage of *Litomosoides sigmodontis* infection in BALB/c mice does not skew host immunity towards a strong T_H2 or T_{REG} phenotype. Mouse strains resistant to infection display an expansion and infiltration of leukocytes in the pleural cavity and excessive production of both type 1 and 2 cytokines; subsequently leading to the destruction of adult worms within 10-30 days post infection (Babayan, Ungeheuer et al. 2003). This response is not evident in susceptible strains. Infection with L4 stage *L. sigmodontis* of susceptible BALB/c strain produces a subtle T_H2 influence on host immunity which subsequently does not alter A/WSN/33 infection. At a dose of 5×10^3 A/WSN/33 (delivered intranasally), mice develop clinical signs of reduced mobility and increased respiratory effort within 4 days of infection. While a reduction in onset of such signs can be observed in the co-infected group, the anorexia associated weight loss consistent with influenza infection is not altered significantly by pre-existing L4 *L. sigmodontis* nematode infection, suggesting unaltered viral pathogenesis. Upon repeat of this experiment, the slight modification was less defined and again not significant. This result is mirrored in the levels of viral replication. Virus titres recovered from lung homogenates 6 days post infection were almost identical in co-infected and A/WSN/33 singly infected mice, confirming that viral replication was not impacted by pre-existing infection. While disease progression is influenced by successful viral replication, a number of studies have concluded that outcome of influenza infection is not exclusively tied to levels of replicating virus (Taubenberger and Morens 2008). Instead, severe clinical signs and fatality in influenza infection in humans and mice are correlated to the excessive production of cytokines and chemokines, termed 'cytokine storm'. A phenomenon most commonly observed in the highly pathogenic sub-strains of the virus (Clark 2007). As the A/WSN/33 singly infected mice were recorded at high severity 6 days post infection the cytokine environment in the lung was monitored. Inflammatory cytokines $IFN\gamma$ and $TNF\alpha$ were not increased to significant levels compared with uninfected mice. These results were measured by ELISA on lung homogenates and therefore a significant increase in such cytokines is required for detection, an issue that is addressed at later time points. $IFN\gamma$ production by $CD8^+$ and $CD4^+$ cells was raised significantly in response to A/WSN/33 infection however the increase was at similar levels in lymphocytes from the lung draining lymph nodes in both singly and co-infected mice suggesting activation of inflammatory T cells by the viral infection was also not altered. The ability to produce normal polarisation of naïve $CD4^+$ T cells to a T_H1 phenotype is therefore intact in mice with pre-

existing nematode infection. TNF α production in CD4⁺ and CD8⁺ cell populations was not increased by infection either. The regulatory cytokine IL-10 increased in incidence in the lung homogenates from co-infected mice. The immunosuppressive qualities of this cytokine, commonly produced by infiltrating CD8⁺ T cells are known to limit pathology during viral infection and supplement recovery processes (Sun, Madan et al. 2009). Total CD8⁺ cells and likewise CD4⁺ lymphocytes, however, did not show any increase in the co-infected group in comparison to singly infected mice and therefore support the theory that *L. sigmodontis* infection at this early time point is not able to skew a subsequent immune response. Furthermore CD4⁺ T cells from the draining lymph nodes of *L. sigmodontis* infected mice did not display increased polarising IL-4 and IL-5 production associated with skewing towards a T_H2 phenotype. This response is observed upon chronic infection with *L. sigmodontis*, with a significant increase in strong T_H2 responses reported previously in BALB/c mice at around day 58 post infection (Marechal, Le Goff et al. 1997). Therefore to determine the extent of inflammatory damage between groups and potential influence of the increased IL-10, lungs were fixed, sectioned and stained by hemoxylin and eosin. Pathology was scored on a scale of 0-3 for a number of signs of influenza infection (Taubenberger and Morens 2008). Interstitial and epithelial necrosis and measures of immune cell infiltration around airways and blood vessels, common signs of influenza infection were not noticeably different between A/WSN/33 and co-infected mice. The extent of the lung damage was consistent with previous experiments at the same infective dose and as viral replication was similar between groups and levels of CD8⁺ and CD4⁺ T cells in the lymph nodes were not significantly increased, these results demonstrate that pre-existing co-infection with immature L4 *Litomosoides sigmodontis* larvae is not sufficient to modulate the immune response to acute influenza infection. This is reinforced by a lack of significant change to the lung pathology caused by the *L. sigmodontis* infection alone.

4.5.2 Co-infection with pre-patent (adult) *Litomosoides sigmodontis* delays the pathogenesis of A/WSN/33 infection

At this pre-patent stage of *Litomosoides sigmodontis* infection, co-infection with A/WSN/33 results in an attenuated phenotype. Weight loss in A/WSN/33 singly infected mice is the same as in the younger mice from the previous time point; reaching a maximum weight loss of around 15% 6 days post infection. Weight loss is coupled with the onset of clinical signs as before, however, by day 6 all A/WSN/33 infected mice do not exceed the moderate severity scoring for combined respiratory effort, reduced mobility, staring coat and hunching stature. The mice at this time point are 10-11 weeks old before infection, which likely explains the slower progression in disease severity. Age is a significant factor contributing to the immune response

to influenza in mice models (Bender, Taylor et al. 1995; Bender, Cottey et al. 1996). Significant differences between A/WSN/33 singly infected mice and co-infected mice occur at the initial stages of clinical presentation. At the onset of influenza clinical signs, (day 3 and 4) 4 out of 6 co-infected mice show only mild signs of infection whilst all A/WSN/33 infected mice already have moderate signs of infection. This correlates with weight loss, which in the A/WSN/33 infected group is significantly increased compared with uninfected and *L. sigmodontis* infected controls from 3 days post infection whilst co-infected mice do not show a statistically significant decrease in weight until 5 days post infection. There is also much greater variation within the co-infected group than others at this time point. Weight loss in co-infected mice is less severe between days 3 and 5, however, as with clinical signs, co-infected mice reach similar weight loss by day 6 suggesting that *L. sigmodontis* affords a delay or initial reduction in response rather than significant protection from viral infection.

The total CD8⁺ T cell response in the draining lymph nodes during A/WSN/33 is not altered by pre-existing *L. sigmodontis* infection however the production of the inflammatory cytokine IFN γ is mediated by the presence of co-infection. IFN γ production by CD8⁺ T cells is, as expected, significantly raised in A/WSN/33 infected mice, however, this is to a lesser extent in those with prior *L. sigmodontis* infection. *L. sigmodontis* infection alone did not produce CD8⁺ T cells capable of IFN γ production. IFN γ production by CD8⁺ T cells is required to recruit other immune cells to the site of infection and mediate the inflammatory environment in the lung (Wiley, Cerwenka et al. 2001). It was therefore of interest to investigate if this cell population was also at decreased concentration in the alveolar spaces of the lung. Interestingly the percentage of total CD8⁺ cells was highly increased in the lungs of co-infected mice in comparison to all other experimental groups. A similar percentage of such CD8⁺ cells are capable of IFN γ production when compared to levels produced by singly A/WSN/33 infected mice.

Pre-existing infection with *Trichinella spiralis*, a parasitic roundworm, is capable of modulating immune responses to influenza by reducing infiltrating numbers of CD8⁺ and CD4⁺ as well as neutrophils (Furze, Hussell et al. 2006). Similarly in *Plasmodium yoelii* / *Litomosoides sigmodontis* co-infection studies, production of IFN γ and TNF α by T_H1 cells is suppressed reducing the inflammatory environment and pathological lesions. (Karadjian, Berrebi et al. 2014). It was therefore expected that *L. sigmodontis* infection would provide protection from influenza pathogenesis by similar interactions or induction of hypo responsiveness in T cells, as is also seen in inhibition of allergic sensitization (Dittrich, Erbacher et al. 2008). An increase in CD8⁺ T cells was therefore unexpected. It is therefore important to consider that CD8a may also be expressed on a number of other cell types, which might explain the increase in percentage of CD8⁺ cells but lack of increase in the percentage of cells producing IFN γ and subsequent

alterations to pathology. The increase is solely seen in the lung lavage and not in the draining lymph nodes. This population in part, may be composed of CD8⁺ dendritic cells. Mouse CD8⁺ DCs have been previously described as non-migratory resident cells which are continuously seeded exclusively to lymph nodes from a bone marrow monocyte precursor (Belz, Smith et al. 2004). Conversely a recently described population of CD8⁺ CD103⁺ dendritic cells in the lung have been shown to increase in response to influenza or parainfluenza infection, although these cells display differential kinetics to CD8- DCs; they migrate less efficiently to lymph nodes and are weaker in regards to T cell activation (Beauchamp, Yammani et al. 2012). However it is not clear if these cells increase upon co-infection and until a repeat experiment is performed with either CD103⁺ or CD3⁺ cell markers the contribution of non T cell CD8⁺ cells to the increased population observed in co-infected mice is purely speculative.

The phenotype of CD4⁺ T cell subsets is also different between groups. A/WSN/33 infection leads to canonical activation of T_H1 cells in the draining lymph node by MHC-II presentation of antigen by antigen presenting cells (Fonteneau, Gilliet et al. 2003). As a result T_H1 cells produce IFN γ leading to an inflammatory immune environment. Alternatively *L. sigmodontis* infection results in production of T_H2 cells governed by production of IL-4 and IL-5 (Allen and Maizels 2011). In the lymph nodes of adult *L. sigmodontis* infected mice there is a robust T_H2 response with significantly increased levels of IL-4 and IL-5 and very low levels of inflammatory cytokines IFN γ and TNF α . A/WSN/33 infected mice however show large increases in production of IFN γ and minimal levels of IL-4 and IL-5. Co-infected mice produce both T_H1 and T_H2 cells, however, all cytokines are produced at intermediary levels compared with the singly infected mice. IL-4 and IL-5 levels are increased significantly less than in solely *L. sigmodontis* infected mice and IFN γ and TNF α levels are similarly moderated compared with singly A/WSN/33 infected mice. However in the case of TNF α , levels of production in the co-infected mice are much more aligned with the *L. sigmodontis* infected mice. These results show that while site of infection for the two pathogens is not the same the resulting production of an adaptive immune response during the co-infection is altered at the site of the draining lymphatics. IL-10, a regulatory cytokine associated with suppression of adaptive immune responses did not appear to be up regulated in any of the infected mice, however within the IFN γ generating CD4⁺ T cells identified in the co-infected mice, IL-10 was co-expressed to a greater level than seen in A/WSN/33. CD4⁺ IFN γ ⁺ IL-10⁺ Tr1 cells with suppressive function have been identified before in chronic infections (Chen and Liu 2009). Alternatively, these cells may represent a population of T_H1 cells that intrinsically negatively regulate IFN γ by production of IL-10 to mediate excessive inflammation in response to other suppressive stimuli, a response usually seen toward the end of the T_H1 cell life cycle. (Cope, Le Friec et al. 2011) While this cell population is only a very small population of the total CD4⁺ cells it may be an indication of

how co-infection with a filarial nematode, can mediate subsequent heterologous responses in the draining lymph node.

The lung environment, however, does not follow the same pattern. Production of IL-4 and IL-5 cytokines is slightly increased in *L. sigmodontis* infected mice as expected although at very low levels. These T_H2 cytokines are not found in the co-infected group. Instead the CD4⁺ cells from the lung lavage show an identical T_H1 phenotype to the CD4⁺ T cells in the singly infected A/WSN/33. Both groups produce similarly increased levels of IFN γ exclusively. The migration of inflammatory CD4⁺ T cells from the lymph node to the site of A/WSN/33 infection in the lung is therefore specific for T_H1 cells despite the mixed T_H1/T_H2 phenotype observed in the lymph nodes of co-infected mice. Alternatively, all cells may migrate into the lung however only upon recognition of influenza antigen in the lung do primed CD4⁺ T cells proliferate and therefore produce IFN γ , as shown previously with the use of an OVA-transgenic influenza virus (Chapman, Castrucci et al. 2005). This would suggest that even if the influenza specific CD4⁺ T cell phenotype is altered in the lymph nodes of co-infected mice, sufficient influenza specific T_H1 CD4⁺ T cells migrate and proliferate in the lungs of co-infected mice by day 6 as in A/WSN/33 singly infected mice. Previous studies have also demonstrated that antigen bearing dendritic cells migrating from the lung have imprinting capacity on the T cells they activate in the lymph node and therefore during influenza infection lung DC-primed CD4⁺ T cells have greater capacity to return to the lung (Mikhak, Strassner et al. 2013). Correspondingly, CD4⁺ T cells migrate predominantly to the pleural cavity during *L. sigmodontis* infection (Taylor, Harris et al. 2007). At day 6 post infection the kinetics of these responding CD4⁺ cells in the lung are identical between co-infected and A/WSN/33 infected mice. This is supported in the pathological scoring of the lung. Interstitial, peribronchial and perivascular inflammation is equivalent in the two groups, as is the extent of lung damage, proposing similar cellular infiltrates and proliferation in both groups. A subtle difference in overall IFN γ production is observed by ELISA of lung homogenates. Whilst not significant when measured at a 95% confidence level, IFN γ is increased to a greater degree in singly A/WSN/33 infected mice compared with co-infected mice which could not be statistically distinguished from the uninfected and solely *L. sigmodontis* infected mice in regards to IFN γ levels. TNF α , IL-10 and TGF β levels were unaltered. Despite spiked sample testing prior to use with lung homogenates, the ELISAs appear to require large increases for detection of differences between groups. To look specifically at the epithelial alveolar environment, broncho-alveolar lavage fluid was collected and examined for the same cytokine levels. In these results IFN γ and IL-10 were both significantly increased in A/WSN/33 infected groups, however, the ability to distinguish between co-infected and singly infected mice was no longer apparent. All of these observations are measured 6 days post infection and therefore represent the time point at which the delay in

pathogenesis of A/WSN/33 infection in the co-infected group was no longer significant. Identifying differences in the lung environment between day 3 and 5 may be useful to determine the mechanism of the delay observed in weight loss and clinical signs.

4.5.3 Co-infection with patent (adult \pm mf) *Litomosoides sigmodontis* exacerbates the pathogenesis of A/WSN/33 infection

As the mice were infected with L3 stage larvae, which progress through a number of developmental stages before reaching patency, equivalent 15-16 week old age matched adult mice were used in all experimental groups. In the A/WSN/33 singly infected group this led to markedly reduced pathology and weight loss from the same 5×10^3 infective dose. Mice at this age showed only mild clinical signs that did not become apparent until day 6 post infection. Similarly significant weight loss occurred from day 6 compared with day 3 in earlier time points and clinical signs were not apparent in the majority of mice in this group. Some individuals showed very mild increase in respiratory effort. Co-infected mice at this time point however had severe clinical signs and weight loss over the time course with strong resemblance to previous time points. Increased respiratory effort and decreased mobility was apparent in all mice from day 4, progressing to severe presentation of infection by day 6. Co-infected mice were therefore significantly worse than A/WSN/33 infected mice in presentation from day 4 onwards and from day 5 in weight loss measurements. This time point is also the only point at which influenza titre in the lung has shown significant difference. Co-infected mice have a statistically significant increase in infectious virus however the difference between groups is unlikely to be biologically significant. To determine the effect of this, an experimental repeat would need to be undertaken until day 8 or 9 to determine changes to viral clearance. Pathology caused by infection is not significantly altered in the lungs of A/WSN/33 and co-infected groups. Inflammatory cell infiltration surrounding both the airways and blood vessels can be seen in both groups, along with epithelial and interstitial necrosis, all to similar levels as the previous time point. A significant difference occurs in the extent of pathology. Previous time points have shown ~50% of the lung to be affected at this dose of viral infection irrespective of pre-existing *L. sigmodontis* infection, however, consistent with the decreased signs and weight loss, influenza infection alone in older mice affects only ~25% of the lung. Co-infection however seems to exacerbate the area of pathology back to ~50%. This response is not validated by the cytokine environment in the lung homogenates. Once again IFN γ is increased in the A/WSN/33 singly infected mice compared with co-infected mice. Both groups also show an increase in IL-10 although variation in the uninfected group means this is not a significant increase. In the BAL fluid IFN γ is increased in both A/WSN/33 groups, although IL-10 is now no longer increased to the same degree. Both cytokines are at much lower levels than in the previous time

point. These cytokines are therefore likely part of the adaptive immune response to A/WSN/33 which is less aggressive in these adult mice. There also seems to be limited evidence to suggest that IFN γ levels detected in the lung homogenate and BAL fluid directly at day 6 are indicative of clinical signs or weight loss associated with influenza infection in these experiments.

CD8⁺ T cell levels in the lymph nodes are again unaltered between experimental groups however *L. sigmodontis* infected mice now show an increase in production of IFN γ . As has been previously described by antigenic stimulation of lymphocytes with microfilaria antigen, (Taubert and Zahner 2001) patent infection leads to a switch in immune phenotype and *L. sigmodontis* infected mice produce type 1 and type 2 cytokines synergistically. This is a response mirrored in the CD4⁺ T cells subsets in the lymph node, where *L. sigmodontis* infected mice now produce elevated IFN γ levels indistinguishable to those that of A/WSN/33 infected and co-infected mice. CD4⁺ T cells in these mice however maintain high production of IL-4 and IL-5, at levels significantly higher than all other experimental groups. Synergistic T_{H1} / T_{H2} responses in *L. sigmodontis* infected mice are required for production of neutrophil responses against adult worms (Saeftel, Arndt et al. 2003). Co-infected mice also show an increase in these T_{H2} cytokines however to a once again intermediary phenotype. TNF α is also still produced in co-infected and *L. sigmodontis* infected mice at significantly lower levels than the A/WSN/33 singly infected group. IL-10 production is not different in CD4⁺ T cells in the lymph nodes of any experimental group and CD4⁺ IFN γ ⁺ IL-10⁺ are identifiable to similar levels in co-infected and A/WSN/33 infected mice.

CD4⁺ T cells identified in the lavage were again IL-4 and IL-5 positive in *L. sigmodontis* infected and to a lesser degree in the co-infected mice but all experimental groups were now capable of IFN γ production. The increase in IFN γ in *L. sigmodontis* infection was coupled with a decrease in IL-10 production that was elevated at the earlier time point. IL-10 may therefore be responsible for inhibiting IFN γ production by CD4⁺ T cells in *L. sigmodontis* infected mice at earlier stages of development. Total numbers of CD8⁺ T cells in the lavage samples were again raised in the co-infected animals. It is therefore uncertain that this population was directly involved in the delayed phenotype at the pre-patent co-infection. IFN γ production by these cells was equivalent to the earlier time point however CD8⁺ T cells in the lungs of A/WSN/33 singly infected mice are now producing high levels of TNF α . During viral infection with lymphochoriomeningitis virus (LCMV) or vesicular stomatis virus (VSV), production of TNF α by CD8⁺ T cells is associated with a virus specific effector population. The spleen contained high proportions of these CD8⁺ TNF α producing cells (Kristensen, Madsen et al. 2004). An increase in effector function by CD8⁺ T cells in response to influenza infection may explain the increasing resistance in mice with age to A/WSN/33. Limited expression of such a population in the co-infected mice may therefore explain why the co-infected mice have similar pathology to

earlier time points. Intrinsic production of TNF α by CD8⁺ T cells is integral for clearance of virus and resolution of pathology during influenza infection (Wortzman, Lin et al. 2013).

A similar pattern of inflammation dependent on the developmental stage of *L. sigmodontis* is observed in mice injected with sub lethal doses of LPS at pre-patent and microfilaraemic stages of *L. sigmodontis* infection. Adult female worm infected mice suppressed cytokine production to subsequent LPS injection compared with sham infected, LPS treated mice. However at patent stage of infection presence of microfilaria induced increased levels of inflammatory cytokines in sera leading to exacerbated sepsis (Hubner, Pasche et al. 2008).

Chapter 5 - Discussion

5.1 Hypotheses

The aim of this project was to test the theory that pre-existing infection with a chronic or persistent pathogen would skew the immune response to a secondary infection with influenza A. It was hypothesised that latent gammaherpesvirus infection would decrease susceptibility to influenza infection by increasing the 'anti-viral' type 1 immune responses in the lung. This hypothesis was also tested in the absence of the inflammatory cytokine IFN γ . A second hypothesis was tested with a persistent filarial nematode infection that was hypothesised to skew the immune response towards a type 2 and suppressive immune response, impairing the ability to produce optimal anti-viral immunity to influenza and increasing susceptibility.

5.2 Context

The importance of understanding co-infections and their potential to adjust immune responses or homeostasis of the host is a relatively new concept. In the context of single infections, much has been gained by studying a single pathogen in a model animal that is completely naïve to other infections. Immune responses may synchronise with, inhibit or have an additive effect on subsequent infection. This means that further understanding can be gained from a model of co-infection. This system of modelling attempts to be more reflective of human infections, where sub-clinical infections with multiple persistent and on-going pathogens are common place. Influenza infection is more highly likely to occur in an individual who is already mounting an immune response to a pre-existing pathogen.

In the preceding chapters two models of co-infection have been investigated. Latent gammaherpesvirus infection appears to provide a protective effect against acute respiratory infection with influenza A in a dose dependent manner, with protection less effective during severe infection. Co-infection led to a reduction in inflammatory cytokines and chemokines resulting in reduced pathology and clinical signs without impacting influenza viral replication. Subtle changes to the CD4⁺ and CD8⁺ cells in the lung may be responsible in part for the attenuation. The effect was not negated by removal of the inflammatory and in some circumstances regulatory, cytokine IFN γ . Chronic infection with *L. sigmodontis*, a model of filarial nematode infection, modulated influenza A infection with differing outcomes depending on the developmental stage of the parasite. Early stage (L4) infection had no significant impact. Pre-patent adult stage of infection delayed the pathogenesis of influenza infection for 1-2 days. Patent, late stage infection resulted in exacerbated disease. At all time points, pathology and

CD4⁺ and CD8⁺ T cell responses were compartmentalised to the site of each infection whilst some interaction was observed in the draining lymph nodes.

5.3 Interaction between divergent immune responses

The project considered that immune responses from unrelated pathogens could interact and alter the outcome of each infection. Immune responses to different pathogens and in particular those that cause polarised immune responses are thought to interact in a number of ways.

5.3.1 Competing responses

CD4⁺ T cells are pivotal in polarising the adaptive immune response. Development of T_H1 and T_H2 cells requires a degree of competition between IL-12, IL-18 and IL-4, IL-13 to influence antigen responsive cells and develop appropriate T helper lineages (Glimcher and Murphy 2000). This is of particular importance for CD4⁺ T cells returning to the epithelial barrier surfaces in the lung and gut where overexpression of GATA-3 and resulting suppression of T-bet can induce asthma and cause chronic inflammation and other immunopathology (Neurath, Finotto et al. 2002). In the context of a chronic infection, a heightened ‘anti-inflammatory’ immune response restricting the chronic infection could lead to modulation of responses to another type 1 co-infecting pathogen. This can be seen in infection with *Schistosoma mansoni* where chronic infection of mice skews the CD4⁺ immune response to a number of unrelated antigens (Kullberg, Pearce et al. 1992) and *Brugia malayi* infection, which alters cytokine production by PPD (*Mycobacterium tuberculosis* antigen) specific T cells due to IL-4 production.

This effect can be seen in the *L. sigmodontis* and A/WSN/33 co-infection experiments when measuring the cytokine responses in the lymph nodes. CD4⁺ and CD8⁺ cells in the co-infected mice consistently showed reduced production of both type 1 and 2 cytokines compared with single infected controls (Figure 4.11A-C). The draining lymph node is an important site of attenuation in the production of appropriately polarised adaptive responses during co-infection. Antigen specific activation of T cells from the lymph nodes would be a logical next step in order to determine if this change in phenotype is due to competition between the IL-4 and IL-12 governed arms of the immune system.

In chronic MHV-68 infected mice (28 days post infection), CD4⁺ T cells in the mediastinal and tracheobronchial lymph nodes were not increased in number or in the amount of inflammatory (IFN γ and TNF α) or regulatory (IL-10) cytokines produced when stimulated non-specifically with ionomycin and PMA (in comparison with uninfected mice). The acute phase of the

gammaherpesvirus infection, which requires expansion of CD4⁺ T cells in the lung draining lymph nodes, is therefore resolved by this time point and the virus has achieved latency. The inflammatory cytokine environment in the lung is also unaltered when detected by ELISA (Figure 3.29A). It is therefore unlikely that ongoing inflammatory immune responses in the lymph node as a result of chronic gammaherpesvirus infection are changing the outcome of A/WSN/33 co-infection.

L. sigmodontis and A/WSN/33 co-infection does alter the cytokines produced (at day 6) by CD4⁺ cells in the lymph nodes. However during co-infection, CD4⁺ cells in the lung at the same time point have similar cytokine production to mice infected with A/WSN/33 alone. Changes to CD4⁺ T cells in the lymph nodes are therefore not apparent in the lungs of co-infected mice. Likewise, pathology at the mesothelium layer also appears unaltered in the co-infected mice compared with the solely *L. sigmodontis* infected mice. The mechanism of delay in severity and weight loss during the adult, pre-patent (day 34-40) *L. sigmodontis* and A/WSN/33 co-infection is therefore unknown.

Counter-inhibitory type 1 cytokines (IFN γ and TNF α) and type 2 cytokines (IL-4 and IL-5) are capable of changing the phenotype of responding CD4⁺ and CD8⁺ cells during co-infection in the lymph nodes, but this effect is not mirrored at the site of influenza infection. This suggests changes to another cell population as a result of pre-existing infection may be responsible for the delay in severity of clinical signs caused by influenza.

The delay in response to A/WSN/33 during co-infection with pre-patent *L. sigmodontis* is consistent with another *L. sigmodontis* co-infection experiment in the literature, where the immune responses to *L. sigmodontis* and co-infecting *Leishmania major* were successfully compartmentalised by the immune system and did not interact, however there was a delay in pathogenesis of *L. major* (Lamb, Graham et al. 2005).

The second touch hypothesis states that activation, polarisation and expansion of adaptive immunity occurs in the lymph nodes and requires antigen presentation and specific cytokine production but effector function at the site of infection is activated by a second antigen specific signal at the point of inflammation where the antigen is derived (Ley 2014). Within the lymph nodes T_H1 and T_H2 prototypical cytokines appear to interact leading to the induction of sufficiently polarised antigen specific responses. Appropriate expression of chemokines by macrophages, innate lymphoid cells, damaged infected cells and dendritic cells at the site of infection (Lebre, Burwell et al. 2005) recruit suitable cell populations back into the peripheral tissues to exert effector function. The interaction between responses in the lymph node may explain the delay in the co-infected mice which take longer to produce an appropriate response on account of the other cytokine responses present. At day 6 appropriate responses are present

in the lungs and there is no difference between *L. sigmodontis* and A/WSN/33 co-infected and singly A/WSN/33 infected mice.

Another reason for the delay may be changes at an earlier time point. Poor antigen presentation, changes to phagocytic capacity of macrophages at the site of infection, inefficient production of cytokines by innate lymphoid cells or impaired NK cell activation could contribute. It would therefore be of interest to compare the lung resident immune cells 6-48 hours after influenza infection in the co-infected mice with those from singly infected mice.

5.3.2 Regulatory responses

As an alternative to competition between T_H1/T_H2 and other polarised responses of the host immune response (T_H17 , T_H9 etc), the interactions between concurrent immune responses may be explained by regulatory mechanisms. *L. sigmodontis* produces a regulatory T cell response from early time points during infection that is capable of suppressing an allergic asthmatic response in the lung (Dittrich, Erbacher et al. 2008). Similarly $CD4^+ CD25^+ CTLA4^+$ T cells are induced during infection to prevent a neutralising T_H2 response in resistant strains of mice (Taylor, Harris et al. 2007). Regulation of cytokine production in the lymph node may explain why reduced type 1 and 2 cytokines were seen in the mice co-infected with *L. sigmodontis* and A/WSN/33 however this is not supported by an increased production of IL-10 by $CD4^+$ T cells, although the percentage of $IFN\gamma^+ IL-10^+ CD4^+$ cells was increased in co-infected mice (Figure 4.11H) suggesting that the effector function of these cells may have been altered despite their ability to produce $IFN\gamma$.

In latent MHV-68 infected mice, macrophages from lung lavage had an increased level of SOCS-1, a suppressor of cytokine production. Down regulation of macrophage cytokine production is found in other herpesvirus infections for example HHV-6 can suppress the activation of macrophages by GM-CSF and IL-3 and similarly KSHV encodes a protein mimic of CD200 to down-regulate macrophage activation (Foster-Cuevas, Wright et al. 2004). Many persistent viruses encode immunosuppressive proteins in order to evade the acute immune response and establish latency. Therefore the requirement to suppress on-going responses to long-lived pathogens to avoid excessive collateral damage may provide an explanation for assuaging the response to A/WSN/33 in infected mice.

5.3.3 Synergistic responses

In reality it is likely that a combination of the previously described factors alter immune responses during co-infection. It is also apparent that polarisation of the immune response is not

simple and sufficient immunity to all pathogens requires interactions between all (T_{H1} , T_{H2} , T_{H17} etc) branches of the immune response to act synergistically or to varying degrees.

In *L. sigmodontis* infection, IL-5 and IFN γ act synergistically following the establishment of patency to eliminate the parasite (Saeftel, Arndt et al. 2003), evidenced in the increased production of IFN γ by CD4⁺ T cells in the solely *L. sigmodontis* infected group in the last developmental stage experiment (Figure 4.18A). Influenza responses combine neutrophil recruiting IL-17a responses, with T_{H1} inflammatory responses. IL-17RA^{-/-} mice have reduced pathology. Therefore activation of different branches (E.g. T_{H1}/T_{H2} etc) of the immune system must be balanced. Increased expression of T_{H17} responses may contribute to hypercytokinemia induced fatality (Bermejo-Martin, Ortiz de Lejarazu et al. 2009) and therefore understanding how MHV-68 infection manages to reduce the production of all cytokines and chemokines measured in the cytokine array (Figure 3.17) could contribute to development of therapeutics against self-propagating inflammatory responses.

It is likely that this synergistic balance in responses is important in influenza infection, where increases in IL-4 and IL-5 expression were seen alongside the expected inflammatory cytokines (Figure 3.17C). Counter-regulation and suppression of these systems is required for resolution of pulmonary damage and therefore, as evidenced in the co-infection experiments, imbalance of this response can greatly alter the outcome of infection without altering influenza replication.

5.4 Mouse strain

Mouse strain specific differences observed in the MHV-68 and A/WSN/33 co-infection experiments in BALB/c and 129Sv/Ev mice provide evidence of host genetic factors contributing to susceptibility to infection. In humans this can be seen in the identification of IFITM3 alleles that make individuals more likely to succumb to influenza infection (Everitt, Clare et al. 2012). In mice this is seen in the presence or absence of Mx proteins (Staeheli, Grob et al. 1988) and both *L. sigmodontis* and MHV-68 infections have been shown to produce differing immune responses in BALB/c and C57BL/6 mice (Hoffmann, Petit et al. 2000; Weinberg, Lutzke et al. 2004). It is consequently unsurprising that different mouse strains may respond differently to the same co-infection, especially considering additional differences such as murine MHC haplotype. Some mice are more adept at producing particular responses than others, which can be seen most clearly in their ability to instigate $T_{H1}/T_{H2}/T_{H17}$ etc. responses. Results of the MHV-68 and A/WSN/33 co-infection in the 129Sv/Ev model had a drawback in the unintended alteration to the diurnal light cycle and this experiment therefore needs repeating before conclusions can be drawn. Understanding genetic differences and their influence on susceptibility during infection may however demonstrate target cell populations that control

immunity during co-infection. This is evidence of the highly complicated network of immune responses that are constantly evolving and interacting to meet the needs of the host and regulate homeostasis.

5.5 Antigen specificity

Evidence of direct cross-reacting immune responses or ‘heterologous immunity’ driven by chronic herpesvirus infection has been observed in some co-infections. EBV antigen-specific CD8⁺ T cells were observed to respond to hepatitis B infection in a human cohort with similar kinetics to that of the total CD8⁺ T cell population (Sandalova, Laccabue et al. 2010). Later individual cross-reactive epitopes were identified between EBV and antigens from influenza A, explaining the reactivity of herpes-specific memory responses during heterologous infection (Clute, Naumov et al. 2010). This could also be a mechanism by which protection against A/WSN/33 is afforded by MHV-68. Specificity of responding CD8⁺ and CD4⁺ T cells in the lung would determine if direct cross-reactivity occurs in the mouse model of MHV-68 and A/WSN/33 co-infection. In this case protective secondary immunity could be compromised as discussed in 3.6.2.

5.6 The role of IFN γ

IFN γ was hypothesised to contribute to the protective effect seen in the MHV-68 co-infection. Co-infected animals displayed a decrease in mean IFN γ levels in lung homogenates measured by ELISA compared with singly A/WSN/33 infected mice. MHV-68 infection, however, had a similar protective effect in IFN γ RA^{-/-} mice. IFN γ is integral to recall responses (Bot, Bot et al. 1998) and cytolytic activity in CD4⁺ T cells (Brown, Lee et al. 2012). IFN γ is expressed by T_{FH} following influenza infection (Luthje, Kallies et al. 2012) and regulates macrophage function (Sun and Metzger 2008). It has been shown to have enough overlap and redundancy with other signalling cascades in the immune system that expression of IFN γ is not essential to mount successful immunity to influenza A (Graham, Dalton et al. 1993). Augmentation of IFN γ responses, however, still showed potential to influence the outcome of influenza infection, as seen in previous co-infection experiments (Metzger 2014). While IFN γ was reported to increase as a result of MHV-68 infection in the serum (Barton, White et al. 2009), the increase reported in the lung by qPCR in other studies (Saito, Ito et al. 2013) was not observed by ELISA during these experiments. The rise in IFN γ in the lung due to latent MHV-68 infection may therefore not be the crucial change caused by gammaherpesvirus infection that alleviates the expansion of other inflammatory cytokines and adaptive cellular immunity at later stages of infection.

MHV-68 infection produces a more evident persistent response in the lung, coupled with infiltration of immune cells in the absence of IFN γ RA, (Figure 3.26) and causes multiple organ fibrosis, alternative activation of macrophages and a significant impact on leukocyte trafficking (Ebrahimi, Dutia et al. 2001; Gangadharan, Hoeve et al. 2008). It is therefore difficult to compare this significantly altered phenotype in the context of the co-infection as lymph nodes cannot be collected due to fibrosis.

Both single infections are changed and normal immune function is compromised by the absence of IFN γ receptor (and subsequent signalling). Targeted depletion of IFN γ with monoclonal antibodies may be more useful to understand its influence at specific time points during infection. This method would also allow for comparison of competent MHV-68 infection prior to co-infection when IFN γ could be depleted for a more direct comparison however this could reactivate MHV-68 as a result.

In the absence of IFN γ signalling, MHV-68 infection in the spleen resulted in increased M2 markers *Ym/1* and *Fizz1* and transcription of type 2 cytokines IL-21, IL-5 and IL-13 was up-regulated suggesting a highly type 2 polarised response (Gangadharan, Hoeve et al. 2008). This environment may share similarity with that seen in the persistent helminthic infection experiments and would suggest that type 2 responses alone are more capable of controlling influenza infection in the complete absence of IFN γ driven type 1 immunity.

MHV-68 and A/WSN/33 co-infection in BALB/c mice had a large reduction in all cytokines and chemokines (Figure 3.17) 6 days post infection. 129Sv/Ev mice produce a more inflammatory response to influenza and are more resistant to weight loss (Figure 3.21A). A significant reduction in inflammatory cytokines does not explain the increased resistance seen in the co-infected BALB/c mice. Therefore the role of IFN γ is contentious.

Ultimately it is likely another mechanism of action that causes protection in the MHV-68 co-infection and further investigation of the early stages of response and in the solely MHV-68 infected mice is required.

5.7 Future directions

5.7.1 Lung homeostasis and early innate responses

In the MHV-68 and A/WSN/33 co-infection no alterations occur in the lymph nodes but subtle changes in the responding populations are evident in the lung. These changes may reflect the alterations to lung homeostasis during latent infection with MHV-68. Macrophages in latently infected mice showed increased SOCS-1 expression while CD4⁺ T cells and cytokines in the

lung were unaltered. The ELISA method of cytokine detection, however, may not be sensitive enough to determine subtle increases in IFN γ required levels to suppress virus replication, as discussed previously. The results of the cytokine array in the MHV-68 and 5×10^3 A/WSN/33 co-infection suggest that all cytokines and chemokines were reduced in co-infected mice by day 6 post A/WSN/33 infection. The ability of MHV-68 to suppress inflammatory responses in the lung must therefore be an on-going effect of latent infection on the immune system.

Currently we do not understand the mechanism underlying the alteration to influenza virus infection by latent MHV-68 infection but early signalling pathways and changes to receptors and anti-viral surveillance molecules may be the source of this transformation. If the production of inflammatory cytokines such as IFN γ is required to control gammaherpesvirus latency, then expression of IFN γ inducible genes or anti-viral receptors such as RIG-I, MDA-5, NOD receptors, type 1 and 3 interferon production and even MHC expression may be altered. The importance of such receptors can be seen in their inhibition, which increases susceptibility to influenza virus infection (Wu, Patel et al. 2011).

In the absence of the IFN γ receptor, the protective effect is still observed and A/WSN/33 replication is not significantly altered by co-infection. This weakens the hypothesis that expression of inhibitors of viral replication would be increased. Instead the effect of MHV-68 infection may be attributed to changes in lung integrity, phenotype of residing immune cells such as macrophages and even the epithelial barrier and its interaction with professional antigen presenting cells.

The regulation and suppression of inflammation at the site of infection lead to reduced infiltration of immune cells. This is observed in the lung pathology (Figure 3.9I and 3.9L). Therefore it would be important to investigate the early time points of influenza infection during co-infection with latent MHV-68. This would require further investigation in order to identify subtle changes in the immune environment caused by the underlying latent MHV-68 infection that subsequently provide protection against influenza A infection.

While the lung environment during latent infection is not known, changes to lung homeostasis may be identifiable in innate recognition molecules such as CD200 expressed on airway epithelium. CD200 is capable of suppressing macrophage responses to influenza infection (Snelgrove, Goulding et al. 2008). Similarly in a steady state the lung environment is governed by IL-10 production by dendritic cells and T_{REG} induction against innocuous antigens. Correspondingly, epithelial cells secrete GM-CSF and NO and TGF- β that alter the responses of dendritic cells to harmless inhaled antigens (Snelgrove, Godlee et al. 2011). If chronic infection can adjust this balance it is likely a source of the protection during co-infection.

The increase in production of type 2 cytokines in response to mechanical damage caused by filarial nematode infection may offer insight into changes in the lung environment that provide the changes in pathogenesis seen in the *L. sigmodontis* and A/WSN/33 co-infection at different developmental stages. Helminth infection induces a range of cytokines and alarmins (TSLP, IL-25, IL-33) and release of DAMPs such as uric acid and extracellular ATP from apoptotic cells that are usually absent in the uninfected lung. It is also apparent in the later developmental stage that *L. sigmodontis* causes a degree of fibrosis in the lung mesothelium. The phenotype of macrophages in the lungs of these mice would also be interesting to delineate, as helminthic infection often induces alternative activation and increased production of MHC-II (Reece, Siracusa et al. 2006).

Key cytokines required to initiate responses in the lung released by epithelial cells such as IL-33 may also be of key consideration in future work to determine how airway homeostasis and remodelling is altered by pre-existing infection. Administration of IL-33 during influenza A infection increases T_H17 and T_H2 cytokine production and as IL-33 is induced upon helminth infection it could be a source of regulation in the early response to co-infection (Yagami, Orihara et al. 2010). Such changes at epithelial barriers could also determine the alleviation of inflammation observed in MHV-68 and A/WSN/33 co-infection. Although production of IL-33 during latent infection is unlikely, changes to IL-33 cause alterations in effector function by CD8⁺ T cells (Ngoi, St Rose et al. 2012) which is seen in the MHV-68 and A/WSN/33 co-infection in the lung.

An unexpected outcome of co-infection with MHV-68 and A/WSN/33 was a reduction in MHV-68 viral load in the lungs of co-infected mice. This is hypothesised to be a result of increased presence of inflammatory cytokines including IFN γ which is responsible for maintaining latency in gammaherpesvirus infection and a reduction in IL-4 which has been shown in helminthic co-infection to reactivate MHV-68 (Steed, Barton et al. 2006; Reese, Wakeman et al. 2014). Dysregulation of early innate responses is a key contribution to the outcome of infection (Vogel, Harris et al. 2014). Therefore understanding of the effect of MHV-68 and *L. sigmodontis* infections on the lung is predicted to determine why these infections can confer a level of protection or exacerbate disease and pathogenesis of influenza A.

5.7.2 Secondary infection and memory responses

While better understanding of the early innate responses could be integral to determining the changes in outcome caused by co-infection, the protective effect and dampened immune responses may come at a cost to memory responses (Beaumier, Mathew et al. 2008; Min-Oo and Lanier 2014). Correspondingly there may also be an impact on antibody responses and class

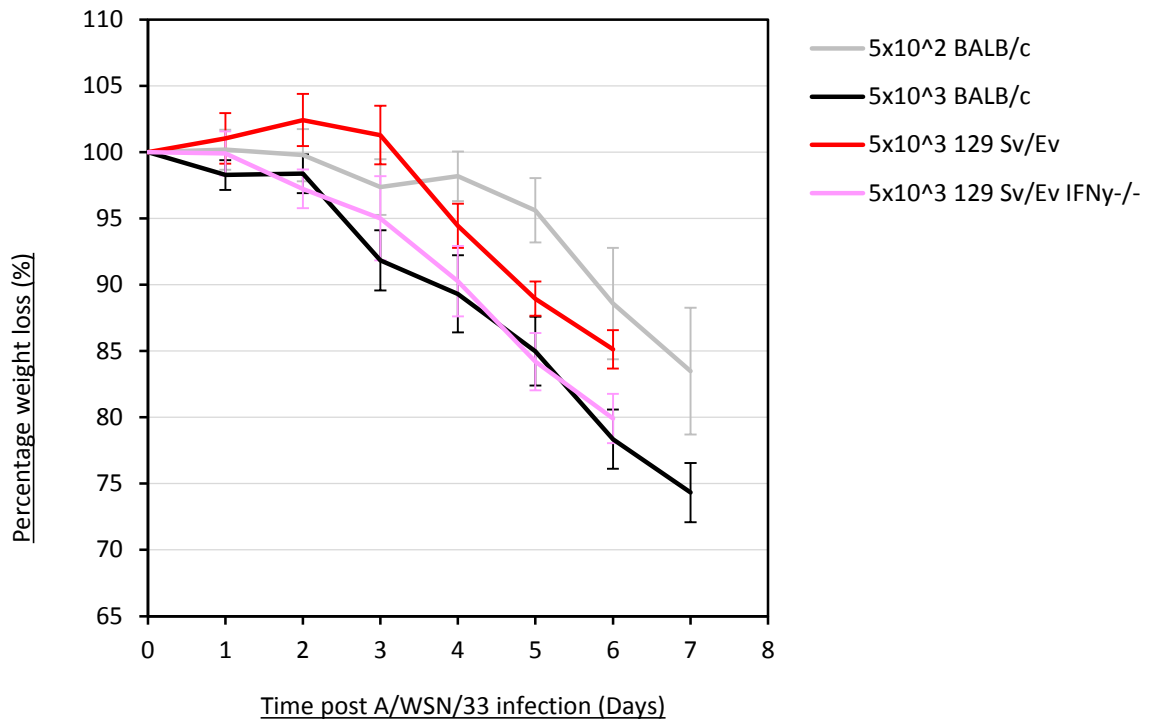
switching if inflammatory cytokines and signalling is reduced by co-infection. Measuring the outcome of A/WSN/33 pathogenesis and long term immune responses may therefore also be of interest in the context of co-infection. Identifying influenza specific IgG1 vs. IgG2a balance following *L. sigmodontis* and A/WSN/33 co-infection was an aim of the project that unfortunately could not be completed.

5.7.3 Impact

The outcome of the two co-infection experiments suggests that immunity to influenza infection is greatly altered by co-infection. Latent gammaherpesvirus infection which is common among human populations, appears to offer protection from inflammatory responses to influenza A in this model. Filarial nematode infection, which is highly prevalent in the tropics also impacted influenza virus pathogenesis and varied due to developmental stage of the worm. These observations could have important implications during the treatment of severe influenza. While many studies have addressed the effect of co-infecting respiratory pathogens during infection and identified the impact of influenza A virus on lung integrity in the promotion of bacterial infection, it has only recently been understood that pre-existing unrelated pathogens, infecting sites away from the lungs can have a significant impact on the outcome of influenza infection. This knowledge could be an integral factor contributing to the wide variations in responses recorded during highly pathogenic influenza infections. Similarly if chronic infection is capable of skewing immune responses to unrelated infection, understanding the mechanism may provide better vaccination strategies or highlight potential targets within the host's immune system for therapeutic intervention.

Chapter 6 - Appendix

Figure 6.1 Comparison of A/WSN/33 infection between mouse strains



A. Comparison of all A/WSN/33 infected groups

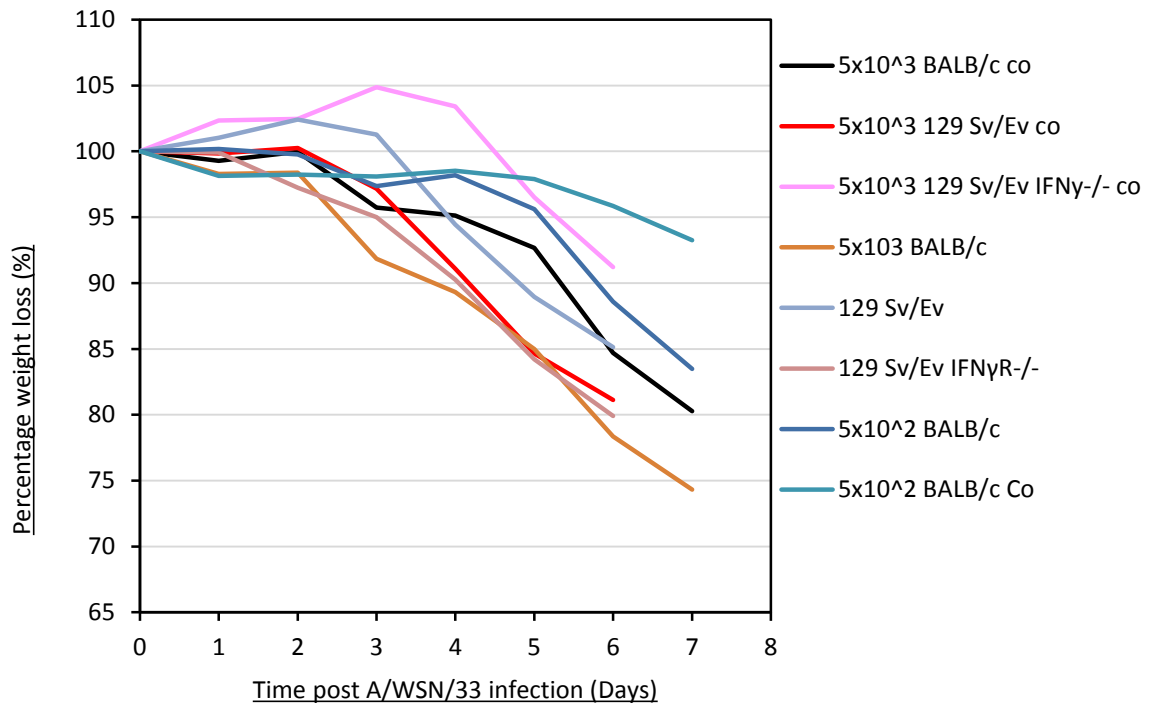


Figure 6.2 FACS Analysis Protocol

Representative plots of FACS analysis and gating strategy to identify lymphocyte populations

1. Sample before analysis

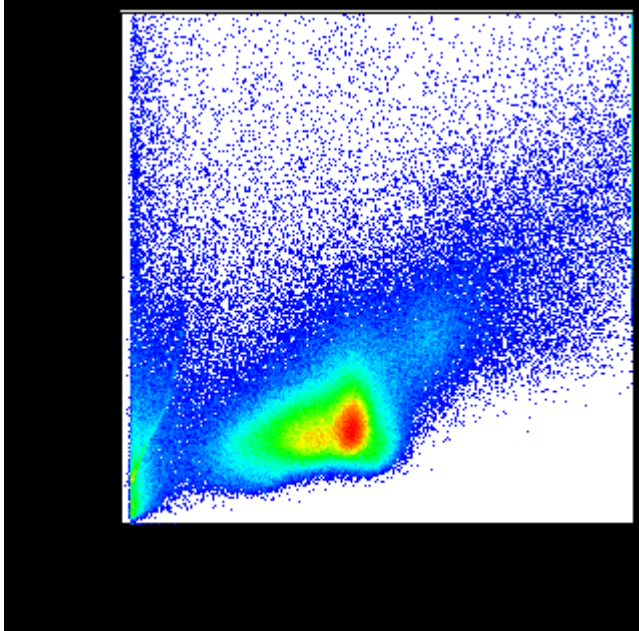


Figure 6.2.1 Whole samples run on SSC-A and FSC-A

2. Removing dead cells

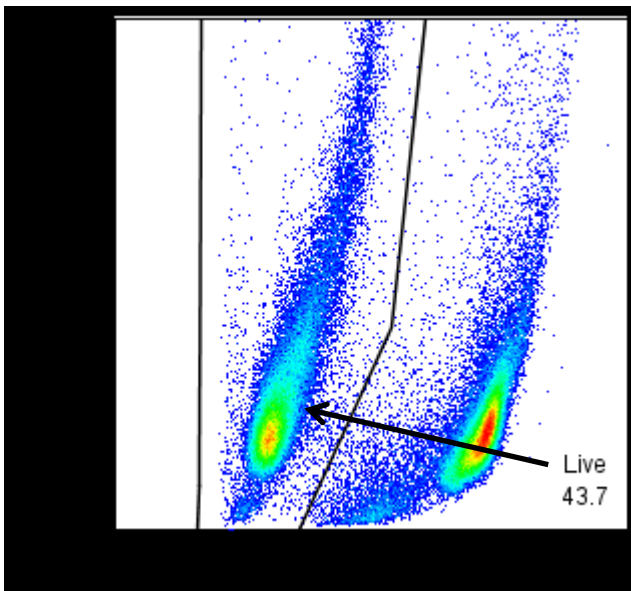


Figure 6.2.2 Live cells are gated based on stain with Zombie cyan live/dead stain (Biolegend). Cells are run in SSC-Area vs. emission at 525/50nm. Dead cells are stained positive and excluded.

3. Removing doublets

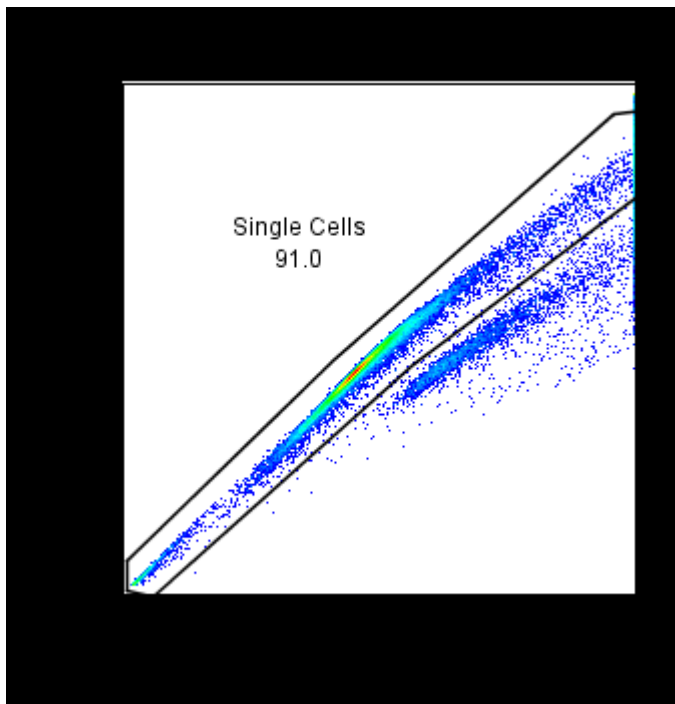


Figure 6.2.3 Live single cells were identified by analysis of live cells on a FSC-height vs FSC-area plot. Single cells were identified as those with tightly correlated height and area detection.

4. Identifying lymphocyte population

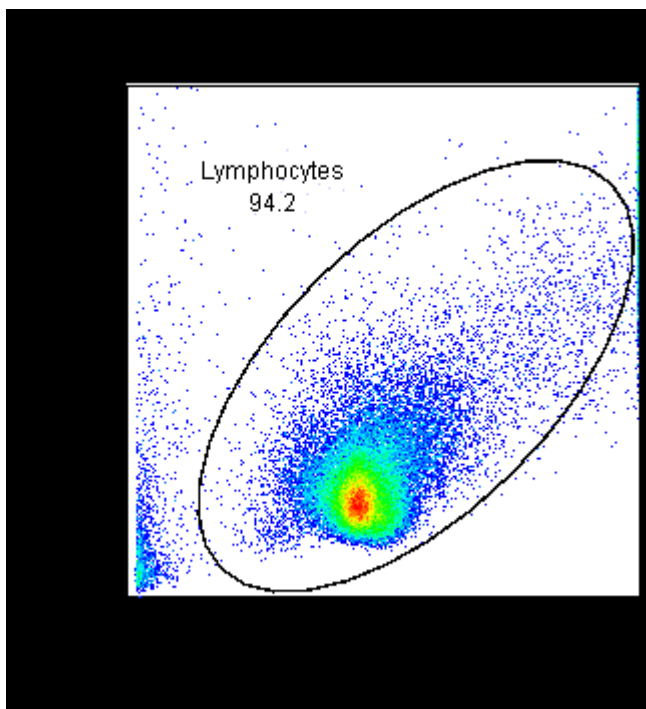


Figure 6.2.4 Live, single lymphocytes were identified by size on a FSC-A vs SSC-A plot.

5. Identifying CD4⁺ and CD8⁺ cells

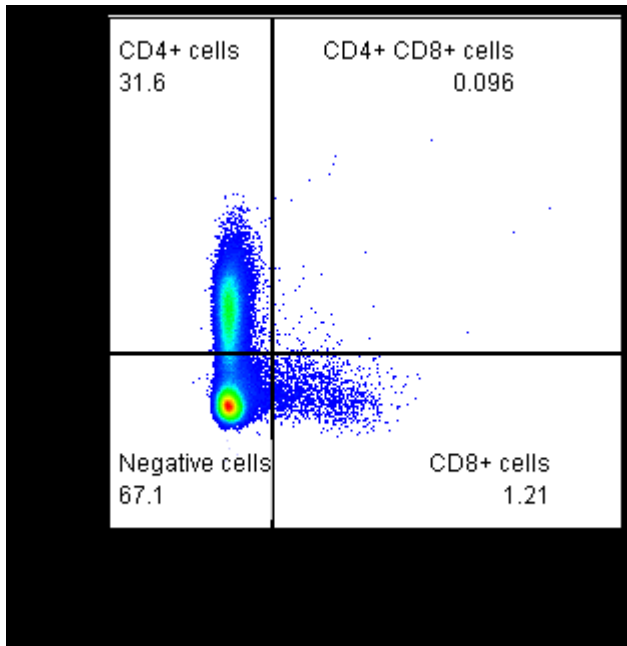


Figure 6.2.5 CD4⁺ and CD8⁺ lymphocytes were identified with population specific antibodies

6. Identifying cytokine expression within CD4⁺ and CD8⁺ cells

A. Experimental sample

B. Isotype negative control

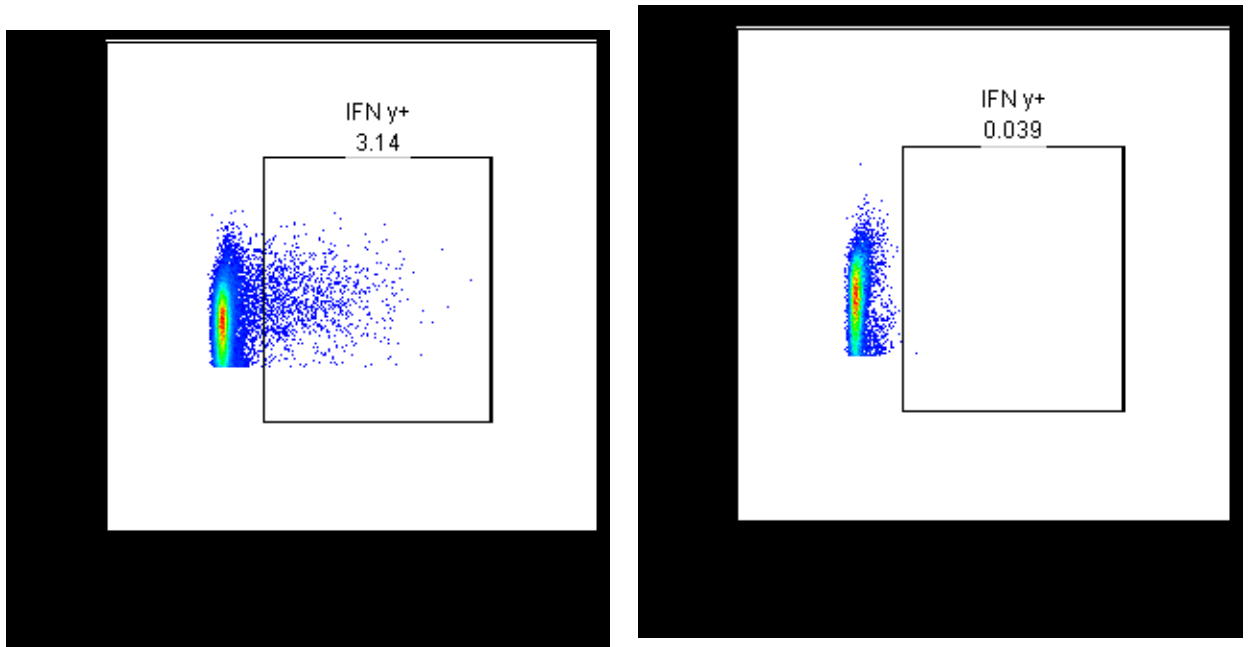


Figure 6.2.6 Intracellular staining was performed on fixed cells to determine production of cytokines after 4 hour stimulation with PMA and Ionomycin. Relevant isotype controls were used to identify nonspecific binding. This value was subtracted from positive samples.

Chapter 7 - References

Website pages

- (NIAID, 2014). "International Collaborative Network for the Study of Human Helminth Co-infections." 2014, from <http://www.niaid.nih.gov/topics/tropicaldiseases/research/pages/helminth.aspx>.
- (CDC, 2014). "Parasites - Lymphatic Filariasis." from <http://www.cdc.gov/parasites/lymphaticfilariasis/>.
- (WHO, 2014). "Lymphatic Filariasis." from <http://www.who.int/mediacentre/factsheets/fs102/en/>.

Journals

- Abbas, O. M., N. A. Omar, et al. (2009). "Schistosoma mansoni coinfection could have a protective effect against mixed cryoglobulinaemia in hepatitis C patients." *Liver Int* **29**(7): 1065-1070.
- Alberts, R., B. Srivastava, et al. (2010). "Gene expression changes in the host response between resistant and susceptible inbred mouse strains after influenza A infection." *Microbes Infect* **12**(4): 309-318.
- Allen, J. E. and R. M. Maizels (2011). "Diversity and dialogue in immunity to helminths." *Nat Rev Immunol* **11**(6): 375-388.
- Andre, P., T. Morooka, et al. (2011). "Critical role for Syk in responses to vascular injury." *Blood* **118**(18): 5000-5010.
- Anthony, R. M., L. I. Rutitzky, et al. (2007). "Protective immune mechanisms in helminth infection." *Nat Rev Immunol* **7**(12): 975-987.
- Apiwattanakul, N., P. G. Thomas, et al. (2014). "Helminth infections predispose mice to pneumococcal pneumonia but not to other pneumonic pathogens." *Med Microbiol Immunol*.
- Arai, K., Z. X. Liu, et al. (2002). "IP-10 and Mig facilitate accumulation of T cells in the virus-infected liver." *Cell Immunol* **219**(1): 48-56.
- Arndt, U., G. Wennemuth, et al. (2002). "Release of macrophage migration inhibitory factor and CXCL8/interleukin-8 from lung epithelial cells rendered necrotic by influenza A virus infection." *J Virol* **76**(18): 9298-9306.
- Attout, T., C. Martin, et al. (2008). "Pleural cellular reaction to the filarial infection *Litomosoides sigmodontis* is determined by the moulting process, the worm alteration, and the host strain." *Parasitol Int* **57**(2): 201-211.
- Babayán, S., M. N. Ungeheuer, et al. (2003). "Resistance and susceptibility to filarial infection with *Litomosoides sigmodontis* are associated with early differences in parasite development and in localized immune reactions." *Infect Immun* **71**(12): 6820-6829.
- Babu, B. V. and A. N. Nayak (2003). "Treatment costs and work time loss due to episodic adenolymphangitis in lymphatic filariasis patients in rural communities of Orissa, India." *Trop Med Int Health* **8**(12): 1102-1109.
- Babu, S., L. M. Ganley, et al. (2000). "Role of gamma interferon and interleukin-4 in host defense against the human filarial parasite *Brugia malayi*." *Infect Immun* **68**(5): 3034-3035.
- Babu, S., L. D. Shultz, et al. (1999). "Immunity in experimental murine filariasis: roles of T and B cells revisited." *Infect Immun* **67**(6): 3166-3167.
- Barton, E. S., D. W. White, et al. (2007). "Herpesvirus latency confers symbiotic protection from bacterial infection." *Nature* **447**(7142): 326-329.
- Barton, E. S., D. W. White, et al. (2009). "Herpesvirus latency and symbiotic protection from bacterial infection." *Viral Immunol* **22**(1): 3-4; author reply 5-6.
- Bauquet AT, Jin H, Paterson AM, et al. Costimulatory molecule ICOS plays a critical role in the development of TH-17 and follicular T-helper cells by regulating c-Maf expression and IL-21 production. *Nature immunology*. 2009;10(2):167-175. doi:10.1038/ni.1690.
- Beauchamp, N. M., R. D. Yammani, et al. (2012). "CD8 marks a subpopulation of lung-derived dendritic cells with differential responsiveness to viral infection and toll-like receptor stimulation." *J Virol* **86**(19): 10640-10650.
- Beaumier, C. M., A. Mathew, et al. (2008). "Cross-reactive memory CD8(+) T cells alter the immune response to heterologous secondary dengue virus infections in mice in a sequence-specific manner." *J Infect Dis* **197**(4): 608-617.
- Belz, G. T., C. M. Smith, et al. (2004). "Distinct migrating and nonmigrating dendritic cell populations are involved in MHC class I-restricted antigen presentation after lung infection with virus." *Proc Natl Acad Sci U S A* **101**(23): 8670-8675.
- Bender, B. S., R. Cotter, et al. (1996). "Body temperature and nesting behavior following influenza challenge in mice: effects of age." *Mech Ageing Dev* **86**(1): 1-9.
- Bender, B. S., S. F. Taylor, et al. (1995). "Pulmonary immune response of young and aged mice after influenza challenge." *J Lab Clin Med* **126**(2): 169-177.
- Bermejo-Martin, J. F., R. Ortiz de Lejarazu, et al. (2009). "Th1 and Th17 hypercytokinemia as early host response signature in severe pandemic influenza." *Crit Care* **13**(6): R201.

- Blackwell, A. D., M. Martin, et al. (2013). "Antagonism between two intestinal parasites in humans: the importance of co-infection for infection risk and recovery dynamics." *Proc Biol Sci* **280**(1769): 20131671.
- Blanco, J. L. and M. E. Garcia (2008). "Immune response to fungal infections." *Vet Immunol Immunopathol* **125**(1-2): 47-70.
- Blasdell, K., C. McCracken, et al. (2003). "The wood mouse is a natural host for Murid herpesvirus 4." *J Gen Virol* **84**(Pt 1): 111-113.
- Blaskovic, D., M. Stancekova, et al. (1980). "Isolation of five strains of herpesviruses from two species of free living small rodents." *Acta Virol* **24**(6): 468.
- Bloomfield, S. F., R. Stanwell-Smith, et al. (2006). "Too clean, or not too clean: the hygiene hypothesis and home hygiene." *Clin Exp Allergy* **36**(4): 402-425.
- Borza, C. M. and L. M. Hutt-Fletcher (2002). "Alternate replication in B cells and epithelial cells switches tropism of Epstein-Barr virus." *Nat Med* **8**(6): 594-599.
- Bot, A., S. Bot, et al. (1998). "Protective role of gamma interferon during the recall response to influenza virus." *J Virol* **72**(8): 6637-6645.
- Bot, A., A. Holz, et al. (2000). "Local IL-4 expression in the lung reduces pulmonary influenza-virus-specific secondary cytotoxic T cell responses." *Virology* **269**(1): 66-77.
- Bouchery, T., G. Denece, et al. (2012). "The chemokine CXCL12 is essential for the clearance of the filaria *Litomosoides sigmodontis* in resistant mice." *PLoS One* **7**(4): e34971.
- Bourgeois, F. T., C. Valim, et al. (2009). "Relative impact of influenza and respiratory syncytial virus in young children." *Pediatrics* **124**(6): e1072-1080.
- Brincks, E. L., A. Katewa, et al. (2008). "CD8 T cells utilize TRAIL to control influenza virus infection." *J Immunol* **181**(7): 4918-4925.
- Brown, D. M. (2010). "Cytolytic CD4 cells: Direct mediators in infectious disease and malignancy." *Cell Immunol* **262**(2): 89-95.
- Brown, D. M., A. M. Dilzer, et al. (2006). "CD4 T cell-mediated protection from lethal influenza: perforin and antibody-mediated mechanisms give a one-two punch." *J Immunol* **177**(5): 2888-2898.
- Brown, D. M., S. Lee, et al. (2012). "Multifunctional CD4 cells expressing gamma interferon and perforin mediate protection against lethal influenza virus infection." *J Virol* **86**(12): 6792-6803.
- Buchmeier, N. A. and R. D. Schreiber (1985). "Requirement of endogenous interferon-gamma production for resolution of *Listeria monocytogenes* infection." *Proc Natl Acad Sci U S A* **82**(21): 7404-7408.
- Bussey, K. A., E. Reimer, et al. (2014). "The gammaherpesviruses Kaposi's sarcoma-associated herpesvirus and murine gammaherpesvirus 68 modulate the Toll-like receptor-induced proinflammatory cytokine response." *J Virol* **88**(16): 9245-9259.
- Cantin EM, Hinton DR, Chen J, Openshaw H. Gamma interferon expression during acute and latent nervous system infection by herpes simplex virus type 1. *Journal of Virology*. 1995;69(8):4898-4905.
- Cantin E, Tanamachi B, Openshaw H, Mann J, Clarke K. Gamma Interferon (IFN- γ) Receptor Null-Mutant Mice Are More Susceptible to Herpes Simplex Virus Type 1 Infection than IFN- γ Ligand Null-Mutant Mice. *Journal of Virology*. 1999;73(6):5196-5200.
- Carbone, A., A. Ghoghini, et al. (2008). "EBV-associated lymphoproliferative disorders: classification and treatment." *Oncologist* **13**(5): 577-585.
- Casiraghi, C., I. Shanina, et al. (2012). "Gammaherpesvirus latency accentuates EAE pathogenesis: relevance to Epstein-Barr virus and multiple sclerosis." *PLoS Pathog* **8**(5): e1002715.
- Castro Sanchez, A. Y., M. Aerts, et al. (2013). "A mathematical model for HIV and hepatitis C co-infection and its assessment from a statistical perspective." *Epidemics* **5**(1): 56-66.
- Cesarman, E. and D. M. Knowles (1999). "The role of Kaposi's sarcoma-associated herpesvirus (KSHV/HHV-8) in lymphoproliferative diseases." *Semin Cancer Biol* **9**(3): 165-174.
- Chan, M. C., C. Y. Cheung, et al. (2005). "Proinflammatory cytokine responses induced by influenza A (H5N1) viruses in primary human alveolar and bronchial epithelial cells." *Respir Res* **6**: 135.
- Chandra, G. (2008). "Nature limits filarial transmission." *Parasit Vectors* **1**(1): 13.
- Chapman, T. J., M. R. Castrucci, et al. (2005). "Antigen-specific and non-specific CD4+ T cell recruitment and proliferation during influenza infection." *Virology* **340**(2): 296-306.
- Chen, J. and X. S. Liu (2009). "Development and function of IL-10 IFN-gamma-secreting CD4(+) T cells." *J Leukoc Biol* **86**(6): 1305-1310.
- Chen, L., D. Zanker, et al. (2014). "Immunodominant CD4+ T-Cell Responses to Influenza A Virus in Healthy Individuals Focus on Matrix 1 and Nucleoprotein." *J Virol* **88**(20): 11760-11773.
- Chertow, D. S. and M. J. Memoli (2013). "Bacterial coinfection in influenza: a grand rounds review." *JAMA* **309**(3): 275-282.
- Chiaretti, A., S. Pulitano, et al. (2013). "IL-1 beta and IL-6 upregulation in children with H1N1 influenza virus infection." *Mediators Inflamm* **2013**: 495848.
- Chiou, W. F., C. C. Chen, et al. (2011). "8-Prenylkaempferol Suppresses Influenza A Virus-Induced RANTES Production in A549 Cells via Blocking PI3K-Mediated Transcriptional Activation of NF-kappaB and IRF3." *Evid Based Complement Alternat Med* **2011**: 920828.

- Choppin, P. W. and A. Scheid (1979). "Role of cellular proteases in viral pathogenicity." Trans Am Clin Climatol Assoc **90**: 56-65.
- Chowaniec, W., R. B. Wescott, et al. (1972). "Interaction of *Nematospiroides dubius* and influenza virus in mice." Exp Parasitol **32**(1): 33-44.
- Christensen, J. P., R. D. Cardin, et al. (1999). "CD4(+) T cell-mediated control of a gamma-herpesvirus in B cell-deficient mice is mediated by IFN-gamma." Proc Natl Acad Sci U S A **96**(9): 5135-5140.
- Christensen, J. P. and P. C. Doherty (1999). "Quantitative analysis of the acute and long-term CD4(+) T-cell response to a persistent gammaherpesvirus." J Virol **73**(5): 4279-4283.
- Clark, I. A. (2007). "The advent of the cytokine storm." Immunol Cell Biol **85**(4): 271-273.
- Clute, S. C., Y. N. Naumov, et al. (2010). "Broad cross-reactive TCR repertoires recognizing dissimilar Epstein-Barr and influenza A virus epitopes." J Immunol **185**(11): 6753-6764.
- Cohen, C., J. Moyes, et al. (2013). "Severe influenza-associated respiratory infection in high HIV prevalence setting, South Africa, 2009-2011." Emerg Infect Dis **19**(11): 1766-1774.
- Cook, P. C., L. H. Jones, et al. (2012). "Alternatively activated dendritic cells regulate CD4(+) T-cell polarization in vitro and in vivo." Proc Natl Acad Sci U S A **109**(25): 9977-9982.
- Cooper, N. R. and G. R. Nemerow (1984). "The role of antibody and complement in the control of viral infections." J Invest Dermatol **83**(1 Suppl): 121s-127s.
- Cope, A., G. Le Friec, et al. (2011). "The Th1 life cycle: molecular control of IFN-gamma to IL-10 switching." Trends Immunol **32**(6): 278-286.
- Correale, J. and M. Farez (2007). "Association between parasite infection and immune responses in multiple sclerosis." Ann Neurol **61**(2): 97-108.
- Cox, F. E. (2001). "Concomitant infections, parasites and immune responses." Parasitology **122** Suppl: S23-38.
- Cross, T. (1996). *Medical Microbiology* 4th Edition. S. Baron, University of Texas Medical Branch at Galveston.
- D'Elia, R. V., K. Harrison, et al. (2013). "Targeting the "cytokine storm" for therapeutic benefit." Clin Vaccine Immunol **20**(3): 319-327.
- Davies, L. C., S. J. Jenkins, et al. (2013). "Tissue-resident macrophages." Nat Immunol **14**(10): 986-995.
- Davison, A. J. (2010). "Herpesvirus systematics." Vet Microbiol **143**(1): 52-69.
- de Jong, M. D., C. P. Simmons, et al. (2006). "Fatal outcome of human influenza A (H5N1) is associated with high viral load and hypercytokinemia." Nat Med **12**(10): 1203-1207.
- de Souza, D. K., B. Koudou, et al. (2012). "Diversity and transmission competence in lymphatic filariasis vectors in West Africa, and the implications for accelerated elimination of *Anopheles*-transmitted filariasis." Parasit Vectors **5**: 259.
- Decman, V., P. R. Kinchington, et al. (2005). "Gamma interferon can block herpes simplex virus type 1 reactivation from latency, even in the presence of late gene expression." J Virol **79**(16): 10339-10347.
- Deng, J., Z. Ma, et al. (2013). "Respiratory virus multiplex RT-PCR assay sensitivities and influence factors in hospitalized children with lower respiratory tract infections." Virology **458**(2): 97-102.
- Deshmane, S. L., S. Kremlev, et al. (2009). "Monocyte chemoattractant protein-1 (MCP-1): an overview." J Interferon Cytokine Res **29**(6): 313-326.
- Dias, P., F. Giannoni, et al. (2010). "CD4 T-cell help programs a change in CD8 T-cell function enabling effective long-term control of murine gammaherpesvirus 68: role of PD-1-PD-L1 interactions." J Virol **84**(16): 8241-8249.
- Dickson, J. H., K. Oegg, et al. (2000). "The omnivorous Tyrolean Iceman: colon contents (meat, cereals, pollen, moss and whipworm) and stable isotope analyses." Philos Trans R Soc Lond B Biol Sci **355**(1404): 1843-1849.
- Dienz, O., J. G. Rud, et al. (2012). "Essential role of IL-6 in protection against H1N1 influenza virus by promoting neutrophil survival in the lung." Mucosal Immunol **5**(3): 258-266.
- Dierksheide, J. E., R. A. Baiocchi, et al. (2005). "IFN-gamma gene polymorphisms associate with development of EBV+ lymphoproliferative disease in hu PBL-SCID mice." Blood **105**(4): 1558-1565.
- Dittrich, A. M., A. Erbacher, et al. (2008). "Helminth infection with *Litomosoides sigmodontis* induces regulatory T cells and inhibits allergic sensitization, airway inflammation, and hyperreactivity in a murine asthma model." J Immunol **180**(3): 1792-1799.
- Droebner, K., S. J. Reiling, et al. (2008). "Role of hypercytokinemia in NF-kappaB p50-deficient mice after H5N1 influenza A virus infection." J Virol **82**(22): 11461-11466.
- Dufour, J. H., M. Dziejman, et al. (2002). "IFN-gamma-inducible protein 10 (IP-10; CXCL10)-deficient mice reveal a role for IP-10 in effector T cell generation and trafficking." J Immunol **168**(7): 3195-3204.
- Ebrahimi, B., B. M. Dutia, et al. (2001). "Murine gammaherpesvirus-68 infection causes multi-organ fibrosis and alters leukocyte trafficking in interferon-gamma receptor knockout mice." Am J Pathol **158**(6): 2117-2125.
- Egan, J. J., J. P. Stewart, et al. (1995). "Epstein-Barr virus replication within pulmonary epithelial cells in cryptogenic fibrosing alveolitis." Thorax **50**(12): 1234-1239.
- Ekiert, D. C., A. K. Kashyap, et al. (2012). "Cross-neutralization of influenza A viruses mediated by a single antibody loop." Nature **489**(7417): 526-532.
- Elliott, D. E., T. Setiawan, et al. (2004). "*Heligmosomoides polygyrus* inhibits established colitis in IL-10-deficient mice." Eur J Immunol **34**(10): 2690-2698.

- Enders, G., M. Biber, et al. (1990). "Prevalence of antibodies to human herpesvirus 6 in different age groups, in children with exanthema subitum, other acute exanthematous childhood diseases, Kawasaki syndrome, and acute infections with other herpesviruses and HIV." *Infection* **18**(1): 12-15.
- England, P. H. (6 October 2014) "Public Health England and the NHS prepare for unpredictable flu season."
- Esper, F. P., T. Spahlinger, et al. (2011). "Rate and influence of respiratory virus co-infection on pandemic (H1N1) influenza disease." *J Infect* **63**(4): 260-266.
- Everitt, A. R., S. Clare, et al. (2012). "IFITM3 restricts the morbidity and mortality associated with influenza." *Nature* **484**(7395): 519-523.
- Fenwick, A. (2012). "The global burden of neglected tropical diseases." *Public Health* **126**(3): 233-236.
- Ferri, E., O. Bain, et al. (2011). "New insights into the evolution of Wolbachia infections in filarial nematodes inferred from a large range of screened species." *PLoS One* **6**(6): e20843.
- Feuerer, M., K. Eulenburg, et al. (2006). "Self-limitation of Th1-mediated inflammation by IFN-gamma." *J Immunol* **176**(5): 2857-2863.
- Fields, B. N., D. M. Knipe, et al. (2007). *Fields virology*. Philadelphia, Wolters Kluwer Health/Lippincott Williams & Wilkins.
- Flano, E., S. M. Husain, et al. (2000). "Latent murine gamma-herpesvirus infection is established in activated B cells, dendritic cells, and macrophages." *J Immunol* **165**(2): 1074-1081.
- Fonteneau, J. F., M. Gilliet, et al. (2003). "Activation of influenza virus-specific CD4+ and CD8+ T cells: a new role for plasmacytoid dendritic cells in adaptive immunity." *Blood* **101**(9): 3520-3526.
- Foster-Cuevas, M., G. J. Wright, et al. (2004). "Human herpesvirus 8 K14 protein mimics CD200 in down-regulating macrophage activation through CD200 receptor." *J Virol* **78**(14): 7667-7676.
- Freeman, G. J., E. J. Wherry, et al. (2006). "Reinvigorating exhausted HIV-specific T cells via PD-1-PD-1 ligand blockade." *J Exp Med* **203**(10): 2223-2227.
- Freeman, M. L., A. D. Roberts, et al. (2014). "Promotion of a subdominant CD8 T cell response during murine gammaherpesvirus 68 infection in the absence of CD4 T cell help." *J Virol* **88**(14): 7862-7869.
- Furze, R. C., T. Hussell, et al. (2006). "Amelioration of influenza-induced pathology in mice by coinfection with *Trichinella spiralis*." *Infect Immun* **74**(3): 1924-1932.
- Gangadharan, B., M. A. Hoeve, et al. (2008). "Murine gammaherpesvirus-induced fibrosis is associated with the development of alternatively activated macrophages." *J Leukoc Biol* **84**(1): 50-58.
- George, P. J., R. Anuradha, et al. (2014). "Helminth infections coincident with active pulmonary tuberculosis inhibit mono- and multifunctional CD4+ and CD8+ T cell responses in a process dependent on IL-10." *PLoS Pathog* **10**(9): e1004375.
- GeurtsvanKessel, C. H., M. A. Willart, et al. (2008). "Clearance of influenza virus from the lung depends on migratory langerin+CD11b- but not plasmacytoid dendritic cells." *J Exp Med* **205**(7): 1621-1634.
- Giannoni, F., A. Shea, et al. (2008). "CD40 engagement on dendritic cells, but not on B or T cells, is required for long-term control of murine gammaherpesvirus 68." *J Virol* **82**(22): 11016-11022.
- Gilsdorf, A. and G. Poggensee (2009). "Influenza A(H1N1)v in Germany: the first 10,000 cases." *Euro Surveill* **14**(34).
- Glimcher, L. H. and K. M. Murphy (2000). "Lineage commitment in the immune system: the T helper lymphocyte grows up." *Genes Dev* **14**(14): 1693-1711.
- Goka, E., P. Vallely, et al. (2013). "Influenza A viruses dual and multiple infections with other respiratory viruses and risk of hospitalisation and mortality." *Influenza Other Respir Viruses* **7**(6): 1079-1087.
- Goodwin, M. M., S. Canny, et al. (2010). "Murine gammaherpesvirus 68 has evolved gamma interferon and stat1-repressible promoters for the lytic switch gene 50." *J Virol* **84**(7): 3711-3717.
- Goodwin, M. M., J. M. Molleston, et al. (2010). "Histone deacetylases and the nuclear receptor corepressor regulate lytic-latent switch gene 50 in murine gammaherpesvirus 68-infected macrophages." *J Virol* **84**(22): 12039-12047.
- Gopinath, R., M. Ostrowski, et al. (2000). "Filarial infections increase susceptibility to human immunodeficiency virus infection in peripheral blood mononuclear cells in vitro." *J Infect Dis* **182**(6): 1804-1808.
- Goulding, J., A. Godlee, et al. (2011). "Lowering the threshold of lung innate immune cell activation alters susceptibility to secondary bacterial superinfection." *J Infect Dis* **204**(7): 1086-1094.
- Graham, A. L., T. J. Lamb, et al. (2005). "Malaria-filaria coinfection in mice makes malarial disease more severe unless filarial infection achieves patency." *J Infect Dis* **191**(3): 410-421.
- Graham, A. L., M. D. Taylor, et al. (2005). "Quantitative appraisal of murine filariasis confirms host strain differences but reveals that BALB/c females are more susceptible than males to *Litomosoides sigmodontis*." *Microbes Infect* **7**(4): 612-618.
- Graham, M. B., V. L. Braciale, et al. (1994). "Influenza virus-specific CD4+ T helper type 2 T lymphocytes do not promote recovery from experimental virus infection." *J Exp Med* **180**(4): 1273-1282.
- Graham, M. B., D. K. Dalton, et al. (1993). "Response to influenza infection in mice with a targeted disruption in the interferon gamma gene." *J Exp Med* **178**(5): 1725-1732.
- Greene, W., K. Kuhne, et al. (2007). "Molecular biology of KSHV in relation to AIDS-associated oncogenesis." *Cancer Treat Res* **133**: 69-127.
- Griffiths, E. C., A. B. Pedersen, et al. (2011). "The nature and consequences of coinfection in humans." *J Infect* **63**(3): 200-206.

- Gyapong, J. O., D. Kyelem, et al. (2002). "The use of spatial analysis in mapping the distribution of bancroftian filariasis in four West African countries." *Ann Trop Med Parasitol* **96**(7): 695-705.
- Hammond, M. E., G. R. Lapointe, et al. (1995). "IL-8 induces neutrophil chemotaxis predominantly via type I IL-8 receptors." *J Immunol* **155**(3): 1428-1433.
- Hay, A. J., V. Gregory, et al. (2001). "The evolution of human influenza viruses." *Philos Trans R Soc Lond B Biol Sci* **356**(1416): 1861-1870.
- Ho, A. W., N. Prabhu, et al. (2011). "Lung CD103+ dendritic cells efficiently transport influenza virus to the lymph node and load viral antigen onto MHC class I for presentation to CD8 T cells." *J Immunol* **187**(11): 6011-6021.
- Hoffmann, W., G. Petit, et al. (2000). "Litomosoides sigmodontis in mice: reappraisal of an old model for filarial research." *Parasitol Today* **16**(9): 387-389.
- Hoffmann, W. H., A. W. Pfaff, et al. (2001). "Determinants for resistance and susceptibility to microfilariemia in Litomosoides sigmodontis filariasis." *Parasitology* **122**(Pt 6): 641-649.
- Horner, G. J. and F. D. Gray, Jr. (1973). "Effect of uncomplicated, presumptive influenza on the diffusing capacity of the lung." *Am Rev Respir Dis* **108**(4): 866-869.
- Hotez, P. J., D. H. Molyneux, et al. (2007). "Control of neglected tropical diseases." *N Engl J Med* **357**(10): 1018-1027.
- Hsieh, Y. J., C. L. Fu, et al. (2014). "Helminth-induced interleukin-4 abrogates invariant natural killer T cell activation-associated clearance of bacterial infection." *Infect Immun* **82**(5): 2087-2097.
- Hu, X., P. K. Paik, et al. (2006). "IFN-gamma suppresses IL-10 production and synergizes with TLR2 by regulating GSK3 and CREB/AP-1 proteins." *Immunity* **24**(5): 563-574.
- Huang, S., W. Hendriks, et al. (1993). "Immune response in mice that lack the interferon-gamma receptor." *Science* **259**(5102): 1742-1745.
- Huber, V. C., R. M. McKeon, et al. (2006). "Distinct contributions of vaccine-induced immunoglobulin G1 (IgG1) and IgG2a antibodies to protective immunity against influenza." *Clin Vaccine Immunol* **13**(9): 981-990.
- Hubner, M. P., K. E. Killoran, et al. (2012). "Chronic helminth infection does not exacerbate Mycobacterium tuberculosis infection." *PLoS Negl Trop Dis* **6**(12): e1970.
- Hubner, M. P., B. Pasche, et al. (2008). "Microfilariae of the filarial nematode Litomosoides sigmodontis exacerbate the course of lipopolysaccharide-induced sepsis in mice." *Infect Immun* **76**(4): 1668-1677.
- Hubner, M. P., M. N. Torrero, et al. (2009). "Litomosoides sigmodontis: a simple method to infect mice with L3 larvae obtained from the pleural space of recently infected jirds (Meriones unguiculatus)." *Exp Parasitol* **123**(1): 95-98.
- Hughes, D. J., A. Kipar, et al. (2010). "Pathogenesis of a model gammaherpesvirus in a natural host." *J Virol* **84**(8): 3949-3961.
- Hui, K. P., S. M. Lee, et al. (2009). "Induction of proinflammatory cytokines in primary human macrophages by influenza A virus (H5N1) is selectively regulated by IFN regulatory factor 3 and p38 MAPK." *J Immunol* **182**(2): 1088-1098.
- Hwang, S., T. T. Wu, et al. (2008). "Persistent gammaherpesvirus replication and dynamic interaction with the host in vivo." *J Virol* **82**(24): 12498-12509.
- Ichikawa, A., K. Kuba, et al. (2013). "CXCL10-CXCR3 enhances the development of neutrophil-mediated fulminant lung injury of viral and nonviral origin." *Am J Respir Crit Care Med* **187**(1): 65-77.
- Ichinohe, T., H. K. Lee, et al. (2009). "Inflammasome recognition of influenza virus is essential for adaptive immune responses." *J Exp Med* **206**(1): 79-87.
- Isobe, Y., K. Sugimoto, et al. (2004). "Epstein-Barr virus infection of human natural killer cell lines and peripheral blood natural killer cells." *Cancer Res* **64**(6): 2167-2174.
- Ito, S., P. Ansari, et al. (1999). "Interleukin-10 inhibits expression of both interferon alpha- and interferon gamma-induced genes by suppressing tyrosine phosphorylation of STAT1." *Blood* **93**(5): 1456-1463.
- Jeisy-Scott, V., W. G. Davis, et al. (2011). "Increased MDSC accumulation and Th2 biased response to influenza A virus infection in the absence of TLR7 in mice." *PLoS One* **6**(9): e25242.
- Johnson, H. M. and C. M. Seifert (1998). "Updating accounts following a correction of misinformation." *J Exp Psychol Learn Mem Cogn* **24**(6): 1483-1494.
- Julkunen, I., T. Sareneva, et al. (2001). "Molecular pathogenesis of influenza A virus infection and virus-induced regulation of cytokine gene expression." *Cytokine Growth Factor Rev* **12**(2-3): 171-180.
- Kaiser, L., R. S. Fritz, et al. (2001). "Symptom pathogenesis during acute influenza: interleukin-6 and other cytokine responses." *J Med Virol* **64**(3): 262-268.
- Kamal, S. M. and K. El Sayed Khalifa (2006). "Immune modulation by helminthic infections: worms and viral infections." *Parasite Immunol* **28**(10): 483-496.
- Kaplan, M. H., J. R. Whitfield, et al. (1998). "Th2 cells are required for the Schistosoma mansoni egg-induced granulomatous response." *J Immunol* **160**(4): 1850-1856.
- Karadjian, G., D. Berrebi, et al. (2014). "Co-infection restrains Litomosoides sigmodontis filarial load and plasmodial P. yoelii but not P. chabaudi parasitaemia in mice." *Parasite* **21**: 16.
- Kash, J. C., K. A. Walters, et al. (2011). "Lethal synergism of 2009 pandemic H1N1 influenza virus and Streptococcus pneumoniae coinfection is associated with loss of murine lung repair responses." *MBio* **2**(5).

- Kim, P. S. and R. Ahmed (2010). "Features of responding T cells in cancer and chronic infection." *Curr Opin Immunol* **22**(2): 223-230.
- Kim, T. S. and T. J. Braciale (2009). "Respiratory dendritic cell subsets differ in their capacity to support the induction of virus-specific cytotoxic CD8+ T cell responses." *PLoS One* **4**(1): e4204.
- Kitagaki, K., T. R. Businga, et al. (2006). "Intestinal helminths protect in a murine model of asthma." *J Immunol* **177**(3): 1628-1635.
- Kourilsky, P. and P. Truffa-Bachi (2001). "Cytokine fields and the polarization of the immune response." *Trends Immunol* **22**(9): 502-509.
- Kristensen, N. N., A. N. Madsen, et al. (2004). "Cytokine production by virus-specific CD8(+) T cells varies with activation state and localization, but not with TCR avidity." *J Gen Virol* **85**(Pt 6): 1703-1712.
- Kullberg, M. C., E. J. Pearce, et al. (1992). "Infection with *Schistosoma mansoni* alters Th1/Th2 cytokine responses to a non-parasite antigen." *J Immunol* **148**(10): 3264-3270.
- Labonte, A. C., A. C. Tosello-Trampont, et al. (2014). "The role of macrophage polarization in infectious and inflammatory diseases." *Mol Cells* **37**(4): 275-285.
- Lamb, T. J., A. L. Graham, et al. (2005). "Co-infected C57BL/6 mice mount appropriately polarized and compartmentalized cytokine responses to *Litomosoides sigmodontis* and *Leishmania major* but disease progression is altered." *Parasite Immunol* **27**(9): 317-324.
- Lampe, M. F., C. B. Wilson, et al. (1998). "Gamma interferon production by cytotoxic T lymphocytes is required for resolution of *Chlamydia trachomatis* infection." *Infect Immun* **66**(11): 5457-5461.
- Lass, S., P. J. Hudson, et al. (2013). "Generating super-shedders: co-infection increases bacterial load and egg production of a gastrointestinal helminth." *J R Soc Interface* **10**(80): 20120588.
- Law, A. H., D. C. Lee, et al. (2010). "Cellular response to influenza virus infection: a potential role for autophagy in CXCL10 and interferon-alpha induction." *Cell Mol Immunol* **7**(4): 263-270.
- Lebre, M. C., T. Burwell, et al. (2005). "Differential expression of inflammatory chemokines by Th1- and Th2-cell promoting dendritic cells: a role for different mature dendritic cell populations in attracting appropriate effector cells to peripheral sites of inflammation." *Immunol Cell Biol* **83**(5): 525-535.
- Lee, E. H., C. Wu, et al. (2010). "Fatalities associated with the 2009 H1N1 influenza A virus in New York city." *Clin Infect Dis* **50**(11): 1498-1504.
- Lee, L. Y., L. A. Ha do, et al. (2008). "Memory T cells established by seasonal human influenza A infection cross-react with avian influenza A (H5N1) in healthy individuals." *J Clin Invest* **118**(10): 3478-3490.
- Lee, N. L. (2009). "Role of cytokines and chemokines in severe and complicated influenza infections." *Hong Kong Med J* **15 Suppl 8**: 38-41.
- Lemaitre, M., L. Watier, et al. (2014). "Coinfection with *Plasmodium falciparum* and *Schistosoma haematobium*: additional evidence of the protective effect of Schistosomiasis on malaria in Senegalese children." *Am J Trop Med Hyg* **90**(2): 329-334.
- Leon, B., J. E. Bradley, et al. (2014). "FoxP3+ regulatory T cells promote influenza-specific Tfh responses by controlling IL-2 availability." *Nat Commun* **5**: 3495.
- Ley, K. (2014). "The second touch hypothesis: T cell activation, homing and polarization." *F1000Res* **3**: 37.
- Li, W., B. Moltedo, et al. (2012). "Type I interferon induction during influenza virus infection increases susceptibility to secondary *Streptococcus pneumoniae* infection by negative regulation of gammadelta T cells." *J Virol* **86**(22): 12304-12312.
- Liang, X., R. L. Crepeau, et al. (2013). "CD4 and CD8 T cells directly recognize murine gammaherpesvirus 68-immortalized cells and prevent tumor outgrowth." *J Virol* **87**(10): 6051-6054.
- Linterman, M. A., L. Beaton, et al. (2010). "IL-21 acts directly on B cells to regulate Bcl-6 expression and germinal center responses." *J Exp Med* **207**(2): 353-363.
- Liu, M. T., D. Armstrong, et al. (2001). "Expression of Mig (monokine induced by interferon-gamma) is important in T lymphocyte recruitment and host defense following viral infection of the central nervous system." *J Immunol* **166**(3): 1790-1795.
- Liu, T., K. M. Khanna, et al. (2000). "CD8(+) T cells can block herpes simplex virus type 1 (HSV-1) reactivation from latency in sensory neurons." *J Exp Med* **191**(9): 1459-1466.
- Luthje, K., A. Kallies, et al. (2012). "The development and fate of follicular helper T cells defined by an IL-21 reporter mouse." *Nat Immunol* **13**(5): 491-498.
- Lv, J., Y. Hua, et al. (2014). "Kinetics of pulmonary immune cells, antibody responses and their correlations with the viral clearance of influenza A fatal infection in mice." *Virol J* **11**: 57.
- MacDonald, A. S., M. I. Araujo, et al. (2002). "Immunology of parasitic helminth infections." *Infect Immun* **70**(2): 427-433.
- Madhi, S. A., B. Schoub, et al. (2000). "Increased burden of respiratory viral associated severe lower respiratory tract infections in children infected with human immunodeficiency virus type-1." *J Pediatr* **137**(1): 78-84.
- Marechal, P., L. Le Goff, et al. (1997). "Immune response to the filaria *Litomosoides sigmodontis* in susceptible and resistant mice." *Parasite Immunol* **19**(6): 273-279.
- Marechal, P., L. Le Goff, et al. (1996). "The fate of the filaria *Litomosoides sigmodontis* in susceptible and naturally resistant mice." *Parasite* **3**(1): 25-31.

- Maroof, A., Y. M. Yorgensen, et al. (2014). "Intranasal vaccination promotes detrimental Th17-mediated immunity against influenza infection." *PLoS Pathog* **10**(1): e1003875.
- Marsland, B. J., N. Schmitz, et al. (2005). "IL-4/alpha signaling is important for CD8+ T cell cytotoxicity in the absence of CD4+ T cell help." *Eur J Immunol* **35**(5): 1391-1398.
- Martin, J. N. (2007). *The epidemiology of KSHV and its association with malignant disease*.
- Masuzawa, T., Y. Beppu, et al. (1992). "Experimental *Borrelia burgdorferi* infection of outbred mice." *J Clin Microbiol* **30**(11): 3016-3018.
- Matheu, M. P., J. R. Teijaro, et al. (2013). "Three phases of CD8 T cell response in the lung following H1N1 influenza infection and sphingosine 1 phosphate agonist therapy." *PLoS One* **8**(3): e58033.
- McCullers, J. A. (2006). "Insights into the interaction between influenza virus and pneumococcus." *Clin Microbiol Rev* **19**(3): 571-582.
- McCullers, J. A. (2014). "The co-pathogenesis of influenza viruses with bacteria in the lung." *Nat Rev Microbiol* **12**(4): 252-262.
- McCullers, J. A. and E. I. Tuomanen (2001). "Molecular pathogenesis of pneumococcal pneumonia." *Front Biosci* **6**: D877-889.
- McGeoch, D. J., F. J. Rixon, et al. (2006). "Topics in herpesvirus genomics and evolution." *Virus Res* **117**(1): 90-104.
- McGill, J., N. Van Rooijen, et al. (2008). "Protective influenza-specific CD8 T cell responses require interactions with dendritic cells in the lungs." *J Exp Med* **205**(7): 1635-1646.
- McKenna, J. J., A. M. Bramley, et al. (2013). "Asthma in patients hospitalized with pandemic influenza A(H1N1)pdm09 virus infection-United States, 2009." *BMC Infect Dis* **13**: 57.
- McKinstry, K. K., T. M. Strutt, et al. (2010). "The potential of CD4 T-cell memory." *Immunology* **130**(1): 1-9.
- Metkar, S. S., C. Menaa, et al. (2008). "Human and mouse granzyme A induce a proinflammatory cytokine response." *Immunity* **29**(5): 720-733.
- Metzger, J. A. (2014). "Adaptive defense mechanisms: function and transcendence." *J Clin Psychol* **70**(5): 478-488.
- Mikhak, Z., J. P. Strassner, et al. (2013). "Lung dendritic cells imprint T cell lung homing and promote lung immunity through the chemokine receptor CCR4." *J Exp Med* **210**(9): 1855-1869.
- Milligan, G. N. and D. I. Bernstein (1997). "Interferon-gamma enhances resolution of herpes simplex virus type 2 infection of the murine genital tract." *Virology* **229**(1): 259-268.
- Mills, C. E., J. M. Robins, et al. (2004). "Transmissibility of 1918 pandemic influenza." *Nature* **432**(7019): 904-906.
- Min-Oo, G. and L. L. Lanier (2014). "Cytomegalovirus generates long-lived antigen-specific NK cells with diminished bystander activation to heterologous infection." *J Exp Med* **211**(13): 2669-2680.
- Mishra, P. K., N. Patel, et al. (2013). "Prevention of type 1 diabetes through infection with an intestinal nematode parasite requires IL-10 in the absence of a Th2-type response." *Mucosal Immunol* **6**(2): 297-308.
- Monteiro, J. M., C. Harvey, et al. (1998). "Role of interleukin-12 in primary influenza virus infection." *J Virol* **72**(6): 4825-4831.
- Mora, A. L., E. Torres-Gonzalez, et al. (2006). "Activation of alveolar macrophages via the alternative pathway in herpesvirus-induced lung fibrosis." *Am J Respir Cell Mol Biol* **35**(4): 466-473.
- Mordstein, M., G. Kochs, et al. (2008). "Interferon-lambda contributes to innate immunity of mice against influenza A virus but not against hepatotropic viruses." *PLoS Pathog* **4**(9): e1000151.
- Morens, D. M., J. K. Taubenberger, et al. (2008). "Predominant role of bacterial pneumonia as a cause of death in pandemic influenza: implications for pandemic influenza preparedness." *J Infect Dis* **198**(7): 962-970.
- Mozdzanowska, K., M. Furchner, et al. (2005). "Roles of CD4+ T-cell-independent and -dependent antibody responses in the control of influenza virus infection: evidence for noncognate CD4+ T-cell activities that enhance the therapeutic activity of antiviral antibodies." *J Virol* **79**(10): 5943-5951.
- A. Muhlethaler-Mottet, W. Di Berardino, L.A. Otten, et al. Activation of the MHC class II transactivator CIITA by interferon-gamma requires cooperative interaction between Stat1 and USF-1 *Immunity*, **8** (1998), pp. 157-166
- Murphy, K. (2011). *Janeway's Immunobiology*.
- Nakamura, S., K. M. Davis, et al. (2011). "Synergistic stimulation of type I interferons during influenza virus coinfection promotes *Streptococcus pneumoniae* colonization in mice." *J Clin Invest* **121**(9): 3657-3665.
- Nash, A. A., B. M. Dutia, et al. (2001). "Natural history of murine gamma-herpesvirus infection." *Philos Trans R Soc Lond B Biol Sci* **356**(1408): 569-579.
- Nayak, D. P., G. W. Kelley, et al. (1964). "The Enhancing Effect of Swine Lungworms on Swine Influenza Infections." *Cornell Vet* **54**: 160-175.
- Nelson, F. K., D. L. Greiner, et al. (1991). "The immunodeficient scid mouse as a model for human lymphatic filariasis." *J Exp Med* **173**(3): 659-663.
- Neurath, M. F., S. Finotto, et al. (2002). "The role of Th1/Th2 polarization in mucosal immunity." *Nat Med* **8**(6): 567-573.
- Ngoi, S. M., M. C. St Rose, et al. (2012). "Presensitizing with a Toll-like receptor 3 ligand impairs CD8 T-cell effector differentiation and IL-33 responsiveness." *Proc Natl Acad Sci U S A* **109**(26): 10486-10491.
- Nguyen YN, McGuffie BA, Anderson VE, Weinberg JB. Gammaherpesvirus Modulation of Mouse Adenovirus Type 1 Pathogenesis. *Virology*. 2008;380(2):182-190. doi:10.1016/j.virol.2008.07.031. Nicol, M. Q. and B. M. Dutia (2014). "The role of macrophages in influenza A virus infection." *Future Virol* **9**(9): 847-862.

- Nielsen, N. O., P. E. Simonsen, et al. (2006). "Cross-sectional relationship between HIV, lymphatic filariasis and other parasitic infections in adults in coastal northeastern Tanzania." *Trans R Soc Trop Med Hyg* **100**(6): 543-550.
- Nilsson, C., A. Linde, et al. (2005). "Does early EBV infection protect against IgE sensitization?" *J Allergy Clin Immunol* **116**(2): 438-444.
- O'Brien, K. B., S. Schultz-Cherry, et al. (2011). "Parasite-mediated upregulation of NK cell-derived gamma interferon protects against severe highly pathogenic H5N1 influenza virus infection." *J Virol* **85**(17): 8680-8688.
- Oh, S. and M. C. Eichelberger (2000). "Polarization of allogeneic T-cell responses by influenza virus-infected dendritic cells." *J Virol* **74**(17): 7738-7744.
- Okada, H., C. Kuhn, et al. (2010). "The 'hygiene hypothesis' for autoimmune and allergic diseases: an update." *Clin Exp Immunol* **160**(1): 1-9.
- Osborne, L. C., L. A. Monticelli, et al. (2014). "Coinfection. Virus-helminth coinfection reveals a microbiota-independent mechanism of immunomodulation." *Science* **345**(6196): 578-582.
- Palm, N. W., R. K. Rosenstein, et al. (2012). "Allergic host defences." *Nature* **484**(7395): 465-472.
- Paludan, C., K. Bickham, et al. (2002). "Epstein-Barr nuclear antigen 1-specific CD4(+) Th1 cells kill Burkitt's lymphoma cells." *J Immunol* **169**(3): 1593-1603.
- Pamer, E. G. (2009). "Tipping the balance in favor of protective immunity during influenza virus infection." *Proc Natl Acad Sci U S A* **106**(13): 4961-4962.
- Paquette, S. G., D. Banner, et al. (2012). "Interleukin-6 is a potential biomarker for severe pandemic H1N1 influenza A infection." *PLoS One* **7**(6): e38214.
- Pawlowski, A., M. Jansson, et al. (2012). "Tuberculosis and HIV co-infection." *PLoS Pathog* **8**(2): e1002464.
- Peacey, M., R. J. Hall, et al. (2010). "Pandemic (H1N1) 2009 and seasonal influenza A (H1N1) co-infection, New Zealand, 2009." *Emerg Infect Dis* **16**(10): 1618-1620.
- Pearce, E. J. and A. S. MacDonald (2002). "The immunobiology of schistosomiasis." *Nat Rev Immunol* **2**(7): 499-511.
- Peiris, J. S., W. C. Yu, et al. (2004). "Re-emergence of fatal human influenza A subtype H5N1 disease." *Lancet* **363**(9409): 617-619.
- Pellet, B. R. P. E. (2001). *Herpesviridae*. Fields Virology.
- Peperzak, V., E. A. Veraar, et al. (2013). "CD8+ T cells produce the chemokine CXCL10 in response to CD27/CD70 costimulation to promote generation of the CD8+ effector T cell pool." *J Immunol* **191**(6): 3025-3036.
- Perrone, L. A., K. J. Szretter, et al. (2010). "Mice lacking both TNF and IL-1 receptors exhibit reduced lung inflammation and delay in onset of death following infection with a highly virulent H5N1 virus." *J Infect Dis* **202**(8): 1161-1170.
- Petney, T. N. and R. H. Andrews (1998). "Multiparasite communities in animals and humans: frequency, structure and pathogenic significance." *Int J Parasitol* **28**(3): 377-393.
- Pothlichet, J., M. Chignard, et al. (2008). "Cutting edge: innate immune response triggered by influenza A virus is negatively regulated by SOCS1 and SOCS3 through a RIG-I/IFNAR1-dependent pathway." *J Immunol* **180**(4): 2034-2038.
- Prabhu, N., A. W. Ho, et al. (2013). "Gamma interferon regulates contraction of the influenza virus-specific CD8 T cell response and limits the size of the memory population." *J Virol* **87**(23): 12510-12522.
- Prakash, G., R. K. Gupta, et al. (2011). "Concurrent infection of candidiasis and strongyloidiasis in an endoscopic biopsy in an immunocompetent host." *Indian J Pathol Microbiol* **54**(3): 644-645.
- Pullan, R. and S. Brooker (2008). "The health impact of polyparasitism in humans: are we under-estimating the burden of parasitic diseases?" *Parasitology* **135**(7): 783-794.
- Quinnell, R. J. (2003). "Genetics of susceptibility to human helminth infection." *Int J Parasitol* **33**(11): 1219-1231.
- Raison, C. L., C. A. Lowry, et al. (2010). "Inflammation, sanitation, and consternation: loss of contact with coevolved, tolerogenic microorganisms and the pathophysiology and treatment of major depression." *Arch Gen Psychiatry* **67**(12): 1211-1224.
- Ramaiah, K. D., P. K. Das, et al. (2000). "The economic burden of lymphatic filariasis in India." *Parasitol Today* **16**(6): 251-253.
- Randolph, A. G., F. Vaughn, et al. (2011). "Critically ill children during the 2009-2010 influenza pandemic in the United States." *Pediatrics* **128**(6): e1450-1458.
- Raso, G., A. Luginbuhl, et al. (2004). "Multiple parasite infections and their relationship to self-reported morbidity in a community of rural Cote d'Ivoire." *Int J Epidemiol* **33**(5): 1092-1102.
- Raz, E. (2007). "Organ-specific regulation of innate immunity." *Nat Immunol* **8**(1): 3-4.
- Reece, J. J., M. C. Siracusa, et al. (2006). "Innate immune responses to lung-stage helminth infection induce alternatively activated alveolar macrophages." *Infect Immun* **74**(9): 4970-4981.
- Reese, T. A., B. S. Wakeman, et al. (2014). "Coinfection. Helminth infection reactivates latent gamma-herpesvirus via cytokine competition at a viral promoter." *Science* **345**(6196): 573-577.
- Reese, T. A., B. S. Wakeman, et al. (2014). "Helminth infection reactivates latent gamma-herpesvirus via cytokine competition at a viral promoter." *Science*.
- Renegar, K. B., P. A. Small, Jr., et al. (2004). "Role of IgA versus IgG in the control of influenza viral infection in the murine respiratory tract." *J Immunol* **173**(3): 1978-1986.

- Reynolds, L. A., K. J. Filbey, et al. (2012). "Immunity to the model intestinal helminth parasite *Heligmosomoides polygyrus*." *Semin Immunopathol* **34**(6): 829-846.
- Rice, T. W., L. Rubinson, et al. (2012). "Critical illness from 2009 pandemic influenza A virus and bacterial coinfection in the United States." *Crit Care Med* **40**(5): 1487-1498.
- Richards, K. A., F. A. Chaves, et al. (2011). "The memory phase of the CD4 T-cell response to influenza virus infection maintains its diverse antigen specificity." *Immunology* **133**(2): 246-256.
- Ridge, J. P., F. Di Rosa, et al. (1998). "A conditioned dendritic cell can be a temporal bridge between a CD4+ T-helper and a T-killer cell." *Nature* **393**(6684): 474-478.
- Riley, J. L., K. Schlienger, et al. (2000). "Modulation of susceptibility to HIV-1 infection by the cytotoxic T lymphocyte antigen 4 costimulatory molecule." *J Exp Med* **191**(11): 1987-1997.
- Rochford, R., M. L. Lutzke, et al. (2001). "Kinetics of murine gammaherpesvirus 68 gene expression following infection of murine cells in culture and in mice." *J Virol* **75**(11): 4955-4963.
- Roman, E., E. Miller, et al. (2002). "CD4 effector T cell subsets in the response to influenza: heterogeneity, migration, and function." *J Exp Med* **196**(7): 957-968.
- Rook, G. A. and A. Dalgleish (2011). "Infection, immunoregulation, and cancer." *Immunol Rev* **240**(1): 141-159.
- Rook, G. A., C. A. Lowry, et al. (2013). "Microbial 'Old Friends', immunoregulation and stress resilience." *Evol Med Public Health* **2013**(1): 46-64.
- Roth, M. D. and S. H. Golub (1993). "Human pulmonary macrophages utilize prostaglandins and transforming growth factor beta 1 to suppress lymphocyte activation." *J Leukoc Biol* **53**(4): 366-371.
- Saadoun, S., M. C. Papadopoulos, et al. (2005). "Involvement of aquaporin-4 in astroglial cell migration and glial scar formation." *J Cell Sci* **118**(Pt 24): 5691-5698.
- Saefel, M., M. Arndt, et al. (2003). "Synergism of gamma interferon and interleukin-5 in the control of murine filariasis." *Infect Immun* **71**(12): 6978-6985.
- Saini, P., P. Gayen, et al. (2014). "Antifilarial effect of ursolic acid from *Nyctanthes arbortristis*: Molecular and biochemical evidences." *Parasitol Int* **63**(5): 717-728.
- Saito, F., T. Ito, et al. (2013). "MHV68 latency modulates the host immune response to influenza A virus." *Inflammation* **36**(6): 1295-1303.
- Salgame, P., G. S. Yap, et al. (2013). "Effect of helminth-induced immunity on infections with microbial pathogens." *Nat Immunol* **14**(11): 1118-1126.
- Salvador, A. R., E. Guivier, et al. (2011). "Concomitant influence of helminth infection and landscape on the distribution of Puumala hantavirus in its reservoir, *Myodes glareolus*." *BMC Microbiol* **11**(1): 30.
- Samarasinghe, A. E., S. N. Woolard, et al. (2014). "The immune profile associated with acute allergic asthma accelerates clearance of influenza virus." *Immunol Cell Biol* **92**(5): 449-459.
- Sandalova, E., D. Laccabue, et al. (2010). "Contribution of herpesvirus specific CD8 T cells to anti-viral T cell response in humans." *PLoS Pathog* **6**(8): e1001051.
- Sarawar, S. R., R. D. Cardin, et al. (1997). "Gamma interferon is not essential for recovery from acute infection with murine gammaherpesvirus 68." *J Virol* **71**(5): 3916-3921.
- Schmitz, N., M. Kurrer, et al. (2005). "Interleukin-1 is responsible for acute lung immunopathology but increases survival of respiratory influenza virus infection." *J Virol* **79**(10): 6441-6448.
- Schroder, K., P. J. Hertzog, T. Ravasi, and D. A. Hume. 2004. Interferongamma: an overview of signals, mechanisms and functions. *J. Leukoc. Biol.* **75**: 163-189
- Semple, S. J., S. A. Strathdee, et al. (2011). "Methamphetamine-using parents: the relationship between parental role strain and depressive symptoms." *J Stud Alcohol Drugs* **72**(6): 954-964.
- Seo, S. H. and R. G. Webster (2002). "Tumor necrosis factor alpha exerts powerful anti-influenza virus effects in lung epithelial cells." *J Virol* **76**(3): 1071-1076.
- Shimeld, C., J. L. Whiteland, et al. (1997). "Cytokine production in the nervous system of mice during acute and latent infection with herpes simplex virus type 1." *J Gen Virol* **78** (Pt 12): 3317-3325.
- Simas, J. P. and S. Efsthathiou (1998). "Murine gammaherpesvirus 68: a model for the study of gammaherpesvirus pathogenesis." *Trends Microbiol* **6**(7): 276-282.
- Slater, H. C., M. Gambhir, et al. (2013). "Modelling co-infection with malaria and lymphatic filariasis." *PLoS Comput Biol* **9**(6): e1003096.
- Small, C. L., C. R. Shaler, et al. (2010). "Influenza infection leads to increased susceptibility to subsequent bacterial superinfection by impairing NK cell responses in the lung." *J Immunol* **184**(4): 2048-2056.
- Smed-Sorensen, A., C. Chalouni, et al. (2012). "Influenza A virus infection of human primary dendritic cells impairs their ability to cross-present antigen to CD8 T cells." *PLoS Pathog* **8**(3): e1002572.
- Smith, A. M., F. R. Adler, et al. (2013). "Kinetics of coinfection with influenza A virus and *Streptococcus pneumoniae*." *PLoS Pathog* **9**(3): e1003238.
- Snelgrove, R. J., A. Godlee, et al. (2011). "Airway immune homeostasis and implications for influenza-induced inflammation." *Trends Immunol* **32**(7): 328-334.
- Snelgrove, R. J., J. Goulding, et al. (2008). "A critical function for CD200 in lung immune homeostasis and the severity of influenza infection." *Nat Immunol* **9**(9): 1074-1083.
- Sparks-Thissen, R. L., D. C. Braaten, et al. (2004). "An optimized CD4 T-cell response can control productive and latent gammaherpesvirus infection." *J Virol* **78**(13): 6827-6835.

- Spencer, L., L. Shultz, et al. (2001). "Interleukin-4 receptor-Stat6 signaling in murine infections with a tissue-dwelling nematode parasite." *Infect Immun* **69**(12): 7743-7752.
- Staehele, P., R. Grob, et al. (1988). "Influenza virus-susceptible mice carry Mx genes with a large deletion or a nonsense mutation." *Mol Cell Biol* **8**(10): 4518-4523.
- Steed, A. L., E. S. Barton, et al. (2006). "Gamma interferon blocks gammaherpesvirus reactivation from latency." *J Virol* **80**(1): 192-200.
- Steel, C. and T. B. Nutman (2003). "CTLA-4 in filarial infections: implications for a role in diminished T cell reactivity." *J Immunol* **170**(4): 1930-1938.
- Stefanska, I., M. Romanowska, et al. (2013). "Co-infections with influenza and other respiratory viruses." *Adv Exp Med Biol* **756**: 291-301.
- Steinmuller, C., G. Franke-Ullmann, et al. (2000). "Local activation of nonspecific defense against a respiratory model infection by application of interferon-gamma: comparison between rat alveolar and interstitial lung macrophages." *Am J Respir Cell Mol Biol* **22**(4): 481-490.
- Stewart, J. P., E. J. Usherwood, et al. (1998). "Lung epithelial cells are a major site of murine gammaherpesvirus persistence." *J Exp Med* **187**(12): 1941-1951.
- Stuller, K. A., S. S. Cush, et al. (2010). "Persistent gamma-herpesvirus infection induces a CD4 T cell response containing functionally distinct effector populations." *J Immunol* **184**(7): 3850-3856.
- Stuller, K. A. and E. Flano (2009). "CD4 T cells mediate killing during persistent gammaherpesvirus 68 infection." *J Virol* **83**(9): 4700-4703.
- Summers, R. W., D. E. Elliott, et al. (2005). "Trichuris suis therapy in Crohn's disease." *Gut* **54**(1): 87-90.
- Sun, J., R. Madan, et al. (2009). "Effector T cells control lung inflammation during acute influenza virus infection by producing IL-10." *Nat Med* **15**(3): 277-284.
- Sun, K. and D. W. Metzger (2008). "Inhibition of pulmonary antibacterial defense by interferon-gamma during recovery from influenza infection." *Nat Med* **14**(5): 558-564.
- Sunil-Chandra, N. P., S. Efstathiou, et al. (1992). "Virological and pathological features of mice infected with murine gamma-herpesvirus 68." *J Gen Virol* **73** (Pt 9): 2347-2356.
- Suswillo, R. R., D. G. Owen, et al. (1980). "Infections of *Brugia pahangi* in conventional and nude (athymic) mice." *Acta Trop* **37**(4): 327-335.
- Sylwester, A. W., B. L. Mitchell, et al. (2005). "Broadly targeted human cytomegalovirus-specific CD4+ and CD8+ T cells dominate the memory compartments of exposed subjects." *J Exp Med* **202**(5): 673-685.
- Talaat, K. R., N. Kumarasamy, et al. (2008). "Filarial/human immunodeficiency virus coinfection in urban southern India." *Am J Trop Med Hyg* **79**(4): 558-560.
- Tan, L. C., N. Gudgeon, et al. (1999). "A re-evaluation of the frequency of CD8+ T cells specific for EBV in healthy virus carriers." *J Immunol* **162**(3): 1827-1835.
- Tate, M. D., H. C. Schilter, et al. (2011). "Responses of mouse airway epithelial cells and alveolar macrophages to virulent and avirulent strains of influenza A virus." *Viral Immunol* **24**(2): 77-88.
- Taubenberger, J. K. and D. M. Morens (2008). "The pathology of influenza virus infections." *Annu Rev Pathol* **3**: 499-522.
- Taubert, A. and H. Zahner (2001). "Cellular immune responses of filaria (*Litomosoides sigmodontis*) infected BALB/c mice detected on the level of cytokine transcription." *Parasite Immunol* **23**(8): 453-462.
- Taylor, M. D., A. Harris, et al. (2007). "CTLA-4 and CD4+ CD25+ regulatory T cells inhibit protective immunity to filarial parasites in vivo." *J Immunol* **179**(7): 4626-4634.
- Taylor, M. J., A. Hoerauf, et al. (2010). "Lymphatic filariasis and onchocerciasis." *Lancet* **376**(9747): 1175-1185.
- Taylor, P. M., J. Davey, et al. (1987). "Class I MHC molecules rather than other mouse genes dictate influenza epitope recognition by cytotoxic T cells." *Immunogenetics* **26**(4-5): 267-272.
- Teixeira, L. K., B. P. Fonseca, et al. (2005). "The role of interferon-gamma on immune and allergic responses." *Mem Inst Oswaldo Cruz* **100** Suppl 1: 137-144.
- Teixeira, L. K., B. P. Fonseca, et al. (2005). "IFN-gamma production by CD8+ T cells depends on NFAT1 transcription factor and regulates Th differentiation." *J Immunol* **175**(9): 5931-5939.
- Thepen, T., G. Kraal, et al. (1994). "The role of alveolar macrophages in regulation of lung inflammation." *Ann N Y Acad Sci* **725**: 200-206.
- Torres, S. F., T. Iolster, et al. (2012). "High mortality in patients with influenza A pH1N1 2009 admitted to a pediatric intensive care unit: a predictive model of mortality." *Pediatr Crit Care Med* **13**(2): e78-83.
- Torti, N. and A. Oxenius (2012). "T cell memory in the context of persistent herpes viral infections." *Viruses* **4**(7): 1116-1143.
- Treanor, J. (2004). "Influenza vaccine--outmaneuvering antigenic shift and drift." *N Engl J Med* **350**(3): 218-220.
- Tripp, R. A., A. M. Hamilton-Easton, et al. (1997). "Pathogenesis of an infectious mononucleosis-like disease induced by a murine gamma-herpesvirus: role for a viral superantigen?" *J Exp Med* **185**(9): 1641-1650.
- Tripp, R. A., S. R. Sarawar, et al. (1995). "Characteristics of the influenza virus-specific CD8+ T cell response in mice homozygous for disruption of the H-2IAb gene." *J Immunol* **155**(6): 2955-2959.
- Tsai, C. Y., Z. Hu, et al. (2011). "Strain-dependent requirement for IFN-gamma for respiratory control and immunotherapy in murine gammaherpesvirus infection." *Viral Immunol* **24**(4): 273-280.

- Uetani, K., M. Hiroi, et al. (2008). "Influenza A virus abrogates IFN-gamma response in respiratory epithelial cells by disruption of the Jak/Stat pathway." *Eur J Immunol* **38**(6): 1559-1573.
- Upham, J. W., D. H. Strickland, et al. (1995). "Alveolar macrophages from humans and rodents selectively inhibit T-cell proliferation but permit T-cell activation and cytokine secretion." *Immunology* **84**(1): 142-147.
- Van Campen, H. (1994). "Influenza A virus replication is inhibited by tumor necrosis factor-alpha in vitro." *Arch Virol* **136**(3-4): 439-446.
- van den Biggelaar, A. H., R. van Ree, et al. (2000). "Decreased atopy in children infected with *Schistosoma haematobium*: a role for parasite-induced interleukin-10." *Lancet* **356**(9243): 1723-1727.
- van Hellemond, J. J., A. G. Vonk, et al. (2013). "Association of eumycetoma and schistosomiasis." *PLoS Negl Trop Dis* **7**(5): e2241.
- VanBuskirk, A. M., V. Malik, et al. (2001). "A gene polymorphism associated with posttransplant lymphoproliferative disorder." *Transplant Proc* **33**(1-2): 1834.
- Veckman, V., P. Osterlund, et al. (2006). "TNF-alpha and IFN-alpha enhance influenza-A-virus-induced chemokine gene expression in human A549 lung epithelial cells." *Virology* **345**(1): 96-104.
- Vogel, A. J., S. Harris, et al. (2014). "Early cytokine dysregulation and viral replication are associated with mortality during lethal influenza infection." *Viral Immunol* **27**(5): 214-224.
- Waithman, J. and J. D. Mintern (2012). "Dendritic cells and influenza A virus infection." *Virulence* **3**(7): 603-608.
- Walk, S. T., A. M. Blum, et al. (2010). "Alteration of the murine gut microbiota during infection with the parasitic helminth *Heligmosomoides polygyrus*." *Inflamm Bowel Dis* **16**(11): 1841-1849.
- Walsh, K. P. and K. H. Mills (2013). "Dendritic cells and other innate determinants of T helper cell polarisation." *Trends Immunol* **34**(11): 521-530.
- Wang, J., M. P. Nikrad, et al. (2012). "Innate immune response of human alveolar macrophages during influenza A infection." *PLoS One* **7**(3): e29879.
- Wang, M., K. Lamberth, et al. (2007). "CTL epitopes for influenza A including the H5N1 bird flu; genome-, pathogen-, and HLA-wide screening." *Vaccine* **25**(15): 2823-2831.
- Wang, W., P. Yang, et al. (2013). "Monoclonal antibody against CXCL-10/IP-10 ameliorates influenza A (H1N1) virus induced acute lung injury." *Cell Res* **23**(4): 577-580.
- Wang, X., C. C. Chan, et al. (2011). "A critical role of IL-17 in modulating the B-cell response during H5N1 influenza virus infection." *Cell Mol Immunol* **8**(6): 462-468.
- Wang, X., K. Yang, et al. (2010). "Coinfection with EBV/CMV and other respiratory agents in children with suspected infectious mononucleosis." *Viral J* **7**: 247.
- Wang, Z., S. Zhou, et al. (2014). "Interferon-gamma Inhibits Nonopsonized Phagocytosis of Macrophages via an mTORC1-c/EBPbeta Pathway." *J Innate Immun*.
- Wareing, M. D., A. Lyon, et al. (2007). "Chemokine regulation of the inflammatory response to a low-dose influenza infection in CCR2-/- mice." *J Leukoc Biol* **81**(3): 793-801.
- Wareing, M. D., A. B. Lyon, et al. (2004). "Chemokine expression during the development and resolution of a pulmonary leukocyte response to influenza A virus infection in mice." *J Leukoc Biol* **76**(4): 886-895.
- Wei, H., S. Wang, et al. (2014). "Suppression of interferon lambda signaling by SOCS-1 results in their excessive production during influenza virus infection." *PLoS Pathog* **10**(1): e1003845.
- Weinberg, J. B., M. L. Lutzke, et al. (2004). "Mouse strain differences in the chemokine response to acute lung infection with a murine gammaherpesvirus." *Viral Immunol* **17**(1): 69-77.
- Weng, M., D. Huntley, et al. (2007). "Alternatively activated macrophages in intestinal helminth infection: effects on concurrent bacterial colitis." *J Immunol* **179**(7): 4721-4731.
- White, D. W., R. Suzanne Beard, et al. (2012). "Immune modulation during latent herpesvirus infection." *Immunol Rev* **245**(1): 189-208.
- WHO (2014) "Influenza A."
- Wiley, J. A., A. Cerwenka, et al. (2001). "Production of interferon-gamma by influenza hemagglutinin-specific CD8 effector T cells influences the development of pulmonary immunopathology." *Am J Pathol* **158**(1): 119-130.
- Wissinger, E., J. Goulding, et al. (2009). "Immune homeostasis in the respiratory tract and its impact on heterologous infection." *Semin Immunol* **21**(3): 147-155.
- Wortzman, M. E., G. H. Lin, et al. (2013). "Intrinsic TNF/TNFR2 interactions fine-tune the CD8 T cell response to respiratory influenza virus infection in mice." *PLoS One* **8**(7): e68911.
- Wu, W., K. B. Patel, et al. (2011). "Cigarette smoke extract suppresses the RIG-I-initiated innate immune response to influenza virus in the human lung." *Am J Physiol Lung Cell Mol Physiol* **300**(6): L821-830.
- Wynd, S. (2007). "Understanding the community impact of lymphatic filariasis: a review of the sociocultural literature." from <http://www.who.int/bulletin/volumes/85/6/06-031047/en/>.
- Yagami, A., K. Orihara, et al. (2010). "IL-33 mediates inflammatory responses in human lung tissue cells." *J Immunol* **185**(10): 5743-5750.
- Yu, X., X. Zhang, et al. (2011). "Intensive cytokine induction in pandemic H1N1 influenza virus infection accompanied by robust production of IL-10 and IL-6." *PLoS One* **6**(12): e28680.

- Yun, H. C., W. H. Fugate, et al. (2014). "Pandemic influenza virus 2009 H1N1 and adenovirus in a high risk population of young adults: epidemiology, comparison of clinical presentations, and coinfection." *PLoS One* **9**(1): e85094.
- Zaccone, P., O. Burton, et al. (2009). "Schistosoma mansoni egg antigens induce Treg that participate in diabetes prevention in NOD mice." *Eur J Immunol* **39**(4): 1098-1107.
- Zaccone, P., T. Raine, et al. (2004). "Salmonella typhimurium infection halts development of type 1 diabetes in NOD mice." *Eur J Immunol* **34**(11): 3246-3256.
- Zavitz, C. C., C. M. Bauer, et al. (2010). "Dysregulated macrophage-inflammatory protein-2 expression drives illness in bacterial superinfection of influenza." *J Immunol* **184**(4): 2001-2013.
- Zhou, W., F. Lin, et al. (2013). "Prevalence of herpes and respiratory viruses in induced sputum among hospitalized children with non typical bacterial community-acquired pneumonia." *PLoS One* **8**(11): e79477.
- Zhu, J. and W. E. Paul (2008). "CD4 T cells: fates, functions, and faults." *Blood* **112**(5): 1557-1569.